TECHNISCHE UNIVERSITÄT MÜNCHEN

Lehrstuhl für Bodenökologie

Dynamic of alkane degrading bacteria at different compartments in soil

Stephan Schulz

Vollständiger Abdruck der von der Fakultät Wissenschaftszentrum Weihenstephan für Ernährung, Landnutzung und Umwelt der Technischen Universität München zur Erlangung des akademischen Grades eines

Doktors der Naturwissenschaften

genehmigten Dissertation.

Vorsitzender:	Univ.-Prof. Dr. J. C. Munch
Prüfer der Dissertation:	1. Hon.-Prof. Dr. M. Schloter
	2. Univ.-Prof. Dr. I. Kögel-Knabner

Die Dissertation wurde am 12.06.2012 bei der Technischen Universität München eingereicht und durch die Fakultät Wissenschaftszentrum Weihenstephan für Ernährung, Landnutzung und Umwelt am 27.09.2012 angenommen.

"Die Neugier steht immer an erster Stelle eines Problems, das gelöst werden will."

(Galileo Galilei 1564 - 1642)

Contents

List of Figures

List of Tables

List of Publications and Contributions

Book chapter

I. Pérez-de-Mora A., **Schulz S.**, Schloter M. (2010). MPN- and real time-based PCR methods for the quantification of alkane-monooxygenase homologous genes (*alkB*) in environmental samples. In: Cunningham S (ed). *Methods in Molecular Biology*. Humana Press: New York. pp 59-68

Research paper

II. **Schulz S.**[*], Pérez de Mora A.[*], Engel M., Munch J.C., Schloter M. (2010). A comparative study of most probable number (MPN)-PCR vs. real-time-PCR for measurement of abundance and assessment of diversity of *alkB* homologous genes in soil. *Journal of Microbiological Methods* 80(3): 295-298

III. **Schulz S.**[*], Giebler J.[*], Chatzinotas A., Wick L.Y., Fetzer I., Welzl G., Harms H., Schloter M. (2012) Plant litter and soil type drive abundance, activity and community structure of *alkB* harbouring microbes in different soil compartments. *The ISME Journal* doi: 10.1038/ismej.2012.17

IV. **Schulz S.**, Yuyunkina T., Pagel H., Wick L.Y., Poll C., Streck T., Kandeler E.[*], Schloter M.[*] (2012) The influence of the herbicide 2-methyl-4-chlorophenoxyacetic acid (MCPA) on the mineralization of litter-derived alkanes and the abundance of the alkane monooxygenase gene (*alkB*) in the detritusphere of *Pisum sativum* (L.). *Biology and Fertility of Soils* doi: 10.1007/s00374-012-0685-2

[*]authors contributed equally

My contributions to the publications were the following.

I. I contributed to the preparation of the manuscript and the gene quantification by real-time PCR. In addition, I optimized the amplification protocol and the *alkB* primer set, published earlier by Kloos *et al.* [107].

II. I was involved in the sampling campaign and the isolation of nucleic acids. Furthermore, I optimized the protocol for successful amplification of *alkB* and accomplished the quantification of this gene via MPN- and real-time PCR. The manuscript is mainly based on my contribution.

III. I carried out the incubation experiment and the soil sampling as well as the isolation of DNA and RNA with subsequent cDNA synthesis. The quantification of *alkB* genes and transcripts via optimized real-time PCR was also done by me. Furthermore, I was mainly involved in the preparation of the manuscript.

IV. I was involved in the planning of the experiment and supervised the executing master student (T. Yuyunkina) during the isolation of nucleic acids and the quantification of *alkB* and 16S rRNA by real-time PCR. The preparation of the manuscript was mainly done by me.

1 Summary

Soils are highly hierarchically structured systems with diverse micro-habitats, which are the result of the interplay of different particles and minerals. The habitats differ in their expansion, due to the various sizes and shapes of those particles as well as their assemblages. Depending on the physico-chemical conditions of soils, the distribution of nutrients, water, oxygen as well as electron acceptors is highly dynamic in time and space. Consequently, so-called hotspots of microbial activity and evolution might be formed trough dependency of the nutrient supply. In previous studies, the micro-habitats and the corresponding microbial turnover processes at the microscale are often overlooked, when samples were taken without maintaining the soil micro-structure. However, diverse studies were accomplished to gain insights into the abundance and community structure of alkane degrading bacteria during the remediation of hydrocarbons. Here again, analyses were done in the range of centimeters, omitting the microscale.
As part of the DFG-priority program 1315 ("Biogeochemical Interfaces in Soil"), the present study was conducted to analyse the abundance and activity of *alkB*-harbouring bacteria in a spatio-temporal manner. In pioneer work, published *alkB*-specific primers were modified in order to increase qPCR amplification efficiency and consequently improve the quantification. Therefore, four-fold degenerated bases were substituted with inosine nucleotides and various PCR reaction protocols were tested. Additionally, different reaction mixture additives like DMSO, BSA and magnesium chloride have been analysed for suitability. By using the modified primers and respective qPCR conditions the following experiments have been conducted.

I. Two arable soils differing significantly in their texture were incubated with litter material of maize and pea. At the beginning and after two, eight and thirty weeks of incubation, the litter layer as well as the litter-soil interface and bulk soil compartments were sampled and analysed. The data clearly suggest a gradient formation from the litter to deeper bulk soil compartments, as a result of heterogeneous nutrient dispersal. Furthermore, despite the different quantities and qualities of maize and pea plant wax alkanes, no impact of the litter type on the *alkB*-harbouring bacteria was monitored. Contrary, the abundance of *alkB* genes and transcripts was strongly influenced by the incubation time and moreover by the soil type.

II. Due to the fact that herbicides might have a hampering effect on certain soil bacteria, abundance of alkane degraders harbouring *alkB* in MCPA amended and control soils was analysed. Therefore, *alkB* genes were quantified in the detritusphere of soils (0 - 3, 3 - 6, 6 - 9 mm), which were incubated with pea litter for up to six weeks. Interestingly, the results could not demonstrate an influence of this herbicide.

III. In order to verify the influence of certain clay minerals on the abundance of *alkB*, eight so-called "artificial soils" with diverse compositions and of two different ages were incubated with litter material of wheat for two weeks. In this regard, no impact of the compositions was monitored. Furthermore, data suggest other factors than litter derived alkanes to be the driving factor for microbial response at different soil compartments.

However, in order to identify hotspots of alkane degrading bacteria and to verify the potential distribution of alkanes in soils, antibodies against AlkB should be produced in the present study. Therefore, different approaches for the overexpression of AlkB in host strains and the specific purification were tested to yield sufficient amounts for immunization.

2 Zusammenfassung

Böden sind hoch hierarchisch strukturierte Systeme mit verschiedenen Mikrohabitaten, die das Resultat eines Zusammenspiels verschiedener Partikel und Mineralien sind. Die Habitate unterscheiden sich in Ihrer Ausdehnung als Folge verschiedener Größen und Formen dieser Partikel und Ihrer Zusammenschlüsse. In Abhängigkeit der physikochemischen Bedingungen in Böden, ist die Verteilung von Nährstoffen, Wasser, Sauerstoff und Elektronenakzeptoren in Raum und Zeit hoch dynamisch. In diesem Zusammenhang entstehen in Abhängigkeit der Nährstoffversorgung so genannte "Hotspots" mikrobieller Aktivität und Entwicklung. In früheren Studien, in denen eine Beprobung ohne den Erhalt der Bodenmikrostruktur erfolgte, wurden solche Mikrohabitate oft nicht beachtet. Des weiteren wurden diverse Studien durchgeführt, um Einblicke in die Abundanz und Struktur alkanabbauender Bakterien während der Verwertung von Kohlenwasserstoffen zu erlangen. Aber auch hier wurden die Analysen unter Ausschluss der Mikroskala nur im Zentimeterbereich gemacht.
Als Teil des DFG-Schwerpunktprogrammes 1315 ("Biogeochemical Interfaces in Soil"), wurde die vorliegende Studien erstellt, um die Abundanz und Aktivität *alkB* tragender Bakterien in einem räumlichen und zeitlichen Kontext zu untersuchen. In Vorarbeiten wurden bereits veröffentlichte *alkB*-spezifische Primer modifiziert, um die Amplifikationseffizienz zu erhöhen und damit die Quantifizierung zu verbessern. Zu diesem Zweck wurden 4-fach degenerierte Basen durch Inosinnukleotide ausgetauscht und diverse PCR-Reaktionsprotokolle getestet. Darüber hinaus wurden verschiedene Additive wie DMSO, BSA und Magnesiumchlorid auf Ihre Eignung untersucht. Unter Zuhilfenahme der modifizierten Primer und entsprechender PCR-Protokolle, wurden folgende Experimente durchgeführt:

I. Zwei landwirtschaftlich genutzte Böden, die sich signifikant in Ihrer Struktur unterscheiden, wurden mit Streumaterial von Mais und Erbse inkubiert. Zu Beginn und nach zwei, acht und dreißig Wochen Inkubation wurden die Streuschicht, die Streu-Boden-Grenzschicht und Boden in 1 cm Tiefe beprobt und untersucht. Die Daten weisen klar auf die Bildung eines Gradienten vom Streu zu tieferen Bodenkompartimenten als Folge einer heterogenen Nährstoffverteilung hin. Des weiteren wurde trotz der unterschiedlichen Quantitäten und Qualitäten der pflanzlichen Alkane von Mais und Erbse, kein Einfluss des Streutypes auf die Abundanz *alkB*-tragender Bakterien beobachtet. Im Gegensatz dazu wurde die Abundanz der *alkB* Gene und Transkripte stark von der Inkubationszeit und dem jeweiligen Bodentyp beeinflusst.

II. Aufgrund des Faktes, das Herbizide eine schädlichen Einfluss auf bestimmte Bodenenzyme haben können, wurde die Abundanz von Alkandegradierern die *alkB* tragen in MCPA versetzten und Kontrollböden untersucht. Interessanterweise konnten die Ergebnisse keinen Einfluss des Herbizides darstellen.

III. Um den Einfluss bestimmter Tonmineralien auf die Abundanz von *alkB* zu bestätigen, wurden acht sogenannte "künstliche Böden" mit diversen Zusammensetzungen und von unterschiedlichem Alter mit Weizenstreu inkubiert. Darüber hinaus deuten die Daten darauf hin, das andere Faktoren als die Alkane aus dem Streumaterial, die antreibenden Faktoren für die mikrobielle Reaktion in verschiedenen Bodenkompartimenten sind.

Um die "Hotspots" von alkanzersetzenden Bakterien identifizieren und die mögliche Verteilung der Alkane im Boden verifizieren zu können, sollten Antikörper gegen AlkB in der vorliegenden Studien hergestellt werden. Aus diesem Grund wurden verschiedene Ansätze für die Überexpression in Produktionsstämmen und eine spezifische Aufreinigung getestet, um geeignete Mengen für die Immunisierung zu erzielen.

3 Introduction

3.1 Introduction to the Ph.D. thesis

Soils play a major role in global nutrient cycles as they are storage, transformation and transport medium for water, gases and also pollutants. Persistence and turnover rates of all substrates are determined by the conditions at so-called biogeochemical interfaces (BGI's) where minerals, organic matter and soil microbes interact with each other. As most recent studies analysed the fate of organic matter on the macroscale, data about the transformation processes on the microscale are still rare. The present study was part of the priority program SPP1315 "Biogeochemical Interfaces in Soils" (www.spp1315.uni-jena.de) funded by the Deutsche Forschungsgemeinschaft (DFG). In this program interdisciplinary research of geological, chemical and biological sciences was done in order to characterize the structure and functionality of biogeochemical interfaces in soil and their potential for degradation of organic compounds. The results of this study contribute to the mechanistic understanding of the microbial degradation of model compounds in soils on the microscale.

3.2 Biogeochemical interfaces in soils

Per definition, interfaces are contact zones between different phases or spheres. In this respect, soils represent extremely large interfaces on the macroscale (m to km), as they mediate the interactions of the biosphere, the hydrosphere, the atmosphere and the lithosphere. Contrarily, depending on its mineralogy, 1 g of soil can contain tens of m^2 of surface, where organic and mineral phases can interact. Hence, soils are are also large and highly complex on the microscale ranging from µm to several mm (Figure 1). As biological and chemical turnover processes take place at such interfaces [264] they are generally termed biogeochemical interfaces. Those interfaces represent the boundary surfaces to soil liquids and gaseous phases [229] and are consequently extended into voids and pores [264]. In such microhabitats, microbes colonizing the surfaces of mineral particles [52; 53] can actively shape their environment. For instance, exopolysaccharides, which were secreted in order to form biofilms or as protective barrier against environmental stresses (e.g. droughts, antibiotic substances), can act as glue between soil particles. As a result, microaggregates might be formed [132] acting as reservoirs for substrates and microbial refuge from predators. During ongoing pedogenesis these microaggregates can be destructed or destabilized by the microbial degradation of organic matter [97; 265]. In addition, iron-oxidizing microbes from the genera *Thiobacillus* or

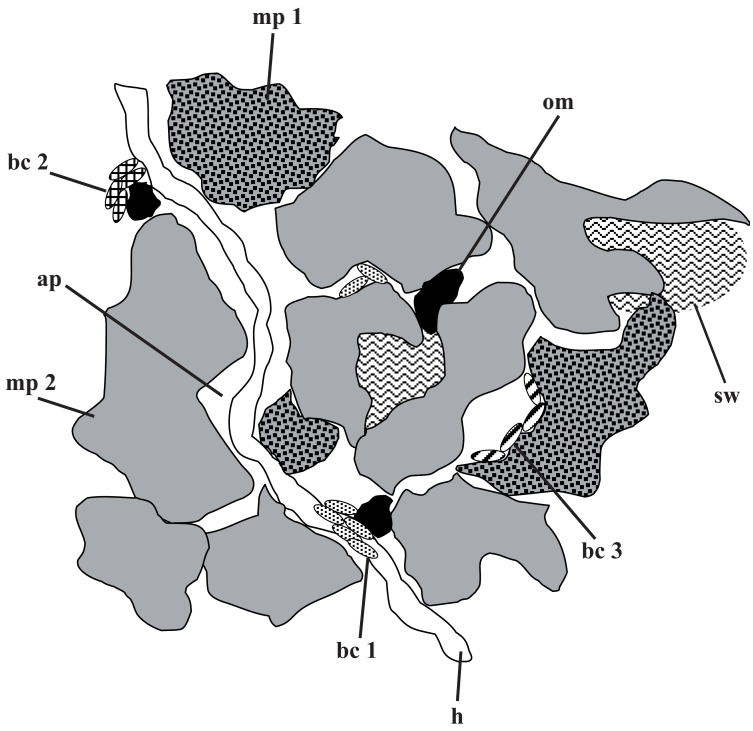

Fig. 1: Biogeochemical interfaces in the soil
Biogeochemical interfaces and microbial hotspots in the highly complex and hierarchically structured soil. ap = air filled pores; bc = bacterial communities with diverse structures; h = hyphae; mp = different kinds of mineral particles; om = organic matter; sw = soil water

Ferroplasma can affect the mineral phase further impacting the stability of such structures. However, the microbial community not only influences their environment, but is also impacted by the microhabitats *vice versa*. Due to biological and non-biological processes like the entanglement of microaggregates by fine roots or fungal mycelium as well as drying/ wetting and freezing/ thawing phenomena, macroaggregates might be formed. In this respect, micro- and macroaggregates in turn affect the distribution of substrates, water or electron acceptors and consequently the abundance, activity and diversity of soil microbial communities.

In spite of various studies focusing on the rhizosphere (soil influenced by root exudates) as well as the detritusphere (soil adjacent to and influenced by plant litter material), microbial processes and community structure at the biogeochemical interfaces are poorly understood.

3.3 Leaf litter degradation

Leaf litter decomposition is an important process in the recycling of carbon and nitrogen and other essential elements. As revealed in several studies dealing with leaf litter decay in terrestrial and aquatic ecosystems, the turnover of organic matter is characterized by two essential stages, differing significantly in their kinetics. In the early stage, which occurs within only few days and weeks, easy degradable compounds (e.g. sugars, hemicellulose, cellulose and proteins) become released and quickly metabolized by the microbial community. It was shown in several studies, that fast growing bacteria like *Acidobacteria* [251] and *Proteobacteria* play a dominant role in that stage [56; 59]. In consequence of the microbial activity and leaching processes, an immense loss of biomass within a relative short time period has been reported in several studies. For example, within six weeks of incubation a loss of almost 10% of the initial amount was monitored in an experiment dealing with oak-leaf litter degradation [225]. Furthermore, by analyzing microbial communities during the decay of beech and spruce plant material, Aneja *et al.* [9] could demonstrate losses of more than 30% of the initial amounts within the first two weeks of incubation.

With ongoing incubation, the chemical composition of the litter material becomes modified, resulting in high concentrations of recalcitrant compounds (e.g. lignin), forming very stable complexes [188]. Consequently, degradation is attenuated [10; 76]. In this stage, fungi like *Basidiomycetes* [115] and *Ascomycetes* [198] become dominant in the later stage of litter degradation. Moreover, bacterial specialists also contribute to the turnover of recalcitrant compounds. For instance, increasing abundances of *Actinobacteria* were monitored during continuing leaf litter decay [209; 226] as those bacteria are able to use lignin-derived compounds [105]. Despite the expected competition of bacteria and fungi for carbon and nitrogen, synergetic effects were reported also [71], where fungi provide bacteria with substrate reservoirs and new colonizing space by macerating leaf tissues with their growing hyphae [215].

Besides the immense hydrolytic potential of litter degrading microbes, litter decay is also influenced by the substrate quality [33; 60; 78; 92; 218]. Especially, the ratios between compounds like carbon, nitrogen and lignin impact litter degradation rates [1; 80; 119; 146; 174]. For example, negative effects of high lignin contents were shown earlier [36], as they can react with ammonia or amino acids, resulting in a nitrogen depletion being detrimental for microbial growth. *Vice versa*, several studies demonstrated that elevated amounts of nitrogen can hamper the decay of lignin [101; 188]. Litter degradation is not only influenced by substrate quality but by anthropogenic activities

as well. For instance, the post-emergence herbicide 4-chloro-2-methylphenoxyacetic acid (MCPA) was shown to have derogatory effects on the microbial community structure and the activity of telluric enzymes [220]. In consequence, litter degradation rates and efficiencies might be reduced.

3.4 Aliphatic hydrocarbons and their role in nature

Aliphatic hydrocarbons like *n*-alkanes are highly abundant and ubiquitously distributed in the environment as a consequence of anthropogenic and natural activities. For example, large amounts are introduced to an ecosystem via oil spills, petroleum exploration and transportation activities as well as municipal waste disposal. Contrarily, the transformation of decaying biomass to crude oil or petroleum gas during geochemical processes also contribute to the alkane appearance. Furthermore, alkanes are actively produced by the living biomass or during the mineralization of organic matter. The biggest natural source of hydrocarbons is represented by epicuticulary waxes, forming the contact zone between plant leaves and the environment [100] as demonstrated in Figure 2. Beside long-chained alcohol esters, alkanes with a chain length between C_{16} and C_{37} [48; 86] are a major component of these waxes which are produced to form a barrier against environmental stresses like phytopathogens or uncontrolled water loss via evaporation [14; 66].

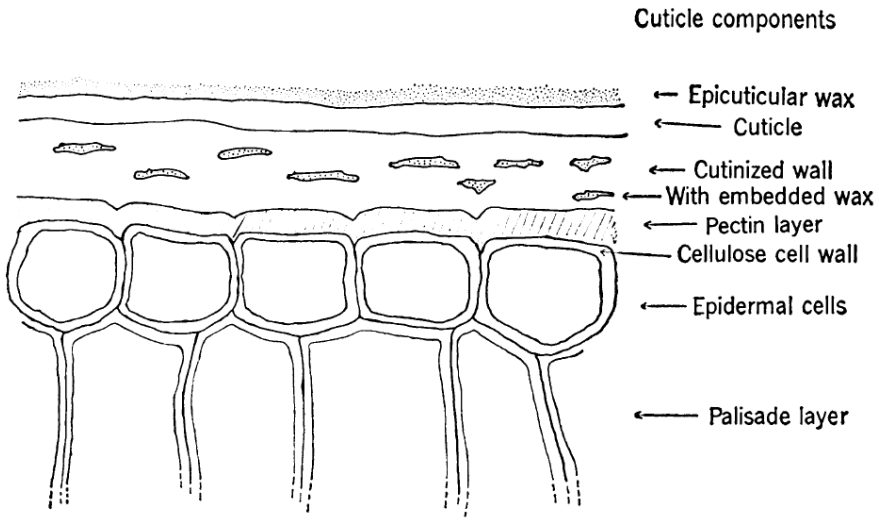

Fig. 2: Schematic cross section of the herbal epicuticle [49]
Cross section of the herbal epicuticle which is composed of the cuticle layer covering the epidermal cells. Epicuticlar and embedded waxes overlaying and crossing the cuticle, to form a barrier against environmental influences, are a large source of middle- and long-chained alkanes.

For example, increased accumulation of cuticular waxes in response to drought events were monitored during earlier studies of stress response in sorghum, tree tobacco or different *Brassica* species [27; 12; 168]. In addition, short chained alkanes like hexadecane, octadecane, eicosane and tetradecane were found to be the main seed oil alkanes in GC and GC-MS studies of 43 *Leguminosae* species [120]. The concentration and composition as well as the carbon isotopic compositions of cuticulary wax alkanes vary between

different plant species and thus allow the differentiation of plant families and metabolic properties like C3 and C4 plants. Different C_{29}/C_{31} ratios for *Umbelliferae* and *Leguminosae* [135] as well as varying $\delta^{13}C$ values (-35 ‰ to -40 ‰ for C3 and -15 ‰ to -25 ‰ for C4) [35; 177] were found in earlier studies. Furthermore, variations in the higher plant *n*-alkane average chain length (ACL), which describes the average number of carbons per molecule based on the abundance of odd-carbon-numbered *n*-alkanes in higher plants [167], can be used to distinguish between vegetation types [38] or climatic conditions [88; 194].

Beside plants, several studies could show that microorganisms (both prokaryotes and eukaryotes) are able to synthezise aliphatic hydrocarbons for physiological purposes. For example, Ladygina et al. [117] demonstrated sulfate reducing bacteria and clostridia being capable of synthesizing extracellular hydrocarbons which appeared to be associated with the formation of capsules protecting the cells from high concentrations of excreted acids. Furthermore, long-chained alkanes from *Pseudomonas fluorescens* are supposed to be involved in the autoregulation of cell adhesion to smooth surfaces as well as the promotion of cell aggregation. Hara *et al.* [77] reported on the ability of marine zooplankton to produce hydrocarbons as well. Anyhow, similar to the taxonomic determination potential of the alkane composition of cuticulary waxes, hydrocarbon configuration of microbes was also assumed to be a chemotaxonomic criterion [95].

The bioavailability of released *n*-alkanes is strongly dependent on their chain length, as the interaction of hydrocarbons with other compounds is influenced by the carbon number. In addition, short chained alkanes can be toxic, as they impair cell membranes acting as solvents for cellular fats [202]. On the contrary, long chained alkanes can induce the formation of oil films and slicks restricting the exchange of water, nutrients and gases between micro- and macro-environments [121].

3.5 Microbial degradation of *n*-alkanes

The large variety of different alkane species occurring in the environment (e.g. short-, middle-, long-chained alkanes) as well as the supply of diverse electron acceptors highly impact the microbial uptake and mineralization and consequently render a broad spectrum of alkane degradative systems with overlapping substrate ranges. As summarized in Figure 3, diverse systems were detected, facilitating the degradation of alkanes under aerobe, semi-anaerobe and anaerobe conditions. However, several studies in the last decades identified bacteria and fungi being the key players in the degradation of hydrocarbons. Contrarily, no hints or only scanty data for a direct alkane metabolization by protozoa and algae are available [179; 247]. In an experiment focusing on the degradation of hexadecane in a sandy loam soil, Song *et al.* [212] pointed out that 82% of the mineralization of C_{16} were attributed to bacteria and only a comparable minor fraction was related to fungal activity. Despite this, fungi and in particular yeasts are regarded to be established members of the alkane degrading soil microbial communities [197].

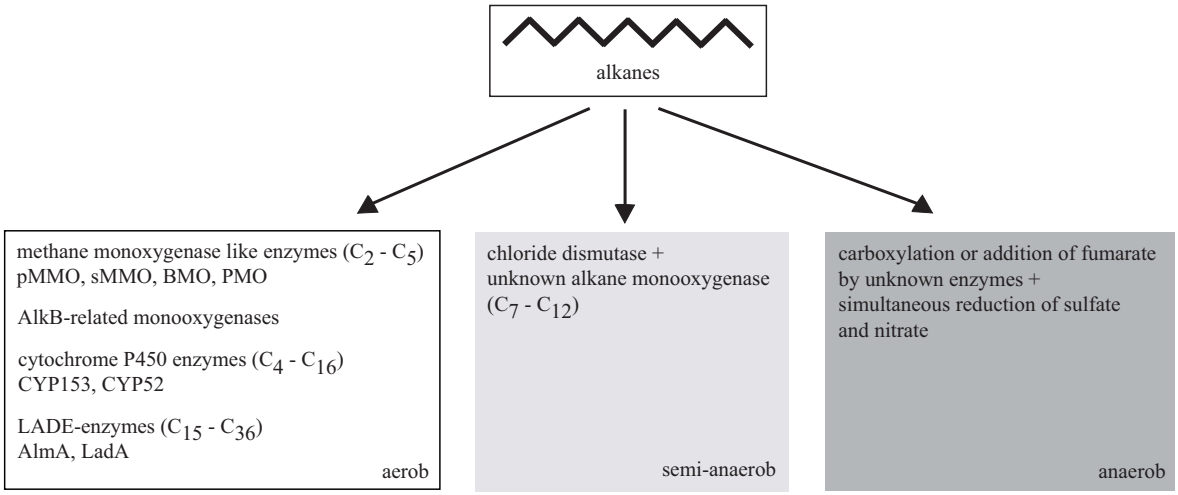

Fig. 3: Schematic overview of known alkane degradation pathways
Due to different availabilities of divers electron acceptors, a broad spectrum of alkane degradative systems under aerobe, semi-anaerobe and completely anaerobe conditions have been developed. See text for detailed information about the individual enzymes. pMMO = particular Methane Monooxygenase, sMMO = soluble Methane Monooxygenase, PMO = Propane Monooxygenase, BMO = Butane Monooxygenase.

Beside facultative alkane degraders, which can also use other carbon sources, so-called obligate alkanotrophs related to strains of *Alcanivorax borkumensis* [190] and *Thalassolituus oleivorans* [263] were found. These strains are able to grown on alkanes and a few related compounds solely. However, strains harbouring multiple alkane hydroxylase systems with overlapping substrate ranges were found to grow on short- (C_1–C_4) [207] and very long-chained alkanes (C_{32}) [216] as well. For example, *A. borkumensis* isolates were found to contain two, AlkB-related particulate alkane hydroxylases (pAH) and two

CYP153 enzymes [190]. Furthermore, van Beilen *et al.* [235] clearly demonstrated five pAHs and two CYP153's in *Rhodococcus erythropolis* HXN-2000. In a recent study, Liu *et al.* [127] reported on *Alcanivorax dieselolei* B-5 harbouring two pAH's, a CYP153 and an AlmA-like alkane hydroxylase facilitating the use of alkanes up to C_{36}. However, solubility of alkanes strongly decreases with increasing chain length as Rojo [181] stated for hexane and hexadecane, where solubility of C_{16} (10^{-10} M) was six orders of magnitude lower compared to C_6 (10^{-4} M). During the last decades various pathways for the sensitive and effective uptake of hydrocarbons by microbes, irrespective of the source, have been monitored. For instance, the production of bioemulsifiers and biosurfactants can improve the bioavailability of alkanes about 10 to 15 times by enhancing the adhesion between cell wall and accessible hydrocarbons which is schematically shown in Figure 4.

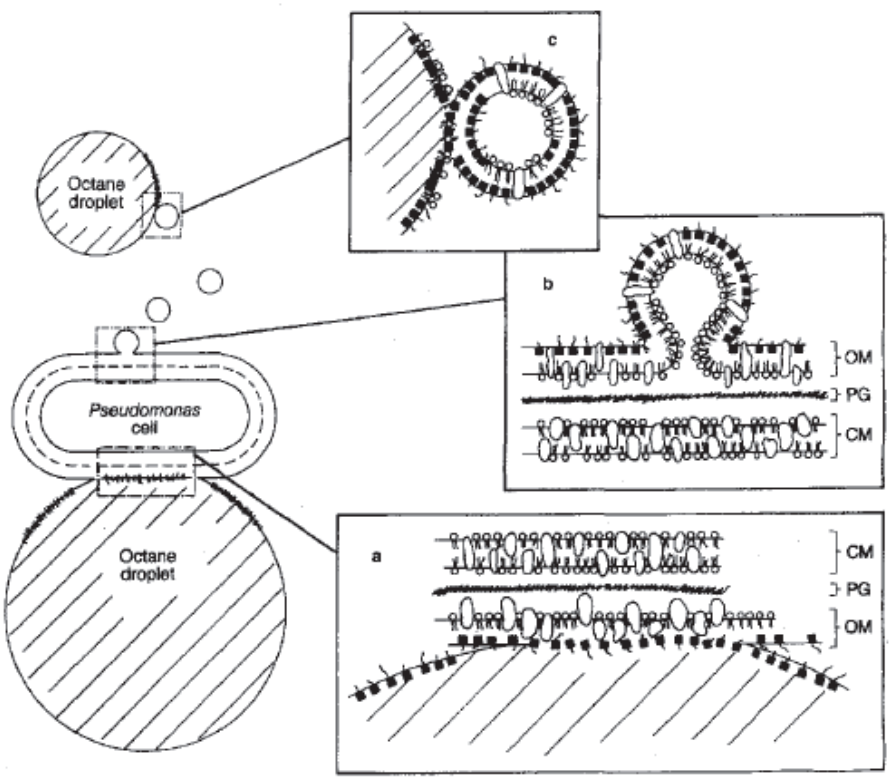

Fig. 4: Model for the uptake of alkanes in *P. putida* GPo1
During direct attachment of the cells to the hydrocarbon droplet, membrane components from the cell wall partition into the apolar droplet (a). Alternatively, water-solubility of alkanes can be increased by the extraction of emulsifiers as part of outer membrane vesicles (b) which interact with the hydrocarbon resulting in a complete coating with an outer layer of hydrophilic sugar chains (c) [256]. OM = outer membrane, PG = peptidoglycan layer, CM = cell membrane

A study by Beal and Betts [20] revealed an increased solubility of *n*-hexadecane from around 2 μg L^{-1} up to almost 25 μg L^{-1} after the synthesis of rhamnolipids by *Pseudomonas aeruginosa* PG201. However, changes in membrane lipid compositions and subsequently increasing hydrophobicities of cell surfaces can also benefit the increase

of alkane diffusion into the cell [20; 252]. In addition, a solubilization of hydrocarbon droplets by encapsulating them in membrane microvisicles (Fig. 4), which are subsequently taken up into cells via active processes was also demonstrated [111; 203]. Several studies proposed that modifications of the cell envelope like the invagination of membranes [199], the production of fimbriae [58; 184] or an increased content of lipopolysaccharides [256] could facilitate the adherence to hydrocarbon droplets and consequently support the utilization of alkanes.

Next to effective uptake mechanisms, the microbial alkane degradation efficiencies (6% to 82% in fungi [96], 0.13% to 50% in bacteria [160]) are also strongly dependent on different environmental conditions. In this respect, Smith *et al.* [206] supposed the optimization of the C:N:P ratio to be the most powerful tool for an enhanced bioremediation of alkanes. Additionally, high mineralization rates were found at a soil pH between 5 and 7.8 [44] further increased by the soil moisture, the salinity, the amount of oxygen as well as the terrestrial nutrient status [75]. Furthermore, the soil temperature is highly relevant for degradation as oil viscosity increases at low temperatures [121] with congruent decreasing hydrocarbon distribution in the soil matrix *vice versa* [250]. In parallel, Bartha and Bossert demonstrated an optimal degradation rate between 30 °C and 40 °C [19]. Due to the fact that *n*-alkanes are relatively inert, with long-chained alkanes being more resistant to degradation than alkanes with low carbon numbers (e.g. methane), activation is needed. This activation is achieved during various alkane degradation pathways, significantly differing under oxic and anoxic conditions (Fig. 3). As a result of their immense importance, the pathways will be highlighted in detail in the following chapter.

Aerobe alkane degradation

In environments with sufficient oxygen supply, alkane degraders were found to be present among prokaryotes, eukaryotes and archaea, which are summarized in Table 1. In 2007, Beilen and Funhoff [234] proposed three categories of unrelated enzyme systems which are relevant for the aerobe microbial alkane metabolisation facilitating the degradation of short- (methane monooxygenase-like enzymes), middle- (AlkB-related and cytochrome P450 enzymes) as well as long-chained alkanes (enzymes with rare data identified as **l**ong-chained **a**lkane **d**egrading **e**nzymes ("LADE") in this thesis).

Bacteria	**Yeast**	**Fungi**	**Archaea**	**Algae**
Achromobacter	*Candida*	*Acremonium*	*Halobacterium*	*Prototheca*
Acinetobacter	*Cryptococcus*	*Aspergillus*	*Haloferax*	
Agrobacterium	*Debaryomyces*	*Cladosporium*	*Halococcus*	
Alcanivorax	*Hansenula*	*Corollasporium*		
Alcaligenes	*Pichia*	*Cunninghamella*		
Bacillus	*Rhodotorula*	*Dendryphiella*		
Brevibacterium	*Saccharomyces*	*Fusarium*		
Burkholderia	*Sporobolomyces*	*Gliocladium*		
Corynebacterium	*Torulopsis*	*Gongronella*		
Dietzia	*Trichosporon*	*Lulworthia*		
Flavobacterium	*Yarrowia*	*Penicillium*		
Geobacillus		*Varicospora*		
Micrococcus		*Verticillium*		
Mycobacterium				
Nocardia				
Pseudomonas				
Rhodococcus				
Sphingomonas				
Streptomyces				
Xanthomonas				
...	...	...	...	...

Tab. 1: Aerobe alkane degrading bacteria
Microorganisms which are able to degrade aliphatic hydrocarbons like *n*-alkanes aerobically [6; 29; 217; 234; 237; 249]

Methane monooxygenase-like enzymes

Gaseous alkanes in the range of C_2-C_5 can be oxidized by two methane monooxygenases as well as the propane and butane hydroxylases which are all strongly related to each other. Whereas the membrane-bound particular monooxygenase (pMMO) seemed to be restricted to alkanes shorter than C_6 [126], bacteria harbouring the soluble methane monooxygenase (sMMO) were found to grow on alkanes with a chain length up to C_{10} [16] also. However, ability of bacteria harbouring propane monooxygenases (PMO) and butane monooxygenases (BMO) to grow on alkanes larger than C_5 was also shown for *Gordonia* sp. TY-5 (C_2-C_8) and *Pseudomonas buntanovora* ATCC 43655 (C_3 and $C_{13}-C_{22}$), respectively [110; 205].

Cytochrome P450 enzymes

Members of the cytochrome P450 superfamily are found in all three domains of life and constitute more than 4000 enzymes which can be subdivided into over 100 families [136; 239]. Remarkably, more than 80% of these enzymes are related to eukaryotes, whereas only a fractional amount is assumed to be present in prokaryotes [239]. Despite this, only a few enzymes being involved in the alkane degradation have been monitored so far, which were divided into two subclasses (class I, II) significantly differing in their structure and substrate range. The bacterial cytochrome CYP153 (class I) is characterized by a three-component system consisting of the cytochrome itself, a ferredoxin and a ferredoxin reductase for the transfer of electrons and oxidizes C_4−C_{16} alkanes [136]. On the contrary, the functionally corresponding fungal cytochrome CYP52 (class II) catalyzes the oxidation of alkanes with a chain length of C_{10}−C_{16} [37] is only composed of the membrane-bound cytochrome and a reductase.

AlkB-related monooxygenases

The alkane monooxygenase gene *alkB*, encoding the corresponding monooxygenase, was first descripted in detail by Chakrabarty *et al.* [30] who analysed its transcription regulation in *Pseudomonas putida* (formerly *P. oelovorans*) during its growth on *n*-octane and substrates beyond. Conjugational transfer experiments proposed a location of *alkB* on the so-called OCT (octane utilizing) plasmid [31; 109; 242; 236]. In contrast to those initial analyses, other studies also demonstrated multiple chromosomal copies of *alkB* in a large variety of alkane degrading bacteria. For example, two to three chromosomal gene copies have been found in different strains of *P. aeruginosa* including PAO1 and ATCC17423 [207; 243]. Furthermore, van Beilen *et al.* [238] could demonstrate four to five paralogues in strains of *Rhodococcus erythropolis*. Interestingly, the transcription of these paralogues genes is strictly regulated and strongly dependent on i) the chain-length variations of the substrates [208], ii) different growth phases [141] and iii) distinct affinities for various alkane species including non-linear aliphatic or aromatic alkanes [239]. Besides this, the expression of *alkB* was also found to be dependent on different alkane derivates like alkanols, aldehydes or fatty acids [70; 140]. In addition, transformation of alkenes and alcohols to epoxides and aldehydes as well as the demethylation of branched methyl esters and sulfoxidation of thioesters catalyzed by the *alkB* transcription product was also demonstrated [98; 99; 142; 143; 144; 241; 256].
Unfortunately a distinct description of the protein structure of AlkB is still missing since crystallization experiments to proof the theory failed up to date. However, early

results suggested six transmembrane domains, represented by gray barrels in Figure 5, forming a hexagonal tube which spans the cytoplasma membrane, with 60 - 65% of the total protein being located within the cytoplasma. The AlkB protein harbours two iron atoms in its catalytic centre being enclosed by four highly conserved histidine motifes as shown earlier by Shanklin *et al.* [200].

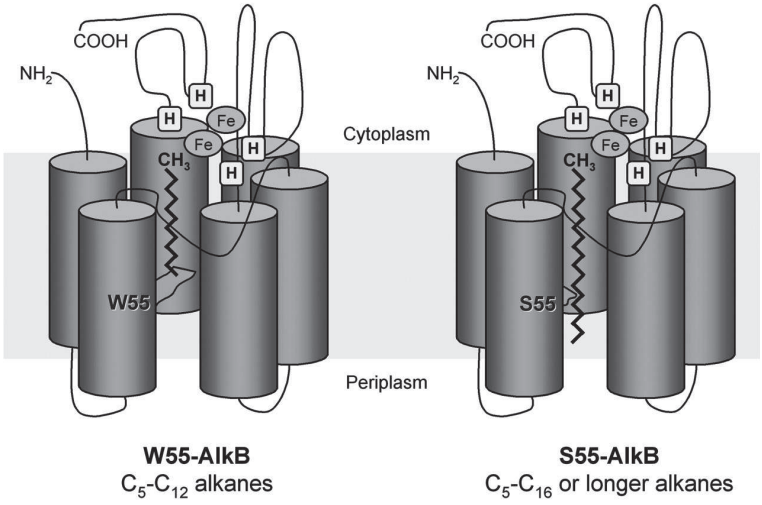

Fig. 5: Substrate range discrimination and cellular orientation of AlkB
A tryptophan residue at position 55 determines substrate affinity in *P. putida*. A substitution with less bulky amino acids changes the affinity to alkanes. See text for explanation. H, histine; Fe, iron atom [180].

Anyhow, Beilen and colleagues [233] could demonstrate that the substrate range of AlkB is determined by a tryptophan in the middle of the hexagonal tube (amino acid position 55 and 58 in *P. putida* and *A. borkumensis* respectively) preventing longer alkanes to fully enter the catalytic center (Fig. 5). With the substitution of this tryptophan by less bulky amino acids (e.g. serine, cysteine) alkane substrate ranges of AlkB can be prolonged to alkanes with a chain-length of 16 carbons without loosing the ability to hydroxylize C_5 - C_{12} [180].

The alkane degradation via the AlkB-related pathway is facilitated by proteins with different regulatory and catalytic functions. As summarized by Beilen *et al.*, the genes encoding the corresponding proteins are clustered in two distinct open reading frames (ORF's). The ORF's *alkST* and *alkBFGHJKL* include the alkane monooxygenase (AlkB) itself, two rubredoxins (AlkG, AlkF), the rubredoxin reductase (AlkT), an alcohol and aldehyde hydroxylase (AlkJ, AlkH), a putative substrate transporter (AlkL) as well as the transcription regulator AlkS. Several studies analyzing the function of AlkS could demonstrate a positive expression regulation of both reading frames [28; 47; 156].

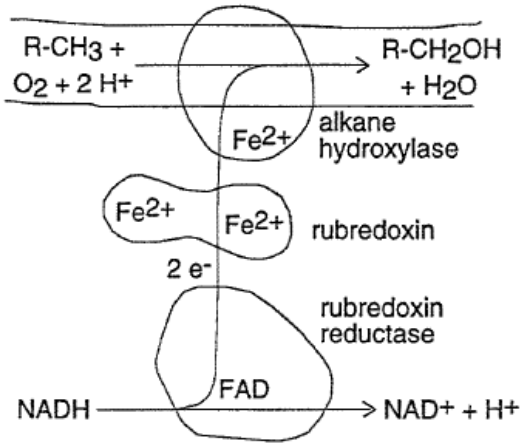

Fig. 6: Component structure of the AlkB-related alkane degradative system [236]
The AlkB-related alkane degradative system consists of an integral membrane bound alkane hydroxylase, a rubredoxin and its corresponding reductase. Electrons for the alkane hydroxylation are transferred from NADH to AlkB via sequential redox-reactions.

However, during sequential reduction and oxidation of rubredoxin and the corresponding reductase, electrons from NADH are transferred to AlkB, as shown in Figure 6, and consequently used for the terminal and subterminal hydroxylation of alkanes [181]. The resulting primary and secondary alcohols [260] are further processed to bi-carbonic acids, succinyl-CoA or acetic acids which can be used in turn as substrates for the β-oxidation or the tricarboxylic acid (TCA) cycle, respectively. The whole process of aerobe alkane degradation using the alkane monooxygenase AlkB as the catalysator for the initial reaction is summarized in Figure 7.

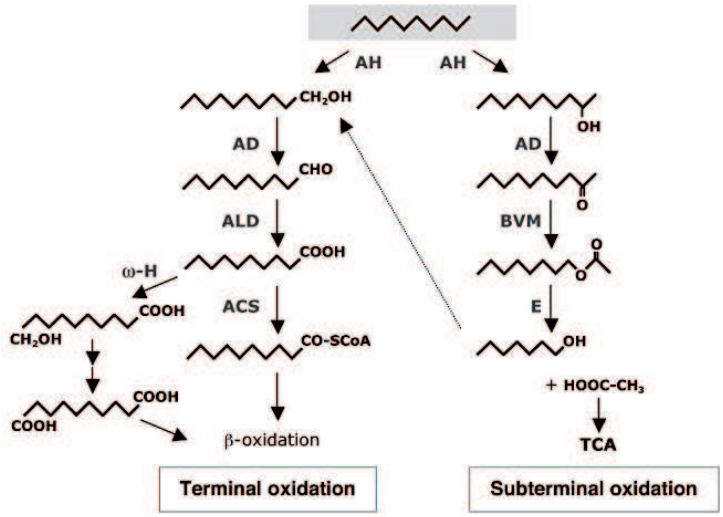

Fig. 7: Aerobe alkane degradation via the *alkB*-related pathway [181]
Under aerobe conditions aliphatic *n*-alkanes are oxidized by AlkB at terminal or subterminal position. Resulting primary and secondary alcohols are further metabolized to bi-carbonic acids, succinyl-CoA and acetic acid which are in turn substrates for the β-oxidation or the TCA cycle.

Long-chained alkane degrading enzymes (LADE-enzymes)

In the last years alkane degrading systems, which are neither related to the cytochrome P450 superfamily nor AlkB-related enzymes nor to methane monooxygenase-like proteins, were monitored. These enzymes are active in microbes growing on very long chained alkanes with up to 36 carbons. Throne-Holst and colleagues [223] described a flavin-binding monoxygenase (AlmA) in *Acinetobacter* strain DSM 17874 which enabled growth on C_{20} - C_{32} alkanes. Gene homologues to *almA* were also found in *Acinetobacter sp.* M1 and *A. borkumensis* SK2. Furthermore, another hydroxylase (LadA) from *Geobacillus thermodenitrificans* NG80-2 generated primary alcohols from alkanes with a chain length of C_{15} - C_{36} [57].

Anaerobe alkane degradation

Contrary to environments with sufficient exchange of the gaseous phase, anoxic conditions might be reached as a result of different factors. For example, high microbial activity with increased oxygen consumption or the depletion of dioxygen during the turnover of substrates might lead to environments with low oxygen. In addition, the saturation of soils with water can also interfere with gas exchange. In such environments only a few specialized alkane degrading microorganisms have been found so far, which are summarized in Table 2.

Bacteria	**Archaea**
Desulfoglaeba	*Methanobacterium*
Desulfosarcina/	
Desulfococcus Cluster	*Methanococcus*
Desulfovibrio	*Methanomicrobiales*
Desulfothermus	*Methanosaeta*
strain AK-01	*Methanosarcinales*
strain Hxd3	*Methanosphaera*
strain HxN1	
strain OcN1	
strain Pnd3	
strain TD3	
...	...

Tab. 2: Anaerobe alkane degraders
Microorganisms which are able to degrade aliphatic hydrocarbons like *n*-alkanes under anaerobe conditions [4; 5; 42; 43; 50; 51; 83; 108; 185; 201; 211; 254]

Interestingly, little is known about the mechanistic pathways of anoxic alkane degradation. However, several studies in the last decades, focusing on bacterial alkane degraders, revealed two mechanistic pathways for alkane degradation without oxygen as demonstrated in Figure 8. On the one hand, activation of inert hydrocarbons is done by the terminal or subterminal addition of carbon dioxide [210]. On the other hand, the attachment of fumarate to the same positions, was also shown to be an approach for activation [181]. In both pathways, sulfate and nitrate were found to be simultaneously used as electron acceptors [26; 42; 108; 113; 254]. Despite these pathways might represent the predominant alkane turnover processes in marine sediments, degradation occurs at negligible rates only and is therefore widely regarded as being of minor ecological relevance [121].

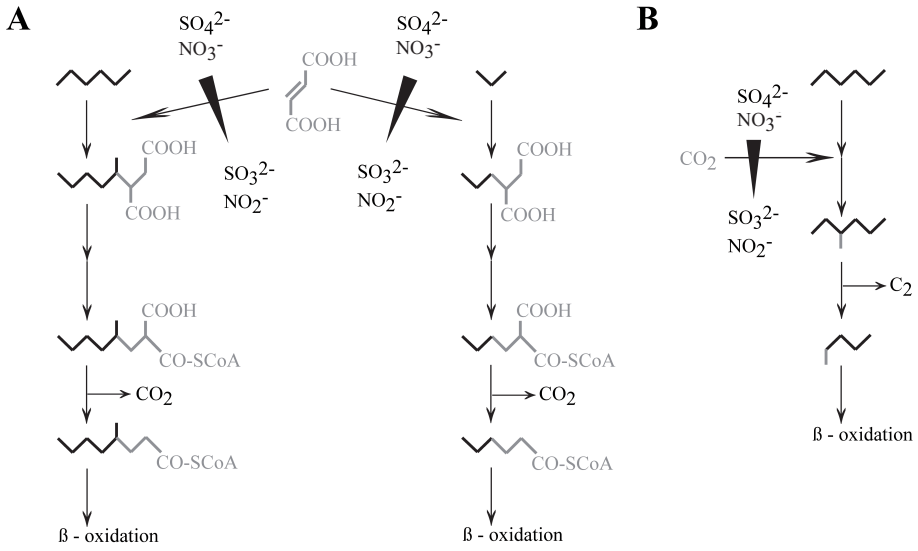

Fig. 8: Bacterial anaerobe degradation of alkanes
Modified mechanistic pathway for the anaerobe alkane degradation [181; 210]. Activation of the inert *n*-alkanes is accomplished by the addition of fumarate (A) as well as carboxylation (B) with concurrent reduction of sulfate and nitrate.

However, Mehboob and colleagues [145] presented data which possibly point to an extraordinary degradation pathway which might link the aerobe and anaerobe alkane metabolization. They could demonstrate that *Pseudomonas chloritidismutans* AW-1T was able to use oxygen or chlorate as electron acceptors during growth on middle-chained *n*-alkanes, but unable to reduce nitrate or sulphate, which is reflected in Figure 9. Under partially anaerobe conditions chlorate reduction renders chlorite which is further processed to Cl^- and O_2 by chlorite dismutase [178; 257]. The released oxygen might be subsequently used for the hydroxylation of alkanes by oxygenases.

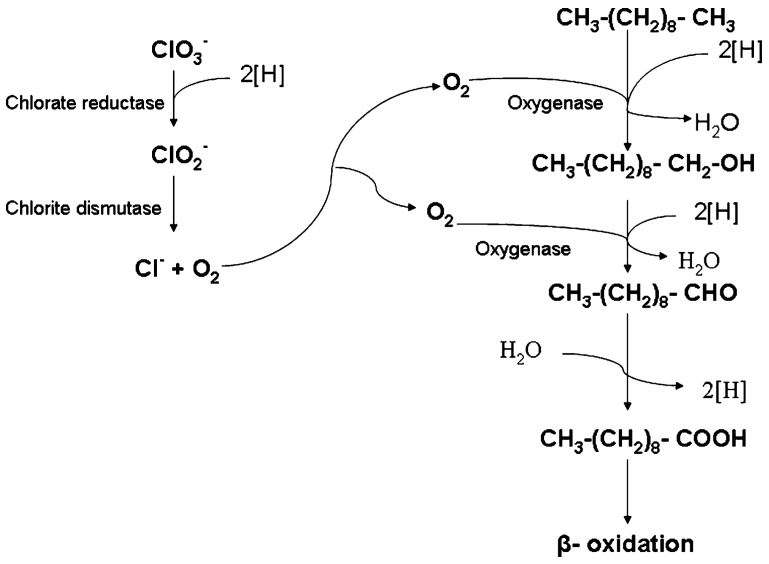

Fig. 9: Hypothetical pathway of alkane degradation under semi-anaerobe conditions
During the reduction of chlorate, molecular oxygen becomes released which can be used in turn for the activation of alkanes and their subsequent degradation via the aerobe degradation pathway [145]

3.6 Detection of functional diversity in soils

Knowledge about the functional diversity is substantial, when targeting the microbial degradative potential in soils. Since only a marginal fraction of soil bacteria can be cultivated [94; 228], phylogentic analyses need to be done with cultivation independent approaches. As demonstrated in Figure 10, functional diversity can be determined on different scales. For instance, detection of functional genes indicate the genetic potential of a microbial community, whereas analyses of the corresponding messenger RNA (mRNA) supplies reliable data about the activity status. However, since the transcription of genes is strongly impacted by post-transcriptional modification and other spatial-temporal factors (e.g. availability of nutrients, position of competitors), life time of mRNA is limited and consequently reflects only a snapshot of activity.

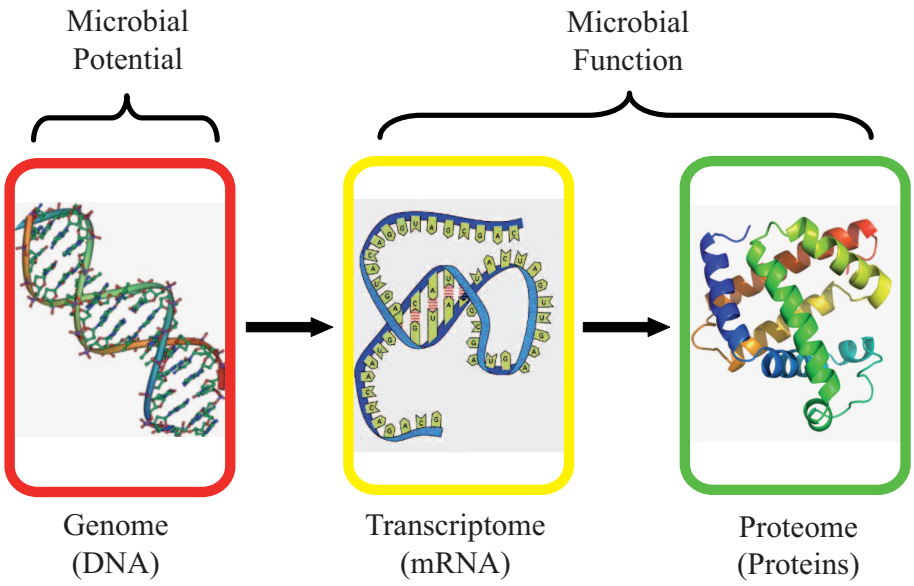

Fig. 10: Different scales for assessing functional diversity
The detection of functional diversity can be accomplished on different scales including the genome, transcriptome and proteome of a microbial community. Modified after Schloter *et al.* [196].

Therefore, analyses on protein level give more insights about the potential activities. For the analysis on nucleic acid level, two fundamental strategies for the isolation of DNA and RNA exist [81]. Extraction of nucleic acids is either done after the cell separation from the soil matrix [84] or directly within the soil samples [182]. The first would minimize contaminations by humic substances, which could hamper downstream applications like PCR [230] or enzymatic digestion [84; 91; 231]. Since cell separation could be ineffective due to microbes trapped in soil microaggregates, the procedure could result in a loss of information. The latter is more feasible and extraction of DNA and RNA is subsequently done by using phenol-chloroform extraction methods or by commercial

kits. In addition, after the isolation and appropriate purification, mRNA is frequently reverse transcripted, to gain stable cDNA.

Knowledge about the dynamic of functional genes and respective transcripts contributes to the mechanistic understanding of processes in soils on the microscale. Quantification is thereby done using two basic techniques, differing significantly in their detection method and accuracy. On the one hand, copy numbers can be determined by using statistic-based most probable number polymerase chain reaction (MPN-PCR), where signal aquisation is done after the reaction was completed. By using sequential dilutions of PCR reaction mixtures, which are done in three or five replicates, the number of mixtures yielding a signal after PCR are monitored. Gene abundances are subsequently calculated with tables, which were firstly described by Cochran [34] for the estimation of bacterial densities in liquid cultures. Despite this method being successfully used for the quantification of different genes (exemplarely [159]), definition of signals is strongly influenced by the subjective setting of the signal threshold. As a result data can be biased, as abundances might be under- or overestimated.

On the other hand, fluorescence dye- or fluorophore-based real-time PCR allows an online signal acquisition directly during the PCR run. For this, signals are detected at the end of each cycle. In general, three different chemistries can be used for quantification: i) fluorescence dyes (e.g. Sybr®Green) which bind double strand DNA or cDNA, ii) fluorochromes bound to sequence-specific probes (e.g. TaqMan®-PCR [85]) and iii) fluorochromes bound to primers [267]. Quantification can either be relative in comparison with other samples or absolute by using serial dilutions of plasmids containing the template. As signal strength is positively correlated with template amounts, gene copy numbers can be calculated by signals exceeding a certain threshold. Although this technique is frequently used in microbial ecology, sufficient quantification is influenced by various factors. For instance, amplification efficiencies might be reduced in case of amplicons significantly exceeding 500 bp [158] or by the presence of inhibitors (e.g. humic acids, pesticides). Furthermore, measurements of gene copies using Sybr® Green can be biased, because it intercalates double stranded DNA, which results in the detection of primer dimers. Anyhow, with the quantification of genes and transcripts only the genetic potential and the transcriptional status of a microbial community can be assessed.

To answer the question, if mRNA is translated to proteins, the respective catalytic enzymes have to be analysed. Since protein detection in soils is still challenging, functional diversity on the proteomic scale was indirectly determined in most studies done so

far. For instance, by measuring respiration rates and the activity of dehydrogenases or lipases [61; 139], conclusions can be made concerning the microbial community structure of hydrocarbon contaminated soils. However, reports on the *in situ* detection of specific enzymes by using antibodies labeled with i) fluorescence dyes, ii) gold particles or iii) alkaline phosphatases are still rare. It was therefore one aim of the present thesis, to produce antibodies against AlkB in order to monitor the spatial distribution of this protein in the soil matrix.

3.7 Aims and hypotheses

In soils, organic and anorganic particles with different sizes and shapes interact with each other and form highly structured matrices. In such matrices the distribution of substrates, water and electron donors is strongly influenced by different physicochemical interactions with minerals resulting in patchy arrangements. Consequently, dispersal and activity of microbes is also extremely heterogeneous and can change within a range of several µm only. Despite many studies examining the spatial distribution of microbial consortia in the detritusphere, knowledge about the distribution patterns of alkane degraders within the bulk soil matrix is still rudimental. Due to the reduced mobility of *n*-alkanes, distribution of these microbes might be different in 1 and 10 mm soil depth. It was therefore the aim of the present study, to analyse the abundance and activity of alkane degraders in a spatial-temporal manner. On this basis, *alkB*-harbouring bacteria, which are representatives of alkane degrading microbes, were detected on the mm-scale in the detritusphere of different soils during the decomposition of litter material. Furthermore, it was tested if divers soil, litter and compartment types have an impact on these bacteria. In addition, the use of herbicides for weed control might also impact the dynamic and activity of alkane degrading microbes. In this context, the following hypotheses have been proposed and tested.

I. During the decay of plant litter material, a gradient of *alkB*-harbouring bacteria is formed in the detritusphere, which is dependent on the bioavailability of litter derived alkanes.

II. The abundance of *alkB* genes and corresponding transcripts is thereby not only influenced by the soil and compartment type, but also impacted by the litter type in relation to varying alkane quantities and qualities, as well as changing C:N ratios.

III. Presence and activity of alkane degraders harbouring *alkB* is differentially influenced by various soil minerals constituting distinct physico-chemical properties.

IV. During the evolution of soils bacterial consortia are formed, resulting in increased response to the supply of litter derived alkanes.

V. The application of 2-methyl-4-chlorophenoxyacetic acid (MCPA), which is a potential inhibitor for enzymatic activities in soils, has a derogatory effect on *alkB*-harbouring bacteria. This effect is consequently reflected by a feedback reduction of *alkB* genes and transcripts.

In order to verify these hypotheses, three different soil microcosm experiments have been conducted, where litter of maize, pea and wheat was used as natural alkane source. Thereby, microcosms with sandy-loamy and silty-loamy soils as well as mixtures of different soil minerals, reflecting natural soil compositions, were used. Three different micro-habitats (litter, litter-soil-interface and bulk soil) were sampled to analyse the amount of *alkB* DNA and mRNA at different soil compartments. The obtained data were related to the total bacteria by additional quantification of *rpoB* and 16S rRNA genes. To analyse the effect of herbicide application, the model compound MPCA was applied to some microcosms. The amplification efficiency, which is directly linked to a sufficient quantification of the *alkB* genes from different strains was improved by modifying the respective primers and PCR protocols (**Publications I and II**). For the purpose of analysing the spatial distribution of the alkane monooxygenase in the soil matrix, antibodies against AlkB should be prepared.

4 Materials and Methods

4.1 Materials

4.1.1 Chemicals and proteins

Compound	Company
AHT (anhydrotetracycline)	IBA GmbH, Germany
BCIP (5-bromo-4-chloro-3-indolylphosphate *p*-toluidine salt)	AppliChem, Germany
BSA (bovine serum albumin)	Sigma-Aldrich, Germany
BsaI	New England Biolabs, Germany
$CaCl_2$	Sigma-Aldrich, Germany
Chloramphenicol	Sigma-Aldrich, Germany
n-DDM (*n*-dodecyl-β-D-maltoside)	Sigma-Aldrich, Germany
DEPC (diethylpyrocarbonate)	Sigma-Aldrich, Germany
DMF (dimethylformamid)	AppliChem, Germany
EDTA (ethylenediaminetetraacetic acid)	Sigma-Aldrich, Germany
Ethanol	Merck, Germany
GeneScan™500 ROX™	Applied Biosystems, USA
Glycine	Sigma-Aldrich, Germany
Goat-anti-Rabbit-IgG	Sigma-Aldrich, Germany
n-hexane	Merck, Germany
HpyCH4V	New England Biolabs, Germany
MCPA (4-chloro-2-methylphenoxyacetic acid)	Sigma-Aldrich, Germany
β-Mercaptoethanol	Sigma-Aldrich, Germany
NaCl	Sigma-Aldrich, Germany
NaN_3	AppliChem, Germany
Na_2SO_4	Sigma-Aldrich, Germany
NBT(nitro-blue tetrazolium chloride)	AppliChem, Germany
PEG-6000 (polyethylene glycol-6000)	Fluka, Germany
Pfu-Polymerase	Invitrogen, Germany
Ponceau-S	Sigma-Aldrich, Germany
Power Sybr®Green Master Mix	Applied Biosystems, USA

SDS (sodiumdodecylsulfate)	Fluka, Germany
SuperScript® II Reverse Transcriptase	Invitrogen, Germany
T4 DNA-Ligase	Fermentas, Germany
Taq-Polymerase	Fermentas, Germany
Taq-PCR Master Mix	Qiagen, Germany
Tris (2-amino-2-hydroxymethyl-propane-1,3-diol)	Merck, Germany
Triton®X-100	AppliChem, Germany
Tween® 20	Sigma-Aldrich, Germany

4.1.2 Kits for nucleic acid extraction and purification

Kit	**Company**
AllPrep DNA/RNA Mini Kit	Qiagen, Germany
NucleoSpin®Plasmid Kit	Macherey-Nagel GmbH, Germany
Wizard® SV Gel & PCR Clean-Up System	Promega, Germany
QIAquick PCR Purification Kit	Qiagen, Germany

4.1.3 Oligonucleotides

		Primer	**5' → 3' sequence**[1,2,3]	**Reference**
real-time	**PCR**	alkB1f	AAYAC*N*GC*N*CAYGARCT*N*GG*N*CAYAA	[107]
		alkB1r	GCRTGRTGRTC*N*GARTG*N*CGYTG	[107]
		16Sf	GGTAGTCYAYGCMSTAAACG	[15]
		16Sr	GACARCCATGCASCACCTG	[15]
		rpoBf	AACATCGGTTTGATCAAC	[41]
		rpoBr	CGTTGCATGTTGGTACCCAT	[41]
antibody	**production**	anti-for1	AGATCGGGTCTCAGCGCATGTTTGCCTCGCTTTCCT	(this study)
		anti-for2	GCCCACAAGACCCGCTGG	(this study)
		anti-rev1	CGTCGTGGTCTCATATCAGATGCGCTGGGTGTCGG	(this study)
		anti-rev2	CCAGCGGGTCTTGTGGGC	(this study)

1) italic bases have been substituted with an inosine
2) underlined bases represent BsaI restriction site
3) bold bases represent point mutation to mask BsaI restriction site

4.2 Methods

4.2.1 Soil microcosm experiments

In the three different incubation experiments, which are displayed in detail in the following sections, microcosms have been designed and prepared as shown in Figure 11. All prepared soil columns were pre-incubated in the dark for two weeks at a temperature of 14 °C in order to equilibrate the soils and restore microbial activity. After pre-incubation, the microcosms were covered with small pieces (25 mm^2) of fresh litter material from various sources (Fig. 11) and incubated under specific conditions. The litter was sampled at the same research site described in experiment 1 (see section 4.2.1.1). To eliminate the potential photodegradation of litter materials [13; 25], the incubation experiments were done under exclusion of light.

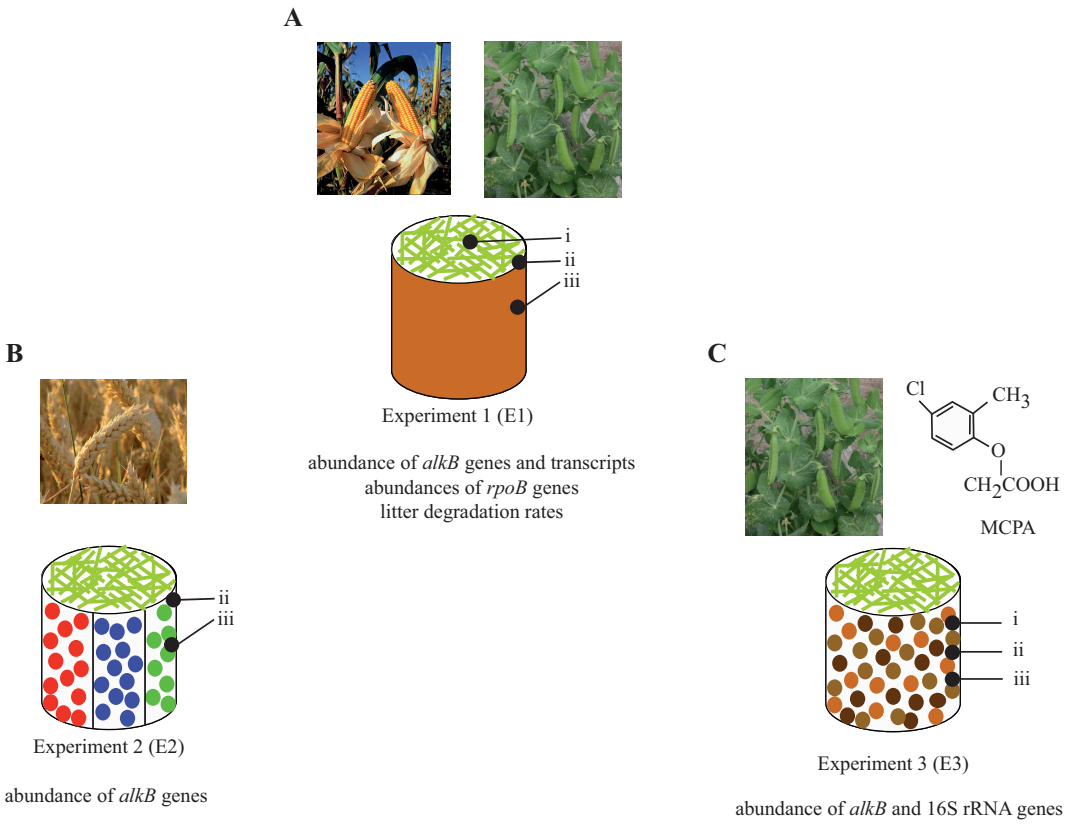

Fig. 11: Schematic overview of the soil microcosm experiments
A) Undisturbed soils (Euric Cambisol, Luvisol) were covered with litter of maize or pea plants, B) Soil columns with different artificial soil mixtures (in each case one) were covered with litter of wheat, C) Destructively sampled Luvisol soil was mixed with MCPA and covered with pea litter. The sampled compartments and the particulate analyses done in each experiment are indicated. i = litter compartment, ii = litter-soil interface compartment (0-3 mm), iii = bulk soil compartment (10-13 mm). Note that in experiment 3 (C) indications represent 0-3, 3-6 and 6-9 mm soil depth respectively

4.2.1.1 Dynamic of *alkB* genes in different soil compartments (E1) of two arable soils

In this experiment the dynamics of *alkB* genes and transcripts in relation to the total bacteria (*rpoB* genes) were analysed in two arable soils with undisturbed structure. For this, 96 soil cores (48 cores each soil type) were taken from the top 5 cm of a sandy-loamy and a silty-loamy soil at the agricultural research farm "Klostergut Scheyern" (www.helmholtz-muenchen.de/scheyern), located 45 km north of Munich. The sampling was done in autumn 2008 after the harvest of maize (*Zea mays* L.) and alfalfa (*Medicago sativa* L.), respectively, by using soil augers made of stainless steel (diameter 5 cm, height 5 cm). After sampling, the current soil moisture as well as the soil pH (using 0.01 M $CaCl_2$) were determined. Beside these parameters, Table 3 summarizes the texture of the two soils, which was previously determined in 2003 by using a protocol of Sinowski & Auerswald [204]. Soil classification was done after a guideline of the World Reference Base for Land Resources [259].

Soil type	**Sand** (%)	**Silt** (%)	**Clay** (%)	**pH** ($CaCl_2$)	**mWHC** (%)
Euric Cambisol (sandy-loamy)	55.2	31.4	13.4	5.9	29.9
Luvisol (silty-loamy)	18.0	60.0	21.4	6.1	34.4

Tab. 3: Parameters of the soils used in experiment 1
Top soil samples were taken from two arable soils and used for microcosm experiments. Soil texture was determined in 2003 after a protocol of Sinowski & Auerswald [204]. Soil classification was subsequently done after the World Reference Base for Land Resources [259]. The measurement of soil pH and moisture was done directly after the top soil samples have been taken.

Before the microcosm experiment started, soil cores were equilibrated for two weeks at 14 °C and 55% of the maximum water holding capacity (mWHC) to reset microbial activity. Three cores of each soil type were sampled after equilibration and served as time point zero treatments (T0). Nine soil cores of each soil type were incubated with 1 g dry weight (dw) of fresh litter material from maize (*Zea mays* L., EC60), respectively pea (*Pisum sativum* L., EC60) which was applied carefully on the top of the soil cores. Additionally, for each litter and soil type nine cores were incubated using litter material in nylon litterbags (1 g litter material per bag; 50 µm mesh size of the bags), which were carefully covered by soil to determine litter degradation rates. Nine cores of each soil type without litter addition served as non-litter controls (NLC). All cores were incubated in the dark up to 30 weeks at a constant temperature of 14 °C and a soil moisture of 55% of mWHC. Sampling of three soil cores per treatment (sand-pea; sand-

maize; sand-control; silt-pea; silt-maize; silt-control) was performed two (T1), eight (T2) and 30 (T3) weeks after litter addition. For each sampling three compartments (litter layer, litter-soil interface and bulk soil 1-1.5 cm below the interface) were sampled from each core and treated as true replicates from the treatments. To obtain the litter-soil interface, the remaining litter material was carefully removed with a pair of forceps and then carefully sampled using a clean spatula up to a depth of 2-3 mm below the litter layer. All taken samples were immediately shock frozen in liquid nitrogen and stored at -80 °C for molecular analysis. For the determination of litter degradation rates, litter bags were removed from the soils of the corresponding treatments at T1, T2 and T3. After air drying the litter material mass losses were determined gravimetrically.

4.2.1.2 Dynamic of *alkB* genes in artificial soils (E2)*,†

To gain more insights into the mechanisms of BGI formation in dependency of single compounds of the fine fraction (< 6.3 µm particle size), microcosm experiments with artificial soils were conducted (Fig. 11B). Eight various soil compositions (Tab. 3) differing in their fine fraction and subsequently in the size of pores were prepared in order to simulate various chemico-physical conditions of natural soils. The soils were subsequently supplied ones with sterilized manure as sole carbon source (15 mg C g^{-1} soil) and inoculated with a water extraction of an Eutric Cambisol soil (Ultuna, Sweden) for three and twelve months (pre-aging) as recently described [79]. During the incubation, the soils were supposed to form organic-mineral complexes with evolution of specific bacterial consortia. Nevertheless, due to the frequent mixing of the soils in order to gain homogeneous distributed soil moisture, no formation of soil layers was expected. However, after the pre-aging of the mixtures, 24 microcosms (three for each soil mixture and pre-aging time respectively) were prepared by stratifying the pre-aged soils (1 cm layer thickness) on a sandy drainage layer using truncated 50 mL falcon tubes (3 cm diameter) as shown in Figure 12.

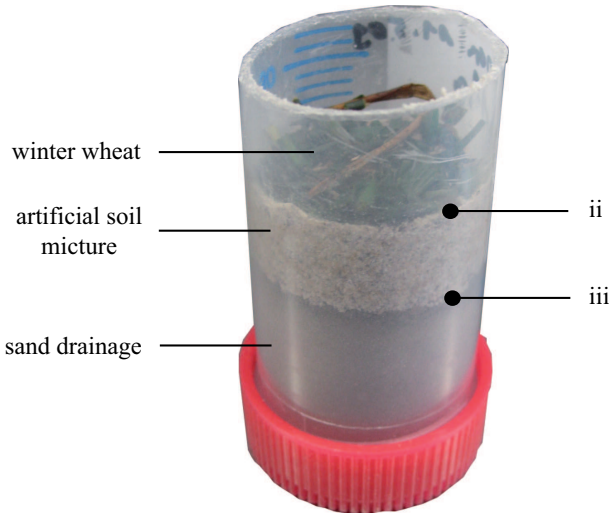

Fig. 12: Design of soil microcosms in experiment E2
After the addition of wheat (*Triticum aestivum* L.) litter, samples were taken from the litter-soil-interface (ii) and the bulk soil compartment (iii) at the beginning and after two weeks of incubation (T1).

*The experiment was part of two bachelor theses (S. Ammermüller, K. Linnemann) under my supervision
†Preparation of artificial soils and subsequent pre-aging were done by G. Pronk and K. Heister (Chair of Soil Science, TU München)

The prepared soil columns were subsequently covered with litter of wheat (*Triticum aestivum* L., EC25) and incubated for two weeks at a temperature of 14 °C. During the whole incubation the soil moisture was determined gravimetrically and kept at 55% of mWHC. At the beginning (T0) of the experiment bulk soil samples from the pre-aged soils were taken as T0, whereas the litter-soil-interface (0-1 mm) and the bulk soil compartment (10-11 mm) were sampled after two weeks of incubation (T1) as indicated in Figure 12. In this experiment only the abundance of *alkB* genes at the different compartments was analysed.

	soil composition (% mass contribution)							
model compound	**I**	**II**	**III**	**IV**	**V**	**VI**	**VII**	**VIII**
quartz (sand)	41.7	40.0	41.4	40.8	41.7	40.0	40.0	40.0
quartz (silt)	52.0	52.0	52.0	52.0	52.0	52.0	52.0	52.0
montmorillonite	6.3	-	-	3.2	4.3	-	-	-
illite	-	8.0	-	4.0	-	7.0	7.0	5.0
quartz	-	-	5.6	-	-	-	-	-
ferrihydrite	-	-	1.0	-	-	1.0	-	1.0
boehmite	-	-	-	-	-	-	1.0	-
charcoal	-	-	-	-	2.0	-	-	2.0
soil pH ($CaCl_2$)	7.7	7.5	7.6	7.6	7.6	7.6	7.6	7.6
mWHC (%)	33.0	31.0	28.0	32.0	33.0	31.0	31.0	31.0

Tab. 4: Composition of artificial soils
Artificial soils with components of different particle sizes were prepared in order to simulate various physico-chemical properties of natural soils. Preparation of mixtures and determination of pH and moisture were done by G. Pronk and K. Heister (Chair of Soil Science, TU München)

4.2.1.3 Dynamic of *alkB* genes in a MCPA contaminated soil (E3)*

During the agricultural use of 4-chloro-2-methylphenoxyacetic acid (MCPA) for weed control, only minor fractions directly reach the plants. The majority is rinsed from the leaves during rain fall or irrigation or directly enters the soil during its dispersion. In this experiment, a possible influence of MCPA on the abundance of *alkB*-harbouring bacteria, which would benefit from the elevated litter derived alkane amounts as a consequence of MCPA induced plant death, was analysed (Fig. 11C) in relation to the total bacterial community (16S rRNA genes). Therefore, sieved (< 2 mm) top soil samples (0-5 cm) which have been compacted to a density of 1.2 g cm^{-3} were used to prepare 32 microcosms in total as demonstrated in an earlier experiment from Poll *et al.* [164] and schematically shown in Figure 13.

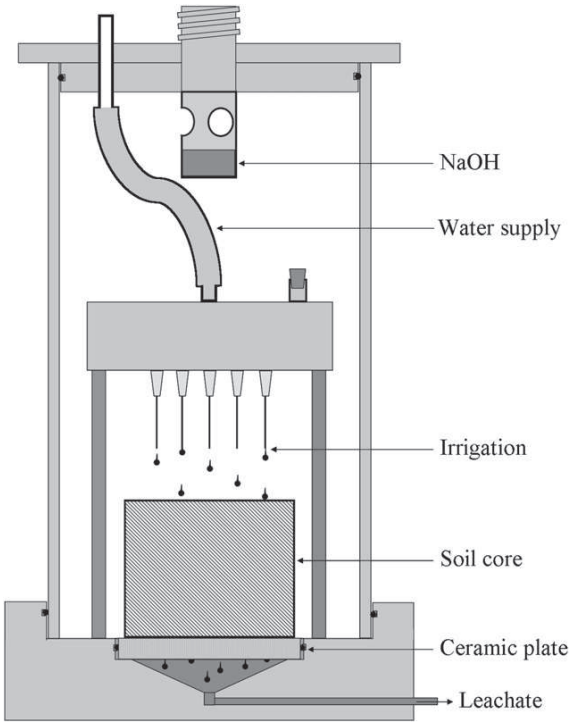

Fig. 13: Design of soil microcosms after Poll *et. al* [164].
During incubation, prepared soil microcosms were weekly irrigated with 0.01 M $CaCl_2$ solution. The NaOH reservoir could be potentially used for measurement of microbial CO_2 production, which was not accomplished during this experiment.

In experiment E3 the same silty soil was used as in E1 (Tab. 3), which was taken in December 2009 after the harvest of wheat (*Triticum aestivum* L.). However, after the pre-incubation 16 soil microcosms were spiked with 50 mg g^{-1} soil (dw) MCPA, whereas the remnants received only water and served as non-contaminated controls. All cores were incubated at 14 °C for up to six weeks with pea litter (*Pisum sativum* L.,

*This experiment was done by a Master student (T. Yuyukina) who was equally supervised by me and colleagues from the Institute of Soil Science and Land Evaluation (University of Hohenheim)

EC63), which was acting as natural alkanes source. A soil moisture corresponding to a water suction of -63 hPa was maintained by weekly irrigation with a solution of 0.01 M $CaCl_2$. Prior the different soil compartments were sampled at the beginning (T0) and after one (T1), three (T2) and six (T3) weeks of incubation, soil columns were frozen to facilitate exact sampling by using a cryostat microtome (HM 500M, MICROM International GmbH, Germany). The different soil compartments were sampled in the following distances to the litter: 0-3 mm, 3-6 mm, 6-9 mm.

4.2.2 Nucleic acid extraction

DNA and RNA have been co-extracted by using a protocol after Griffiths et al. [69]. This protocol was found to be suitable for the extraction of soil and plant litter related nucleic acids. In order to optimize the yield of DNA and RNA, the protocol was modified by Töwe *et al.* [232]. In detail, 0.5 g of fresh litter material were extracted in lysis tubes (PreCellys Ceramic Kit, Peqlab, Germany) with 0.5 mL extraction buffer containing cetyl trimethylammonium bromide and the same volume of a mixture of phenol, chloroform and isoamyl alcohol (25: 24: 1) (pH 8.0). In contrast to Töwe *et al.* no β-mercaptoethanol was added to the extraction buffer. The samples were subsequently lysed by using the Precellys®24 Homogenizer (Peqlab, Germany) for 2 x 30 sec., resulting debris were pelleted during centrifugation at 4 °C and 16,100 x g for 5 min. The resulting aqueous phase was recovered and mixed with an equal volume of a mixture of chloroform and isoamyl alcohol (24: 1) by vigorous shaking to remove phenol residues. After a second centrifugation this purification step was repeated. Afterwards nucleic acids were precipitated by adding one volume of a precipitation solution (10% PEG 8000, 1.2 M NaCl), incubation on ice for 2 h and centrifugation for 10 min. at 4 °C. To remove the polyethylenglycol and the sodium chloride which would interfere with downstream applications, the resulting nucleic acids were washed in ice-cold 70% ethanol and precipitated again by centrifugation (10 min., 4 °C). After air drying, the pellet was resuspended in 50-100 µL nuclease-free water. DNA and RNA were separated by spin columns using the AllPrep DNA/RNA Mini Kit (Qiagen, Germany) following the manufacturer's instructions.

Quality and quantity of the seperated nucleic acids were subsequently determined spectrophotometrically at 230, 260 and 280 nm (Nanodrop® ND-1000, Peqlab, Germany). In addition, the quality of the RNA was tested by screening for DNA residues. For this purpose RNA extracts were used as template for PCR with 16S rRNA specific primers (see 4.1.3). To overcome the false-positive signals for 16S rRNA genes which can occur in PCRs performed with *Taq*-polymerase [172], a more specific *Pfu*-polymerase was used. Since no signals could be detected after gel electrophoresis, the used nucleic acid separation method was found to be sufficient. First strand cDNA was therefore synthesized with SuperScript® II Reverse Transcriptase using 1 pmol of random hexamer primer.

4.2.3 Optimization of *alkB*-specific primers and PCR reaction mixtures

In 2006, Kloos and colleagues [107] proposed a set of primers which covered a broad range of different *alkB*-harbouring bacteria (refer to section 4.1.3). These primers were highly degenerated and therefore enabled phylogenetic analyses in environmental samples. As illustrated in Figure 14, the binding sites of the proposed primers were located in the coding regions of the histidine motifs one and four. Subsequently the amplicon covers the whole catalytic center of the alkane monooxygenase, which is highly conserved among the different species.

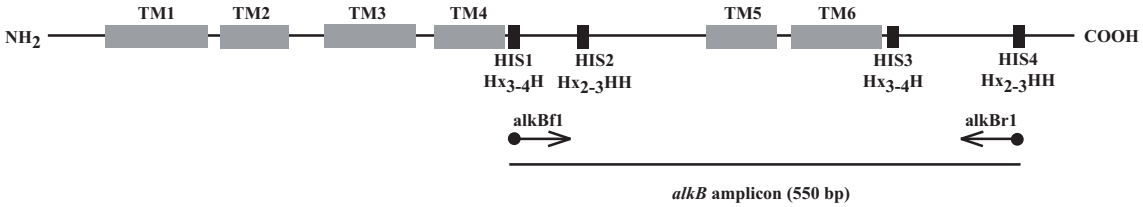

Fig. 14: Binding sites of degenerated *alkB* primers
Degenerated primers (alkBf1, alkBr1) published by Kloos *et al.* [107] for the amplification of *alkB* gene fragments bind in the coding regions of histidine motifs 1 and 4. The amplicon, which is shown in relation to the AlkB protein, covers all four histidine motifs (HIS1 - 4), representing the catalytic center of the hydroxylase. Transmembrane domains are indicated by light-gray boxes (TM1 - 6).

However, due to their high degeneracy, 4096 fold and 512 fold for alkBf1 and alkBr1 respectively, the effective concentrations of the individual primer sequences is very low (1/4096 alkBf1, 1/512 alkBr1). In consequence, the amplification of the individual *alkB* sequences is stoichiometrically limited. This might result in an underestimation of the gene copy numbers. Additionally, a biased quantification is also strongly impacted by the amplification efficiency during a PCR. For example, after 30 cycles of a PCR with only 90% efficiency, detected gene copy numbers are one order of magnitude lower, compared to reactions with 100% efficiency. As demonstrated in Table 5, these enormous differences are further enhanced in reactions with 80% efficiency or below.

As known from literature, effectivity of polymerase chain reactions can be enhanced by the addition of different compounds. For example, bovine serum albumin (BSA) can interact with potential inhibitors, which would hamper the activity of the DNA-polymerase. Tsai *et al.* [231; 230] postulated that humic substances, which might contaminate nucleic acid extracts from soil samples, have inhibitory effects on downstream enzymatic applications like PCR. Furthermore, the addition of dimethylsulfoxide (DMSO) might increase the amplification of GC-rich templates, resulting in elevated efficiencies also. Besides, $MgCl_2$ can improve the binding of the primers to their target and form complexes with dNTPs, which can be used as substrates for the polymerase.

	Gene copy numbers			
Cycle	100% Effeciency	90% Effeciency	80% Effeciency	70% Effeciency
0	1	1	1	1
5	32	25	19	14
10	1,024	613	357	202
15	$3.2 * 10^4$	$1.5 * 10^4$	$6.0 * 10^3$	$2.0 * 10^3$
20	$1.0 * 10^6$	$3.8 * 10^5$	$1.3 * 10^5$	$4.0 * 10^4$
25	$3.3 * 10^7$	$9.3 * 10^6$	$2.4 * 10^6$	$5.8 * 10^5$
30	$1.0 * 10^9$	$2.3 * 10^8$	$4.5 * 10^7$	$8.2 * 10^6$

Tab. 5: Effect of different amplification efficiencies
Assuming a doubling of the copy numbers of a target gene in a PCR with 100% effeciency, immense underestimations would be the result in lower effective amplifications.

Anyhow, as frequently reported in the manuals of commercial real-time PCR kits, high amounts of DNA and cDNA could also diminish the amplification efficiencies. In order to improve the amplification of *alkB* gene fragments from soil samples, the respective primers were modified. For this, every four folded base was substituted by an inosine nucleotide. As inosine indiscriminately pairs with adenine, thymine or cytosine; degeneracy would be reduced drastically. In contrast, the individual concentrations of the single primer sequences would be increased (e.g. 1/256 alkBf1, 1/128 alkBr1). In addition, various tests including the application of BSA, DMSO and extra $MgCl_2$ were done, to check for their impact on the efficiency. Due to their high degeneracy, the used primers have a broad spectrum of optimal annealing temperatures and tend to form dimer complexes also. Consequently, the effects of an initial touchdown step with two different temperature ranges as well as the signal detection at 78 °C was tested.

4.2.4 Quantitative real-time PCR

In order to analyse the abundance of *alkB* genes and transcripts as well as 16S rRNA and *rpoB* genes at the different soil compartments, Sybr®Green-based real-time PCR's were accomplished. Based on the results of the preliminary tests, which will be presented in subsection 5.1, adapted PCR reaction mixtures and protocols have been used for the amplification of *alkB*. As mentioned earlier, high amounts of nucleic acids can impact the amplification efficiency. Therefore, samples of soils and litter material were diluted 16 fold and 32 fold respectively. As a result, amounts of DNA and cDNA used in the reaction mixtures are fluctuating. Reaction mixtures have been prepared as summarized in Table 6.

	E1		**E2**	**E3**	
	alkB	***rpoB***		***alkB***	**16S rRNA**
template (DNA)	5.0-15.0 ng	5.0-15.0 ng	4.0-30.0 ng	2.0-25.0 ng	2.0-25.0 ng
template (cDNA)	10.0-40.0 ng	-	-	-	-
alkB1f	0.1 µM	-	0.1 µM	0.1 µM	-
alkB1r	0.1 µM	-	0.1 µM	0.1 µM	-
rpoBf	-	0.1 µM	-	-	-
rpoBr	-	0.1 µM	-	-	-
16Sf	-	-	-	-	0.01 µM
16Sr	-	-	-	-	0.01 µM
$MgCl_2$	2.0 mM	2.0 mM	2.0 mM	2.0 mM	2.0 mM
BSA	0.06 %	0.06 %	0.06 %	0.06 %	0.06 %
Sybr®Green Master Mix	1x	1x	1x	1x	1x
DEPC-water	add to 25 µL respectively				

Tab. 6: Real-time PCR reaction mixtures

In contrast to *alkB*, amplification efficiencies of 16S rRNA and *rpoB* genes were found to be at 92% and 87% respectively. Therefore respective primers and protocols were used without modification as previously described in each case by Bach *et al.* [15] and Powell *et al.* [166]. As an exception, the signal detection was done similar to *alkB* at 78 °C for 30 seconds. All modifications of the amplification protocols are summarized in Table 7.

	alkB	16S rRNA	*rpoB*
Stage 1 (1x)			
Hotstart	10 min., 95 °C	10 min., 95 °C	15 min., 95 °C
Stage 2 (5x)			
Denature	45 sec., 95 °C	-	-
Anneal	1 min., 62 °C (-1 °C/cycle)	-	-
Extend	45 sec., 72 °C	-	-
Stage 3 (40x)			
Denature	45 sec., 95 °C	20 sec., 95 °C	30 sec., 88 °C
Anneal	1 min., 57 °C	1 min., 62 °C	30 sec., 50 °C
Extend	45 sec., 72 °C	30 sec., 72 °C	30 sec., 72 °C
Data Collection	30 sec., 78 °C	30 sec., 78 °C	30 sec., 78 °C
Stage 4 (1x)			
Denature	15 sec., 95 °C	15 sec., 95 °C	15 sec., 95 °C
Anneal	30 sec., 60 °C	30 sec., 60 °C	30 sec., 60 °C
Extend	15 sec., 95 °C	15 sec., 95 °C	15 sec., 95 °C

Tab. 7: Modified real-time PCR protocols for the amplification of *alkB*, 16S rRNA and *rpoB*

Absolute quantification of the different genes was done by using fragments of *alkB* (550 bp) and *rpoB* (345 bp) from *P. putida* as well as 16S rRNA (260 bp) from *Clavibacter michiganensis michiganensis* respectively. These fragments were amplified and subsequently cloned into commercial pCR2.1 vectors (Invitrogen, Germany). With the assumption, that only single fragments were introduced into the vector, amounts of gene copy numbers were calculated by using Equation 1. Serial dilutions of the real-time PCR standards produced linear standard curves ($r^2 > 0.99$) over five orders of magnitude.

$$n \leq \left(\frac{c}{m * l}\right) * N_A \tag{1}$$

n = copy numbers μl^{-1}, c = concentration of recombinant vector ($\mu g\ \mu l^{-1}$), m = molecular weight of 1 bp (666 $\mu g\ \mu mol^{-1}$), l = length of recombinant vector (bp), N_A = Avogadro constant (μmol)

4.2.5 Statistical data analysis

One- or multifactorial ANOVA calculations were done by using log-transformed data, which fulfilled assumptions of normal data distribution and homogeneity of variances. Both have been checked by histograms and the Kolmogorov-Smirnov test at a level of significance of $P \leq 0.05$. Statistical analyses of the litter degradation and the abundances of *rpoB* (E1) and 16S rRNA (E3), as well as *alkB* genes (E1-E3) and transcripts (E1) were done by using the statistical software SPSS version 11.5 (IBM Deutschland GmbH, Ehningen, Germany).

4.2.6 Production of anti-AlkB antibodies

In order to localize the alkane monooxygenase AlkB directly in the soil matrix, anti-AlkB antibodies should be produced in the present thesis. Although, the AlkB protein was successfully overexpressed in earlier studies [152; 157; 214; 213], a sufficient purification for the effective production of anti-AlkB-antibodies was not accomplished. Consequently, the resulting immunoglobulins might recognize unspecific proteins, leading to a large number of false positive signals. Therefore an application for the *in situ* localization of AlkB might be not feasible.

In order to simplify the specific isolation of AlkB and consequently reduce the potential synthesis of antibodies binding unspecific epitopes, overexpression of the target protein and its direct isolation was in the focus of the present experiment.

Therefore, only the *alkB* gene itself was directly fused behind a promoter which was under the control of an extra inducer, facilitating the secretion into the periplasm. The produced AlkB protein was purified with strep-tag specific affinity columns and subsequently used for the production of polyclonal anti-AlkB antibodies. The single steps which have been accomplished to produce the antibodies are displayed in detail in the following subsections. In addition, a schematic overview is illustrated in Figure 15.

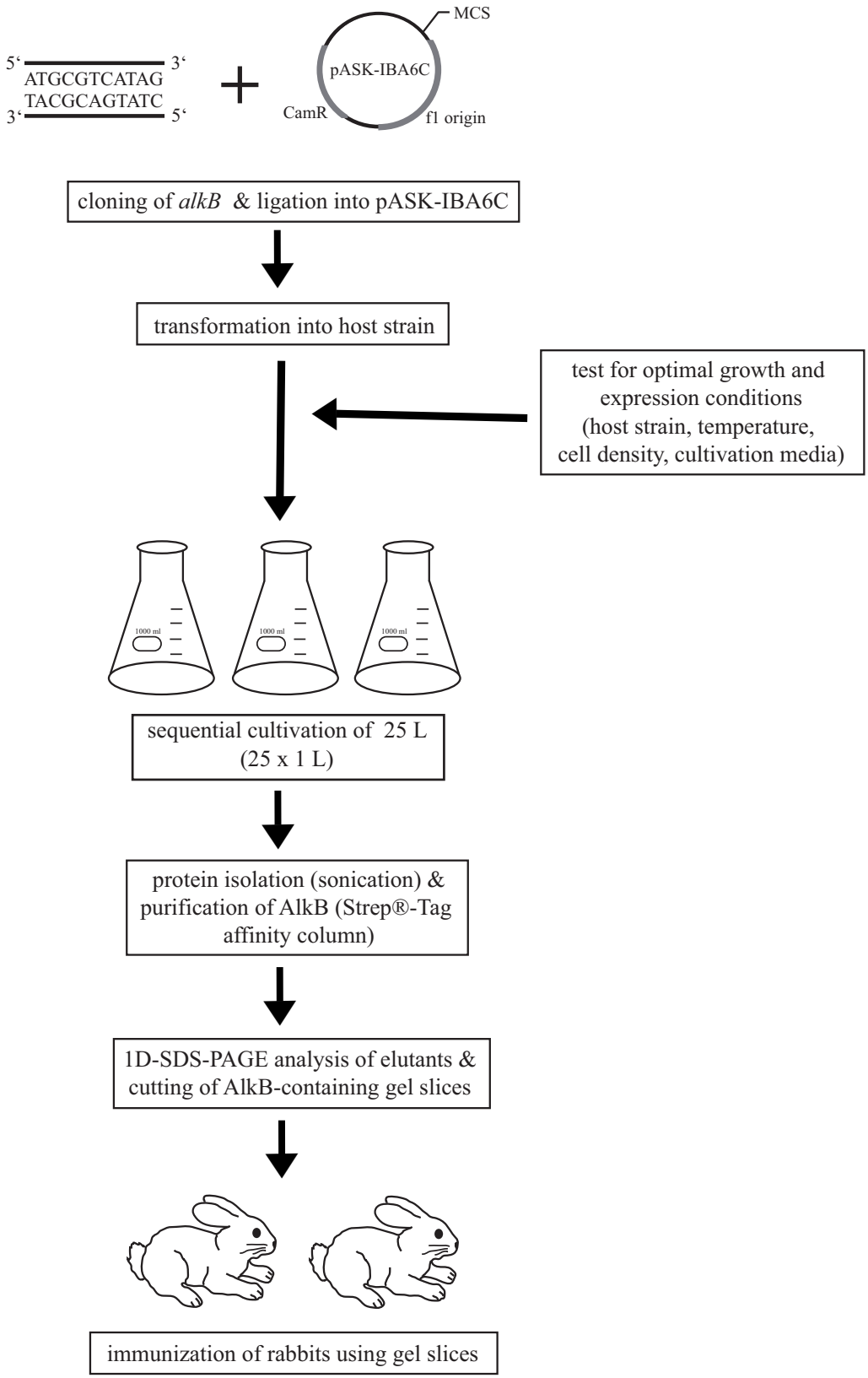

Fig. 15: Flowchart of the anti-AlkB production

Single steps from the cloning of *alkB* and the subsequent ligation into the commercial expression vector pASK-IBA6C. Transformation of recombinant vectors into different host strains were facilitated in order to overexpress and consequently purify AlkB. Afterwards gained proteins were used for the immunization of rabbits.

4.2.6.1 Synthesis and cloning of recombinant *alkB*

For the overexpression of AlkB recombinant expression vectors (pASK-IBA6C, IBA GmbH, Germany) were synthezised after manufacturer's instructions by using amplified copies of *alkB2* from *P. aeruginosa*. However, *in silico* restriction analyses of the PCR products revealed an intra-gene restriction site of BsaI which was used for preparing the ligation. Therefore, a single base substitution was introduced resulting in a replacement of cytosine with thymine and subsequent masking of the restriction site.

In detail, two gene fragments from *alkB* were amplified with proof-reading active *Pfu*-Polymerase by using the primer sets anti-for1/anti-rev2 and anti-rev1/anti-for2 (see 4.1.3). Prior combination via Fusion-PCR (using primers anti-for1 and anti-rev1), fragments were purified using MinElute PCR Purification Kit (Qiagen, Germany). Successful amplification and effective masking of the intra-gene BsaI restriction site was checked by digest of DNA aliquots with BsaI and subsequent agarose gel electrophoresis after Sambrook *et al.* [192]. After successful ligation, recombinant expression vectors were transferred into cells of *Escherichia coli* strain W3110 via electrotransformation (1.8 kV, 5.2 msec.) using a MicroPulser Electroporator 165-2100 (Bio-Rad Laboratories GmbH, Germany) according to manufacturer's recommendations. Selection of transformed cells was subsequently done in an overnight incubation at 37 °C using LB agar plates and chloramphenicol (30 µg ml^{-1}). Resulting colonies were used for the production of storage cultures using 20% (v/v) sterile glycerine, which were subsequently aliquoted and stored at -80 °C until further use. Accessorily, the recombinant vectors were isolated using the NucleoSpin®Plasmid Kit (Macherey-Nagel, Germany) and subsequently analysed to check for the correct *alkB* sequence.

4.2.6.2 Overexpression and isolation of strep-tagged AlkB

Prior to the large scale cultivation of recombinant *E. coli* cells for synthesis of AlkB, tests for optimal growth and protein expression conditions were done. These tests included i) different incubation temperatures, ii) different optical densities at which induction was initiated and iii) three cultivation media (LB, 1/5 LB, R2A after [173]) with different nutrition levels. During the temperature test, synthesis of AlkB was analysed on proteomic and transcriptomic scale, where isolated RNA was transcribed into cDNA and used as template for PCR using anti_for1/anti_rev1 primer set (see 4.1.3) and *Taq*-polymerase. PCR products were subsequently analysed by gel electrophoresis with 1% agarose gels. Beyond the results which are discussed in detail in section 5.5, incubation was done at 30 °C in LB medium (25 L in total), supplemented with chloramphenicol (30 µg ml^{-1}). At an optical density of 0.5 - 0.7 (measured at 550 nm), which was corrsponding to 1.25 - 1.75 x 10^8 cells ml^{-1} [147], the induction of the AlkB overexpression was induced by the addition of 0.1% (w/v) glucose and 250 ng ml^{-1} anhydrotetracycline (AHT). After 2h of induction, where no significant increase of the optical density was monitored, cells were harvested by centrifugation (9700 x g, 4 °C) and obtained pellets were resuspended in buffer W. All buffers, which have been used for the resuspension of the cell pellets and the purification of the protein extracts via Strep-Tactin affinity columns, are demonstrated in Table 8.

Unfortunately, a periplasmatic expression of the AlkB-Streptag-fusion protein was not successful. Therefore, the impact of the addition of Triton®X-100 and SDS on the protein isolation was analysed. Additionally, cell disruption by pressure (French Press, 2 x 1000 bar) or sonication (2 x 3 min, 30% Cycle, 60% Power) was tested (see section 5.5.4). Despite the results could not proof a hampered cell disruption effeciency for pressure, sonication was used for protein isolation, as handling of large volumina with FrenchPress was not feasible. After sonication on ice using a Sonoplus HD-2070 sonicator equipped with a standard horn SH70G and a microtip MS73 (all Carl Roth GmbH + Co. KG, Germany), proteins have been received by centrifugation (30 min., 22,200 x g, 6 °C). The supernatant which included cytoplasmatic as well as membrane related proteins (loosened membrane bound and freed transmembrane proteins) was diluted with buffer W to improve binding of the strep-tagged AlkB and prevent clogging of the affinity column by high protein concentration.

4.2.6.3 Protein purification and immunization of rabbits

To purify the strep-tagged Alkane monooxygenase from the cellular proteom the extracted proteins were passed through Strep-Tag/Strep-Tactin affinity columns after manufacturer's instructions (Strep-Tactin MacroPrep®, IBA GmbH, Germany), where only strep-tagged and highly biotinylated proteins would bind to the matrix. Bound residues were washed again with fresh buffer W and subsequently released by stepwise elution with buffer E (Tab. 8), which substituted the proteins with desthiobiotin. Afterwards, the columns were regenerated using buffer R including water soluble 2-(4-hydroxyphenylazo)benzoic acid (HABA) (Tab. 8) replacing desthiobiotin *vice versa* and preparing the column for further applications. The single elution fractions were tested for the occurance of AlkB by using 1D-SDS-PAGE according to Laemmli and colleagues [118] and Spectra™Multicolor Broad Range Protein Ladder (Fermentas, Germany). Positive fractions were pooled and mixed with 0.1% *n*-DDM (*n*-dodecyl-β-D-maltoside) to prevent protein aggregation during concentration. After this, the protein solution was inspissated by using centrifugation (4000 x g, 15 °C) and 10 kDa Amicon Ultra Centrifugal Filter Devices (Millipore, USA) which restrained proteins greater than 10 kDa. Concentrates were accordingly washed twice with buffer W and checked again for the occurance of proteins with the respective size of recombinant AlkB (44 kDa) by 1D-SDS-PAGE.

Strep-tag® buffer W		**Strep-tag® buffer E**	
Tris/HCl (pH 8.0)	100.0 mM	Tris/HCl (pH 8.0)	100.0 mM
NaCl	150.0 mM	NaCl	150.0 mM
EDTA	1.0 mM	EDTA	1.0 mM
		Desthiobiotin	2.5 mM
Strep-tag® buffer R			
Tris/HCl (pH 8.0)	100.0 mM		
NaCl	150.0 mM		
EDTA	1.0 mM		
HABA	1.0 mM		

Tab. 8: Buffers for protein purification with affinity column

As shown in Figure 34 (see section 5.5.5), a lot of contaminating proteins of different sizes were co-eluted from the affinity columns. To get rid of these contaminants, different strategies have been done including addition of avidin to the cell extract prior column

load as well as adding 2.5 M NaCl to increase ionic strength and decrease non-covalent complexing. Since these methods were not successful, concentrated elution fractions solution was loaded on a preparative 1D-SDS-PAA gel and subsequently separated in the electric field in order to isolate AlkB. Bands with the respective molecular weight of AlkB were additionally cut from the gel and analysed by mass spectrometry (University of Greifswald, Germany). After the confirmation of a sufficient AlkB quality, the gel slices were used for the immunization of two female New Zealand rabbits, which have prior been negatively tested for already existing anti-AlkB antibodies. In detail, primary immunization was done by subcutaneous injection of the gel slices, which were amended with Freund's complete adjuvant. After several boosts with incomplete Freund's adjuvant, first sampling of the immune-serum was done after 60 days. Immunization was subsequently prolonged and aliquots of serum were sampled monthly in order to monitor the synthesis of anti-AlkB immunoglobulins. Animal husbandry, immunization and extraction of serum were commercially done by Pineda-Antikörper-Service (Germany).

4.2.6.4 Testing of anti-AlkB antibody

Testing of anti-sera taken at 120, 180, 210 and 240 days after first immunization was done by Western-Blot analyses. Therefore, protein solutions from restrained elution fractions, which included the recombinant AlkB were separated by 1D-SDS-PAGE and afterwards transfered on methanol activated membranes of polyvinylidene fluoride (PVDF) (Applichem, Germany) via semi-dry Western-Blot procedure using a Fastblot-B32 apparatus (Biometra GmbH, Germany).

Western-Blot		**Protein detection**	
SP-UL buffer		**CBB R-250**	
Tris	25.0 mM	Brilliant Blue R-250	0.2% (w/v)
Na_2HPO_4	10.0 mM	Methanol	40.0% (v/v)
Glycine	205.0 mM	Acetic acid	7.0% (v/v)
Urea	6.0 M	Water	52.8% (v/v)
SDS	1.1% (w/v)		
β-Mercaptoethanol	1.0% (v/v)		
		Ponceau-S	
		Ponceau-S	0.1% (w/v)
		Acetic acid	5.0% (v/v)
		Water	94.9% (v/v)

Tab. 9: Buffer for semi-dry Western Blot and dyes for protein staining

Since blotting of membrane proteins can be difficult due to their high percentage of hydrophobe amino acids (AlkB contains six transmembrane domains), a two-component transfer buffer (SP-UL buffer) after Abeyrathne and Lam [2] was used. In Table 11 the single components of the different buffers and staining solutions are summarized. Successful transfer of proteins was checked by staining the PAA-gels with Coomassie Brilliant Blue R-250 (CBB R-250), whereas the air dried membranes were reversible stained with Ponceau-S (Tab. 11).

To test the sampled anti-sera for quality and quantity of anti-AlkB antibodies, the dried PVDF-membranes were incubated with a mixture of blocking buffer and different dilutions of rabbit anti-sera respectively (Tab. 10). Afterwards, the membranes were washed twice with fresh blocking buffer to mask unspecific binding sites and subsequently incubated with goat-anti-rabbit-IgG as secondary antibody, which was additionally conjugated with alkaline phosphatase (1:200,000). The membranes were then incubated with AP-buffer, which provides optimal conditions for the phosphatase reaction, fol-

lowing a last incubation with blocking buffer and a two-step wash with water. For the detection of the secondary immunoglobulins, a chromogen solution (Tab. 11) was used where the dephosphorylation of BCIP and congruent reduction of NBT yielded a black-purple-colored precipitate.

	Stage	Duration
1	Semi-dry Western Blot	5 mA/cm^2, 20 min.
2	Incubation of PVDF-membrane with blocking buffer and rabbit anti-serum	over night, RT
3	Wash Step (blocking buffer)	2 x 5 min.
4	Incubation of PVDF-membrane with blocking buffer and goat-anti-rabbit-IgG/AP	1 x 2h, RT
5	Wash Step (blocking buffer)	1x 15 min.
6	Wash Step (water)	2 - 3x 30 sec.
7	Incubation with AP-buffer	1 x 15 min.
8	Incubation with Chromogen solution	until protein bands appear

Tab. 10: Semi-Dry Western Blot detection protocol

Blocking buffer		**NBT stock solution**	
Tris/ HCl (pH7.6)	50.0 mM	NBT	5.0% (w/v)
NaCl	150.0 mM	DMF	70.0% (v/v)
NaN_3	0.05% (w/v)	Water	52.8% (v/v)
skim milk	2.5% (w/v)		
Tween 20	0.05% (v/v)		
AP-buffer		**BCIP stock solution**	
NaCl	100.0 mM	BCIP	5.0% (w/v)
$MgCl_2$	5.0 mM	DMF	95.0% (v/v)
Tris/ HCl (pH 9.5)	100.0 mM		
Chromogen solution			
AP-buffer	99.0% (v/v)		
NBT stock	0.66% (v/v)		
BCIP stock	0.33% (v/v)		

Tab. 11: Buffer for semi-dry Western Blot and dyes for protein staining

5 Results

5.1 PCR-amplification of *alkB* in environmental samples

The primers used in the present study for the quantification of *alkB* genes and transcripts, covered a broad range of different alkane degraders. Due to their high degeneracy, the use of these primers during real-time PCR was limited. Amplification efficiencies did not exceed 75% which resulted in an understimation of gene copy numbers. Therefore several tests were done to optimize the amplification and consequently gain more reliable results. These tests included not only the improvement of the primers itself, but also different additives in the reatcion mixtures, as well as an alternated PCR protocol. As a consequence of the results of these preliminary tests, which will be presented in the following subsections, the amplification efficiency could be increased to almost 86%. The modification of the primers as well as the adapted protocol for Sybr®Green-based real-time PCR have been published successfully (**Publication I, II**).

5.1.1 Modification of *alkB* primers with inosine nucleotides

The substitution of every four fold degenerated base by an inosine nucleotide did not change the specific binding at highly conserved sites, as demonstrated by Kloos and colleagues (refer to Fig. 14). Using *in silico* analyses, the modified primers were aligned against a selection of *alkB*-harbouring bacteria, including members of *Acinetobacteria*, β- and γ-proteobacteria. The results, which are displayed in Figure 16, clearly demonstrate a significant convergence between the primers and the sequences coding for histidine motifs one and four. As these motifs are highly conserved among a broad spectrum of alkane degrading bacteria, the optimized primers are potentially suitable for phylogenetic analyses. To verify this, gene fragments of *alkB* were amplified from different environmental samples using the inosine containing primers and subsequently sequenced. The results apparently indicate the detection of *alkB* genes without any discrimination between known bacterial groups (**Publication II**). Several sequences showed high similarity to *alkB* genes from *Nocardoides sp.* CF8 or strains belonging to *Mycobacteria*. Interestingly, similarities to the marine strain *Microscilla marina* ATCC23134 were also found in this study.

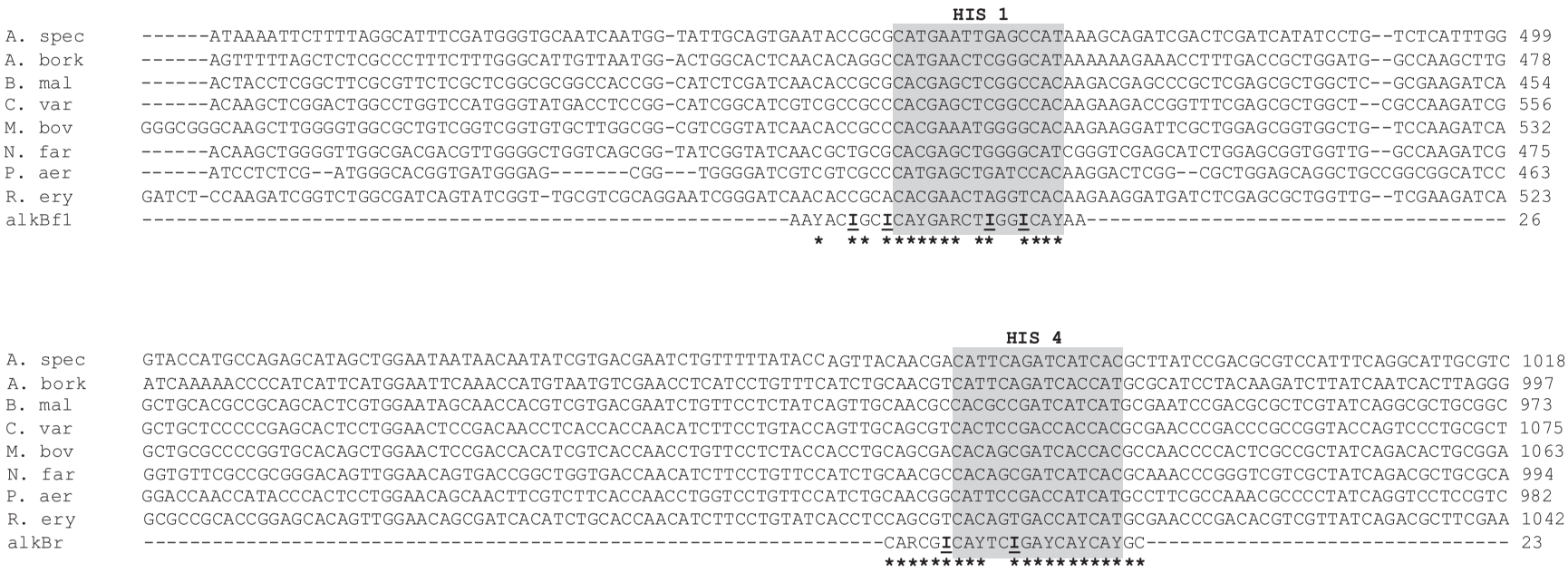

Fig. 16: Alignment of modified *alkB*-primers
The *alkB*-primer set earlier published by Kloos *et al.* [107] was modified in order to improve the amplification efficiencies during real-time PCR. For this, every four fold degenerated base was substituted by an inosine nucleotide (bold underlined letters). The improved primers were aligned against the *alkB* gene sequences of selected representatives. Note that only the coding regions of histidine motifs 1 and 4 are shown (refer to text and Fig. 14). Highly conserved nucleotides are marked by an asterix (*). A.spec = *Acinetobacter sp.* ADP1, A.bork = *Alcanivorax borkumensis* SK2, B.mal = *Burkholderia mallei* ATCC23344, C.var = *Corynebacterium variable* DSM44702, M.bov = *Mycobacterium bovis* AF2122/97, N.far = *Nocardia farcinica* IFM10152, P.aer = *Pseudomonas aeruginosa* PAO1, R.ery = *Rhodococcus erythropolis* PR4, alkBf1 = forward *alkB* primer, alkBr1 = reverse *alkB* primer (refer to 4.1.3).

5.1.2 Data collection during an extra-ordinary reaction step

Despite the introduction of inosine nucleotides, the primers remained highly degenerated. Especially in samples with low amounts of target DNA, this could lead to increased formation of primer dimers. As gene quantification was based on a Sybr®Green assay, even such short double-strained DNA fragments might be detected and increasing total fluorescence signal strength. As a result, gene quantification might be biased. As known from several PCR applications, primer dimers mostly disintegrate at temperatures above 75 °C. Therefore, the effect of signal acquisition at 78 °C was tested with non-template controls (NTC), where potential dimers were the only source for fluorescence signals. As shown in Figure 17, primer dimers were still intact at 72 °C (Fig. 17B) leading to fluorescence signals above the threshold (Fig. 17A). Conversely, dimers were dissociated during data collection at 78 °C (Fig. 17D), leading to signal strengths below the threshold (Fig. 17C). Consequently, primer dimers were not detected.

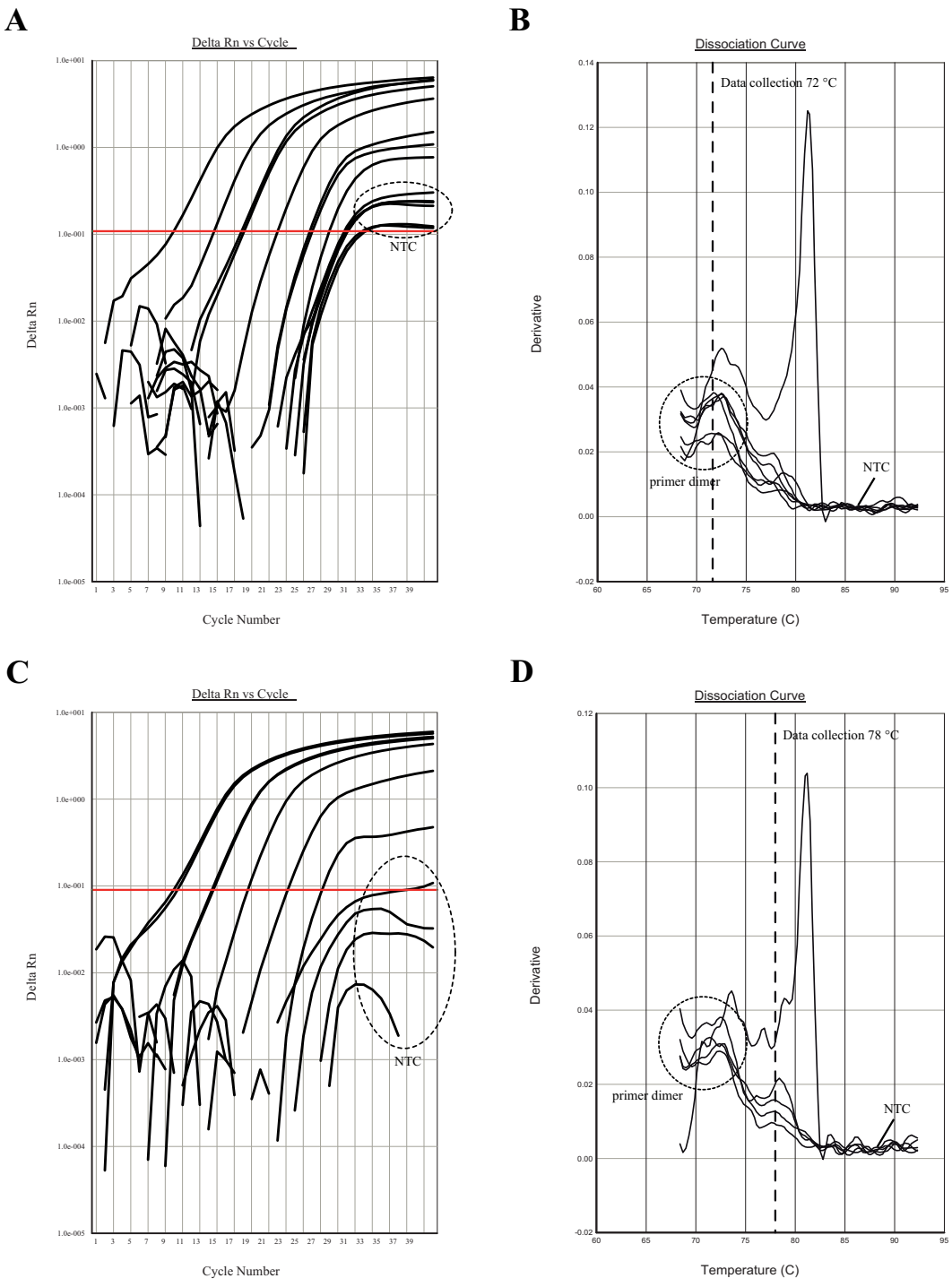

Fig. 17: Reduction of primer dimers during signal detection at 78 °C
Primer dimers bias quantification during data collection at 72 °C (A, B), as they not disintegrate at this temperature (B, dashed circle) and resulting signals are above the threshold (A, red line). During data collection at 78 °C (C, D) dimers (D, dashed circle) are dissociated and disappeared. As a result signal strength is below the threshold (C, red line) and not detected. Contribution of dimers to signal acquisition was tested in non-template controls (NTC). Vertical dashed lines represent data collection at distinct temperatures.

5.1.3 Use of DMSO, BSA and $MgCl_2$ as additives for real-time PCR

As humic substances can act as inhibitors for the activity of the DNA-polymerase, three different additives have been tested for improving the amplification of *alkB* from environmental samples. Figure 18 clearly demonstrates, that the addition of 0.06% (w/v) BSA improved the amplification of the *alkB* genes and resulted in an effeciency of 89% (slope: -3,623). Without extra BSA, activity and binding of the polymerase to the target was hampered. As a result a theoretical effeciency of more than 100% (slope: -2,939) was calculated, which is not feasable. In most studies concerning samples with GC-rich target DNA, dimethylsulfoxid (DMSO) is added to improve amplification. Interestingly, the application of this additive in an *alkB* real-time PCR seemed to be disadvantageous. As displayed in Figure 19, amplification in DMSO supplemented reaction mixtures was low and showed efficiencies around 76% (slope: -4,089) only. In contrast, preparations containing no extra DMSO seemed to result in higher amplification efficiencies, as the calculated slope was -3.667 (efficiency of 87%). Magnesium chloride is supposed to form complexes with dNTPs, which are subsequently used as substrate for DNA-polymerases. Consequently, the addition of $MgCl_2$ to PCR reaction mixtures is commonly used for the improvement of amplification efficiencies. Interestingly, the concentration has thereby a strong influence. For example, Williams [255] could demonstrate a low binding of primers to the target, when amounts of used $MgCl_2$ are too low. In contrast, Ellsworth *et al.* [54] monitored a hampering effect of $MgCl_2$ when used in excess. With high amounts of this compound, base pairing between primer and target DNA is too strong, preventing the primer/DNA-complex to disintegrate during denaturation at 94 °C. In the instructions of commercial reaction mixtures, an amount of 3-7 mM $MgCl_2$ is recommended for a successful real-time PCR. However, since the exact amount of $MgCl_2$ in the used Sybr®Green Master Mix is not known, the effect of extra $MgCl_2$ was tested. As demonstrated in Figure 20 the addition of 2 mM $MgCl_2$ to the Master Mix increased the amplification efficiency about almost 15% from 78% (slope: -4.002) to 92% (slope: -3.512).

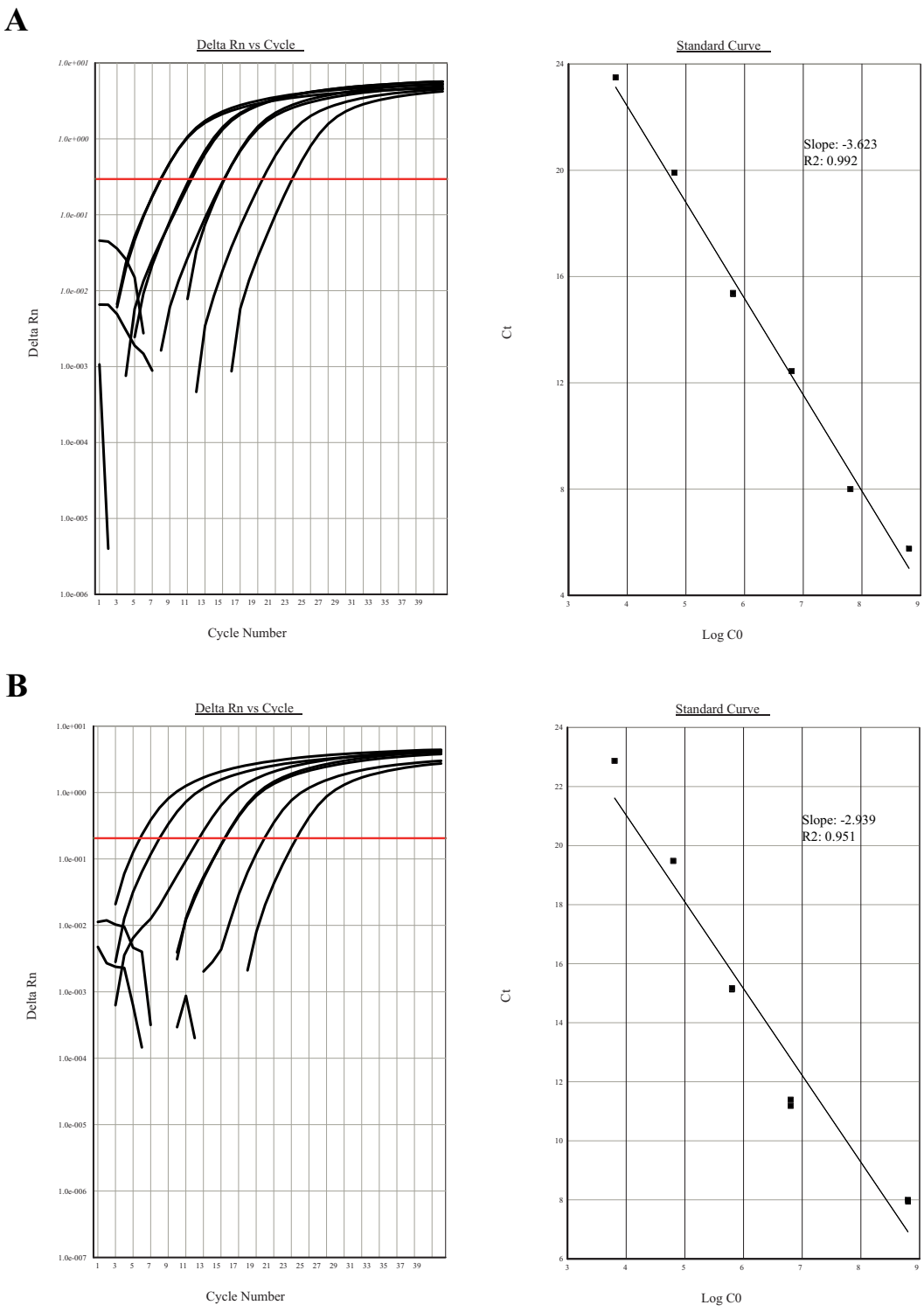

Fig. 18: Addition of bovine serum albumin for elevated *alkB* amplification
The addition of 0.06% bovine serum albumin (A) improved the amplification effeciencies compared to mixtures without BSA application (B). The red line represents the threshold for signal detection. See text for details.

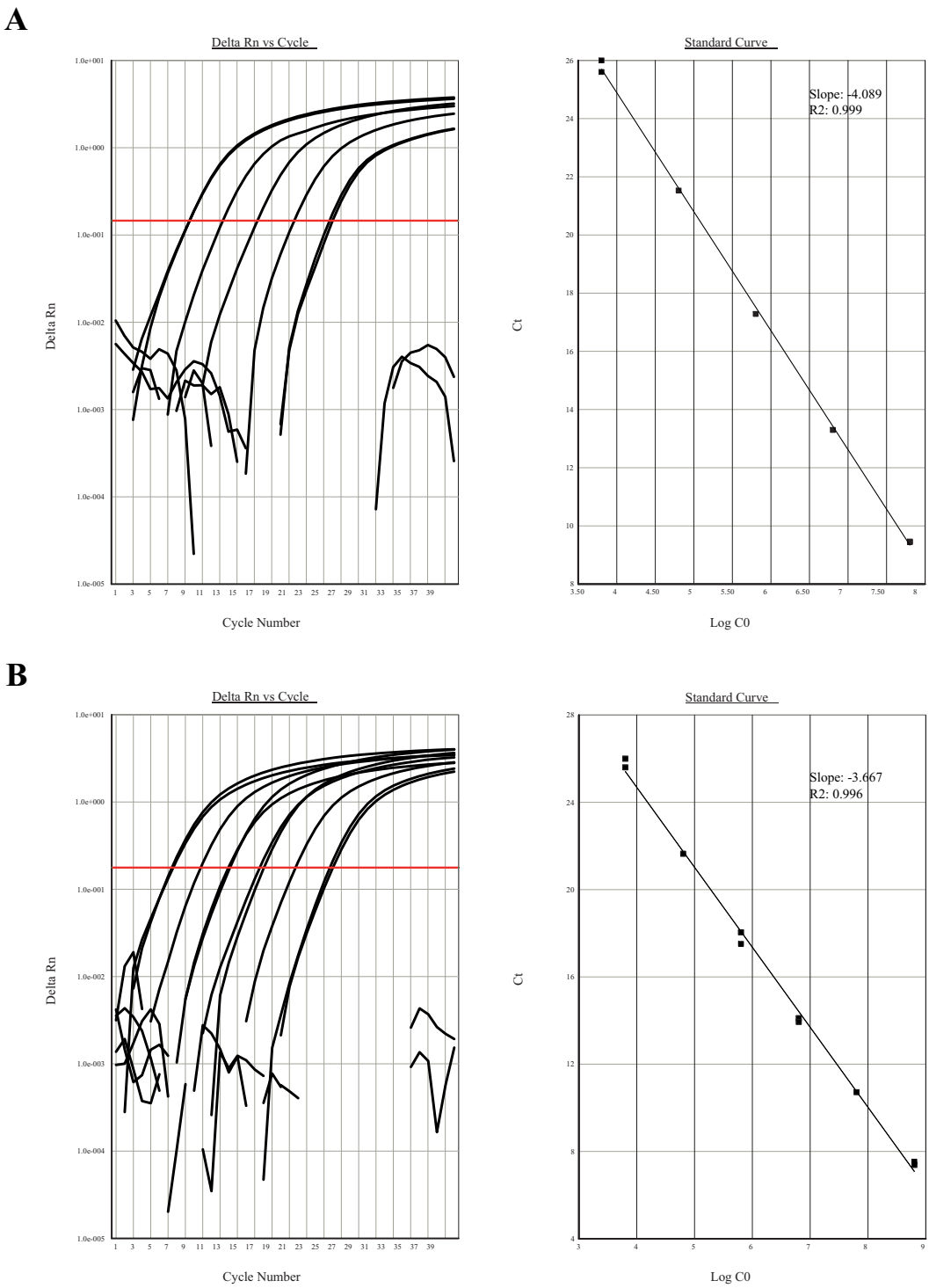

Fig. 19: Effects of DMSO addition on amplification efficiency
Amplification efficiencies of *alkB* genes with (A) and without (B) addition of DMSO in the reaction mixtures. Note that despite standard curves look quite similar, efficiencies strongly differ from each other (see text for details). The red line represents the threshold for signal detection.

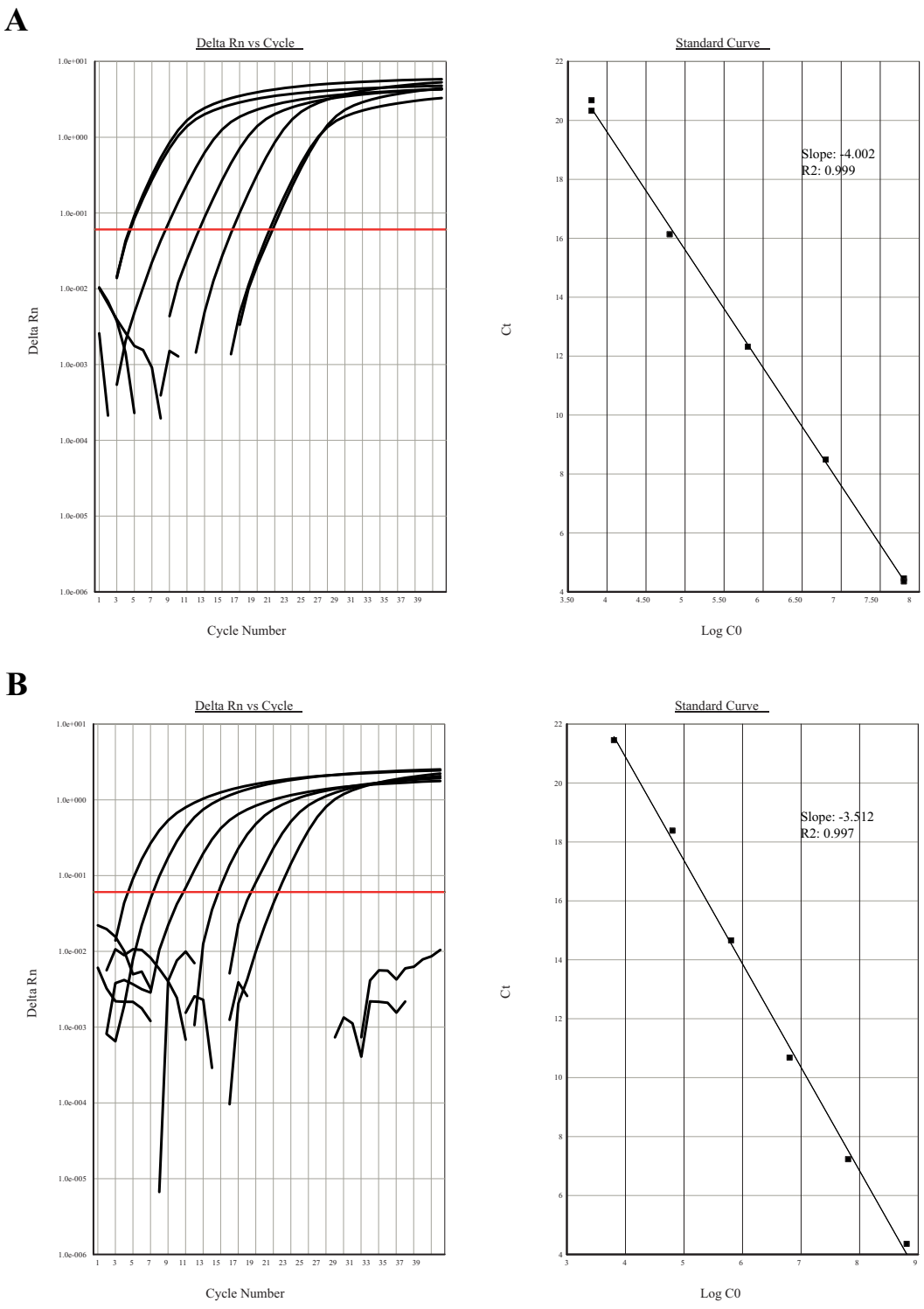

Fig. 20: Effect of extra $MgCl_2$ on the amplification of *alkB*
In PCR reactions without the addition of extra $MgCl_2$ (A), amplification efficiencies were very low at 78%. After mixtures were spiked with 2 mM $MgCl_2$ (B), efficiencies increased up to almost 92% (see text for details). The red line represents the threshold for signal detection.

5.1.4 Introduction of touchdown steps with different temperature ranges

As a consequence of high degeneracy, the used primers reflected a broad range of annealing temperatures. If the highest temperatures were chosen, only a minor fraction of the individual primers would bind to the template. As a result, gene copy numbers might be underestimated. By using lower temperatures, unspecific primer binding would be benefited in some cases. To allow for the specific binding of all sequences of the respective primers, a touchdown with a temperature reduction of about 1 °C per cycle was introduced. Two touchdown protocols covering temperatures between 62 °C and 57 °C as well as 57 °C to 52 °C were tested. As demonstrated in Figure 21, the touchdown from 62 °C to 57 °C resulted not only in clearer standard curve signals but also revealed a higher amplification efficiency of 87%.

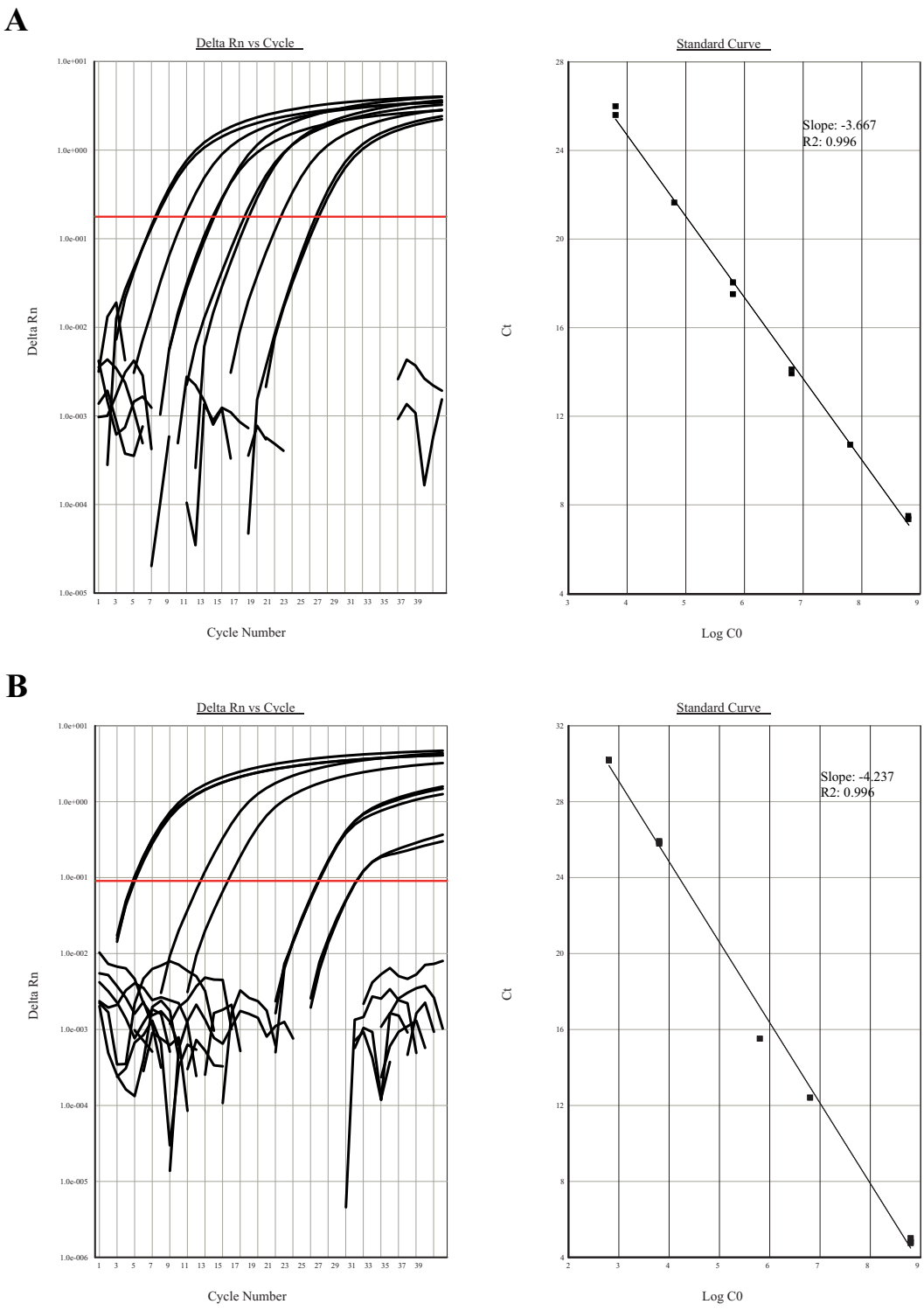

Fig. 21: Use of touchdown cycles with different temperatures
To optimize the binding of the different primer sequences, especially in the first cycles of real-time PCR, touchdown steps (-1 °C/ cycle) were introduced. Two ranges of annealing temperatures covering 62 °C to 57 °C (A) and 57 °C to 52 °C (B) were thereby tested. Serial dilutions (1/10) were used for the standard. Dilutions which showed no appropriate signals were rejected (B). The red line represents the threshold for signal detection.

5.2 Litter degradation and the dynamic of *alkB* in different soil compartments (E1)

In the following section the litter degradation rates as well as the dynamic of *alkB*-harbouring bacteria in different compartments are presented. Next to the effectivity of litter decay, the abundances of *alkB* DNA and mRNA in litter as well as different soil compartments were analysed. Obtained data were correlated to the occurance and activity of total bacteria. For this experiment, sandy and silty soil cores were incubated with maize and pea plant litter. Samples were frequently taken during the incubation (T0-T3) from the litter layer, the litter-soil interface layer as well as the bulk soil.

5.2.1 Litter degradation

As summarized in Figure 22, immense losses of organic matter were monitored already after the first two weeks of incubation, independent of the soil type. Interestingly, significant higher decomposition rates could be observed for pea litter compared to maize ($P < 0.001$). For example, whereas only 50% of the initial maize litter were degraded in sandy soil, more than 80% of pea plant material were mineralized in the same time.

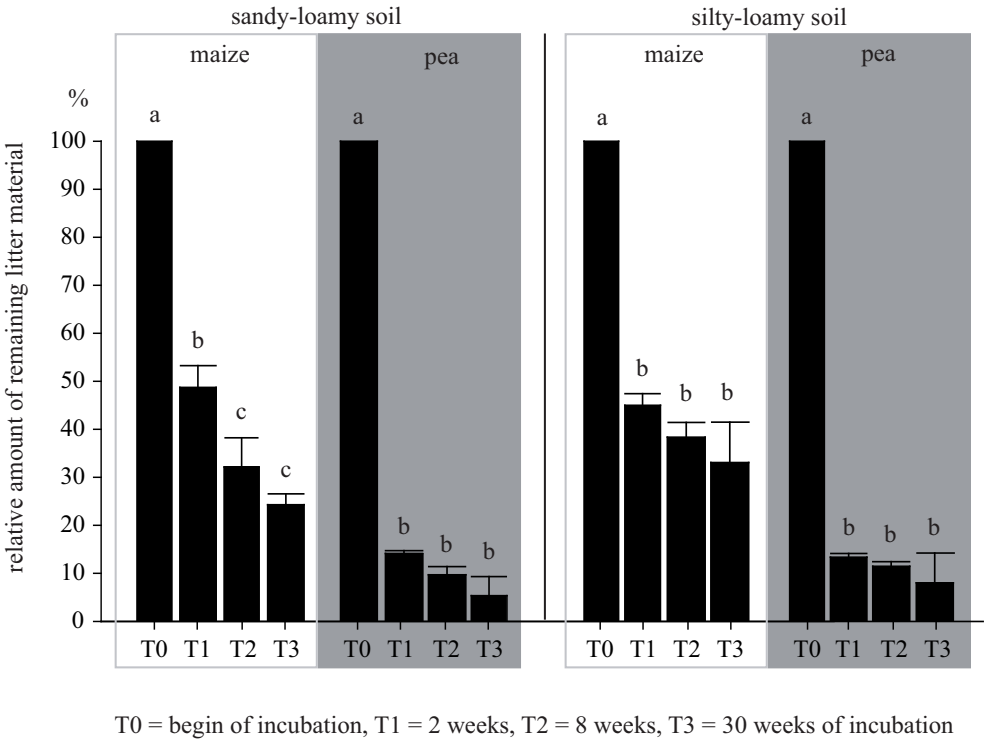

Fig. 22: Litter degradation rates
Relative amount of remaining maize or pea litter after the burial in sandy or silty soil and subsequent incubation. The residual amounts are referred to an initial input of 1 g (dw) of fresh litter material. Error bars represent standard deviations (n = 3). Significant differences ($P < 0.05$) between the samples are indicated by different small letters.

A similar trend was observed during the incubation of silty soil microcosms. With ongoing time, decay was attenuated in both litter types with comparable minor changes in the quantity of remaining litter material at T2 and T3. For instance, contrary to the enormous reductions at T1, dry weights decreased about 5% to 10% only. However, significant changes in the remaining amounts were only observed for sandy soil microcosms covered with maize litter ($P = 0.002$).

5.2.2 Quantification of *rpoB* and *alkB* genes and transcripts

Abundance of *alkB* in microcosms with litter cover

The high amounts of easy degradable compounds make the litter layer a reservoir for a large abundance and diversity of micro-organisms. In the present study the dynamic of *alkB* genes and respective transcription products were analysed. As expected high amounts of *alkB*-harbouring bacteria were found in fresh litter material before the incubation experiment was set. Interestingly, abundances of pre-colonizing alkane degrading bacteria in maize and pea litter differed significantly ($P < 0.05$) from each other. Whereas $3 * 10^{10}$ copies g^{-1} litter (dw) were detected in maize straw, copy numbers found in fresh pea litter were one order of magnitude lower as demonstrated in Figure 23A and B. For instance, at T1 abundances declined to $6 * 10^{9}$ copies g^{-1} litter in maize but recovered in all samples at the end of incubation after 30 weeks (T3). In contrast, a steady increase of gene copies was monitored throughout the experiment in pea litter material. Although such differences were detected, comparable amounts of *alkB* were monitored in both litter types at T3. To this time quantities of almost $1 * 10^{11}$ gene copies g^{-1} dry straw material occurred. ANOVA analyses of the litter layer revealed significant interactions between incubation time and litter type ($P = 0.001$), reflecting the influence of both factors on *alkB*. However, a significant impact of the soil type could not be identified.

Compared to the litter layers, significant lower ($P < 0.001$) abundances of *alkB* were monitored in the litter-soil interface (0-1 mm) and bulk soil (10-11 mm) layers of sandy and silty soil microcosms. In these compartments, gene copy numbers were two to three orders of magnitude lower and ranged between $4.5 * 10^{7}$ and $8 * 10^{8}$ copies g^{-1} dry soil. In general, the dynamic of *alkB* in the different compartments of sandy and silty soils, was not influenced by the litter type. In the bulk soil layers, only minor changes in the course of time were monitored (Fig. 23A, B). Nevertheless, a strong impact of the soil type was observed ($P = 0.000$). In contrast to the bulk soils, oppositional tendencies of *alkB* gene copies have been reflected in the litter-soil interface layers. Whereas copy numbers kept constant in sandy soils covered with maize and pea, abundance increased constantly in the silty soils. Opposite to the bulk soil layers, significant influences of the soil type were only observed in microcosms covered with maize litter ($P = 0.03$). Anyhow, significantly different abundances of *alkB* in the interface layer and bulk soil compartments, were only monitored in silty soils ($P < 0.01$). Conversely, no gradient formation was found in the respective compartments of sandy soil microcosms. The quantification of the *alkB* genes only indicates the genetic potential in the different

soil layers. Subsequently, information about the activity of the alkane degraders is not retrieved. Therefore, the amount of the *alkB* transcripts was determined in order to estimate the activity of *alkB*-harbouring bacteria.

In this study, the cDNA was related to the respective genomic DNA, where the ratios can be used to indicate the specific induction in response to litter derived alkanes. As demonstrated in Figure 23C, the activity of *alkB*-harbouring bacteria colonizing the maize litter increased within the first two weeks of incubation. As expected, this tendency was independent from the soil type. With ongoing incubation, activity decreased by trend in the litter layer covering both soils, but showed different dynamics. For example, in maize litter covering sandy soils, the specific induction which indicates the bacterial activity, collapsed at T2 and changed only slightly until the end of incubation (T3). On the contrary, the specific induction receded constantly over the same time in silty soil microcosms. Interestingly, an increase in the cDNA/ DNA ratio at T1, as reported for the litter layer, was not monitored in the interface and bulk soil layers of both soils. Nevertheless, different dynamics in the activity of *alkB*-harbouring bacteria in these compartments were detected. For instance, the specific induction decreased constantly during the incubation in silty soils, whereas no or only slight changes occurred in sandy soils (Fig. 23C).

In opposite to the maize litter, activity of alkane degrading bacteria using *alkB* uniformly declined in the first eight weeks of incubation in pea plant material (Fig. 23D). Despite this, specific induction slightly recovered at T3. In the soil layers the dynamic of the cDNA/DNA ratio was comparable to silty soil microcosms covered with maize. Consequently, no changes of the specific induction where observed until T1 in sandy and silty soils with pea coverage (Fig. 23D). In the course of time, transcript copy numbers rapidly reduced at T2, but remained constant until T3. However, monitored changes in the bacterial activity were not significant as revealed by statistical analyses.

Abundance of *alkB* in non-litter control microcosms

The presented results do not allow for the discrimination between litter induced effects on the *alkB*-harbouring bacteria and those derived from soil. To overcome this and congruently evaluate the impact of alkanes derived from the litter layer by trend, microcosms devoid of litter coverage were incubated as non-litter controls. Here again, abundances of the *alkB* genes and their specific induction, reflecting the activity, were detected and are summarized in Figure 24. A clear, significant ($P = 0.000$) gradient formation from the interface layer to the bulk soil occoured in the silty soil microcosms,

whereas no significant differentiation between the compartments could be observed in the sandy soil. In addition, abundances of *alkB* in the individual compartments were strongly impacted by the soil type ($P = 0.000$) and in the case of bulk soil by the incubation time also ($P < 0.05$). However, in the interface layer of the sandy soil, copy numbers dropped about one order of magnitude after eight weeks of incubation. In contrast, a steady increase in the abundance of *alkB* up to $1 * 10^8$ gene copies was detected in the same layer of silty soil microcosms (Fig. 24A). Variable tendencies were also observed in the bulk soil compartments. Here, abundances declined within two weeks of incubation in sandy soil, whereas no changes over the time could be monitored in the silty soil.
Anyhow, a gradient formation in the specific induction of *alkB* genes was neither observed in sandy nor in silty soils. Remarkably similar tendencies in the activity of *alkB*-harbouring bacteria were monitored in the interface layer of both soil types. Here, statistical analysis reflected a significant impact by the soil type ($P < 0.05$). In detail, a strong and significant ($P < 0.05$) increase of the specific induction of *alkB* within the first two weeks of incubation occured in sandy soil microcosms (Fig. 24B). In contrast, the activity rose only slightly in the same time in silty soil microcosms. In addition, dynamics of the specific induction of *alkB* were also comparable by trend in the respective bulk soil layers. Here, activity increased during the incubation of both soils, but was more pronounced in the silty soil microcosms ($P < 0.05$).

Abundance of *rpoB* at different soil compartments

To disclose if the dynamic of *alkB* was related to bioavailable alkanes or to factors benefiting general microbial growth, additional quantification of *rpoB* was done. This constitutively expressed gene encodes the β-subunit of the bacterial DNA-Polymerase and can be used as a marker for total bacterial abundance. Due the fact that *rpoB* is a single copy gene, more reliable results compared to the quantification of multicopy 16S rRNA genes are gained.
As demonstrated in Figure 25, the abundance of *rpoB* in the litter layer was significantly higher ($P = 0.000$) compared to the soil layers. Interestingly, one exception was observed at T1 in the interface layer of pea litter covered microcosms. Here, amounts of total bacteria almost reached the copy numbers found in the respective litter layers. Anyhow, significant ($P < 0.05$) different dynamics of *rpoB* in maize and pea were monitored. In detail, copy numbers significantly ($P < 0.05$) decreased within the first two weeks of incubation in maize litter, whereas only a minor increase occurred in pea litter. With ongoing incubation quantities of *rpoB* further decreased or changed only slightly

in the most cases. Conversely, abundances of *rpoB* in the maize litter material covering silty microcosms recovered at the end of incubation after 30 weeks and reached initial amounts around 1 * 10^{10} gene copies g^{-1} soil. As revealed by statistical analyses, gene quantities during the decay of plant material from both litter types were not impacted by the soil type.

In the interface layer of soils covered with maize, gene copy numbers were neither impacted by the soil type nor the incubation time and leveled off between 1 * 10^6 and 2 * 10^7 copies g^{-1} soil until T3 (Fig. 25A). In contrast, numbers of total bacteria dramatically increased two weeks after the start of the experiment in the interface layer of pea covered microcosms (Fig. 25B). Here, copy numbers reached up to 3 * 10^9 genes g^{-1} soil. In the following six weeks (until T2) of incubation, abundances dropped about almost two orders of magnitude and subsequently changed only slightly until T3. In the bulk soil compartments, gene quantities fluctuated throughout the incubation, but did not exceed 1 * 10^7 copies g^{-1} soil. Interestingly, neither the soil nor the litter type impacted abundances of *rpoB* and an influence of the incubation time was only monitored in silty soil microcosms covered with pea litter ($P < 0.05$).

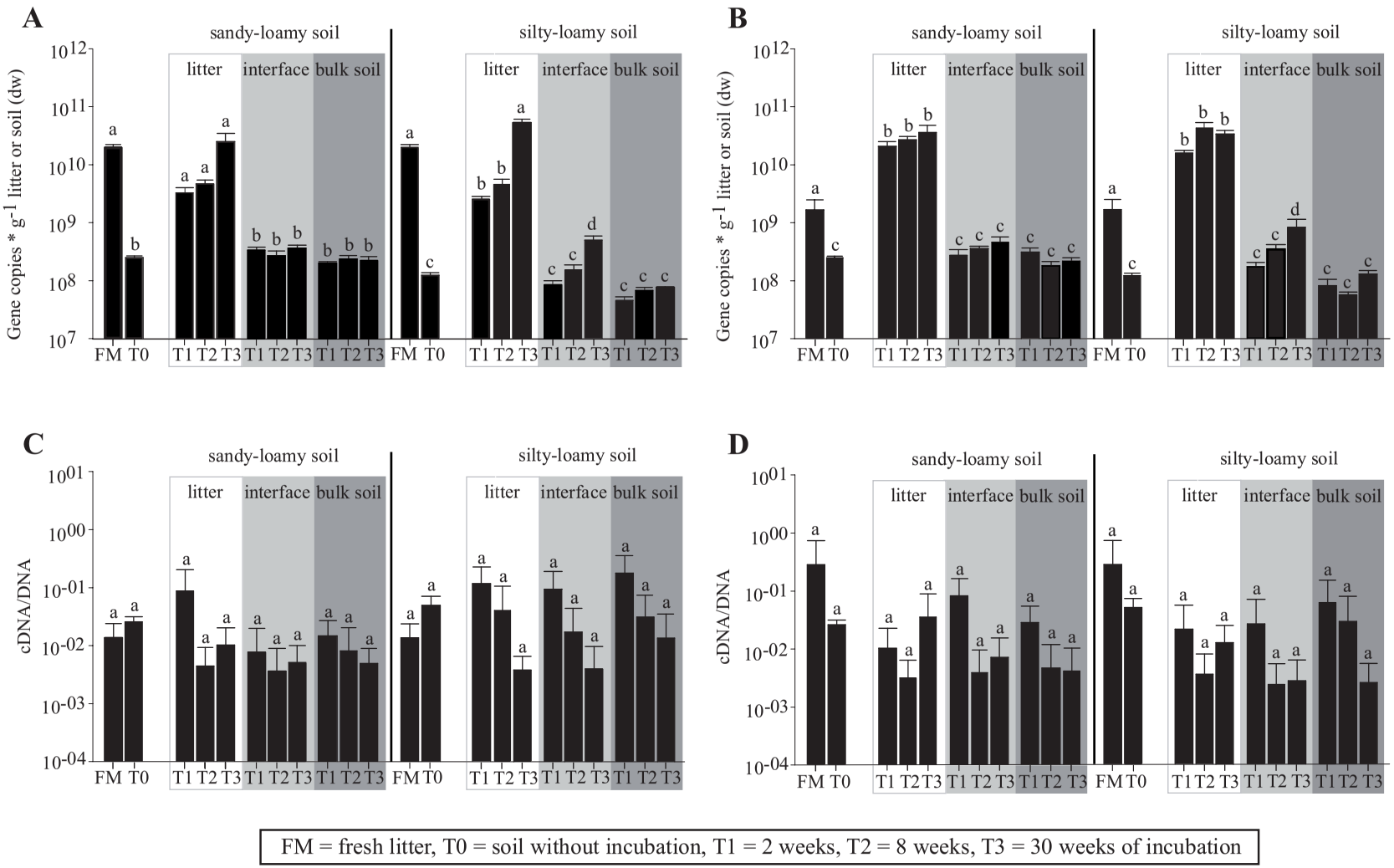

Fig. 23: Abundance of *alkB* genes at different soil layers
Changes in the abundance of *alkB* genes (A, B) and their specific induction (C, D) during the incubation with maize (A, C) or pea (B, D) litter material. The analysed layers are indicated. The specific induction is refered to the ratio of *alkB* cDNA to DNA. Error bars indicated standard deviations (n = 3). Significant differences ($P < 0.05$) are indicated by different small letters.

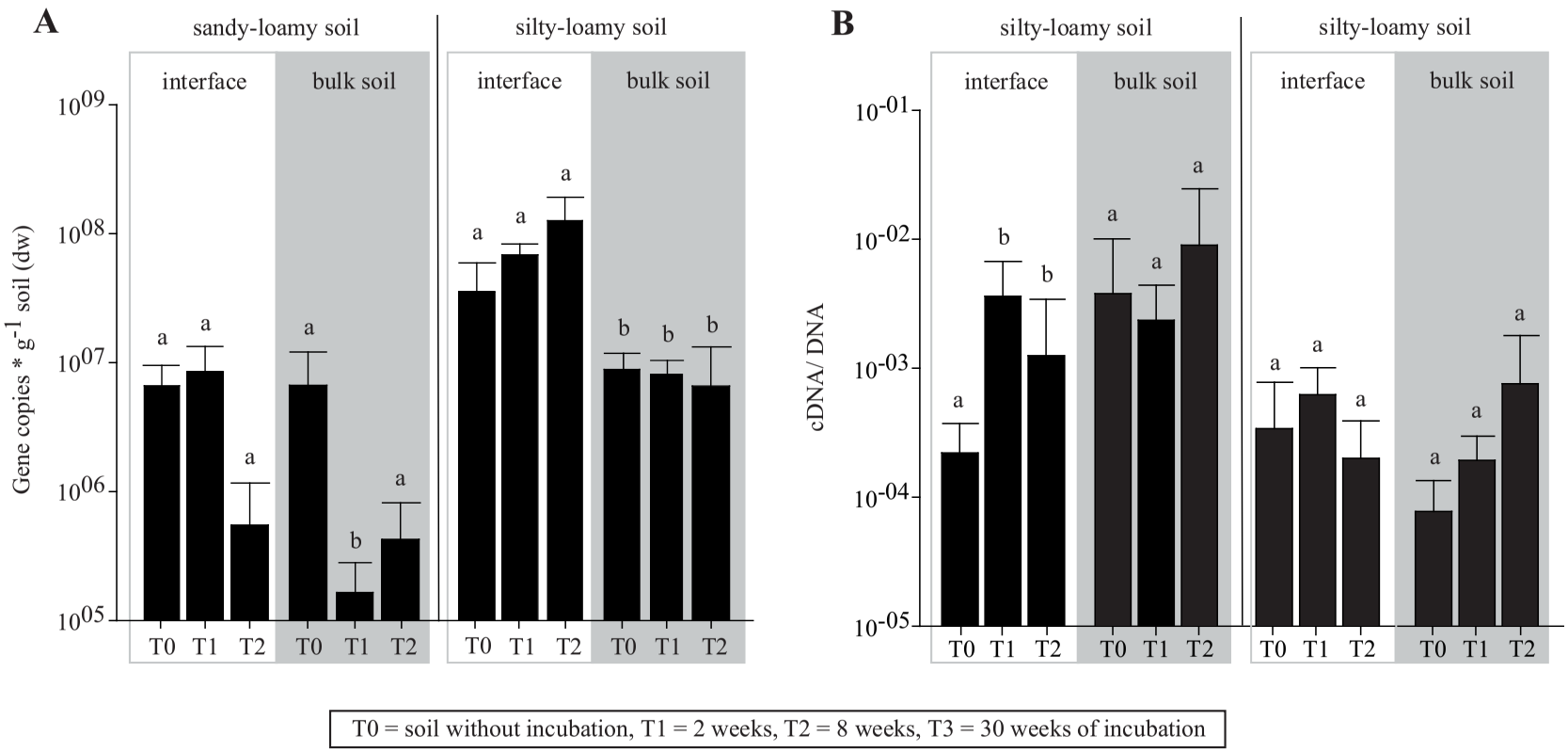

Fig. 24: Gene copy numbers of *alkB* in the non-litter controls
Microcosms composed of sandy and silty soils were incubated without litter cover. The abundance (A) of *alkB* genes and the activity of *alkB*-harbouring bacteria (B) were measured at the beginning (T0) and after two (T1) and eight (T2) weeks of incubation at the litter-soil interface as well as in bulk soil. Error bars represent standard deviations (n = 3). Significant differences ($P < 0.05$) are indicated by different small letters.

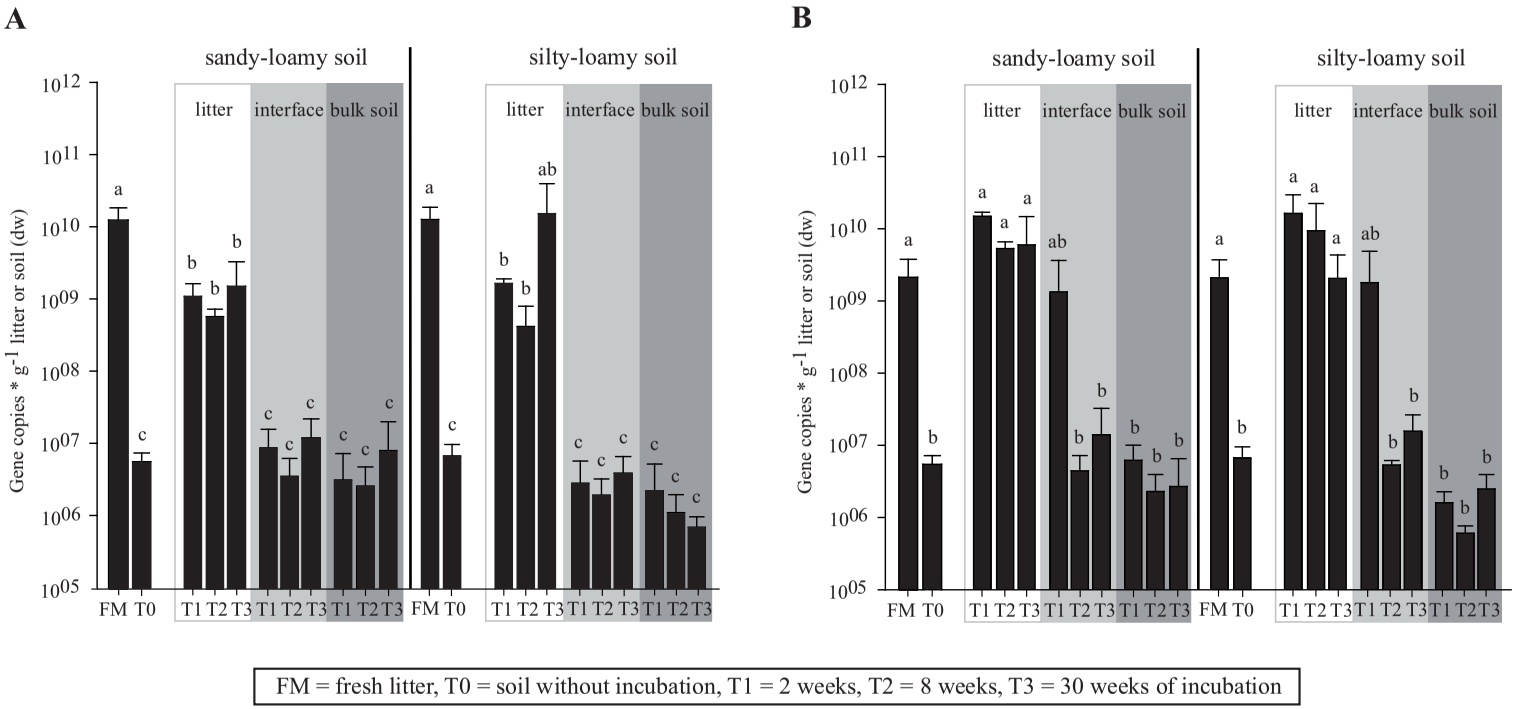

Fig. 25: Abundance of *rpoB* genes during plant litter decay
Abundance of *rpoB* genes in sandy and silty soil microcosms covered with maize (A) or pea litter (B). The *rpoB* gene copy number was measured at the beginning (T0) and after two (T1) and eight (T2) and thirty weeks (T3) of incubation in order to determine the abundance of total bacteria. Error bars represent standard deviations (n = 3). Significant differences ($P < 0.05$) are indicated by different small letters.

5.3 Gradient formation of *alkB* in differently pre-aged artificial soils (E2)

To elucidate the dynamic of *alkB* during the formation of organo-mineral complexes and consequently the genesis of BGI's, artificially prepared soils were used. These mixtures contained particles with different sizes to simulate natural soils with various textures (see Table 4). Prior incubation experiments with litter material were accomplished, mixtures were pre-incubated for three and twelve months without additional nutrient source. In the following section, the dynamic of *alkB* in two different soil compartments during the maturation of the artificial soils is demonstrated.

Initial amounts of *alkB* in three and twelve months matured soils

Before the artificial soils with different ages were incubated with litter material of wheat, initial amounts of *alkB* were detected. Like demonstrated in Figure 26, comparable gene copy numbers were found in the different mixtures, which were pre-aged for three months. Here, copy numbers ranged from $2 * 10^6$ to $8 * 10^6$ copies, but did not exceed $1 * 10^7$ copies g^{-1} dry soil. Conversely, abundances of *alkB* were significantly ($P < 0.05$) reduced in most twelve months pre-aged soils, independent from the soil composition. Monitored gene abundances in these soils ranged between $1 * 10^4$ and $8 * 10^5$ copies g^{-1} soil.

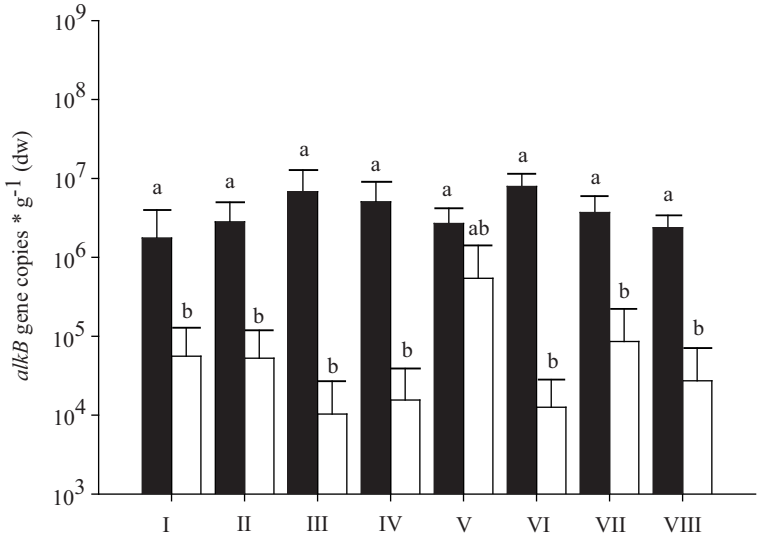

Fig. 26: Amounts of *alkB* genes in differently aged artificial soils at T0
Quantification of *alkB* genes in different three (black bars) and twelve (open bars) month pre-aged artificial soils (roman numerals) was done before incubation with litter material was started (T0). Note that at T0 no compartments were developed. Error bars denote standard deviation (n = 3). Significant differences ($P < 0.05$) are indicated by different small letters.

In the soils containing charcoal and montmorillonite (soil V), no significant differences between three and twelve month old mixtures were monitored (P = 0.206). Here, copy numbers of *alkB* in twelve month old soils reached almost 1 * 10^6 and were consequently comparable to the results found in the younger ones.

Amounts of *alkB* after the incubation with litter material for two weeks

After the addition of wheat litter material and subsequent incubation for two weeks, a differentiation of the bulk soil into distinct compartments has been expected. Therefore the uppermost soil layer, representing the litter-soil interface, as well as the bulk soil 10 mm below were sampled. Figure 27 summarizes the gene copy numbers of *alkB* in the respective compartments. Congruently to the initial abundances, copy numbers in three and twelve months old mixtures differed in general up to two orders of magnitude in both compartments (P < 0.01). In the interface layer of mixtures with both ages, a significant (P < 0.05) increase of *alkB* genes copies was monitored after the incubation with litter material. Although the elevation of copy numbers was independent from the mixture composition, abundances and increasing intensities were fluctuating. For instance, in three month pre-aged mixtures the amount of gene copies increased about one order of magnitude in most cases and reached up to 1.5 * 10^8 copies g^{-1} soil (dw). On the contrary, abundance of *alkB* in twelve month old mixtures was in general two orders of magnitude higher, resulting in copy numbers between 1 * 10^6 and 8 * 10^6.

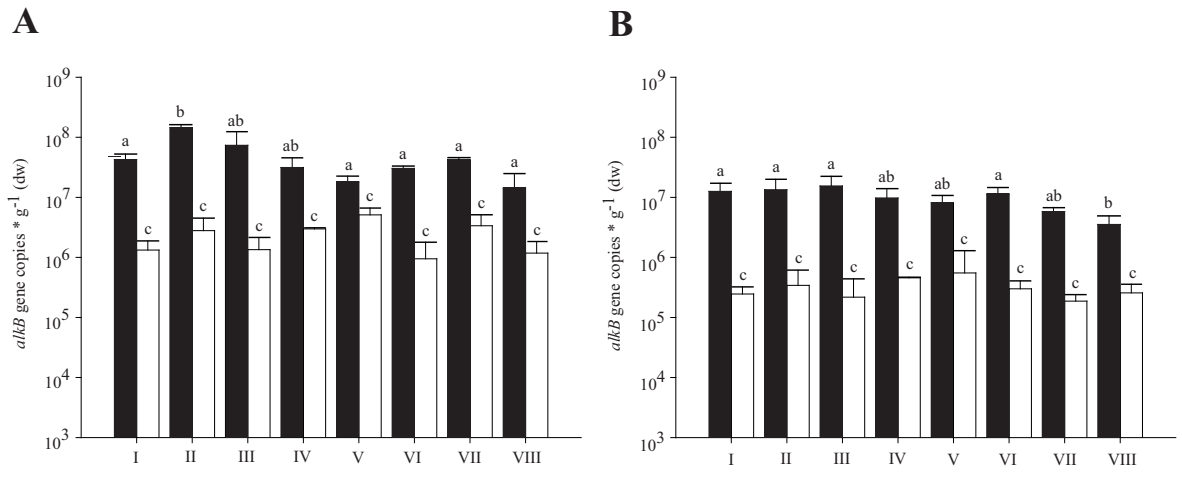

Fig. 27: Quantities of *alkB* genes in interface and bulk soil compartments of divers mixtures at T1
After the incubation of the different soil mixtures with litter of wheat for two weeks (T1), abundances of *alkB* genes were quantified in the interface (A) and bulk soil (B) layer of three (black bars) and twelve (open bars) month pre-aged artificial soil mixtures (roman numerals). Error bars denote standard deviation (n = 3). Significant differences (P < 0.05) are indicated by different small letters.

The increase of copy numbers after the litter application was attenuated in the bulk soil layer of respective microcosms (Fig. 27B). Here, quantities leveled off around 1 * 10^7 and 5 * 10^6 gene copies in three and twelve months old mixtures respectively. Anyhow, comparable amounts of *alkB* were detected at T0 and T1 in three month old mixtures. Remarkably, gene copy numbers in twelve month old mixtures were 4 - 30 timer higher after the litter amendment than found at the beginning of the incubation.
Besides, during the degradation of litter material, a clear and significant ($P < 0.05$) *alkB* gradient was monitored from the interface layer to the bulk soil compartments in all artificial mixtures of both ages. In addition, whereas the abundance of *alkB* was significantly ($P < 0.05$) impacted by the composition in three months pre-aged mixtures, no significant influence was observed in the mixtures aged for twelve month.

Calculation of T1/T0 to determine the response to litter supply

During pre-aging the soil mixtures, interactions of microbes and soil particles might have been developed leading to organo-mineral complexes. In dependency of the minerals used as additives in this experiment, developed microbial communities might differentially deal with the reapplication of nutrients. In order to illustrate and examine the increase in the microbial biomass of *alkB*-harbouring alkane degraders in response to the incubation with plant litter material, ratios of T1/ T0 were individually calculated for the different mixture types and ages.

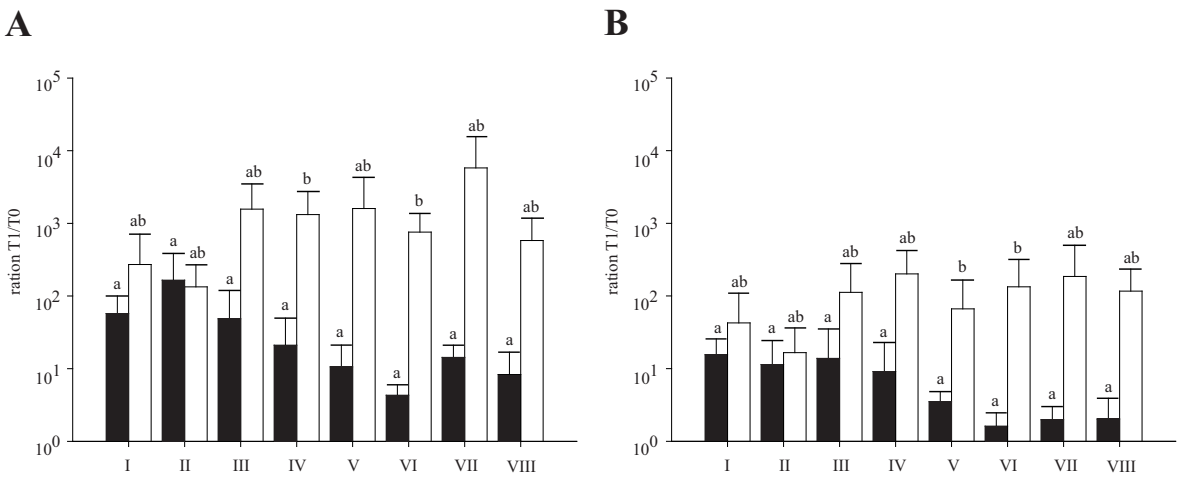

Fig. 28: Ratio of T1/ T0 to illustrate the increase of *alkB* genes after litter amendment
The increase of *alkB* gene copies from the beginning (T0) to the end of incubation with wheat litter after two weeks (T1) is represented by the ratios of T1/ T0 in three (black bars) and twelve (open bars) months aged soils at the litter-soil interface (A) and bulk soil (B). Error bars denote standard deviation (n = 3). Significant differences ($P < 0.05$) are indicated by different small letters.

As demonstrated in Figure 28, comparable dynamics of the microbial response were monitored in the interface and bulk soil layers of the different mixtures. Despite this, differences between the individual soil mixtures occured. In detail, the ratios of T1/ T0 from three and twelve month pre-aged soils were comparable in mixtures composing only one reactive compound (mixtures I and II).

Contrarily, remarkable differences between "younger" (three month) and "older" (twelve month) soils could be found in more complex mixtures (mixtures III-VIII) . Here, ratios of twelve month pre-aged soils exceeded those from three month pre-aged soils about one to two orders of magnitude. However, in the mixtures of the respective ages, ratios fluctuated but were not impacted by the composition. Furthermore, despite the discrepancies between three and twelve month pre-aged mixtures, a significant impact of the maturing time was only found in the interface layer of mixtures IV and VI as well as the bulk soil of mixtures V and VI ($P < 0.05$ in both cases).

5.4 Dynamic of *alkB* and 16S rRNA in MCPA amended soils (E3)

In this experiment, a gradient formation of total bacteria as well as *alkB* genes was monitored by trend from the litter-soil interface (0-3 mm) towards deeper bulk soil layers (3-6, 6-9 mm). This gradient formation was neither influenced by the incubation time nor the treatment type as reflected by ANOVA-analyses. Despite this, soil depths' dependent differences (compartment type) in the abundances of total and *alkB*-harbouring bacteria were only found in control soils ($P < 0.05$).

However, as summarized in detail in Figure 29A and B, a constant and comparable increase within three weeks of incubation was monitored in the interface layers of both treated soils. Copy numbers reached thereby almost $1 * 10^5$ genes g^{-1} dry soil. In water amended soils, quantities dropped after six weeks of incubation to the initial amount of $7 * 10^4$ genes (Fig. 29A), whereas a stabilized rise occurred in the MCPA treated microcosms (Fig. 29B). With escalating distance to the litter-soil interface, abundances declined incessantly in water treated soils, further promoting the gradient formation. On the contrary, amounts of *alkB* changed only slightly during the same time in MCPA spiked soils and reduced, if at all, in the deepest analysed compartment (6-9 mm) at the end of the experiment (T3). To evaluate if changes in the *alkB* copy numbers were the result of the litter derived alkanes and the specific soil treatment only, abundances of total bacteria were also analysed. As expected, copy numbers of 16S rRNA genes were three to four orders of magnitude higher than abundances of *alkB* and ranged around $2 * 10^8$ gene g^{-1} soil. In the interface layer of water and MCPA spiked soils, dynamics of 16S rRNA genes were highly comparable to those found for *alkB*. As demonstrated in Figure 29C - D, constantly increasing quantities in soils of both treatment types were detected within the first three weeks of incubation. At the end of the experiment after six weeks, gene copies slightly decreased in soils which have been spiked with water. In contrast, abundance of 16S rRNA further increased at the same time up to $8 * 10^8$ copies in soils spiked with MCPA. In the deeper soil compartments (3-6, 6-9 mm) dynamics of total bacteria were slightly different between water and MCPA-treated soils. For instance, no or only slight changes in the abundance of total bacteria were observed in soils which have been spiked with water (Fig. 29C), where gene abundances leveled off around $4 * 10^8$ copies g^{-1} soil. Conversely, a constant but only slight increase in the amounts of 16S rRNA was observed until T2 in the same compartments of microcosms incubated with MCPA (Fig. 29D). With ongoing incubation, total bacteria were slightly reduced in these microcosms at the end of the incubation after six weeks.

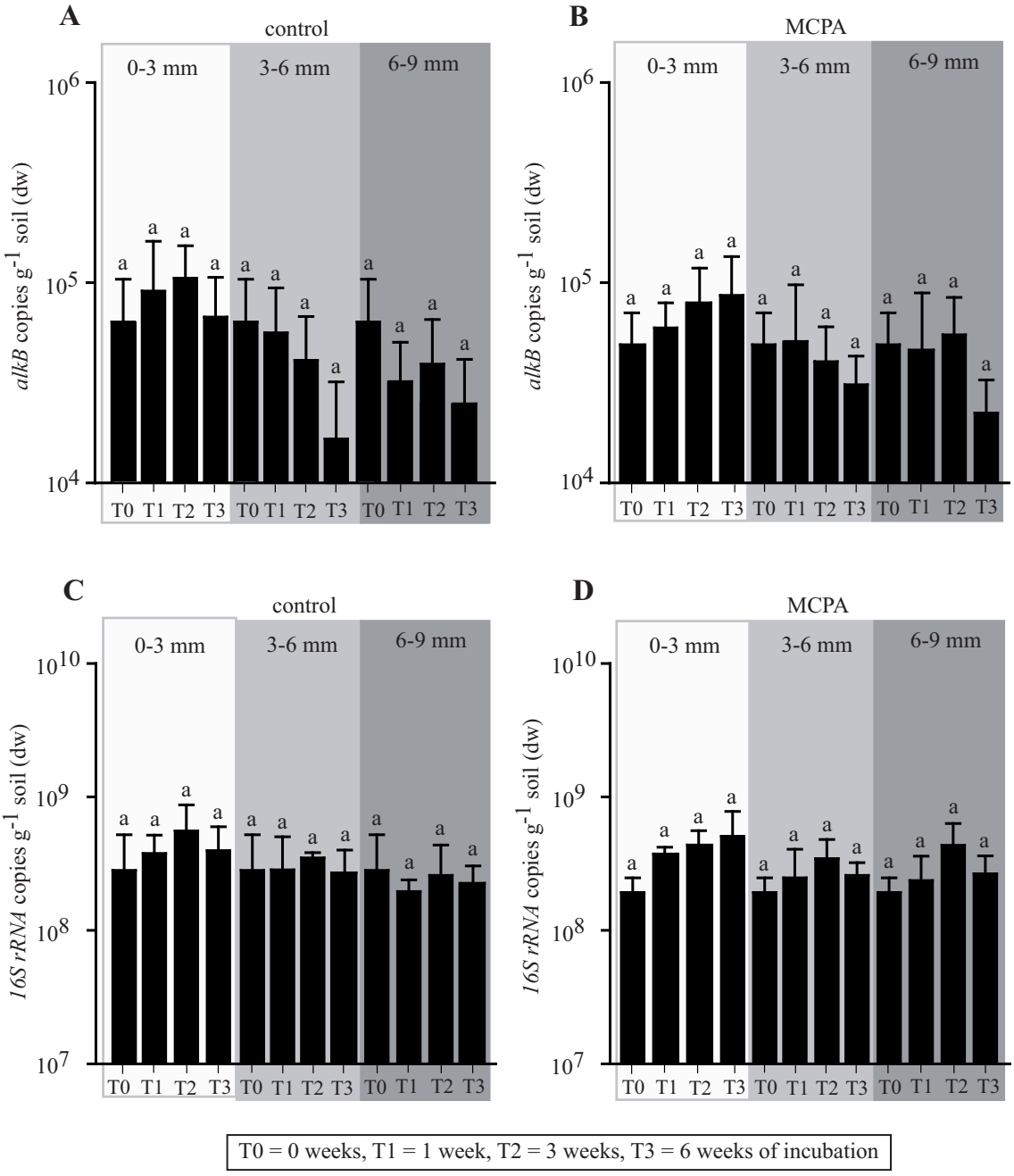

Fig. 29: Abundance of *alkB* and 16S rRNA genes during soil incubation with MCPA (E3)
The abundances of *alkB* (A, B) and 16S rRNA genes (C, D) were measured during the incubation of control (A, C) and MCPA spiked (B, D) soils at the beginning (T0) and after one (T1), three (T2) and six (T3) weeks of incubation. Error bars indicate standard deviations (n = 4). Significant temporal differences in the individual soil compartments ($P < 0.05$) are indicated by different small letters.

5.5 Overexpression of AlkB and production of anti-AlkB antibodies

5.5.1 Test of different incubation temperatures

Overnight cultures were used to inoculate two aliquots of fresh LB medium which were subsequently incubated at 30 °C until a OD_{550nm} of 0.6-0.7 was reached. After this, the expression of recombinant AlkB was induced by the addition of 200 ng mL^{-1} AHT and 0.1% (w/v) glucose followed by a prolonged incubation for additionally four hours at 20 °C and 30 °C respectively. During incubation, samples for monitoring the expression of *alkB* and subsequent synthesis of the respective enzyme, were taken hourly and analysed by gel electrophoresis of PCR products from *alkB* cDNA and 1D-SDS-PAGE as well. As shown in Figure 30C, expression of *alkB* reached its maximum at 20 °C already one hour after the application of the inducer (AHT).
With ongoing incubation, expression rates decreased and completely stopped four hours after induction. Contrarily, in cultivations done at 30 °C, expression rates were the highest three hours after induction but kept stable during ongoing incubation. Despite these differences, newly synthesized AlkB was detected one hour after induction at both temperatures. Interestingly, although expression rates were remarkably different between the two cultivation temperatures, synthesis of AlkB did not change with prolonged incubation and was additionally comparable for 20 °C and 30 °C (Fig. 30B, C).

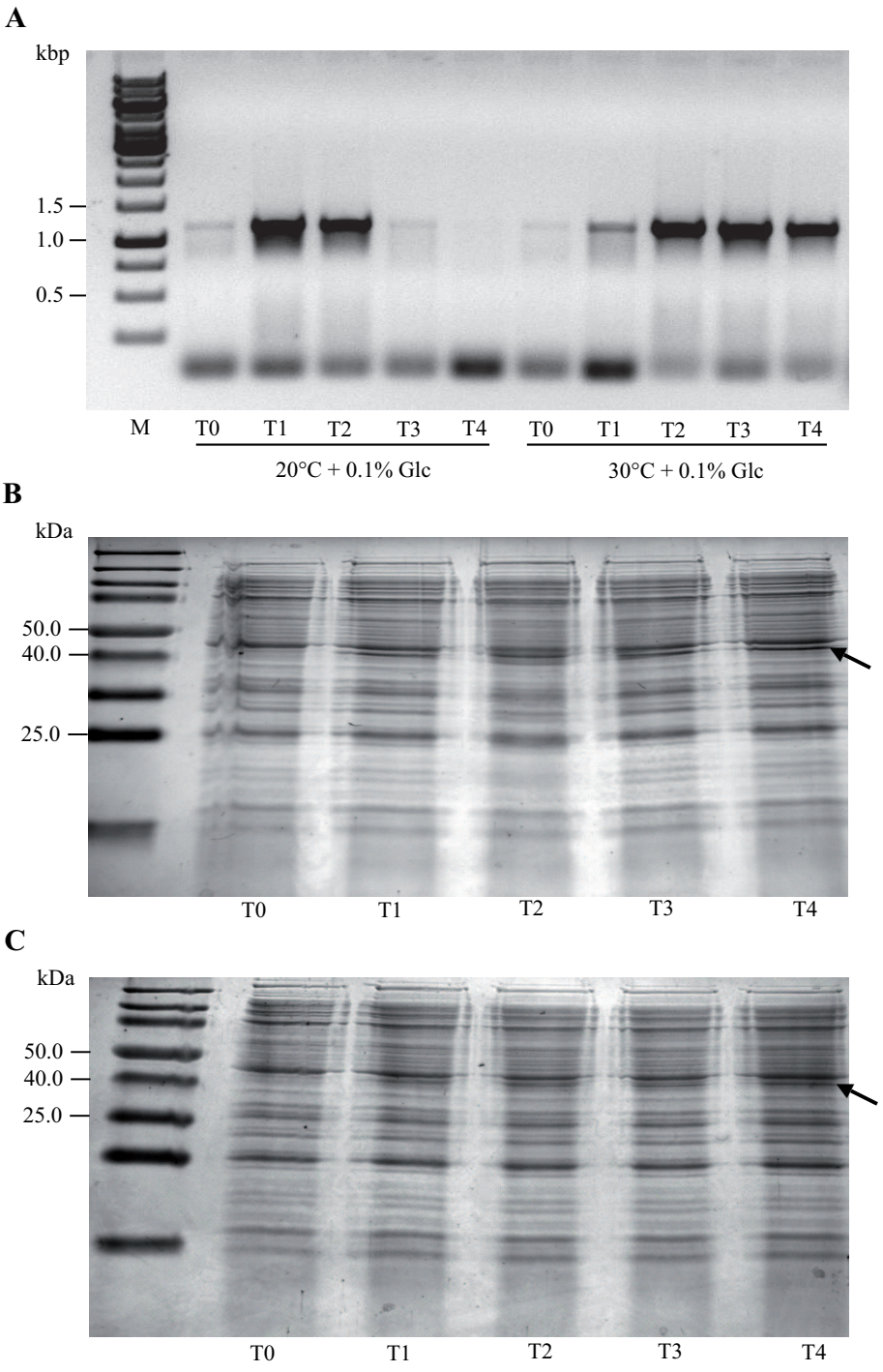

Fig. 30: Test of different incubation temperatures
The expression (A) of *alkB* and the consequent synthesis of the respective protein (B, C) was analysed during a four hour incubation at 20 °C (B) and 30 °C (C) by using gel electrophoresis and 1D-SDS-PAGE. Samples of amplified *alkB* cDNA as well as whole cell proteins were taken before (T0) and up to 4 hours (T1-T4) after induction of *E. coli* W3110 with AHT. The position of newly synthesized AlkB protein is indicated by an arrow.

5.5.2 Evaluation of the best cell densities for optimal induction

As the overexpression of membrane proteins is less sufficient as known for cytoplasmatic proteins, the yield of AlkB at moderate cell densities was very low. Therefore, it was tested if induction at higher cell densities would result in higher concentrations of AlkB *per se*. Cells of *E. coli* were grown at 37 °C and induction was accomplished by the application of AHT at late log-phase (OD_{550nm} = 0.8), early stationary-phase (OD_{550nm} = 1.7) and late stationary-phase (OD_{550nm} = 2.9). Sampling for qualitative 1D-SDS-PAGE was done two hours after induction respectively. Due to the high cell densities, disruption was done using FrenchPress (2x 1000 bar) since sonication was found to be unsuitable. The results presented in Figure 31 clearly demonstrate that despite an effect of the induction on the cell growth was monitored, an overexpression of AlkB neither occurred at the late log-phase nor the stationary phase. Subsequently, the overexpression of AlkB was induced at an optical density (550 nm) between 0.5-0.6 in the incubations used for large scale protein synthesis.

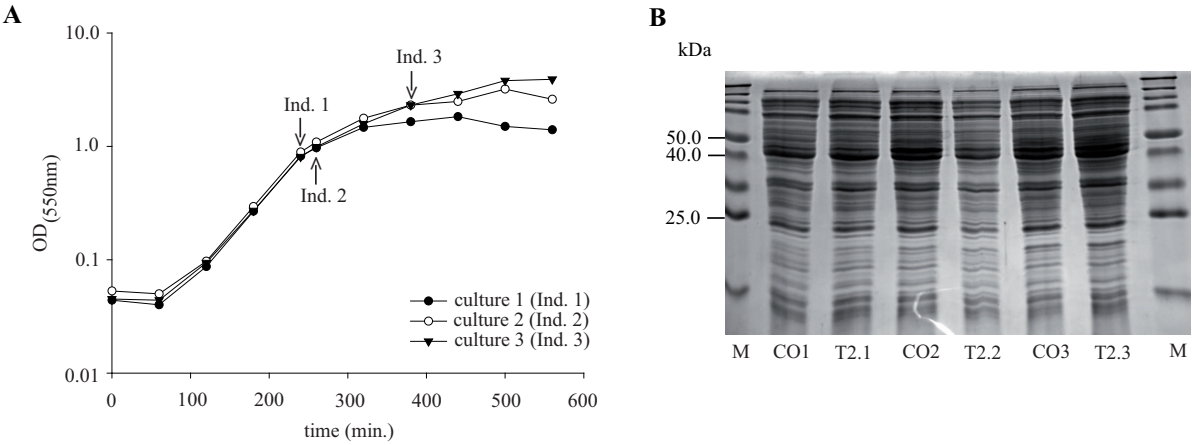

Fig. 31: Test of induction at different cell densities (OD_{550nm})
A) Growth of cells with induction of AlkB expression at the late log-phase (Ind. 1), the early-stationary phase (Ind. 2) and the late-stationary phase (Ind. 3). B) Synthesis of AlkB was monitored using 1D-SDS-Page of samples from non-induced cells (CO1-CO3) and cells 2h after induction (T2.1-T2.3).

5.5.3 Test of diverse cultivation media

Since overexpression of a protein in fast growing host strains can lead to the formation of inclusion bodies (not secreted misfolded proteins) and consequently low protein yield, growth and expression under different nutrition levels was tested. Therefore, an eutrophic (LB) and two nutrition-poor media (1/5 LB, R2A) were used, facilitating fast growth with high overexpression rate or slow growth with moderate protein expression respectively. The induction was set at a OD_{550nm} = 0.4-0.75 of cell cultures grown at 30 °C. This test was only done to monitor the bacterial growth after induction. The results, presented in Figure 32, clearly show that growth stopped after addition of AHT in LB and 1/5 LB media, whereas the supply with inducer had no influence on the growth in R2A medium. Nevertheless, the highest cell numbers were reached with LB medium after Bertani [23].

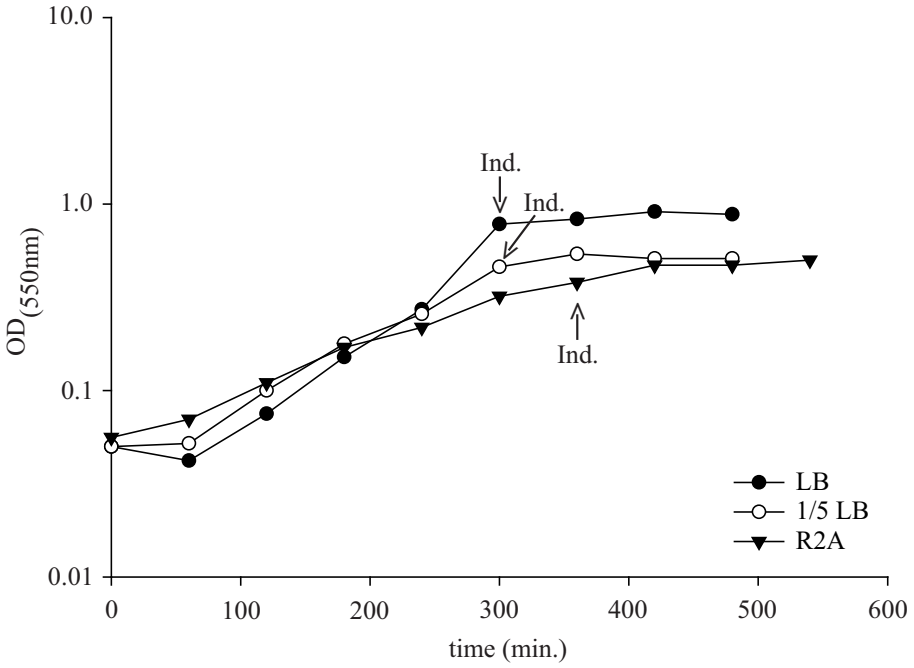

Fig. 32: Test of diverse cultivation media
Growth of *E. coli* W3110 in three different media with changing nutrition levels at 30 °C. Induction (Ind.) was done at optical densities between 0.4-0.75 (OD_{550nm})

5.5.4 Test of detergents as additives for effective cell disruption

By using the pASK-IBA6C expression vector, the recombinant proteins should be secreted into periplasm after synthesis. Unfortunately, no isolation of target protein was accomplished by forming spheroplasts or with isolation of the whole intracellular proteome (data not shown). Since six transmembrane domains were reported for AlkB, the protein could have been incorporated into the plasma membrane. To test this, ionic (SDS) and non-ionic (Triton® X-100) detergents were used to isolate membrane bound as well as membrane associated proteins. The extraction efficiency was tested by using these detergents in combination with sonication or pressure for cell disruption respectively. The results clearly demonstrate that no improvement of AlkB isolation was reached by using Triton® X-100, whereas the use of SDS was successful as summarized in Figure 33. Since no differences between the two cell disruption methods were monitored, sonication was used for large scale isolation of proteins due to reasons of feasibility.

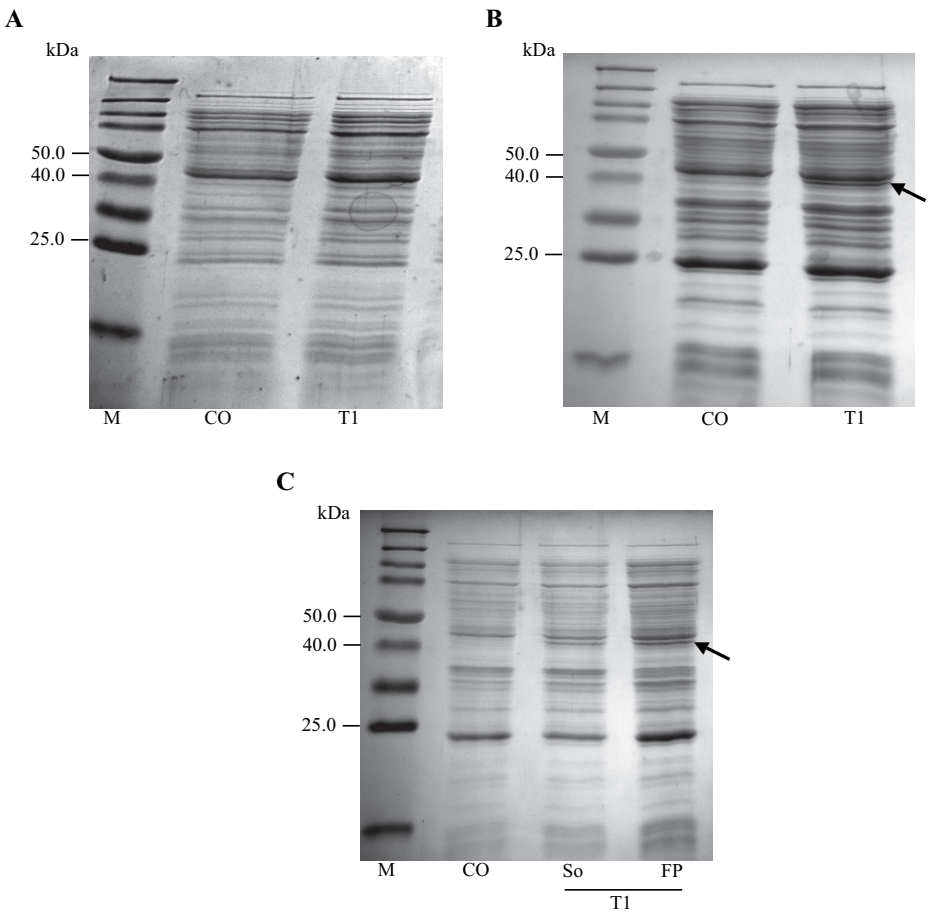

Fig. 33: Test of effective extraction of membrane proteins
1D-SDS-PAGE of membrane proteins from control cells (CO) and 2h after induction (T1). Protein extraction was done with sonication and the addition of Triton® X-100 (A) or 1.5% SDS (B) respectively. No differences in cell disruption efficiency were monitored during sonication (So) or FrenchPress (FP) with 1.5% SDS as additive (C). The presence of AlkB is indicated by an arrow.

5.5.5 Purification of AlkB with affinity columns

For the purification of overexpressed AlkB from whole cell protein extracts, a system was used where theoretically only proteins with a StrepTag would bind to the column matrix. Although a cultivation medium with low concentration of free biotin was used and cells of the host strain *E. coli* W3110 were known to have only limited amounts of biotinylated proteins, several contaminations have been observed after elution of AlkB from the column as demonstrated in Figure 34. Since all efforts done to get rid of the contaminants (e.g. increased ionic strength, blocking of biotin and biotinylated proteins with avidin) failed, the raw elution fractions could not be used and had to be further processed. For this, elution fractions E1-E5 have been pooled and loaded on a preparative PAA-gel. After electrophoretic separation of the proteins, the respective band representing AlkB was cut from the gel and used for the immunization of rabbits.

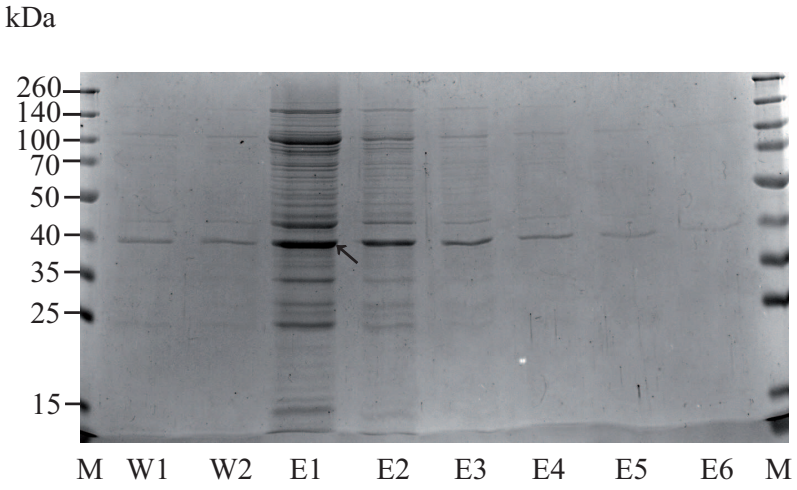

Fig. 34: Contaminants after column purification
Several contaminants were monitored after the purification of whole cell proteins with a StrepTactin column. With 1D-SDS-PAGE the purity of two wash steps (W1-W2) and all elution fractions (E1-E6) was tested. Presence of AlkB is indicated (arrow) and was additionally confirmed by mass spectrometry.

5.5.6 Test of antisera from different immunization stages

Four months after the first subcutaneous injection of the gel slices, aliquots of rabbit anti-sera were sampled, to analyse them for the occurrence of anti-AlkB immunoglobulins (Ig). As shown in Figure 35A, low amounts of anti-AlkB Igs could be detected already after 120 days when whole cell protein extracts of induced cultures were compared to the respective extracts of non-induced cells. Since AlkB was overexpressed in strains of *E.coli*, gained antisera also included antibodies against non specific target proteins. Subsequently, biased signals would be retrieved during the *in situ* detection of the alkane monooxygenase protein AlkB in environmental samples. To overcome this, immunization was prolonged to increase the specific amounts of anti-AlkB Igs. Antisera with high content of the respective antibodies could be used in high dilutions resulting in a decrease of unspecific binding. Therefore, samples taken after 180, 210 and finally 240 days were also tested for anti-AlkB by using elution fractions E2 and E3. Detected signals were related to Western Blot analyses using pre-immune sera. Unfortunately, signal intensities of proposed AlkB did not increase compared to the signals of unspecific target proteins (Fig. 35B, C). Furthermore, intensities decreased in some cases indicating decreasing amounts of anti-AlkB antibodies.

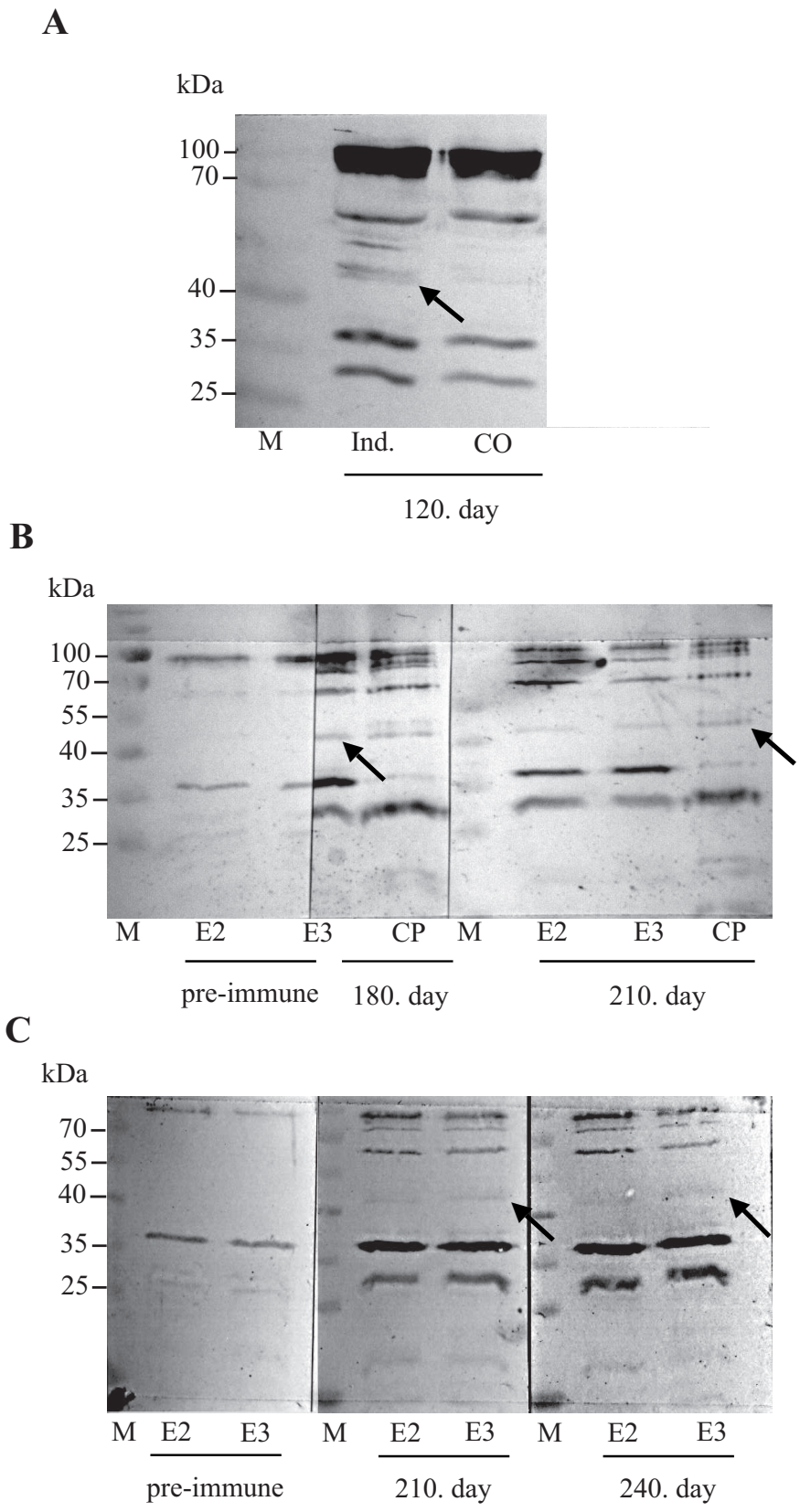

Fig. 35: Test of different immunization stages using Western Blots
The sensitivity of polyclonal anti-AlkB immunoglobulins was tested either by using whole cell proteins (CP) of induced (Ind.) and non-induced (CO) *E.coli* W3110 cells (A) or by using elution fractions (E2, E3) after affinity column purification (B, C). For tests using the elution fractions pre-immune sera were used as negative controls. Arrows indicate AlkB protein.

6 Discussion

Aliphatic hydrocarbons are highly abundant and ubiquitously distributed in the environment as a consequence of geochemical or anthropogenic activities. Due to the immense ecological and economical relevance, most studies focused on the bioremediation of hydrocarbons via the AlkB degradative pathway by analyzing artificially contaminated soils. For example, Alvarez *et al.* [7] examined the diversity of *alkB* in petroleum-contaminated soils from Brazil. In other studies, antarctic soils polluted with diesel oil or fuel were used to examine the abundance and diversity of *alkB* in environmental samples [166; 165; 246]. Furthermore, in experiments done by Margesin *et al.* [138] and Pérez de Mora *et al.* [169] the dynamic of *alkB* genes in alpine and forest soils was detected in relation to increasing amounts of total hydrocarbons (TH) with up to 35 g TH * kg^{-1} soil. Despite many efforts have been done in the last decades to analyse and optimize the bioremediation of hydrocarbons in soils, degradation of alkanes from natural sources was studied only marginally. Kloos *et al.* [107] were among the first who monitored high copy numbers of *alkB* in agricultural and forest soils that have not been artificially contaminated. Consequently, they proposed that the abundance of *alkB* was related to alkanes originated from decaying organic material like plant litter. In addition, in the analyses reported above, no attention on the microscale has been payed, as samples were destructively taken in most cases without maintaining the soil microhabitats. The present thesis links the dynamic of *alkB* genes and transcripts at distinct microhabitats with the degradation of plant litter material. Therefore not only the processes in the litter layer but also in different soil compartments were analysed in the course of time.

6.1 Decay of plant material and dynamic of *alkB* in the detritusphere and different soil compartments

During the first weeks of litter decay, easy degradable and water soluble compounds (e.g. amino acids, sugars, proteins) become congruently metabolized or transported into adjacent soil layers via leaching processes [116]. As a result, high losses of plant mass can be observed at this time. With ongoing incubation, litter quality changes with increasing concentrations of more recalcitrant substrates (e.g. lignin). As decomposition of these substrates is much complex, degradation rates become attenuated [72; 248]. Such two-step degradation of litter material was also observed in the present study. Here, the degradation of pea litter was significantly higher than detected for maize. This finding

might be explained by the remarkable discrepancies in the carbon to nitrogen ratios (C/N = 30 for maize [93], C/N = 12 - 16 for pea [131]), as nitrogen was found to be a driving factor for sufficient decomposition [59; 150; 224]. Moreover, by using mass spectrometry analyses of the litter types used in this Ph.D. thesis, differences in the alkane quality and quantity between the two plants were detected (**Publication III**). These findings support data of earlier studies, where significant higher wax alkane fractions were found in pea compared to maize [14; 66]. Nevertheless, amounts of alkanes are not only correlated to the genotype, but also impacted by the phenotype of the plant. As demonstrated for leaves of tree tobacco [27], accumulation of cuticular waxes and the corresponding amounts of alkanes was increased in response to environmental stresses like drought events. As a result of varying phytomorphologic conditions, the release of *n*-alkanes during the litter decay might be different and consequently influencing the abundance and activity of *alkB*-harbouring bacteria. Conversely, the dynamic of these bacteria might not be related to the degradation of alkanes only, as their amounts in the litter material were to low (**Publication III**). Therefore, the use of other litter derived easy degradable compounds [9; 163], released in higher amounts in pea litter, as well as co-metabolic degradation must be postulated, which is further supported by the general growth of total bacteria (*rpoB* genes). Despite this, succession of the bacterial community by epiphytic fungi, already present on the fresh litter [89], must be considered also. In consequence of potential antimycotic agents found in pea [40], growth of these fungi could be hampered in pea compared to maize litter, leading to increased bacterial growth.

Since *n*-alkanes are a major part of cuticulary waxes, they become released during the decomposition of plant litter material and subsequently enter the soil with the water flow. In response to the rising availability of nutrients, microbial activities in the detritusphere increase. Beare *et al.* [21] reported on a general progression of microbial biomass in a spatial and temporal manner, as a result of plant litter decay. The subsequent dispersion of released alkanes is thereby extremely linked to the chain length and the soil composition. For example, Leythaeuser and Schae [123] demonstrated decreasing mobility of light alkanes with increasing chain length, as a result of decreasing dissolving abilities in liquids. Furthermore, interactions of *n*-alkanes and soil compounds were identified as key players in their bioavailability. For instance, chain length dependent adsorption to soil organic matter (SOM) and clay minerals as well as the diffusion into smaller soil pores, inaccessible for microbes, were both demonstrated in several studies [24; 137; 176]. As a result, the macro-porosity of sandy soils in opposite to the micro-porosity of silty soils

might favor the alkane transport [11; 64]. Consequently, the activity and abundance of *alkB*-harbouring bacteria is differently impacted in the two soils. Anyhow, Löser *et al.* [130] reported on the ability of sand to restrain alkanes as well, which was supposed to be the consequence of a micro-porous surface of the sand particles. Besides, humic acids can act as reservoirs for aliphatic hydrocarbons and carboxylic acids (fatty acids) [102]. Alkanes introduced by plant residues before the incubation experiment started, could have been persisting in arable soils. Consequently, the microbial community might be impacted during the incubation experiment. In addition, this phenomenon could be more pronounced in silty than in sandy soils [189; 193] as a result of higher clay mineral contents. Interestingly these hypotheses are underlined by the detected dynamic of *alkB* genes in the control microcosms which were not incubated with litter material. As a result of the mentioned factors impacting the bioavailability of alkanes, hot spots of microbial activities occur, which have been pointed out to be highly important for the mineralization of litter derived compounds [63; 162]. However, the quantification of *alkB* in the litter-soil-interface compartment further support the hypothesis of a soil texture induced alkane sequestration. For instance, due to the properties of silty soil, alkanes were not removed by leaching processes leading to increased copy numbers of *alkB*. Conversely, alkane losses due to leaching resulted in constant amounts of *alkB* in the same compartment in sandy soils. Despite gene abundances kept constant or increased only slightly during the incubation, alkane concentrations decreased constantly (**Publication III**). Furthermore, the specific induction was reduced by trend in the same time in some compartments, indicating an attenuated gene expression. These findings might be explained by isochronic expression of *alkB* paralogues genes, which are expressed in dependence of the alkane chain length and the growth state of the cells respectively. For example, Tani *et al.* [216] reported on two alkane monooxygenase genes in *Acinetobacter* sp. M-1 which were differently expressed either by growth on medium- (C_{16} - C_{22}) or long-chained alkanes ($> C_{22}$), respectively. Furthermore, expression of *alkB2* from *P. aeruginosa* was highest during the early exponential phase, whereas *alkB1* was induced at the late exponential phase [141]. Beside this, the results could also point to alkane degradative systems relying on other catalytic enzymes including cytochromes P450 (CYP153, CYP52) [90; 235], AlmA [223], AlmA-related enzymes [134] as well as LadA [57]. Furthermore, it is considerable, that alkane derivates like fatty acids, alkanols and long-chained aldehydes, derived from metabolic pathways occurring in these systems, might be further metabolized by *alkB*-harbouring bacteria without using this gene (Fig. 7).

Anyhow, independent of the soil type, significant lower quantities of *alkB* were found in the soil compartments, compared to the litter layer. Beside the remarkable higher amounts of available nutrients in that layer, different community structures of *alkB*-harbouring bacteria in litter and soil compartments might lead to varying quantities. For example, as *alkB* can occur in up to five gene copies [240], increased quantities would be detected in communities including strains harbouring multiple *alkB* gene copies. As shown in **Publication III**, significantly different *alkB*-harbouring communities were detected in litter and soil compartments. Congruently, differences in the gene copy numbers of *alkB* in the litter-soil-interface layer of sandy and silty soil microcosms might also be the result of alternating communities. Interestingly, the respective layers shared more similarity with each other than to the corresponding bulk soil compartments. This further supports the hypothesis of the soil type dependent bioavailability of alkane in that compartment. In addition, co-metabolization of alkanes and other nutrients in litter type dependent amounts might also occur. In consequence of higher nitrogen amounts in pea litter, alkane degradation could be more effective leading to increasing amounts of *alkB*-harbouring bacteria. Nevertheless, no or only slight differences between the compartments of the individual soil microcosms were found on the expression level. It is therefore reasonable that other compounds than litter derived alkanes and the corresponding interaction with soil particles (e.g. minerals, organic matter) might play a role. For example, water soluble nutrients or electron receptors might influence the activity of *alkB*-harbouring alkane degraders rather than the compartment type. Furthermore, in most cases comparable tendencies in the specific induction of *alkB* were found between the different soil types, further supporting the impact of other factors.

6.2 Abundance of *alkB*-harbouring bacteria in different compartments of MCPA spiked soils

Herbicides like MCPA frequently reach the soils by getting washed from the leaves during rain fall or irrigation. Furthermore, the chemicals can enter the detritusphere, when litter material is introduced to it by the activity of soil eukaryotes (e.g. earthworms) or by tillage. Despite many studies focusing on the fate of MCPA in the environment were accomplished in the last decades (e.g. [39; 82; 128; 227]), knowledge about the impact on distinct functional bacteria is still rudimental. Tejada *et al.* [220] reported that MCPA is a potential inhibitor for the activity of telluric enzymes. Contrary, no negative effect on the soil microbial community was monitored, even after excessive application [8; 45; 244; 266; 220]. Nevertheless, it is considerable that the alkane monooxygenase

AlkB could also be hampered by this herbicide. MCPA, which is an acid anionic herbicide, can potentially adsorb to minerals in dependency of the soil pH (e.g. [46; 222]) or the soil organic matter content (e.g. [22; 73; 74]). Consequently, abundance of MCPA might be heterogeneous in the soil matrix, with comparatively high amounts in the litter-soil-interface layer and lower concentrations in bulk soil. Therefore, the influence of MCPA on *alkB*-harbouring bacteria in different soil depths was analysed.

The present study could not reveal a significant impact of MCPA on the abundance of *alkB* genes. Comparable trends in the dynamic of *alkB*-harbouring bacteria were monitored in all soil compartments of water and MCPA amended microcosms. In the litter-soil-interface layer, increasing amounts of *alkB* were congruent to copy numbers of 16S rRNA suggesting that easy degradable compounds (e.g. glucose, amino acids) rather than litter derived alkanes might be the driving factors for bacterial growth. The dynamic of *alkB* revealed comparable tendencies to the dynamic of *alkB*-harbouring bacteria found in experiment 1. Although completely different time points were sampled and various plant litter was used in both experiments (maize and pea in E1, wheat in E3), an increase in the abundance of *alkB* in the litter-soil interface layer during the incubation was observed. Conversely, dynamics differed in the bulk soil layers. Furthermore, gene copy numbers were about three orders of magnitude lower in E3, despite the same soil type was used in both experiments. As reviewed by Bardgett *et al.* [17], soil microbial community structures seasonally change depending on the nutrient availability. For example, bacteria dominate microbial biomass in autumn, whereas fungi are more pronounced in winter. Consequently, preparation of soil samples for the incubation experiments at different seasons (e.g. autumn in case of E1 and winter in case of E3 respectively) might explain variations in the copy numbers.

However, the data of the present thesis revealed a direct influence of the herbicide on the amount of total bacteria. The slight increase of 16S rRNA in the bulk soil layers (3 - 6 mm, 6 - 9 mm) of MPCA amended microcosms, could point to the promotion of MCPA degrading bacteria. In addition, **Publication IV** could demonstrate the complete dispersal of the herbicide within six weeks after application, which further supports this theory. Besides, a stimulation of MCPA degraders in these compartments could also be accomplished by water soluble biostimulants derived from the decaying litter material [164; 220]. In contrast to this, recent studies [82; 164] proposed that the observed tendency could be the result of MCPA loss via leaching processes or adsorption to minerals and organic matter. Nevertheless, by high resolution quantification of 16S rRNA genes in microcosms covered with maize, Poll *et al.* [164] demonstrated a steep gradient for-

mation of total bacteria with the source at the litter-soil interface and the sink in deeper bulk soil layers. Conversely, the present thesis revealed only slight changes in the abundance of total bacteria in the different soil compartments. On the one hand, this could be the consequence of a low resolution due to methodical limitations. On the other hand, discrepancies could also be the result of different C:N ratios as various plant litter types were used. In the present thesis pea litter was used, which has a higher nitrogen content compared to maize. Consequently, leaching nitrogen might result in an improved supply in the soil compartments, leading to elevated bacterial growth. Furthermore, soil fungi in the detritusphere might play in important role in the translocation of bacteria. For instance, in a study of Wong and Griffin [258] bacterial movement along the hyphae of dead fungi was demonstrated. Moreover, several studies revealed the active translocation of bacteria in the water films coating the hyphae of proliferating fungi [122; 253]. Anyhow, the differences in the relative distributions of short- and long-chained alkanes monitored in water and MCPA amended soils suggest slight changes in the community structure of alkane degrading microorganisms. In MCPA contaminated soils alkane degrading systems other than the AlkB-related pathways (e.g. Cyp153, Cyp52) could be privileged. Temporal shifts in the bacterial community structure, which were induced by the addition of MCPA, were demonstrated earlier by Vieublé Gonod *et al.* [244]. Furthermore, as a consequence of an impeded enzymatic activity of AlkB as shown for authochthonous laccases and glutamine-dehydrogenases [161; 187], response to litter derived alkanes could be delayed.

6.3 Dynamic of *alkB* in artificial soils

During litter decay, easy degradable compounds as well as alkanes are released into the detritusphere. By entering the soil, these compounds differentially interact with clay minerals leading to alternating bioavailabilities. In consequence of this interaction, distribution of substrates in the soil matrix as well as abundances of microbial consumers is very heterogeneous.

However, due to their hydrophilic surface, clay minerals are supposed to be ineffective sorbents for adsorbing organic compounds like hydrocarbons [104; 171]. In fact, several studies focusing on the clay minerals montmorillonite and illite were done, reporting on sufficient adsorption of aromatic hydrocarbons like toluene, xylene or benzene [125; 124; 151]. On the contrary, no interaction between aliphatic hydrocarbons and montmorillonite was monitored in earlier studies. For instance, MacEwan [133] found no adsorption of *n*-hexane and *n*-heptane, even when boiling the mineral in these liquids.

Furthermore, Barshad [18] supposed these findings to be the result of the non-polar nature of the minerals. Anyhow, the results of the present experiment clearly demonstrated a gradient formation in the soils of both ages. The highest abundances of *alkB* genes were monitored in the litter-soil-interface layers, whereas lower amounts were found in the bulk soils. On the one hand, this could be a direct response of *alkB*-harbouring bacteria to the release of litter derived alkanes as also indicated by the data from E1 and E3. On the other hand, retention of alkanes in natural soils is mediated by the adsorption to soil organic matter (e.g. humic substances), which is drastically reduced in the artificial soils. Since no binding of saturated hydrocarbons to clay minerals was observed before, leaching of alkanes into deeper soil layers is considerable. Conversely, persistence of hydrocarbons in the analysed soils could be impacted by weak van der Waals forces. These forces mediate the temporal limited attraction between non-polar molecules like alkanes. As physico-chemical analyses of different compounds like montmorillonite, illite and charcoal revealed surface areas between 100,000 and 800,000 m^2 kg^{-1} [55; 125; 148], the van der Waals forces might be increased. In consequence weak interactions between alkanes and these compounds could occur. However, no significant differences between the mixtures were found indicating other factors than alkanes to be the driving factor for bacterial performance. For example, the enhanced growths of total bacterial after litter amendment might be the consequence of easy degradable compounds. Interestingly, *alkB* gene copy numbers in the artificial soils were significantly reduced compared to natural soils where amounts up to 5.5 * 10^5 copies ng^{-1} DNA were detected [107]. Due to the fact, that manure was supplied only once at the beginning of pre-aging, nutrients might become depleted during the incubation. As a result, microbial activity would be reduced after twelve months of pre-aging, where microbial response to retreated nutrient supply (e.g. via litter application) would be increased. *Vice versa*, due to the fact that residues of manure would be still available at this time, the response to substrate addition after three months of pre-aging would be attenuated as demonstrated by the T1/T0 ratios. Anyhow, decreasing microbial activity during pre-aging was confirmed by CO_2 respiration measurements frequently done in parallel to the incubation [170]. Moreover, increased response to litter amendment in the twelve month pre-aged soils could be the result of recombination processes also. As demonstrated in several studies, clay minerals potentially act as reservoirs for free DNA [67; 68; 155], facilitating spontaneous recombination of microbial cells [103; 129]. It is therefore considerable, that non-alkane degraders could be transformed with released *alkB* genes, contributing to the microbial alkane degrading community.

6.4 Methodical consideration

In the present Ph.D. thesis quantities of genes and transcripts were compared. Since the extraction of nucleic acids from environmental samples is challenging and influenced by various factors (e.g. incomplete cell disruption [62], sorption of released nucleic acids to minerals [114]), a successful isolation in sufficient amounts is neither guaranteed nor reproducible. To reduce insufficient yields, DNA and RNA can either be extracted separately by divers affinity column extraction kits or simultaneously by using a phenol-chloroform extraction protocol after Griffiths *et al.* [69]. Interestingly, none of the protocols mentioned above can effectively remove humic substances due to physico-chemical properties being comparable to those of nucleic acids. These substances are potential inhibitors for enzymatic downstream applications and were shown to i) interfere with lytic enzymes [91], ii) bind DNA and Proteins in general [261] or iii) influence the interaction of DNA polymerase and their targets [219]. However, to enhance comparability of the abundances of genes and transcripts, co-extraction of DNA and RNA by using phenol-chloroform was done in the present thesis. Hampering effects of eventually remained inhibitors were reduced by the dilution of samples below the contaminant's minimum inhibitory concentration (MIC) during real-time PCR. For instance, several studies demonstrated the MIC of humic substances in the range of 0.1 and 0.2 ng μL^{-1} [112; 221]. Furthermore, additives like BSA can also reduce the hampering effects by increasing the MIC of humic substances.

In the present study, serial dilutions of the samples and the addition of BSA to the PCR reaction mixture were used. Furthermore, the efficiency of gene quantification by real-time PCR is strongly dependent on i) the effective binding of the primers to the template, ii) a sufficient denaturation of the target DNA and iii) high activity of the DNA polymerase. Beside the use of degenerated primers, which have been improved by the introduction of inosine nucleotides, magnesium chloride and BSA were added to the PCR reaction mixtures (**Publication II**). As a result, amplification efficiencies could be improved and increased up to 86%.

Anyhow, after data achievement a decision needed to be done, whether the results should be related to i) one gram of soil, to ii) ng of isolated DNA or cDNA or to iii) copy numbers of housekeeping genes like 16S rRNA or *rpoB* respectively. In the first case an increase in abundances of genes and transcripts is directly linked to an elevated biomass and enhanced activity. On the contrary, linking data to extracted nucleic acids might lead to an overestimation, as DNA and cDNA which are not corresponding to certain bacterial or fungal groups might be co-extracted (e.g. herbal DNA or DNA from small inverte-

brates). In the latter case, amounts of target genes are related to different functional groups, which can be challenging. As known from literature, numbers of 16S rRNA operons can vary between the different bacterial taxa [3] leading to a total of one to 15 chromosomal copies [106]. In contrast, relation of the data to the abundance of the highly conserved *rpoB* gene, could be an alternative as it occurs in single chromosomal copies only [41]. In the present study data about the abundance of *alkB* genes and transcripts were correlated to the amount of soil used for extraction. Analyses of the abundance of total bacteria were dependent on the respective experiment and were either related to 16S rRNA (E3) or *rpoB* (E1). Temporal shifts in the community structure from r- to k-strategists and soil type dependent availability of nutrients and water, require the analysis of a single copy gene (*rpoB*) when comparing two different soils (E1) with each other. Conversely, in an experiment, where only different compartments within one soil should be analysed during a short time (E3) incubation, the more frequently used 16S rRNA genes were the best standard.

6.5 Overexpression of AlkB and synthesis of polyclonal anti-AlkB antibodies

Despite becoming a standard procedure in the most laboratories, large scale protein synthesis is still challenging. Numerous factors like i) the codon usage of the host strain, ii) the nutrient level of the cultivation medium and iii) the incubation temperature influence the effectivity of protein production and secretion, particularly of membrane proteins like AlkB. The protein production at non-physiological levels might lead thereby to a stalled secretion, due to the limited capacity of the protein translocation machinery in *Escherichia coli* (e.g Sec-dependent pathways) [183]. In consequence nascent proteins are not formed correctly during the passage through the membrane, resulting in truncated polypetides and inclusion bodies. Under those conditions, decreased yields might be the consequence of a secretion stress induced protease activity. To overcome this, incubation was done at 30 °C as a reduction of incubation temperatures was shown to be beneficial (exemplarely [65; 195]), which was also indicated in the present study by a constant growth rate after induction. By using *E. coli* strain W3110 the maximum synthesis rate of AlkB was achieved already one hour after induction. Congruently, AlkB amounts reached only around 4.5% of the total protein, which is in contradiction to the 10 - 15% reported in other studies where overexpression using the pGEc47-vector was done [153; 157].

In order to simplify the purification of overexpressed AlkB, the protein was fused to

the signal sequence of membrane protein OmpA, accomplishing its secretion into the periplasm. The AlkB protein could not be isolated from the periplasm but was extractable from whole cell extracts by the use of sodium-dodecylsulfate (SDS), which was confirmed by mass spectrometry analysis. As SDS facilitates the disintegration of phospholipid layers, this finding might either indicate the formation of intracellular low-density vesicles containing AlkB [153] or a stalled translocation of the protein due to the six hydrophobic transmembrane domains (TMD) acting as molecular anchors. In consequence, AlkB could be accumulated in the cell membranes of the host strains as proposed earlier by Nieboer *et al.* [154].

However, large amounts of contaminating proteins with molecular weights between 25 and 100 kDa were monitored after the purification of whole cell extracts from *E. coli*. On the one hand those contaminants could be co-isolated biotinylated proteins like the biotin carboxyl carrier protein (BCCP), which is one of the subunits of the acetyl-CoA carboxylase complex (ACC) [32]. This highly unstable complex could disintegrate during gel electrophoresis with 0.1% SDS resulting in numerous bands of different molecular weights (e.g. BCCP = 16.7 kDa, Carboxyltransferase = 35 kDa, Biotin Carboxylase = 49.4 kDa). On the other hand, Ruettinger *et al.* [186] proposed that the alkane monooxygenase itself (also known as ω-hydroxylase) can occour in large complexes with a molecular weight up to $2 * 10^3$ kDa. In solutions with low SDS contents (e.g. 0.075% SDS as used during the load of the purification column) such complexes would be intact but collapse into smaller subunits (e.g. up to 42 kDa) at higher amounts of SDS as used in the 1D-SDS-PAGE-running buffer after Laemmli *et al.* [118].

Anyhow, neither the specific blocking of BCCP with avidin nor the disruption of bound ACC by increased ionic strength, in order to get protein fractions below 40 kDa, were successful.

In the present study, excised gel slices containing AlkB were used for the immunization of rabbits. Due to the low protein yield, only minor contents could be used for subcutaneous injection at once. The subsequent antisera, which where supposed to contain anti-AlkB antibodies, were tested monthly with samples from non-induced and induced cells. In the latter, bands were detected which were absent in non-induced cells and might consequently indicate the production of low amounts of anti-AlkB antibodies already 120 days after first injection. Despite the frequent injection of gel slices, increasing amounts of anti-AlkB were not detected, as signal strength remained constant. In addition, detected bands which were supposed to represent AlkB, offered higher molecular weights as expected. Anyhow, during gel electrophoresis, proteins are separated

by their molecular weight and not by their conformation. In this context, migration of membrane proteins can be different from cytoplasmatic ones, as more SDS is bound to the increased number of TMD's. For instance, significant higher amounts of SDS adsorbed to the transmembrane protein CP-B_2 from *Rhodospirillum rubrum* [149] compared to cytoplasmatic proteins [175]. Furthermore, aggregation of highly hydrophobic membrane associated proteins was observed when they were boiled in classical Laemmli buffer [191]. This phenomenon was also reported earlier for lactose permease [245] and bacteriorhodopsin [87]. As a result, a shifted protein migration during SDS-PAGE was monitored. Hence, the exact determination of the molecular weight by using general molecular size standards is hampered.

Regardless of the reported difficulties, Xie *et al.* [262] were recently able to isolate large amounts of overexpressed AlkB from the phospholipid fraction of *E. coli* strain DE3. In their study, yields of approximately 1 mg of biological active AlkB were reported, when disruption and solubilisation of the cytoplasmatic membrane was done using 10 times the critical micillium concentration (CMC) of lauryldimethylamino oxide (LDAO). This detergent showed no interference during the binding of strep-tagged proteins to the Streptactin residues as monitored with 1.5% SDS (6.5 CMC). Consequently, the new protocol might be suitable for the general isolation of high amounts of membrane proteins. Nevertheless, other strategies for the production of mono- or polyclonal anti-AlkB antibodies should be considered also. For instance, the *in vitro* synthesis of short AlkB peptides representing the interregional parts between the different transmembrane domains (refer to Figure 5) could be used for the production of peptide antibodies. Since the extracellular located regions are to short to result in sufficient polypetides, the use of the corresponding intracellular linkers might be more successful. In order to get an suitable peptide sequence for immunization, AlkB1 (NP_251264.1) and AlkB2 (NP_250216.1), which both catalyze the initial step in the degradation of middle-chained alkanes ($C_{16}-C_{24}$ and $C_{12}-C_{20}$ respectively), were analysed *in silico* in the present Ph.D. thesis. Therefore, sequences of both proteins were individually blasted against all microbial protein sequences available up to date at the NCBI database. All amino acid sequences from fakultativ and obligate soil microorganisms which showed a query coverage of $>85\%$ were subsequently blasted against each other to find conserved regions. As a result, only a few conserved regions beside the histidine motifs were found. A region directly located next to histdine motif four (HIS 4) revealed high convergence and was consequently chosen for the extraction of a consensus sequence (ANPTRSYQALRHFDDAPQLP) as shown in Figure 36. To check for

its specificity, the chosen sequence was blasted once more against all available microbial AlkB proteins. As Table 12 summarizes, only alkane degrading bacteria using the AlkB-related alkane degradation pathway were revealed. Interestingly, representatives from α-, β-, γ-proteobacteria, Actinobacteria as well as the Bacteroidetes/ Chlorobi-group and thereby also inhabitants of marine environments were retrieved, which emphasises the overall detection in different habitats.

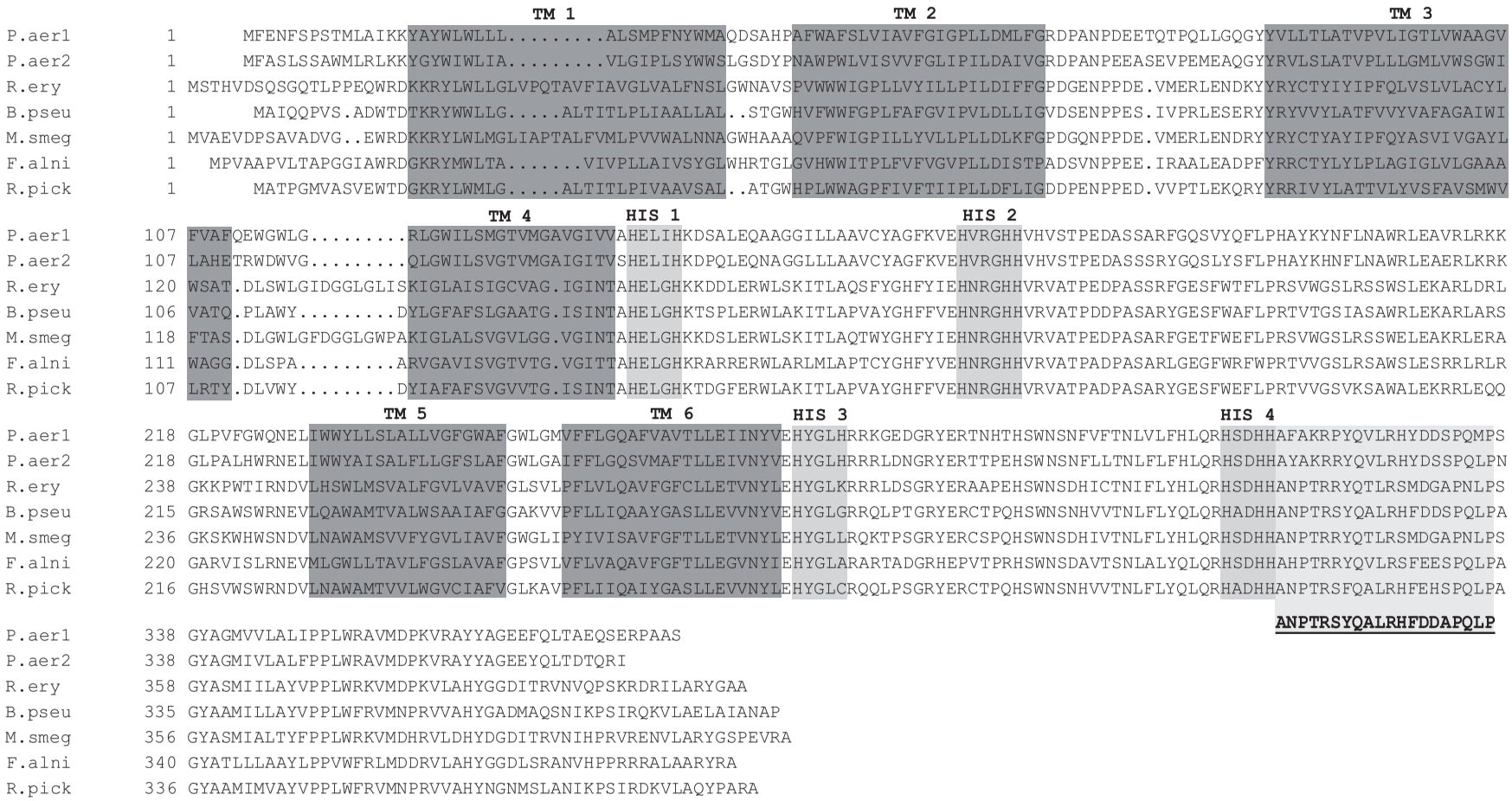

Fig. 36: Alignment of AlkB from different organisms
Alignment of amino acid sequences of AlkB from different strains. Four highly conserved histidine motifs (HIS 1-4) represent the catalytic center of the monooxygenase. Helices spanning the cytoplasma membrane are also indicated (TM 1-6). Conserved regions for the extraction of the consensus sequence suitable for the production of polypeptide antibody are labeled also (bold underlined). P.aer1 = AlkB1, *Pseudomonas aeruginosa* PAO1; P.aer2 = AlkB2, *P. aeruginosa* PAO1; R.ery = *Rhodococcus erythropolis* SK121; B.pseu = *Burkholderia pseudomallei* 305; M.smeg = *Mycobacterium smegmatis* MC2 155; F.alni = *Frankia alni*; R.pick = *Ralstonia pickettii*12J

strain	accession number (NCBI)	e-value
Alcanivorax borkumensis SK2*	YP_694427.1	$6 * 10^{-2}$
Acinetobacter sp. DR1	YP_003732938.1	$1 * 10^{-4}$
A. junii SH205	ZP_06065934.1	$8 * 10^{-3}$
A. baumannii ATCC19606	ZP_05827357.1	$8 * 10^{-3}$
A. calcoaceticus RUH2202	ZP_06056754.1	$8 * 10^{-3}$
A. haemolyticus ATCC19194	ZP_06725872.1	$8 * 10^{-3}$
Burkholderia ubonensis Bu	ZP_02380481.1	$3 * 10^{-6}$
B. cenocepacia AU1054	YP_620386.1	$3 * 10^{-6}$
B. multivorans ATCC17616	YP_001945311.1	$3 * 10^{-6}$
B. ambifara AMMD	YP_772734.1	$7 * 10^{-6}$
B. pseudomallei 305	ZP_01764629.1	$7 * 10^{-6}$
B. gladioloi BSR3	YP_004361423.1	$6 * 10^{-5}$
Caulobacter sp. K31*	YP_001672212.1	$5 * 10^{-2}$
Conexibacter woesei DSM14684	YP_003397515.1	$2 * 10^{-3}$
Microscilla marina ATCC23134*	ZP_01689499.1	$1 * 10^{-2}$
Mycobacterium sp. JDM601	YP_004525252.1	$1 * 10^{-2}$
Pseudomonas fluorescens Pf-5	YP_260041.1	$9 * 10^{-6}$
P. mendocina ymp	YP_001188237.1	$2 * 10^{-2}$
P. aeruginosa PAO1	ZP_06878434.1	$3 * 10^{-2}$
Psychrobacter sp. PRwf-1	YP_001280943.1	$2 * 10^{-2}$
Ralstonia sp. 5_7_47FAA	ZP_07673680.1	$6 * 10^{-4}$
R. pickettii 12J	YP_001892637.1	$6 * 10^{-4}$
Rhodococcus erythropolis SK121	ZP_04388098.1	$3 * 10^{-3}$
R. opacus B4	YP_002776786.1	$2 * 10^{-2}$
R. jostii RHA1	YP_702497.1	$6 * 10^{-2}$
Runella slithyformis DSM19594	YP_004654946.1	$3 * 10^{-2}$
Tsukamurella paurometabola DSM20162	YP_003647687.1	$9 * 10^{-3}$

Tab. 12: Specifity of AlkB polypeptide consensus sequence
Selection of strains with sequence homology to the polypeptide consensus sequence of AlkB for the production of polyclonal anti-AlkB peptide antibodies. *) associated with marine environments

7 Conclusion and Outlook

As a consequence of the interplay of different clay minerals and organic matter, soil matrices comprise an extremely large surface area. In various soil compartments, microbial turnover processes take place, which are dependent on the bioavailability of substrates like litter derived *n*-alkanes. In dependency of their physico-chemical properties, interaction with clay particles might be different resulting in declining concentrations. Thus, a gradient might be formed from the litter to deeper soil compartments, also impacting the abundance of microbial alkane degraders. In the present thesis, gradients of *alkB*-harbouring bacteria have been monitored in agricultural as well as artificially mixtured soils mimicking natural habitats. In arable soils gene abundances were thereby dependent on the soil type, as no gradient formation was observed in sandy soil microcosms. Contrarily, experimental results of the artificial soils gave no hint for the impact of distinct soil minerals. Despite differences in the herbal alkane quantity and quality, no impact of the litter type on the dynamic of *alkB* genes along the gradient was found in natural or artificial soils. Nevertheless, litter quality slightly influenced the activity of *alkB*-harbouring bacteria as demonstrated in experiment 1. However, the results indicate other components (e.g. easy degradable compounds or electron acceptors) than litter derived alkanes as the driving factors for the abundance of *alkB* genes and transcripts at the different soil compartments.
In spite of the potential inhibitory effects of herbicides on the soil microbial community, an impact of MCPA on *alkB*-harbouring bacteria was not found.

Since alkane degradation processes at the soil microscale are complex and still poorly understood, further analyses highlighting the microbial community structure and activity need to be done. For instance, the dynamic of other alkane degraders (e.g. bacteria and fungi harbouring *cyp52* and *cyp153* genes) in relation to the total bacterial and fungal community would be interesting. The combination of FISH-techniques and the use of antibodies against soil proteins could give insights about the distribution of *alkB*-harbouring alkane degraders and the corresponding AlkB-proteins. Anyhow, the adsorption of free DNA to clay minerals rises questions about the microbial evolution at different soil compartments and the dispersal of alkane degrading ability. Consequently, analyses including artificial soils with different clay minerals should be expanded. Finally, questions should be asked, whether similar results would be obtained with other substrates with different physico-chemical properties (e.g. glucose, aromatic hydrocarbons).

References

[1] Aber, J., and Melillo, J. Litter decomposition: measuring relative contributions of organic matter and nitrogen to forest soils. *Canadian Journal of Botany 58* (1980), 416–421.

[2] Abeyrathne, P., and Lam, J. Conditions that allow for effective transfer of membrane proteins onto nitrocellulose membrane in Western blots. *Canadian Journal of Microbiology 53* (2007), 526–532.

[3] Acinas, S., Marcelino, L., Klepac-Ceraj, V., and Polz, M. Divergence and redundancy of 16S rRNA sequences in genomes with multiple rrn operons. *Journal of Bacteriology 186* (2004), 2629–2635.

[4] Aeckersberg, F., Bak, F., and Widdel, F. Anaerobic oxidation of saturated hydrocarbons to CO_2 by a new type of sulfate-reducing bacterium. *Archives of Microbiology 156*, 1 (1991), 5–14.

[5] Aeckersberg, F., Rainey, F. A., and Widdel, F. Growth, natural relationships, cellular fatty acids and metabolic adaptation of sulfate-reducing bacteria that utilize long-chain alkanes under anoxic conditions. *Archives of Microbiology 170*, 5 (1998), 361–369.

[6] Al-Mailem, D., Sorkhoh, N., Al-Awadhi, H., Eliyas, M., and Radwan, S. Biodegradation of crude oil and pure hydrocarbons by extreme halophilic archaea from hypersaline coasts of the arabian gulf. *Extremophiles 14* (2010), 321–328.

[7] Alvarez, V., Santos, S., Casella Rda, C., Vital, R., Sebastin, G., and Seldin, L. Bioremediation potential of a tropical soil contaminated with a mixture of crude oil and production water. *Journal of Microbiology and Biotechnology 18* (2008), 1966–1974.

[8] Anderson, J. Pesticide effects on non-target soil microorganisms. In *Pesticide Microbiology*, I. Hill and S. Wright, Eds. Academis Press, London, 1978, pp. 611–628.

[9] Aneja, M., Sharma, S., Fleischmann, F., Stich, S., Heller, W., Bahnweg, G., Munch, J., and Schloter, M. Microbial colonization of beech and spruce litter - influence of decomposition site and plant litter species on the diversity of microbial community. *Microbial Ecology 52* (2006), 127–135.

[10] Aneja, M., Sharma, S., Munch, J., and Schloter, M. RNA fingerprinting - a new method to screen for differences in plant litter degrading microbial communities. *Journal of Microbiological Methods 59* (2004), 223–231.

[11] Arthurs, P., Stiver, W., and Zytner, R. Passive volatilization of gasoline from soil. *Journal of Soil Contamination 4* (1995), 123–135.

[12] Ashraf, M., and Mehmood, S. Response of four brassica species to drought stress. *Environmental and Experimental Botany 30* (1990), 93–100.

[13] Austin, A., and Vivanco, L. Plant litter decomposition in a semi-arid ecosyszem controlled by photodegradation. *Nature 442* (2006), 555–558.

[14] Avato, P., Bianchi, G., and Pogna, N. Chemosystematics of surface lipids from maize and some related species. *Phytochemistry 29* (1990), 1571–1576.

[15] Bach, H.-J., Tomanova, J., Schloter, M., and Munch, J. Enumeration of total bacteria and bacteria with genes for proteolytic activity in pure cultures and in environmental samples by quantitative PCR mediated amplification. *Journal of Microbiological Methods 49* (2002), 235–245.

[16] Baik, M., Newcomb, M., Friesner, R., and Lippard, S. Mechanistic studies on the hydroxylation of methane by methane monooxygenase. *Chemical Reviews 103* (2003), 2385–2419.

[17] Bardgett, R., Bowman, W., Kaufmann, R., and Schmidt, S. A temporal approach to linking aboveground and belowground ecology. *TRENDS in Ecology and Evolution 20*, 11 (2005), 634–641.

[18] Barshad, I. Factors affecting the interlayer expansion of vermiculite and montmorillonite with organic substances. *Soil Science Society of America - Proceedings 16* (1952), 176–182.

[19] Bartha, R., and Bossert, I. The treatment and disposal of petroleum wastes. In *Petroleum Microbiology*, R. Atlas, Ed. Macmillan, New York, NY, USA, 1984, pp. 553–578.

[20] Beal, R., and Betts, W. Role of rhamnolipids in the uptake and mineralization of hexadecane in *Pseudomonas aeruginosa*. *Journal of Applied Microbiology 89* (2000), 158–168.

[21] Beare, M., Coleman, D., Crossley, D., Hendrix, P., and Odum, E. A hierarchical approach to evaluating the significance of soil biodiversity to biogeochemical cycling. *Plant and Soil 170* (1995), 5–22.

[22] Bekbölet, M., Yenigün, O., and Yücel, I. Sorption studies of 2,4-D on selected soils. *Water, Air and Soil Pollution 111* (1999), 75–88.

[23] Bertani, G. Studies on lysogenesis I. The mode of phage liberation by lysogenic *Escherichia coli*. *Journal of Bacteriology 62* (1951), 293–300.

[24] Bosma, T. N. P., Middeldorp, P. J. M., Schraa, G., and Zehnder, A. J. B. Mass transfer limitation of biotransformation: quantifying bioavailability. *Environmental Science and Technology 31* (1996), 248–252.

[25] Brandt, L., King, J., Hobbie, S., Milchunas, D., and Sinsabaugh, R. The role of photodegradation in surface litter decomposition across a grassland ecosystem precipitation gradient. *Ecosystems 13* (2010), 765–781.

[26] Callaghan, A., Gieg, L., Kropp, K., Suflita, J., and Young, L. Comparison of mechanisms of alkane metabolism under sulfate-reducing conditions among two bacterial isolates and a bacterial consortium. *Applied and Environmental Microbiology 72* (2006), 4274–4282.

[27] Cameron, K., Teece, M., and Smart, L. Increased accumulation of cuticular wax and expression of lipid transfer protein in response to periodic drying events in leaves of tree tobacco. *Plant Physiology 140* (2006), 176–183.

[28] Canosa, I., Sanchez-Romero, J., Yuste, L., and Rojo, F. A positive feedback mechanism controls expression of AlkS, the transcriptional regulator of the *Pseudomonas oleovorans* alkane degradation pathway. *Molecular Microbiology 35* (2000), 791–799.

[29] Chaineau, C., Morel, J.-L., and Oudot, J. Microbial degradation in soil microcosms of fuel oil hydrocarbons from drilling cuttings. *Environmental Science and Technology 29* (1995), 1615–1621.

[30] Chakrabarty, A., Chou, G., and Gunsalus, I. Genetic regulation of octane dissimilation plasmid in *Pseudomonas*. *Proceedings of the National Academy of Sciences of the United States of America 70* (1973), 1137–1140.

[31] Chen, Q., Janssen, D., and Witholt, B. Physiological changes and *alk* gene instability in *Pseudomonas oleovorans* during induction and expression of *alk* genes. *Journal of Bacteriology 178* (1996), 5508–5512.

[32] Choi-Rhee, E., and Cronan, J. The biotin carboxylase-biotin carboxyl carrier protein complex of *Escherichia coli* acetyl-CoA carboxylase. *The Journal of Biological Chemistry 278* (2003), 30806–30812.

[33] Christensen, B. Barley straw decomposition under field conditions: effect of placement and initial nitrogen content on weight loss and nitrogen dynamics. *Soil Biology and Biochemistry 18* (1986), 523–529.

[34] Cochran, W. Estimation of bacterial densities by means of the "most probable number". *Biometrics 6*, 2 (1950), 105–116.

[35] Collister, J., Rieley, G., Stern, B., Eglinton, G., and Fry, B. Compound-specific δ13C analyses of leaf lipids from plants with differing carbon dioxide metabolisms. *Organic Geochemistry 21* (1994), 619–627.

[36] Coûteaux, M., Monrozier, J., and Bottner, P. Increased atmospheric CO_2 chemical changes in decomposing sweet chestnut (*Castanea sativa*) leaf litter incubated in microcosms under increasing food web complexity. *Oikos 76* (1996), 553–563.

[37] Craft, D., Madduri, K., Eshoo, M., and Wilson, C. Identification and characterization of the CYP52 family of *Candida tropicalis* ATCC20336, important for the conversion of fatty acids and alkanes to α,ω-dicarboxylic acids. *Applied and Environmental Microbiology 69* (2003), 5983–5991.

[38] Cranwell, P. Chain-length distribution of n-alkanes from lake sediments in relation to post-glacial environmental change. *Freshwater Biology 3* (1973), 259–265.

[39] Crespín, M., Gallego, M., and Valcárcel, M. Study of the degradation of the herbicide 2,4-D and MCPA at different depths in contaminated agricultural soil. *Environmental Science and Technology 35*, 21 (2001), 4265–4270.

[40] Cruickshank, I., and Perrin, D. Isolation of a phytoalexin from *Pisum sativum* L. *Nature 187* (1960), 799–800.

[41] Dahllhöf, I., Baillie, H., and Kjelleberg, S. rpob-based microbial community analysis avoids limitations inherent in 16S rRNA gene intraspecies heterogeneity. *Applied and Environmental Microbiology 66*, 8 (2000), 3376–3380.

[42] Davidova, I., Duncan, K., Choi, O., and Suflita, J. *Desulfoglaeba alkanexedes* gen. nov., sp. nov., an alkane-degrading, sulfate-reducing bacterium. *International Journal of Systematic and Evolutionary Microbiology 56* (2006), 2737–2742.

[43] Davis, J., and Yarbrough, H. Anaerobic oxidation of hydrocarbons by *Desulfovibrio desulfuricans*. *Chemical Geology 1* (1966), 137–144.

[44] Dibble, J., and Bartha, R. Effect of environmental parameters on the biodegradation of oil sludge. *Applied and Environmental Microbiology 37* (1979), 729–739.

[45] Duah-Yentumi, S., and Johnson, D. Changes in soil microflora in response to repeated applications of some pesticides. *Soil Biology and Biochemistry 18* (1986), 629–635.

[46] Dyson, J., Beulke, S., Brown, C., and Lane, M. Adsorption and degradation of the weak acid mesotrione in soil and environmental fate implications. *Journal of Environmental Quality 31* (2002), 613–618.

[47] Eggink, G., Engel, H., Vriend, G., Terpstra, P., and Witholt, B. Rubredoxin reductase of *Pseudomonas oleovorans* - Structural relationship to other flavoprotein oxidoreductases based on one NAD and two FAD fingerprints. *Journal of Molecular Biology 212* (1990), 135–142.

[48] Eglinton, G., Gonzalez, A. G., Hamilton, R. J., and Raphael, R. A. Hydrocarbon constituents of the wax coatings of plant leaves: A taxonomic survey. *Phytochemistry 1*, 2 (1962), 89–102.

[49] Eglinton, G., and Hamilton, R. J. Leaf epicuticular waxes. *Science 156* (1967), 1322–1335.

[50] Ehrenreich, P. Anaerobes Wachstum neuartiger sulfatreduzierender und nitratreduzierender Bakterien auf *n*-Alkanen und Erdöl. *PhD thesis*, *University of Bremen*, 1996.

[51] Ehrenreich, P., Behrends, A., Harder, J., and Widdel, F. Anaerobic oxidation of alkanes by newly isolated denitrifying bacteria. *Archives of Microbiology 173*, 1 (2000), 58–64.

[52] Eickhorst, T., and Tippkötter, R. Detection of microorganisms in undisturbed soil by combining fluorescence in situ hybridization (FISH) and micropedological methods. *Soil Biology and Biochemistry 40*, 6 (2008), 1284–1293.

[53] Eickhorst, T., and Tippkötter, R. Improved detection of soil microorganisms using fluorescence in situ hybridization (fish) and catalyzed reporter deposition (card-fish). *Soil Biology and Biochemistry 40* (2008), 1883–1891.

[54] Ellsworth, D., Rittenhouse, K., and Honeycutt, R. Artifactual variation in randomly amplified polymorphic DNA banding patterns. *BioTechniques 14* (1993), 214–217.

[55] Endo, S., Grathwohl, P., Haderlein, S., and Schmidt, T. Characterization of sorbent properties of soil organic matter and carbonaceous geosorbents using *n*-alkanes and cycloalkanes as molecular probes. *Environmental Science and Technology 43* (2009), 393–400.

[56] Esperschütz, J., Welzl, G., Schreiner, K., Buegger, F., Munch, J., and Schloter, M. Incorporation of carbon from decomposing litter of two pioneer plant species into microbial communities of the detritusphere. *FEMS Microbiology Letters 320* (2011), 48–55.

[57] Feng, L., Wang, W., Cheng, J., Ren, Y., Zhao, G., Gao, C., Tang, Y., Liu, X., Han, W., Peng, X., Liu, R., and Wang, L. Genome and proteome of long-chain alkane degrading *Geobacillus thermodenitrificans* NG80-2 isolated from a deep-subsurface oil reservoir. *Proceedings of the National Academy of Sciences of the United States of America 104* (2007), 5602–5607.

[58] Finnerty, W., and Singer, M. Membranes of hydrcarbon-utilizing microorganisms. In *Microbial Metabolism of Straight-Chain and Branched Alkanes*, R. Atlas, Ed. Macmillan, New York, 1985, pp. 1–60.

[59] Fioretto, A., Di Nardo, C., Papa, S., and Fuggi, A. Lignin and cellulose degradation and nitrogen dynamics during decomposition of three leaf litter species in a mediterranean ecosystem. *Soil Biology and Biochemistry 37* (2005), 1083–1091.

[60] Fogel, P., and Cromack, K. J. Effect of habitat and substrate quality on Douglas fir litter decomposition in western Oregon. *Canadian Journal of Botany 33* (1977), 1632–1640.

[61] Frankenberger, W., and Johanson, J. Influence of crude oil and refined petroleum products on soil dehydrogenase activity. *Journal of Environmental Quality 11* (1982), 602–607.

[62] Frostegård, A., Courtois, S., Ramisse, V., Clerc, S., Bernillon, D., Le Gall, F., Jeannin, P., Nesme, X., and Simonet, P. Quantification of bias related to the extraction of dna directly from soils. *Applied and Environmental Microbiology 65* (1999), 5409–5420.

[63] Gaillard, V., Chenu, C., and Recous, S. Carbon mineralisation in soil adjacent to plant residues of contrasting biochemical quality. *Soil Biology and Biochemistry 35* (2003), 93–99.

[64] Galin, T., Gerstl, Z., and Yaron, B. Soil pollution by petroleum products, iii. kerosene stability in soil columns as affected by volatilization. *Journal of Contaminant Hydrology 5* (1990), 375–385.

[65] Georgiou, G., and Valax, P. Expression of correctly folded proteins in *Escherichia coli*. *Current Opinion in Biotechnology 7* (1996), 190–197.

[66] Gniwotta, F., Vogg, G., Gartmann, V., Carver, T., Riederer, M., and Jetter, R. What do microbes encounter at the plant surface? Chemical composition of pea leaf cuticular waxes. *Plant Physiology 139* (2005), 519–530.

[67] Goring, C., and Bartholomew, W. Adsorption of mononucleotides, nucleic acids and nucleoproteins by clays. *Soil Science 74* (1952), 149–164.

[68] Greaves, M., and Wilson, M. The adsorption of nucleic acids by montmorillonite. *Soil Biology and Biochemistry 1* (1969), 317–323.

[69] Griffiths, R., Whiteley, A., O'Donnell, A., and Bailey, M. Rapid method for coextraction of DNA and RNA from natural environments for analysis of ribosomal DNA- and rRNA-based microbial community composition. *Applied and Environmental Microbiology 66* (2000), 5488–5491.

[70] Grund, A., Shapiro, J., Fennewald, M., Bacha, P., Leahy, J., Markbreiter, K., Nieder, M., and Toepfer, M. Regulation of alkane oxidation in *Pseudomonas putida*. *Journal of Bacteriology 123* (1975), 546–556.

[71] Gulis, V., and Suberkropp, K. Effect of inorganic nutrients on relative contributions of fungi and bacteria to carbon flow from submerged decomposing leaf litter. *Microbial Ecology 45* (2003), 11–19.

[72] Ha, K., Marschner, P., BÃijnemann, E., and Smernik, R. Chemical changes and phosphorus release during decomposition of pea residues in soil. *Soil Biology and Biochemistry 39* (2007), 2696–2699.

[73] Haberhauer, G., Pfeifer, L., Gerzabek, M., Kirchmann, H., Aquino, A., Tunega, D., and Lischka, H. Response of sorption processes of MCPA to the amount and origin of organic matter in a long-term field experiment. *European Journal of Soil Science 52* (2001), 279–286.

[74] Haberhauer, G., Pfeiffer, L., and Gerzabek, M. Influence of molecular structure on sorption of phenoxyalkanoic herbicides on soil and its particle size fractions. *Journal of Agricultural and Food Chemistry 48* (2000), 3722–3727.

[75] Hamamura, N., Fukui, M., Ward, D. M., and Inskeep, W. P. Assessing soil microbial populations responding to crude-oil amendment at different temperatures using phylogenetic, functional gene (*alkB*) and physiological analyses. *Environmental Science and Technology 42* (2008), 7580–7586.

[76] Hammel, K. Fungal degradation of lignin. In *Driven by nature: Plant litter quality and decompostion.*, G. Cadish and K. Giller, Eds. CAB International, Wallingford, 1997, pp. 33–45.

[77] Hara, A., Baik, S., Syutsubo, K., Misawa, N., Smits, T. H. M., and Beilen, J. B. v. Cloning and functional analysis of *alkB* genes in *Alcanivorax borkumensis* SK2. *Environmental Microbiology 6* (2004), 191–197.

[78] Harper, S., and Lynch, J. The chemical components and decomposition of wheat straw leaves, internodes and nodes. *Journal of the Science of Food and Agriculture 32* (1981), 1057–1062.

[79] Heister, K., Höschen, C., Pronk, G., Müller, C., and Kögel-Knabner, I. NanoSIMS as a tool for characterizing soil model compounds and organomineral associations in artificial soils. *Journal of Soils and Sediments* (2011), 35–47.

[80] Hendrickson, O. Variation in the c :n ratio of substrate mineralized during forest humus decomposition. *Soil Biology and Biochemistry 17* (1985), 435–440.

[81] Herrera, A., and Cockell, C. Exploring microbial diversity in volcanic environments: A review of methods in DNA extraction. *Journal of Microbiological Methods 70* (2007), 1–12.

[82] Hiller, E., Bartal', M., Milicka, J., and Ceranský, S. Environmental fate of the herbicide MCPA in two soils as affected by the presence of wheat ash. *Water, Air and Soil Pollution 197* (2009), 395–402.

[83] Hinrichs, K.-U., Hayes, J., Sylva, S., Brewer, P., and Delong, E. Methane-consuming archaebacteria in marine sediments. *Nature 398* (1999), 802–805.

[84] Holben, W., Jansson, J., Chelm, B., and Tiedje, J. DNA probe method for the detection od specific microorganisms in the soil bacterial community. *Applied and Environmental Microbiology 54* (1988), 703–711.

[85] Holland, P., Abramson, R., Watson, R., and Gelfand, D. Detection of specific polymerase chain reaction product by utilizing the 5' → 3' exonuxlease activity of *Thermus aquaticus* DNA polymerase. *Proceedings of the National Academy of Sciences of the United States of America 88* (1991), 7276–7280.

[86] Holloway, P. Plant cuticles: physicochemical characteristics and biosynthesis. In *Air pollutants and the leaf cuticle*, K. Percey, J. Cape, R. Jagels, and C. Simpson, Eds., vol. 36. NATA ASI Series, 1994, pp. 1–13.

[87] Huang, K.-S., Bayley, H., Liao, M.-J., London, E., and Khorana, H. Refolding of an integral membrane protein. *The Journal of Biological Chemistry 256* (1981), 3802–3809.

[88] Huang, Y., Dupont, L., Samtheim, M., Hayes, J., and Eglinton, G. Mapping of C4 plant input from North West Africa into North East Atlantic sediments. *Geochimica 64* (2000), 3505–3513.

[89] Hudson, H. The ecology of fungi on plant remains above the soil. *New Phytologist 67* (1968), 837–874.

[90] Iida, T., Sumita, T., Ohta, A., and Takagi, M. The cytochrome P450 *alk* multigene family of an *n*-alkane-assimilating yeast, *Yarrowia lipolytica*: Cloning

and characterization of genes coding for new CYP52 family members. *Yeast 16* (2000), 1077–1087.

[91] Jacobsen, C., and Rasmussen, O. Development and application of a new method to extract bacterial DNA from soil based on seperation of bacteria from soil with cation-exchange resin. *Applied and Environmental Microbiology 58* (1992), 2458–2462.

[92] Jawson, M., and Elliott, L. Carbon and nitrogen transformations during wheat straw and root decomposition. *Soil Biology and Biochemistry 18* (1986), 15–22.

[93] Johnson, J., Barbour, N., and Lachnicht Weyers, S. Chemical composition of crop biomass impacts its decomposition. *Soil Biology and Biochemistry 71* (2007), 155–162.

[94] Jones, J. The effect of environmental factors on estimated viable and total populations of planktonic bacteria in lakes and experimental enclosures. *Freshwater Biology 7* (1977), 67–91.

[95] Jones, J., Knight, M., and Byron, J. Effect of gross population by kerosene hydrocarbons on the microflora of a moorland soil. *Nature 227* (1970), 1166.

[96] Jones, J., and Young, B. Major parrafin constituents of microbial cells with particular references to *Chromatium sp. Archives of Microbiology 70* (1970), 82–88.

[97] Kappler, A., and Newman, D. Formation of Fe(iii)-minerals by Fe-oxidizing photoautotrophic bacteria. *Geochimica et Cosmochimica Acta 68* (2004), 1217–1226.

[98] Katopodis, A. G., Smith, H. A., and May, S. W. New oxyfunctionalization capabilities for ω-hydroxylases. asymmetric aliphatic sulfoxidation and branched ether demethylation. *Journal of the American Chemical Society 110* (1988), 897–899.

[99] Katopodis, A. G., Wimalasena, K., Lee, J., and May, S. W. Mechanistic studies on non-heme iron monooxygenase catalysis: epoxidation, aldehyde formation and demethylation by the ω-hydroxylation system of *Pseudomonas oleovorans*. *Journal of the American Chemical Society 106* (1984), 7928–7935.

[100] Kerstiens, G. Signalling across the divide: a wider perspective of cuticular structure-function relationships. *Trends in Plant Science 1* (1996), 125–129.

[101] Keyser, P., Kirk, T., and Zeikus, J. Ligninolytic enzyme system of *Phanerochaete chrysosporium*: Synthesized in the absence of lignin in response to nitrogen starvation. *Journal of Bacteriology 135* (1978), 790–797.

[102] Khan, S., and Schnitzer, M. The retention of hydrophobic organic compounds by humic acid. *Geochimica et Cosmochimica Acta 36* (1972), 745–754.

[103] Khanna, M., and Stotzky. Transformation of *Bacillus subtilis* by DNA bound on montmorillonite and effect of DNase on the transforming ability of bound DNA. *Applied and Environmental Microbiology 58* (1992), 1930–1939.

[104] Kim, J., Shin, W., Kim, Y., Choi, S., Jeon, Y., and Song, D. Sequential sorption and desorption of chlorinated phenols in organoclays. *Water Science & Technology 47* (2003), 59–64.

[105] Kirby, R. Actinomycetes and lignin degradation. *Advances in Applied Microbiology 58* (2006), 125–168.

[106] Klappenbach, J., Dunbar, J., and Schmidt, T. rRNA operon copy number reflects ecological strategies of bacteria. *Applied and Environmental Microbiology 66* (2000), 1328–1333.

[107] Kloos, K., Munch, J., and Schloter, M. A new method for the detection of alkane-monooxygenase homologous genes (*alkB*) in soils based on PCR-hybridization. *Journal of Microbiological Methods 66* (2006), 486–496.

[108] Kniemeyer, O., Musat, F., Sievert, S., Knittel, K., Wilkes, H., Blumenberg, M., Michaelis, W., Classen, A., Bolm, C., Joye, S., and Widdel, F. Anaerobic oxidation of short-chain hydrocarbons by marine sulphate-reducing bacteria. *Nature 449* (2007), 898–901.

[109] Kok, M., Oldenhuis, R., van der Linden, M. P., Raatjes, P., Kingma, J., van Lelyveld, P. H., and Witholt, B. The *Pseudomonas oleovorans* alkane hydroxylase gene. Sequence and expression. *Journal of Biological Chemistry 264* (1989), 5435–5441.

[110] Kotani, T., Yamamoto, T., Yurimoto, H., Sakai, Y., and Kato, N. Propane monooxygenase and NAD(+)-dependent secondary alcohol dehydrogenase in propane metabolism of *Gordonia sp.* strain TY-5. *Journal of Bacteriology 185* (2003), 7120–7128.

[111] Käppeli, O., and Finnerty, W. Partition of alkanes by an extracellular vesicle derived from hexadecane-grown *Acinetobacter*. *Journal of Bacteriology 140* (1979), 707–712.

[112] Kreader, C. Relief of amplification inhibition in PCR with bovine serum albumin or T4 gene 32 protein. *Applied and Environmental Microbiology 62* (1996), 1102–1106.

[113] Kropp, K., Davidova, I., and Suflita, J. Anaerobic oxidation of *n*-dodecane by addition reaction in a sulfate-reducing bacterial enrichment culture. *Applied and Environmental Microbiology 66* (2000), 5393–5398.

[114] Krsek, M., and Wellington, E. Comparison of different methods for the isolation and purification of total community DNA from soil. *Journal of Microbiological Methods 39* (1999), 1–16.

[115] Kubartová, A., Ranger, J., Berthelin, J., and Beguiristain, T. Diversity and decomposing ability of saprophytic fungi from temperate forest litter. *Microbial Ecology 58* (2009), 98–107.

[116] Kumar, K., and Goh, K. Crop residues and management practices: effects on soil quality, soil nitrogen dynamics, crop yield, and nitrogen recovery. *Advances in Agronomy 68* (2000), 197–319.

[117] Ladygina, N., Dedyukhina, E., and Vainshtein, M. A review on microbial synthesis of hydrocarbons. *Process Biochemistry 41* (2006), 1001–1014.

[118] Laemmli, U. Cleavage of structural proteins during the assembly of the head of bacteriophage T4. *Nature 227* (1970), 680–685.

[119] Laishram, I., and Yadava, P. Lignin and nitrogen in the decomposition of leaf litter in sub-tropical forest ecosystem at Shiroy hills in north-eastern India. *Plant and Soil 106* (1988), 59–64.

[120] Lamarque, A., Fortunato, R., and Guzmán, C. Seed oil alkanes from leguminosae species: Evencarbon number preference. *Phytochemistry 49* (1998), 731–736.

[121] Leahy, J., and Colwell, R. Microbial degradation of hydrocarbons in the environment. *Microbiological Reviews 54* (1990), 305–315.

[122] Leben, C. Spread of plant pathogenic bacteria with fungal hyphae. *Phytopathology 74* (1984), 983–986.

[123] Leythaeuser, D., and Schae, R. Role of diffusion in primary migration of hydrocarbons. *American Association of Petroleum Geologists Bulletin 66* (1982).

[124] Li, Y., and Gupta, G. Adsorption of hydrocarbons by clay minerals from gasoline. *Journal of Hazardous Materials 38* (1994), 105–112.

[125] Li, Y., and Gupta, G. Adsorption/desorption of hydrocarbons on clay minerals. *Chemosphere 28* (1994), 627–638.

[126] Lieberman, R., and Rosenzweig, A. Biological methane oxidation: Regulation, biochemistry, and active site structure of particulate methane monooxygenase. *Critical Reviews in Biochemistry and Molecular Biology 39* (2004), 147–164.

[127] Liu, C., Wang, W., Wu, Y., Zhou, Z., Lai, Q., and Shao, Z. Multiple alkane hydroxylase systems in a marine alkane degrader, *Alcanivorax dieselolei* B-5. *Environmental Microbiology 13* (2011), 1168–1178.

[128] Loos, M., Schlosser, I., and Mapham, W. Phenoxy herbicide degradation in soils: Quantitative studies of 2,4-D- and MCPA-degrading microbial populations. *Soil Biology & Biochemistry 11* (1979), 377–385.

[129] Lorenz, M., and Wackernagel, W. Natural genetic transformation of pseudomonas stutzeri by sand-adsorbed dna. *Archives of Microb 154* (1990), 380–385.

[130] Löser, C., Seidel, H., Hoffmann, P., and Zehnsdorf, A. Bioavailability of hydrocarbons during microbial remediation of a sandy soil. *Applied Microbiology and Biotechnology 51* (1999), 105–111.

[131] Ludidi, N., Pellny, T., Kiddle, G., Dutilleul, C., Groten, K., van Heerden, P., Dutt, S., Powers, S., RÃűmer, P., and Foyer, C. Gentic

variation in pea (*Pisum sativum* L.) demonstrates the importance of root but not shoot C/N ratios in the control of plant morphology and reveals a unique relationship between shoot length and nodulation intensity. *Plant, Cell and Environment 30* (2007), 1256–1268.

[132] Lynch, J. Promotion and inhibition of soil aggregate stabilization by microorganisms. *Journal of General Microbiology 126* (1981), 371–375.

[133] MacEwan, D. Complexes of clays with organic conpounds. i. complex formation between montmorillonite and halloysite and certain organic liquids. *Transactions of the Faraday Society 44* (1948), 349–367.

[134] Maeng, J., Sakai, Y., Tani, Y., and Kato, N. Isolation and characterization of a novel oxygenase that catalyzes the first step of *n*-alkane oxidation in *Acinetobacter sp.* strain M-1. *Journal of Bacteriology 178* (1996), 3695–3700.

[135] Maffei, M. Chemotaxonomic significance of leaf wax *n*-alkanes in the *Umbelliferae, Cruciferae* and *Leguminosae* (subf. *Papilionoideae*). *Biochemical Systematics and Ecology 24* (1996), 531–545.

[136] Maier, T., Foerster, H.-H., Asperger, O., and Hahn, U. Molecular characterization of the 56-kDa CYP153 from *Acinetobacter sp.* EB104. *Biochemical and Biophysical Research Communications 286* (2001), 652–658.

[137] Manilal, V., and Alexander, M. Factors affecting the microbial degradation of phenanthrene in soil. *Applied Microbiology and Biotechnology 35* (1991), 401–405.

[138] Margesin, R., Labbe, D., Schinner, F., Greer, C. W., and Whyte, L. G. Characterization of hydrocarbon-degrading microbial populations in contaminated and pristine alpine soils. *Applied and Environmental Microbiology 69* (2003), 3085–3092.

[139] Margesin, R., and Schinner, F. Bioremediation of diesel-oil-contaminated alpine soils at low temperatures. *Applied Microbiology and Biotechnology 47* (1997), 462–468.

[140] Marin, M. M., Smits, T. H. M., Beilen, J. B. v., and Rojo, F. The alkane hydroxylase gene of *Burkholderia cepacia* RR10 is under catabolite repression control. *Journal of Bacteriology 183* (2001), 4202–4209.

[141] Marin, M. M., Yuste, L., and Rojo, F. Differential expression of the components of the two alkane hydroxylases from *Pseudomonas aeruginosa*. *Journal of Bacteriology 185* (2003), 3232–3237.

[142] May, S. W., and Abbott, B. J. Enzymatic epoxidation I. Alkene epoxidation by the ω-hydroxylation system of *Pseudomonas oleovorans*. *Biochemical and Biophysical Research Communications 48* (1972), 1230–1234.

[143] May, S. W., and Katopodis, A. G. Oxygenation of alcohol and sulphide substrates by a prototypical non-haem iron monooxygenase: catalysis and biotechnological potential. *Enzyme and Microbial Technology 8* (1986), 17–21.

[144] McKenna, E. J., and Coon, M. J. Enzymatic ω-oxidation: IV. Purification and properties of the ω-hydroxylase of *Pseudomonas oleovorans*. *Journal of Biological Chemistry 245* (1970), 3882–3889.

[145] Mehboob, F., Junca, H., Schraa, G., and Stams, A. Growth of *Pseudomonas chloritidis* mutants AW-1T on *n*-alkanes with chlorate as electron acceptor. *Applied Microbiology and Biotechnology 83* (2009), 739–747.

[146] Melillo, J., Aber, J., and Muratore, J. Nitrogen and lignin control of hardwood leaf litter decomposition dynamics. *Ecology 63* (1982), 621–626.

[147] Membrillo-Hernández, J., Núnez-De La Mora, A., Rio-Albrechtsen del, T., Camocho-Carranza, R., and Gomez-Eichelmann, M. Thermally-induced cell lysis in *Escherichia coli* K12. *Journal of Basic Microbiology 35*, 1 (1995), 41–46.

[148] Mingelgrin, U., and Prost, R. Surface interactions of toxic organic chemicals with minerals. In *Toxic organic chemicals in porous media*, Z. Gerstl, Y. Chen, U. Mingelgrin, and B. Yaron, Eds. Springer Verlag, New York, NY, 1989.

[149] Miyake, J., Ochiai-Yanagi, S., Kasumi, T., and Takagi, T. Isolation of a membrane protein from *R. rubrum* chromatophores and its abnormal behaviour in SDS-polyacrylamide gel electrophoresis due to a high binding capacity for SDS. *The Journal of Biochemistry 83* (1978), 1679–1686.

[150] Moore, T. Litter decomposition rates in canadian forests. *Global Change Biology 5* (1999), 75–82.

[151] Morrissey, F., and Grismer, M. Kinetics of volatile organic compound sorption/desorption on clay minerals. *Journal of Contaminant Hydrology 36* (1999), 291–312.

[152] Nieboer, M., Gunnewijk, M., Beilen van, J. B., and Witholt, B. Determinants for overproduction of the *Pseudomonas oleovorans* cytoplasmic membrane protein alkane hydroxlyase in *alk*$^+$ *Escherichia coli* W3110. *Journal of Bacteriology 179* (1997), 762–768.

[153] Nieboer, M., Kingma, J., and Witholt, B. The alkane oxidation system of *Pseudomonas oleovorans*: Induction of the *alk* genes in *Escherichia coli* W3110 (pGEc47) affects membrane biogenesis and results in overexpression of alkane hydroxylase in a distinct cytoplasmic membrane subfraction. *Molecular Microbiology 8* (1993), 1039–1051.

[154] Nieboer, M., Vis, A.-J., and Witholt, B. Overproduction of a foreign membrane protein in *Escherichia coli* stimulates and depends on phospholipid synthesis. *European Journal Biochemistry 241* (1996), 691–696.

[155] Ogram, A., Mathot, M., Harsh, J., Boyle, J., and Pettigrew, C. Effects of DNA polymer length on its adsorption to soils. *Applied and Environmental Microbiology 60* (1994), 393–396.

[156] Panke, S., Meyer, A., Huber, C., Witholt, B., and Wubbolts, M. An alkane-responsive expression system for the production of fine chemicals. *Applied and Environmental Microbiology 65* (1999), 2324–2332.

[157] Peters, J., and Witholt, B. Solubilization of the overexpresses integral membrane protein alkane monooxygenase of the recombinant *Escherichia coli* W3110[pGEc47]. *Biochemica et Biophysica Acta 1196* (1994), 145–153.

[158] Pfaffl, M. A new mathematical model for relative quantification in real-time rt-pcr. *Nucleic Acids Research 29*, 9 (2001), –e45.

[159] Picard, C., Ponsonnet, C., Paget, E., Nesme, X., and Simonet, P. Detection and enumeration of bacteria in soil by direct dna extraction and polymerase chain reaction. *Applied and Environmental Microbiology 58*, 9 (1992), 2717–2722.

[160] Pinholt, Y., Struwe, S., and Kjoller, A. Microbial changes during oil decomposition in soil. *Holarctic Ecology 2* (1979), 195–200.

[161] Polemio, M., Genchi, G., Palmieri, F., and Testini, C. Glutamic-dehydrogenase activity inhibition by phenoxyacilic acids. *Plant and Soil 63* (1981), 369–375.

[162] Poll, C., Ingwersen, J., Stemmer, M., Gerzabek, M., and Kandeler, E. Mechanisms of solute transport affect small-scale abundance and function of soil microorganisms in the detritusphere. *European Journal of Soil Science 57* (2006), 583–595.

[163] Poll, C., Marhan, S., Ingwersen, J., and Kandeler, E. Dynamics of litter carbon turnover and microbial abundance in a rye detritusphere. *Soil Biology and Biochemistry 40* (2008), 1306–1321.

[164] Poll, C., Pagel, H.and Devers-Lamrani, M., Martin-Laurent, F., Ingwersen, J., Streck, T., and Kandeler, E. Regulation of bacterial and fungal MCPA degradation at the soil-litter interface. *Soil Biology and Biochemistry 42*, 10 (2010), 1879–1887.

[165] Powell, S., Bowman, J., Ferguson, S., and Snape, I. The importance of soil characteristics to the structure of alkane-degrading bacterial communities on sub-Antarctic Macquarie Island. *Soil Biology and Biochemistry 42* (2010), 2012–2021.

[166] Powell, S. M., Ferguson, S. H., Snape, I., and Siciliano, S. Fertilization stimulates anaerobic fuel degradation of artic soils by denitrifying microorganisms. *Environmental Science and Technology 40* (2006), 2011–2017.

[167] Poynter, J., and Eglinton, G. Molecular composition of three sediments from hole 717C: The Bengal Fan. In *Proceedings of the Ocean Drilling Program, Scientific Results* (1990), J. Cochran, Ed., vol. 116, pp. 155–161.

[168] Premachandra, G., Saneoka, H., Fujita, K., and Ogata, S. Leaf water relations, osmotic adjustment, cell membrane stability, epicuticular wax load and growth as affected by increasing water deficits in sorghum. *Journal of Experimental Botany 43* (1992), 1569–1576.

[169] Pérez de Mora, A., Engel, M., and Schloter, M. Abundance and diversity of *n*-alkane-degrading bacteria in a forest soil co-contaminated with hydrocarbons and metals: a molecular study on *alkB* homologous genes. *Microbial Ecology 62* (2011), 959–972.

[170] Pronk, G. Biogeochemical interfaces in natural and artificial soil systems: specific surface area, phenanthrene sorptive properties and formation of organo-mineral associations. *PhD thesis*, *Technische Universität München*, 2011.

[171] Prost, R., and Yaron, B. Use of modified clays for controlling soil environmental quality. *Soil Science 166* (2001), 880–895.

[172] Rand, K., and Houck, H. Taq polymerase contains bacterial DNA of unknown origin. *Molecular and Cellular Probes 4* (1990), 445–450.

[173] Reasoner, D., and Geldreich, E. A new medium for the enumeration and subculture of bacteria from potable water. *Applied and Environmental Microbiology 49* (1985), 1–7.

[174] Reinertsen, S., Elliott, L., Cochran, V., and Campbell, G. Role of available carbon and nitrogen is determining the rate of wheat straw decomposition. *Soil Biology and Biochemistry 16* (1984), 459–464.

[175] Reynolds, J., and Tanford, C. Binding of dodecyl sulfate to proteins at high binding ratios. possible implications for the state of proteins in biological membranes. *Proceedings of the National Academy of Sciences of the United States of America 66* (1970), 1002–1003.

[176] Richnow, H. H., Seifert, R., Kästner, M., Mahro, B., Horsfield, B., Tiedgen, U., Böhm, S., and Michaelis, W. Rapid screening of PAH-residues in bioremediated soils. *Chemosphere 31* (1995), 3991–3999.

[177] Rieley, G., Collister, J., Stern, B., and Eglinton, G. Gas chromatography/ isotope ration mass spectrometry of leaf wax *n*-alkanes from plants of differing carbon dioxide metabolisms. *Rapid Communications in Mass Spectrometry 7* (1993), 488–491.

[178] Rikken, G., Kroon, A., and van Ginkel, C. Transformation of (per)chlorate into chlorite by a newly isolated bacterium: reduction and dismutation. *Applied Microbiology and Biotechnology 45* (1996), 420–426.

[179] Rogerson, A., and Berger, J. Effect of crude oil and petroleum-degrading micro-organisms on the growth of freshwater and soil protozoa. *Journal of General Microbiology 124* (1981), 53–59.

[180] Rojo, F. Specifity at the end of the tunnel: Understanding substrate length discrimination by the AlkB alkane hydroxylase. *Journal of Bacteriology 187* (2005), 19–22.

[181] Rojo, F. Degradation of alkanes by bacteria. *Environmental Microbiology 11* (2009), 2477–2490.

[182] Roose-Amsaleg, C., Garnier-Sillam, E., and Harry, M. Extraction and purification of microbial DNA from soil and sediment samples. *Applied Soil Ecology 18* (2001), 47–60.

[183] Rosenberg, H. Isolation of recombinant secretory proteins by limited induction and quantitative harvest. *BioTechniques 24* (1998), 188–191.

[184] Rosenberg, M., Bayer, E. A., Delarea, J., and Rosenberg, E. Role of thin fimbriae in adherence and growth of *Acinetobacter calcoaceticus* RAG-1 on hexadecane. *Applied and Environmental Microbiology 44* (1982), 929–937.

[185] Rueter, P., Rabus, R., Wilkes, H., Aeckersberg, F., Rainey, F. A., Jannasch, H., and Widdel, F. Anaerobic oxidation of hydrocarbons in crude oil by new types of sulphate-reducing bacteria. *Nature 372* (1994), 455–458.

[186] Ruettinger, R., Olson, S., Boyer, R., and Coon, M. Identification of the ω-hydroxylase of pseudomonas oleovorans as a nonheme iron protein requiring phospholipid for catalytic activity. *Biochemical and Biophysical Research Communications 57* (1974), 1011–1017.

[187] Ruggiero, P., and Radogna, V. Inhibition of soil humus-laccase complexes by some phenoxyacetic acid and s-triazine herbicides. *Soil Biology & Biochemistry 17* (1985), 309–312.

[188] Rutigliano, F., De Santo, A., Berg, B., Alfani, A., and Fioretto, A. Lignin decomposition in decaying leaves of *Fagus sylvatica* L. and needles of *Abies alba* Mill. *Soil Biology and Biochemistry 28* (1996), 101–106.

[189] Saada, A., Gaboriau, H., Cornu, S., Bardot, F., Villiéras, F., and Croué, J. Adsorption of humic acid onto kaolinitic clay studied by high-resolution argon adsorption volumetry. *Clay Minerals 38* (2003), 433–443.

[190] Sabirova, J. S., Ferrer, M., Regenhardt, D., Timmis, K. N., and Golyshin, P. N. Proteomic insights into metabolic adaptions in *Alcanivorax*

borkumensis induced by alkane utilization. *Journal of Bacteriology 188* (2006), 3763–3773.

[191] Sagné, C., Isambert, M.-F., Henry, J.-P., and Gasnier, B. Sds-resistant aggregation of membrane proteins: application to the purification of the vesicular monoamine transporter. *Biochemical Journal 316* (1996), 825–831.

[192] Sambrook, J., Fritsch, E., and Maniatis, T. *Molecular Cloning: A Laboratory Manual*, vol. 3. Cold Spring Harbor Laboratory Press, Cold Spring Harbor, New York, 1989.

[193] Scheffer, F., and Schachtschabel, P. *Lehrbuch der Bodenkunde*. Spektrum Akademischer Verlag, Heidelberg, Berlin, 2002.

[194] Schefuss, E., Ratmeyer, V., Stuut, J., Jansen, J., and Sinninghe Damste, J. Carbon isotope analyses of n-alkanes in dust from the lower atmosphere over the central eastern Atlantic. *Geochimica et Cosmochimica Acta 67* (2003), 1757–1767.

[195] Schein, C., and Noteborn, M. Formation of soluble recombinant proteins in *Escherichia coli* is favored by lower growth temperature. *Nature Biotechnology 6* (1988), 291–294.

[196] Schloter, M., Schauss, K., Munch, J., Radl, V., Hai, B., and Gattinger, A. Emission von Treibhausgasen aus landwirtschaftlich genutzten Böden. *Biospektrum 2* (2008), 148–149.

[197] Schmitz, C., Goebel, I., Wagner, S., Vomberg, A., and Klinner, U. Competition between n-alkane-assimilating yeasts and bacteria during colonization of sandy soil microcosms. *Applied Microbiology and Biotechnology 54* (2000), 126–132.

[198] Schneider, T., Keiblinger, K., Schmid, E., Sternflinger-Gleixner, K., Ellersdorfer, G., Roschitzki, B., A., R., Eberl, L., Zechmeister-Boltenstern, S., and Riedel, K. Who is who in litter decomposition? Metaproteomics reveals major microbial players and their biogeochemical functions. *The ISME Journal* (2012).

[199] Scott, C., and Finnerty, W. Characterisation of intracytoplasmic hydrocarbon inclusions from the hydrocarbon-oxidising *Acinetobacter* species HO1-N. *Journal of Bacteriology 127* (1976), 481–489.

[200] Shanklin, J., and Whittle, E. Evidence linking the *Pseudomonas oleovorans* alkane ω-hydroxylase, an integral membrane diiron enzyme and the fatty acid desaturase family. *FEBS Letters 545* (2003), 188–192.

[201] Siddique, T., Penner, T., Semple, K., and Foght, J. Anaerobic biodegradation of longer-chain n-alkanes coupled to methane procduction in oil sands tailings. *Environmental Science & Technology 45* (2011), 5892–5899.

[202] Sikkema, J., De Bint, J., and Poolman, B. Mechanisms of membrane toxicity of hydrocarbons. *Microbiological Reviews 59* (1995), 201–222.

[203] Singer, M., and Finnerty, W. Microbial metabolism of straight-chain and branched alkanes. In *Petroleum Microbiology*, R. Atlas, Ed. Macmillan, New York, 1984, pp. 1–59.

[204] Sinowski, W., and Auerswald, K. Using relief parameters in a discriminant analysis to stratify geological areas with different spatial variability of soil properties. *Geoderma 89* (1999), 113–128.

[205] Sluis, M., Sayavedra Soto, L., and Arp, D. Molecular analysis of the soluble butane monooxygenase from *Pseudomonas butanovora*. *Microbiology 148* (2002), 3617–3629.

[206] Smith, V., Graham, D., and Cleland, D. Application of resource-ratio theory to hydrocarbon biodegradation. *Environmental Science 32* (1998), 3386–3395.

[207] Smits, T., Balada, S., Witholt, B., and Beilen, J. v. Functional analysis of alkane hydroxylases from gram-negative and gram-positive bacteria. *Journal of Bacteriology 184* (2002), 1733–1742.

[208] Smits, T. H. M., Witholt, B., and Van Beilen, J. Functional characterization of genes involved in alkane oxidation by *Pseudomonas aeruginosa*. *Antonie van Leeuwenhoek 84* (2003), 193–200.

[209] Snajdr, J., Cajthaml, T. andValaskova, V., Merhautova, V., Petrankova, M., Spetz, P., Leppänen, K., and Baldrian, P. Transformation of *Quercus petreae* litter: successive changes in litter chemistry are reflected in differential enzyme activity and changes in the microbial community composition. *FEMS Microbiology Ecology 75* (2011), 291–303.

[210] So, C. M., Phelps, C. D., and Young, L. Y. Anaerobic transformation of alkanes to fatty acids by a sulfate-reducing bacterium, strain Hxd3. *Applied and Environmental Microbiology 69* (2003), 3892–3900.

[211] So, C. M., and Young, L. Y. Isolation and characterization of a sulfate-reducing bacterium that anaerobically degrades alkanes. *Applied and Environmental Microbiology 65* (1999), 2969–2976.

[212] Song, H. G., Pedersen, T. A., and Bartha, R. Hydrocarbon mineralization in soil: Relative bacterial and fungal contribution. *Soil Biology and Biochemistry 18* (1986), 109–111.

[213] Staijen, I., and Witholt, B. Synthesis of alkane hydroxylase of *Pseudomonas oleovorans* increases the iron requirement of *alk+* bacterial strains. *Biotechnology and Bioengineering 57* (1997), 228–237.

[214] Staijen, I. E., Hatzimanikatis, V., and Witholt, B. The AlkB monooxygenase of *Pseudomonas oleovorans* synthesis, stability and level in recombinant *Escherichia coli* and the native host. *European Journal Biochemistry 244* (1997), 462–470.

[215] Suberkropp, K., and Klug, M. The maceration of deciduous leaf litter by aquatic hyphomycetes. *Canadian Journal of Botany 58* (1980), 1025–1031.

[216] Tani, A., Ishige, T., Sakai, Y., and Kato, N. Gene structures and regulation of the alkane hydroxylase complex in *Acinetobacter sp.* strain M-1. *Journal of Bacteriology 183* (2001), 1819–1823.

[217] Tapilatu, Y., Grossi, V., Acquaviva, M., Militon, C., Bertrand, J.-C., and Cuny, p. Isolation of hydrocarbon-degrading extremely halophilic archaea from an uncontaminated hypersaline pond (Camargue, France). *Extremophiles 14* (2010), 225–231.

[218] Taylor, B., Parkinson, D., and Parsons, W. Nitrogen and lignin content as predictors of litter decay rates: a microcosm test. *Ecology 70* (1989), 97–104.

[219] Tebbe, C., and Vahjen, W. Interference of humic acids and DNA extracted directly from soil in detection and transformation of recombinant DNA from bacteria and a yeast. *Applied and Environmental Microbiology 59* (1993), 2657–2665.

[220] Tejada, M., García-Martínez, A., Gómez, I., and Parrado, J. Application of MCPA herbicide on soils amended with biostimulants: Short-time effects on soil biological properties. *Chemosphere 80* (2010), 1088–1094.

[221] Thompson, D., Rajal, V., De Batz, S., and Wuertz, S. Detection of *Salmonella* in water samples using magnetic capture-hybridization combined with PCR or real time PCR. *Journal of Water and Health 4* (2006), 67–75.

[222] Thorstensen, C., Lode, O., and Eklo, O. Sorption of bentazone, dichlorprop, MCPA and propiconazole in reference soils from Norway. *Journal of Environmental Quality 30* (2001), 2046–2052.

[223] Throne-Holst, M., Wentzel, A., Ellingsen, T. E., Kotlar, H.-K., and Zotchev, S. B. Identification of novel genes involved in long-chain *n*-alkane degradation by *Acinetobacter sp.* strain DSM 17874. *Applied and Environmental Microbiology 73* (2007), 3327–3332.

[224] Tian, G., Kang, B., and Brussard, L. Biological effects of plant residues with contrasting chemical compositions und humid tropical conditions: Decomposition and nutrient release. *Soil Biology and Biochemistry 24* (1992), 1051–1060.

[225] Tietema, A., and Wessel, W. Microbial activity and leaching during the initial oak leaf litter decomposition. *Biology and Fertility of Soils 18* (1994), 49–54.

[226] Torres, P., Abril, A., and Bucher, E. Microbial succession in litter decomposition in the semi-arid Chaco woodland. *Soil Biology and Biochemistry 37* (2005), 49–54.

[227] Torstensson, L., Stark, J., and Göransson, B. The effect of repeated applications of 2,4-d and mcpa on their breakdown in soil. *Weed Research 15* (1975), 159–164.

[228] Torsvik, V., Goksoyr, J., and Daae, F. L. High diversity in DNA of soil bacteria. *Applied and Environmental Microbiology 56* (1990), 782–787.

[229] Totsche, K., Rennert, T., Gerzabek, M., Kögel-Knabner, I., Smalla, K., Spiteller, M., and Vogel, H.-J. Biogeochemical interfaces in soil: The interdisciplinary challenge for soil science. *Journal of Plant Nutrition and Soil Science 173* (2010), 88–99.

[230] Tsai, Y., and Olson. Detection of low numbers of bacterial cells in soils and sediments by polymerase chain reaction. *Applied and Environmental Microbiology 58* (1992), 754–757.

[231] Tsai, Y., and Olson, B. Rapid method for seperation of bacterial DNA from humic substances in sediments for polymerase chain reaction. *Applied and Environmental Microbiology 58* (1991), 2292–2295.

[232] Töwe, S., Wallisch, S., Bannert, A., Fischer, D., Hai, B., Haesler, F., Kleineidam, K., and Schloter, M. Improved protocol for the simultaneous extraction and column-based separation of dna and rna from different soils. *Journal of Microbiological Methods 84*, 3 (2011), 406–412.

[233] van Beilen, J., and Funhoff, E. Expanding the alkane oxygenase toolbox: new enzymes and applications. *Current Opinion in Biotechnology 16* (2005), 308–314.

[234] van Beilen, J., and Funhoff, E. Alkane hydroxylases involved in microbial alkane degradation. *Applied Microbiology and Biotechnology 74* (2007), 13–21.

[235] van Beilen, J., Funhoff, E., Loon, A. v., Just, A., Kaysser, L., Bouza, M., Holtackers, R., Röthlisberger, M., Li, Z., and Witholt, B. Cytochrome P450 alkane hydroxylases of the CYP153 family are common in alkane-degrading eubacteria lacking integral membrane alkane hydroxylases. *Applied and Environmental Microbiology 72* (2006), 59–65.

[236] van Beilen, J., Kingma, J., Jonas, A., and Witholt, B. *Alkane oxidation by* Pseudomonas oleovorans*: Genes and proteins.* PhD thesis, University of Groningen, 1994.

[237] van Beilen, J., Li, Z., Duetz, W., Smits, T., and Witholt, B. Diversity of alkane hydroxylase systems in the environment. *Oil and Gas Science and Technology 58* (2003), 427–440.

[238] van Beilen, J., Neuenschwander, M., Smits, T. H. M., Roth, C., Balada, S., and Witholt, B. Rubredoxins involved in alkane oxidation. *Journal of Bacteriology 184* (2002), 1722–1732.

[239] van Beilen, J., Smits, T. H. M., Roos, F. F., Brunner, T., Balada, S. B., Rothlisberger, M., and Witholt, B. Identification of an amino

acid position that determines the substrate range of integral membrane alkane hydroxylases. *Journal of Bacteriology 187* (2005), 85–91.

[240] van Beilen, J., Smits, T. H. M., Whyte, L. G., Schorcht, S., Röthlisberger, M., Plaggemeier, T., Engesser, K.-H., and Witholt, B. Alkane hydroxylase homologues in gram-positive strains. *Environmental Microbiology 4*, 11 (2002), 676–682.

[241] van Beilen, J., Wubbolts, M., and Witholt, B. Genetics of alkane oxidation by *Pseudomonas oleovorans*. *Biodegradation 5* (1994), 161–174.

[242] van Beilen, J. B., Panke, S., Lucchini, S., Franchini, A. G., Rothlisberger, M., and Witholt, B. Analysis of pseudomonas putida alkane-degradation gene clusters and flanking insertion sequences: evolution and regulation of the alk genes. *Microbiology 147* (2001), 1621–1630.

[243] van Beilen, J. B., Veenhoff, L., and Witholt, B. Alkane hydroxylase systems in *Pseudomonas aeruginosa* strains able to grow on *n*-octane. In *New Frontiers in Screening for Microbial Biocatalysts, Proceedings of an International Symposium*, K. Kieslich, C. van der Beek, J. de Bont, and W. van den Tweel, Eds., vol. 53. Elsevier, 1998, pp. 211–215.

[244] Vieublé Gonod, L., Martin-Laurent, F., and Chenu, C. 2,4-D impact on bacterial communities, and the activity and genetic potential of 2,4-D degrading communities in soil. *FEMS Microbiol Ecology 58*, 3 (2006), 529–537.

[245] Viitanen, P., Newman, M., Foster, D., Wilson, T., and Kaback, H. Purification, reconstitution, and characterization of the lac permease of *Escherichia coli*. *Methods in Enzymology 125* (1986), 429–452.

[246] Vázquez, S., Nogales, B., Ruberto, L., Hernández, E., Christie-Oleza, J., Lo Balbo, A., Bosch, R., Lalucat, J., and Mac Cormack, W. Bacterial community dynamics during bioremediation of diesel oil-contaminated antarctic soil. *Microbial Ecology 57* (2009), 598–610.

[247] Walker, J., Colwell, R., Vaituzis, Z., and Meyer, S. Petroleum-degrading achlorophyllous alga *Prototheca zopfi*. *Nature 254* (1975), 423–424.

[248] Wang, W., Baldock, J., Dalal, R., and Moody, P. Decomposition of plant materials in relation to nitrogen availability and biochemistry determined

by NMR and wet-chemical analysis. *Soil Biology & Biochemistry 36* (2004), 2045–2058.

[249] Wang, X.-B., Chi, C.-Q., Nie, Y., Tang, Y.-Q., Tan, Y., Wu, G., and Wu, X.-L. Degradation of petroleum hydrocarbons (C6 - C40) and crude oil by a novel *Dietzia* strain. *Bioresource Technology 102* (2011), 7755–7761.

[250] Ward, D. M., and Brock, T. Hydrocarbon biodegradation in hypersaline environments. *Applied and Environmental Microbiology 35* (1978), 353–359.

[251] Ward, N. L., Challacombe, J. F., Janssen, P. H., Henrissat, B., Coutinho, P. M., Wu, M., Xie, G., Haft, D. H., Sait, M., Badger, J., Barabote, R. D., Bradley, B., Brettin, T. S., Brinkac, L. M., Bruce, D., Creasy, T., Daugherty, S. C., Davidsen, T. M., DeBoy, R. T., Detter, J. C., Dodson, R. J., Durkin, A. S., Ganapathy, A., Gwinn-Giglio, M., Han, C. S., Khouri, H., Kiss, H., Kothari, S. P., Madupu, R., Nelson, K. E., Nelson, W. C., Paulsen, I., Penn, K., Ren, Q., Rosovitz, M. J., Selengut, J. D., Shrivastava, S., Sullivan, S. A., Tapia, R., Thompson, L. S., Watkins, K. L., Yang, Q., Yu, C., Zafar, N., Zhou, L., and Kuske, C. R. Three genomes from the phylum *Acidobacteria* provide insight into the lifestyles of these microorganisms in soils. *Applied and Environmental Microbiology 75* (2009), 2046–2056.

[252] Watkinson, R., and Morgan, P. Physiology of aliphatic hydrocarbon-degrading microorganisms. *Biodegradation 1* (1990), 79–92.

[253] Wick, L. Y., Remer, R., Würz, B., Reichenbach, J., Braun, S., Schäfer, F., and Harms, H. Effect of fungal hyphae on the access of bacteria to phenanthrene in soil. *Environmental Science and Technology 41* (2007), 500–505.

[254] Wilkes, H., Rabus, R., Fischer, T., Armstroff, A., Behrends, A., and Widdel, F. Anaerobic degradation of *n*-hexane in a denitrifying bacterium: Further degradation of the initial intermediate (1-methylpentyl)-succinate via C-skeleton rearragement. *Archives of Microbiology 177* (2002), 235–243.

[255] Williams, J. Optimization strategies for the polymerase chain reaction. *BioTechniques 7* (1989), 762–769.

[256] Witholt, B., de Smet, M.-J., Kingma, J., van Beilen, J., Kok, M., Lageveen, R., and Eggink, G. Bioconversions of aliphatic compounds by

Pseudomonas oleovorans in multiphase bioreactors: Background and economic potential. *TRENDS in Biotechnology 8* (1990), 46–52.

[257] Wolterink, A., Jonker, A. B., Kengen, S. W. M., and Stams, A. J. M. *Pseudomonas chloritidismutans sp.* nov., a non-denitrifying, chlorate-reducing bacterium. *International Journal of Systematic and Evolutionary Microbiology 52* (2002), 2183–2190.

[258] Wong, P., and Griffin, D. Bacterial movement at high matric potentials - II. In fungal colonies. *Soil Biology and Biochemistry 8* (1976), 219–223.

[259] World Reference Base for Land Resources. *Guidelines for Soil Description*, 4th ed. Food and Agriculture Organization of the United Nations, 2006.

[260] Wyatt, J. The microbial degradation of hydrocarbons. *Trends in Biochemical Sciences 9* (1984), 20–23.

[261] Xia, J., Yason, C., and Kibenge, F. Comparison of dot blot hybridization, polymerase chain reaction, and vuirus isolation for detection of bovine herpesvirus-1 (BHV-1) in artificially infected bovine semen. *Canadian Journal of Veterinary Research 59* (1995), 102–109.

[262] Xie, M., Alonso, H., and Roujeinikova, A. An improved procedure for the purification of catalytically active alkane hydroxlyase from *Pseudomonas putida* GPo1. *Applied Biochemistry and Biotechnology* (2011), 823–831.

[263] Yakimov, M., Giuliano, L., Denaro, R., Crisafi, E., Chernikova, T., Abraham, W., Luensdorf, H., Timmis, K., and Golyshin, P. *Thalassolituus oleivorans gen. nov., sp.* nov., a novel bacterium that obligately utilizes hydrocarbons. *International Journal of Systematic and Evolutionary Microbiology 54* (2004), 141–148.

[264] Young, I., and Crawford, J. Interactions and self-organization in the soil-microbe complex. *Science 304* (2004), 1634–1637.

[265] Young, I., and Ritz, K. Tillage, habitat space and function of soil microbes. *Soil & Tillage Research 53* (2000), 201–213.

[266] Zabaloy, M., Garland, J., and Gómez, M. An integrated approach to evaluate the impacts of the herbicides glyphosate, 2,4-D and metasulfuron-methyl

on soil microbial communities in the Pampas region, Argentina. *Applied Soil Ecology 40* (2008), 1–12.

[267] Zhang, T., and Fang, H. H. P. Applications of real-time polymerase chain reaction for quantification of microorganisms in environmental samples. *Applied Microbiology and Biotechnology 70* (2006), 281–289.

Acknowledgment

First of all I want to thank the examination committee for the verification of this Ph.D. thesis, which was part of the priority program 1315 "Biogeochemical Interfaces in Soil". Therefore, I thank the "Deutsche Forschungsgemeinschaft (DFG)" for the financial support.

I gratefully thank Prof. Dr. Jean Charles Munch for the opportunity to work at his institute and to benefit from the provided hardware. In addition, I thank for the improving recommendations to this thesis.

Special thanks go to Prof. Dr. Michael Schloter for the supervision of my thesis and the numerous chances to present the data to an international audience. This and the possibility to attend divers exciting sampling campaigns at some of the most beautiful places on earth (Damma glacier, Rhône glacier, Argentina) were definitely the highlights of my Ph.D. thesis. Furthermore, I really enjoyed the freedom to find my own way of scientific working and to improve my "soft skills" during the frequent supervision of Bachelor and Master students.

As I often visited the research farm Scheyern for my own scientific purpose and for providing soil samples to my cooperation partners within the priority program, I thank the "Scheyern specialists" Dr. Karin Schreiner, Dr. Karin Pritsch, Rolf Schilling and Georg Gerl for their support.

During the years this thesis took, the members of office 110 changed quite frequently. In this context I gratefully acknowledge the friendly mood of Dr. Karin Schreiner and Dr. Jürgen Esperschütz who both helped me a lot, particularly at the beginning of my Ph.D. thesis.

I cooperated with a lot of interesting people from different scientific research fields resulting in several successful publications. Therefore I thank Julia Giebler, Dr. Lukas Wick, Dr. Antonis Chatzinotas and Prof. Dr. Hauke Harms from the Hemholtz Center for Environmental research (UFZ), Dr. Christian Poll, Holger Pagels and Prof. Dr. Ellen Kandeler from the University of Hohenheim as well as Dr.Geertje Pronk, Dr. Katja Heister and Prof. Dr. Ingrid Kögel-Knabner from the Chair of Soil Science at the TUM for collaboration.

I furthermore gratefully acknowledge the efforts of Joshua Gnizak, who carefully reviewed this manuscript.

Last but not least I want to thank my family and my wonderful wife Stefanie Schulz for all the support and encouraging words. They pushed me up frequently, during times when I was about to quit the job. Thanks a lot.

Publication I

Chapter 4

MPN- and Real-Time-Based PCR Methods for the Quantification of Alkane Monooxygenase Homologous Genes (*alkB*) in Environmental Samples

Alfredo Pérez-de-Mora, Stephan Schulz, and Michael Schloter

Abstract

Hydrocarbons are major contaminants of soil ecosystems as a result of uncontrolled oil spills and wastes disposal into the environment. Ecological risk assessment and remediation of affected sites is often constrained due to lack of suitable prognostic and diagnostic tools that provide information of abiotic–biotic interactions occurring between contaminants and biological targets. Therefore, the identification and quantification of genes involved in the degradation of hydrocarbons may play a crucial role for evaluating the natural attenuation potential of contaminated sites and the development of successful bioremediation strategies. Besides other gene clusters, the *alk* operon has been identified as a major player for alkane degradation in different soils. An oxygenase gene (*alkB*) codes for the initial step of the degradation of aliphatic alkanes under aerobic conditions. In this work, we present an MPN- and a real-time PCR method for the quantification of the bacterial gene *alkB* (coding for rubredoxin-dependent alkane monooxygenase) in environmental samples. Both approaches enable a rapid culture-independent screening of the *alkB* gene in the environment, which can be used to assess the intrinsic natural attenuation potential of a site or to follow up the on-going progress of bioremediation assays.

Key words: Most probable number-PCR, real time PCR, alkane monooxygenase homologous genes.

1. Introduction

Aliphatic *n*-alkanes are saturated hydrocarbons present in crude and refined oils. Although *n*-alkanes can be produced by plants and microorganisms (e.g., waxes) (1,2), they are mainly released into the environment by seepage from reservoirs or through anthropogenic activities related to the extraction, transportation,

S.P. Cummings (ed.), *Bioremediation*, Methods in Molecular Biology 599,
DOI 10.1007/978-1-60761-439-5_4,

further processing, handling, and disposal of oil (3). Some algae that degrade *n*-alkanes have been described; however, bacteria and fungi are the most important groups capable of using long-chain *n*-alkanes as a carbon and energy source (4). Bacterial degradation of *n*-alkanes is possible under aerobic and anaerobic conditions, although the former allows much faster rates of transformation (5).

During the past decades, research related to alkane degradation has focused on the identification and characterization of enzymes involved in the initial step of aerobic bacterial catabolic pathways. Recently, two unrelated classes of enzymes for long-chain *n*-alkane oxidation have been proposed (6): (1) Cytochrome-P450-related enzymes in both yeasts and bacteria, e.g., bacterial CYP153 enzymes, and (2) bacterial particulate alkane hydroxylases (pAHs). The latter class of integral membrane non-heme di-iron monooxygenases of the *alkB*-type catalyzes the terminal or subterminal oxidation of *n*-alkanes to primary or secondary alcohols, which is the initial step in the aerobic degradation of *n*-alkanes (3). This enzyme allows a wide range of Proteobacteria and Actinomycetales to grow on *n*-alkanes with carbon chain lengths from C5 to C16.

Most studies dealing with the detection of *alkB* in microbial communities to date are based on PCR methods using cultured isolates (7, 8, 9). Due to the high diversity of *alkB* sequences in bacteria from different taxonomic groups, analysis of environmental samples required the use of multiple primer and probe sets targeting the respective groups. In order to allow a specific and sensitive detection of *alkB* genes in environmental samples without discriminating any of the known bacterial groups harboring this gene, a PCR hybridization method was described recently (10). Based on this initial work, we present here an improved MPN- and a real-time PCR methods, which allow rapid quantification of *alkB* gene in numerous environmental samples. Furthermore, the amplified products can be directly used for assessing community diversity using fingerprinting or cloning techniques.

2. Materials

2.1. Cell Lysis and Nucleic Acid Extraction

1. FastDNA SPIN Kit for soil (MP Biomedicals, Heidelberg, Germany)
2. PreCellys24 homogeniser (Peqlab Biotechnologie GmbH, Erlangen, Germany)
3. PreCellys ceramic kit 1.4 mm (Peqlab Biotechnologie GmbH, Erlangen, Germany)

2.2. MPN-PCR Amplification of alkB

1. Autoclaved MiliQ water (*see* **Note 1**).
2. 3% bovine serum albumin solution. After sterilization by filtration (22 μm) store in aliquots at −20°C (*see* **Note 1**).
3. dNTPs (Fermentas GmbH, St. Leon-Rot, Germany)
4. Taq polymerase (5 U/μL) (Invitrogen, Carlsbad, CA, USA).
5. 10× buffer provided with Taq polymerase.
6. $MgCl_2$ (50 mM) provided with Taq polymerase or self prepared (in this case *see* **Note 1**).
7. Degenerate PCR primer (10) (Metabion, Martinsried, Germany)
8. alkB-forward (5′AAY ACI GCI CAY GAR CTI GGI CAY AA 3′)
9. alkB-reverse (5′ GCR TGR TGR TCI GAR TGI CGY TG 3′)
10. Template DNA (*see* **Note 2**). Dilutions of template DNA should be prepared directly before use (*see* **Note 3**). We recommend the use of freshly prepared dilutions for every new PCR reaction.
11. Thermocycler (T3 Thermocycler, Biometra, Goettingen, Germany)

2.3. Real-Time PCR Amplification of alkB

1. 3% bovine serum albumin solution. After sterilization by filtration store in aliquots at −20°C. Use filters with 22 μm pore size (*see* **Note 1**).
2. $MgCl_2$ solution (50 mM) (*see* **Note 1**).
3. Power SYBR® Green PCR Master Mix (Applied Biosystems, Foster City, CA, USA). Store Master Mix in single-use aliquots at 28°C for short-term storage (*see* **Note 4**).
4. Degenerated PCR primer (10) (Metabion, Martinsried, Germany) (*see* **Note 5**):
   alkB-forward (5′AAY ACI GCI CAY GAR CTI GGI CAY AA 3′)
   alkB-reverse (5′ GCR TGR TGR TCI GAR TGI CGY TG 3′)
   Store aliquots of appropriate dilution at −20°C (*see* **Note 3**).
5. Template DNA (*see* **Note 2**). Dilutions of template DNA should be prepared directly before use (*see* **Note 3**). Use freshly prepared dilutions for every new PCR reaction.
6. Thermo-Fast® 96 detection plate (Thermo Scientific)
7. MicroAmp™ optical adhesive film (Applied Biosystems, Foster City, CA, USA)

8. Domed 12 cap strips (Thermo Scientific)
9. Cooled centrifuge for detection plates (e.g., Omnifuge 2.0 RS, Heraeus Sepatech Osterode, Germany)
10. A repeater-step pipette (e.g., Distriman®, Gilson Inc., Middleton, WI, USA)
11. 7300 real-time PCR system (Applied Biosystems, Foster City, CA, USA)

2.4. Agarose Gel Electrophoresis

1. Agarose for gel electrophoresis is dissolved in 1× TAE buffer to a final concentration of 2% and should be prepared before use.
2. TAE buffer: 40 mM Tris-base, 1 mM disodium ethylendiamintetraacetate dihydrate dissolved in water pH 8.0 (*see* **Note 1**).
3. Loading dye 6× (Fermentas **GmbH**,St. Leon-Rot, Germany)
4. GeneRuler™ 100 bp or 1 kb DNA ladder (Fermentas GmbH, St. Leon-Rot, Germany)
5. PerfectBlue Gelsystem Mini L (Peqlab Biotechnologie GmbH, Erlangen, Germany) with Power Supply Power Pac 300 (Biorad, Hercules, CA, USA)
6. Gel documentation system

3. Methods

In this work we present two quantitative PCR methods to study the relative abundance of the bacterial *alkB* gene in environmental samples. The first one is based on an MPN PCR approach, while the second one is a real-time PCR procedure. Both methods were tested using a wide range of samples. These included different types of soil: forest and agricultural, low (<1%) and high (>5%) organic C content, noncontaminated (<100 mg total hydrocarbons/kg soil dry weight) and contaminated with hydrocarbons (5000 mg total hydrocarbons/kg soil dry weight), sand and loam texture. In addition, plant residual material was evaluated (pea and maize). For a more detailed discussion on the advantages and disadvantages of quantitative PCR procedures, we refer to (11). A brief introduction is given below.

The MPN PCR approach is based on the combination of PCR with the statistical MPN (most probable number) procedure developed by McCrady (12) and later improved by other authors (13). This method consists of serial dilutions of DNA/cDNA samples until extinction and replicated PCR reactions for every

dilution. The result of each reaction is scored positive or negative after gel electrophoresis analysis. The number of gene copies is calculated using the MPN statistics.

The real-time PCR technique is based on the detection of fluorescence signals emitted due to the synthesis of PCR amplicons by Taq polymerase (2). In the present method, amplicon synthesis is monitored using SYBR® Green, a fluorescent dye that binds to double-stranded DNA. In contrast to other PCR methods, quantification using real-time PCR is a non-end-point measurement and based on a continuous increase of a fluorescence signal, which is measured after each cycle.

3.1. Cell Lysis and Nucleic Acid Extraction

1. To ensure good homogeneity of samples, these may be additionally ground in liquid N until a fine powder is obtained.
2. Weigh 0.5 g of ground sample (fresh weight) into a lysis tube containing ceramic balls.
3. Add the corresponding buffers (*see* **Note 2**).
4. Lyse cells in a homogenizator (30 s at 5.5 m/s)
5. Proceed with the extraction protocol as indicated by the author's or the manufacturer's instructions.
6. Depending on the protocol, used nucleic acids may be either resuspended or eluted with water (*see* **Note 1**).

3.2. Quantification Using MPN-PCR

1. The extracts obtained in the previous section are used for the MPN PCR approach. Prepare a succession of 1/10 serial dilutions of the sample of interest (*see* **Notes 1** and **6**). At least three replicates of each dilution are required.
2. Prepare a PCR reaction mix (23 μl) following this scheme:

Reagents	Volume (μL)	Final concentration
10× buffer	2.5	1×
$MgCl_2$ (50 mM)	1	2 mM
dNTPs (2 mM)	1.25	0.1 mM
Fwd primer (4 μM)	0.625	0.1 μM
Rev primer (4 μM)	0.625	0.1 μM
BSA (3%)	0.5	0.06%
Taq polymerase (5 U/μL)	0.25	0.01 U/μL
Water	16.25	

3. We suggest that a Master Mix is prepared for the desired number of samples.

Stage	Time	Temperature (°C)	Touchdown	Cycles
Stage 1				
Hotstart	10 min	95	(*see* **Note 7**)	×1
Stage 2				
Denature	45 s	95		×5
Anneal	1 min	62	−1°C/cycle	
Extend	45 s	72	(*see* **Note 8**)	
Stage 3				
Denature	45 s	95		×30
Anneal	1 min	57		
Extend	45 s	72		
Stage 4				
Final extension	10 min	72		×1
Pause	–	4		

4. Load 23 μL of reaction mix in each reaction tube.
5. Add 2 μL of template. Store on ice until you are done with all samples. Vortex briefly and centrifuge.
6. Run the following PCR program:
7. When the PCR is completed, vortex the samples briefly for 2 s and centrifuge for 5 s) using a microcentrifuge (14000 × *g*).
8. Carry out an agarose gel electrophoresis (2% agarose). A total of 15 μL PCR product and 4 μL of loading dye should be sufficient for detection of the amplified product. Let the samples run for 1 h at 120 V. At least 100 bp DNA ladder should be included on one of the gel lanes.
9. Following gel electrophoresis, visualize amplicons on the gel with ethidium bromide. In general, a 10–15 min bath is enough if the bath has been recently prepared or has not been used too many times.
10. Detect amplified products with a gel documentation system – the size of the band of interest is approximately 550 bp.
11. Identify the three sets of tubes/reactions that show dilution of the gene to "extinction."
12. Note the number of positive and negative scores resulting from each reaction (e.g., 3 positives for the first dilution, 2 for the second, and 0 for the last).

13. Use an MPN-Table or MPN-calculator (*see* **Note 9**) to compute the most probable number of gene copies in 1 μL of the original dilution.
14. Since the amount of nucleic acids in the original extract is known (nondiluted sample), the final result can be expressed as the number of gene copies/mg of DNA or the number of gene copies/g of soil material (dry weight).

3.3. Quantification Using Real-Time PCR

1. Make 1/10 serial dilutions for the standard (*see* **Notes 3, 10, 11, and 12**). For samples we recommend that 1 in 2 or 1 in 3 serial dilutions are performed to find out the dilution that gives the highest copy number for that sample following PCR reaction (*see* **Notes 3, 11, and 13**).
2. Prepare a PCR reaction mix (23 μl) following this scheme (*see* **Note 14**):

Reagents	Volume (μL)	Final concentration
$MgCl_2$ (50 mM)	1	2 mM
Foward primer (4 μM)	0.625	0.1 μM
Reverse primer (4 μM)	0.625	0.1 μM
BSA (3%)	0.5	0.06%
SyberGreen Master Mix	12.5	
Water	7.75	

3. Prepare a master mix for the desired number of samples.
4. Load 23 μL of reaction mix in each reaction well of the plate (*see* **Note 15**).
5. Cover the negative controls with cap strips to prevent contamination.
6. Add 2 μl of the template DNA to each reaction well of the plate following your working scheme. The final volume of each reaction is 25 μL.
7. When you are done with the templates, add 2 μL of water to template-free reaction wells. These will act as negative controls. Use at least three wells for this purpose.
8. Seal the PCR plate with the MicroAmp™ optical adhesive film. Remove air bubbles by pushing the film to the plate tightly.
9. Spin down the plate for 30 s and load the qPCR system.
10. Run the following PCR program:
11. Values can be calculated based on the Ct value.

Stage	Time	Temperature (°C)	Touchdown	Cycles
Stage 1				
Hotstart	10 min	95	(*see* **Note 7**)	×1
Stage 2				
Denature	45 s	95		×5
Anneal	1 min	62	−1°C/cycle	
Extend	45 s	72	(*see* **Note 8**)	
Stage 3				
Denature	45 s	95		×40
Anneal	1 min	57		
Extend	45 s	72		
Data Collection	30 s	78	(*see* **Note 16**)	
Stage 4 (termination)				
Denature	15 s	95		×1
Anneal	30 s	60	(*see* **Note 17**)	
Extend	15 s	95		

12. To ensure that the quantified amplicons possess the right size, run an agarose gel as described in the MPN PCR approach.
13. As for MPN PCR the final result can be expressed either as the number of gene copies/mg of DNA or the number of gene copies/g of soil material (dry weight).

4. Notes

1. All solutions should be prepared in water treated with 0.1% diethylpyrocarbonate (DEPC) (Sigma-Aldrich, Munich, Germany). This standard is referred to as "water" in this text.
2. For extraction and isolation of nucleic acids, follow the instructions proposed by the authors of the method or the manufacturer's instructions in those cases where different kit systems are used. When measuring the concentration of the isolated nucleic acids, the ratio of sample absorbance at 260 and 280 nm (260/280) should be in the range of 1.8–2.2 for "pure" nucleic acids. A ratio appreciably lower

might be indicative for the presence of co-purified contaminants such as humic acids or phenol.

3. Make all dilutions with water.
4. The SYBR® Green 1 Dye in the master mix is light-sensitive and should be kept in the dark. See manufacturer's instructions for long-term storage and safety.
5. We inserted inosine where the bases were fourfold degenerated to reduce the degeneracy and improve binding of the primers to template.
6. For samples with low copy numbers, a succession of serial dilutions up to 10^4 might be sufficient. Dilutions up to 10^5 or 10^6 may be necessary for samples with high copy numbers.
7. The hotstart stage allows specific annealing reactions to occur and prevents nonspecific annealing events. With a lack of nonspecific hybridization of primers to template or to one another, the resulting amplified DNA bands are cleaner.
8. Due to the degeneracy of the primers and hence differing melting temperature ranges, a touchdown PCR step greatly improves annealing to the template.
9. MPN-tables are available in numerous books, e.g., (15). Instead, you can download a free MPN-calculator from the Internet. Both MPN-tables and calculators should provide the upper and lower limit of the 95% confidence interval.
10. We found copy numbers of the standard from $10^8/\mu l$ to $10^2/\mu l$ to be appropriate for this protocol.
11. When drops are located on the lid of the reaction tube, spin down the tubes. This helps to reduce the danger of cross-contaminations when opening the tubes.
12. We used a 550 bp long fragment of the *alkB* gene of *Pseudomanos putida* Gpo1 cloned into pCR 2.1-Topo vector (Invitrogen, Carlsbad, CA, USA) as the external standard. After plasmid isolation the DNA concentration was measured and the number of copies of the fragment calculated. Alkane monooxygenase genes from other strains may also be used as well.
13. In general, dilutions higher than 1/100 are not necessary for environmental samples.
14. We have used the 7300 Real-Time PCR System (Applied Biosystems, Foster City, CA, USA) and optimized the qPCR-protocol for this system. When other systems are used, other optimization steps might be necessary. Please follow the manufacturer's instructions for each system.

15. A repeater-step pipette may reduce pipetting errors when processing a large number of samples.
16. Due to high primer degeneracy primer-dimers can occur during the annealing step. These will give a positive signal using the Sybr Green detection system. To avoid this, an additional data collection step at 78°C is included to ensure that no primer-dimers are detected, since the latter have a denaturation temperature below 78°C.
17. During this step the dissociation curve is recorded, allowing the detection of unspecific PCR products.

References

1. Bird, C.W., and Lynch, J.M. (1974) Formation of hydrocarbons by microorganisms. *Chem. Soc. Rev.* 3, 309–328.
2. Taylor, S.E., and Calvin, M. (1987) Hydrocarbons from plants: biosynthesis and utilization. *Comm. Agric. Food Chem.* 1, 1–26.
3. Martin dos Santos, V.A.P., Yakimov, M.M., Timmis, K.N., and Golyshin, P.N. (2008) Genomic Insights into oil biodegradation in marine systems. In Díaz. E. (ed.) *Microbial Biodegradation. Genomics and Molecular Biology.* Caister Academic Press, Norfolk, UK, pp. 219–268.
4. van Beilen, J.B., Li, Z., Duetz, W.A., Smits, T.H., and Witholt, B. (2003) Diversity of alkane hydroxylase systems in the environment. *Oil Gas Sci Technol* 58, 427–440.
5. Widdel, F., and Rabus, R. (2001) Anaerobic biodegradation of saturated and aromatic hydrocarbons. *Curr. Opin. Biotechnol.* 12, 259–276.
6. van Beilen, J.B., and Funhoff, E.G. (2007) Alkane hydroxylases involved in microbial alkane degradation. *Appl Microbiol. Biotechnol.* 74, 13–21.
7. Smits, T.H.M., Röthlisberger, M., Witholt, B., and van Beilen, J.B. (1999) Molecular screening for alkane hydroxylase genes in Gram-negative and Gram-positive strains. *Environ. Microbiol.* 1, 307–317.
8. Vomberg, A., and Klinner, U. (2000) Distribution of *alkB* genes within n-alkane-degrading bacteria. *J. Appl. Microbiol.* 89, 339–348.
9. van Beilen, J.B., Funhoff, E.F., van Loon, A., Just, A., Kaysser, L., Bouza, M. et al. (2006) Cytochrome P450 Alkane hydroxylases of the CYP153 family are common in alkane-degrading eubacteria lacking integral membrane alkane hydroxylases. *Appl. Environ. Microbiol.* 72, 59–65.
10. Kloos, K., Munch, J.C., and Schloter, M. (1996) A new method for the detection of alkane-monooxygenase homologous genes (alkB) in soils based on PCR-hybridization. *J. Microbiol. Meth.* 66, 486–496.
11. Sharma, S., Radl, V., Hai, B., Kloos, K., Mrkonjic-Fuka, M., Engel, M. et al. (2007) Quantification of functional genes from prokaryotes in soil by PCR. *J. Microbiol. Meth.* 68, 445–452.
12. Mc Crady, M.H. (1915) The numerical interpretation of fermentation-tube results. *J. Infect. Dis.*17, 183–212.
13. Cochran, W.G. (1950) Estimation of bacterial densities by means of the Most Probable Number. *Biometrics* 4, 105–106.
14. Lee, L.G., Connell, C.R., and Bloch, W. (1993) Allelic discrimination by nick translation PCR with fluorogenic probes. *Nuc. Acid. Res.*21, 3761–3766.
15. Alef, K., and Nannipieri, P. (1995) *Methods in Applied Soil Microbiology and Biochemistry*, Academic Press Inc, San Diego, USA, 576 pp.

Publication II

Journal of Microbiological Methods 80 (2010) 295–298

Contents lists available at ScienceDirect

Journal of Microbiological Methods

journal homepage: www.elsevier.com/locate/jmicmeth

Note

A comparative study of most probable number (MPN)-PCR vs. real-time-PCR for the measurement of abundance and assessment of diversity of *alkB* homologous genes in soil

Stephan Schulz [a,1], Alfredo Peréz-de-Mora [a,1], Marion Engel [b], Jean Charles Munch [a], Michael Schloter [b,*]

[a] Technische Universität München, Chair of Soil Ecology, Ingolstädter Landstr. 1, 85764 Neuherberg, Germany
[b] Helmholtz Zentrum München, German Research Center for Environmental Health (GmbH), Institute of Soil Ecology, Department of Terrestrial Ecogentics, Ingolstädter Landstr. 1, 85764 Neuherberg, Germany

ARTICLE INFO

Article history:
Received 15 November 2009
Received in revised form 1 January 2010
Accepted 1 January 2010
Available online 15 January 2010

Keywords:
Quantitative PCR
Real-time PCR
MPN-PCR
Alkane monooxygenase gene *alkB*

ABSTRACT

The utilization of quantitative PCR (qPCR) approaches such as MPN-qPCR and real-time-qPCR for *in situ* assessment of functional genes yields substantial quantitative and qualitative differences. We show this by targeting the *alkB* gene related to biodegradation of aliphatic alkanes in a set of environmental samples with differing hydrocarbon content.

Quantitative PCR (qPCR) assays based on most-probable-number (MPN) or real-time (rt) techniques have become increasingly popular in the last decade to determine abundance of phylogenetic or functional microbial groups in samples from different environments (Baldwin et al., 2003; Margesin et al., 2003). Even if the same primer system is used different qPCR techniques differ in their chemistry, the mathematical approach to quantify the number of gene copies of interest and the type of *Taq* polymerase enzyme used. However there is still insufficient knowledge regarding the differences in terms of ecological information that these methods may generate. Questions about gene copy numbers obtained or which fraction of the microbial community is targeted using different qPCR approaches but the same primer system have never been answered. Therefore it was the aim of this study to compare MPN-qPCR and rt-qPCR data using the same primer system, to give in depth information about the comparability of different qPCR techniques.

As an example the bacterial gene *alkB*, which codes for a rubredoxin-dependent alkane monooxygenase that catalyzes the first step in the aerobic oxidation of *n*-alkanes was chosen. A wide range of oligonucleotide primers and DNA probes targeting *alkB* genes have been recently developed (Baek et al., 2006; Hara et al., 2004; Kloos et al., 2006; Kuhn et al., 2009; Marchant et al., 2006; Mehboob et al., 2009; Powell et al., 2006; Smits et al., 2002; Whyte et al., 1996, 2002). While most studies dealing with the detection of *alkB* in the past were based on the identification of the gene by PCR from isolates (Beilen van et al., 2006; Throne-Holst et al., 2007; Vomberg and Klinner, 2000), direct application of PCR to measure abundance or diversity of *alkB* from environmental samples has been increasing (Hamamura et al., 2008; Kloos et al., 2006; Powell et al., 2006).

Soil samples from 12 sites (S01–S12) differing in total hydrocarbon concentrations were used in this study (Table 1). Samples were taken in triplicates from topsoil (0–15 cm) using a soil auger (diameter 5 cm) and stored at −20 °C until further use. The three samples obtained from each site were analyzed individually and treated as true replicate. Cells were lysed mechanically as described by Pérez-de-Mora et al. (2008) and nucleic acids were isolated according to the protocol proposed by Griffiths et al. (2000). Primers published by Kloos et al. (2006) with no discrimination of known bacterial groups harbouring *alkB* were used. These primers were slightly modified by substituting every four-fold degenerated base with inosine-nucleotides to reduce degeneracy and improve amplication efficiency. Amplicon length was 550 bp.

MPN-qPCR consisted of stepwise 1:10 dilutions of the DNA samples (5 replicates per dilution). PCR reaction (25 µl volume) was performed with 2 mM $MgCl_2$, 0.1 µM of forward and reverse primer each, 0.06% bovine serum albumine, 0.25 U *Taq* polymerase including the corresponding buffer (Invitrogen, USA) and 2 µl DNA. Amplification was performed as touchdown PCR (10 min 95 °C, 5 cycles of 45 s 95 °C, 1 min 62 °C (stepwise reduced to 57 °C) and 45 s 72 °C,

* Corresponding author. Tel.: +49 89 3187 2304; fax: +49 89 3187 2800.
E-mail address: schloter@helmholtz-muenchen.de (M. Schloter).
[1] Authors contributed equally.

0167-7012/$ – see front matter © 2010 Elsevier B.V. All rights reserved.
doi:10.1016/j.mimet.2010.01.005

Table 1
Soil properties.

Sample	Location	Coordinates	Soil use	Texture	pH	Total carbon (mg kg^{-1})	Total nitrogen (mg kg^{-1})	Total hydrocarbon (mg kg^{-1})	Co-contamination
S01	Munich	48°12′ N 11°35′ E	Grassland close to a highway	Sandy	7.1	87,175	5660	385	Heavy metals, PAH
S02	Munich	48°22′ N 11°58′ E	Park grassland	Loamy sand	6.5	60,131	5150	116	–
S03	Münsingen	48°37′ N 09°48′ E	Mowed pasture	Silty loam	5.2	53,791	5812	100	–
S04	Münsingen	48°37′ N 09°48′ E	Pasture	Silty loam	7.2	102,365	4511	114	–
S05	Kronach	50°14′ N 11°18′ E	Mixed forest-beech	Sandy loam	3.2	35,348	2368	158	Heavy metals
S06	Kronach	50°14′ N 11°18′ E	Mixed forest-beech	Sandy loam	5.4	104,676	4294	3748	Heavy metals
S07	Kronach	50°14′ N 11°18′ E	Mixed forest-beech	Sandy loam	5.5	92,157	4160	2878	Heavy metals
S08	Kronach	50°14′ N 11°18′ E	Mixed forest-beech	Sandy loam	3.6	81,693	3768	1158	Heavy metals
S09	Kronach	50°14′ N 11°18′ E	Mixed forest-beech	Sandy loam	4.9	314,278	10,883	13,021	Heavy metals
S10	Kronach	50°13′ N 11°19′ E	Mixed forest-fir	Loamy sand	3.2	43,139	617	31,768	Heavy metals
S11	Kronach	50°13′ N 11°19′ E	Mixed forest-fir	Loamy sand	3.3	52,891	2024	627	Heavy metals
S12	Kronach	50°13′ N 11°19′ E	Mixed forest-fir	Loamy sand	2.8	77,795	1748	2595	Heavy metals

30 cycles of 45 s 95 °C, 1 min 57 °C and 45 s 72 °C; the final extension was done for 10 min at 72 °C. Signals of MPN-PCR were analyzed after gel electrophoresis with ImageJ Software (Rasband, 1997–2009) after a signal threshold of 10% above background was set. MPN values were calculated according to Cochran (1950).

Rt-qPCR reactions (25 µl volume) were performed with 2 mM $MgCl_2$, 0.1 µM forward and reverse primer each, 0.06% bovine serum albumine, SybrGreen Master Mix (including polymerase; Applied Biosystems, Germany) and 2 µl of 1:32 diluted DNA to overcome inhibitory effects of coextracted humic acids. Amplification reactions were performed in triplicates in the same way as described for MPN-qPCR by using 7300 Real-Time PCR System (Applied Biosystems, Germany). Rt-qPCR amplification efficiencies were calculated according to the following equation:

$$e = 10^{(-1/slope)} - 1 \quad [1]$$

e-values ranged from 83% to 87%. Standard curves for the rt-qPCR assays were linear ($r^2 > 0.99$) over seven orders of magnitude. No signals were observed in the non-template controls. Clone libraries for the diversity analysis of PCR products were created using the pCR2.1 vector system and the TOPO TA Cloning® Kit (Invitrogen, Germany) following the manufacturer's instructions from amplicons obtained from soil S01 (Table 1). PCR products of the replicates, from PCR reactions with 1:10 diluted template DNA, were pooled for clone library studies. After the isolation of recombinant plasmids (Birnboim and Doly, 1979), sequencing was done using M13 forward and reverse primer (Invitrogen, Germany), the Terminator Kit 3.1 (Applied Biosystems, USA) and a capillary sequencer (ABI 3730, Applied Biosystems). Nucleotide sequences were translated into protein sequences *in silico* using the ExPasy proteomic server software (Gasteiger et al., 2003) and subsequently aligned with the blastp-software (NCBI, http://www.ncbi.nlm.nih.gov). The phylogenetic tree was calculated with the ARB Software (Ludwig et al., 2004) using Maximum-Likelihood as well as Parsimony and Neighbour-Joining methods for stability testing (data not shown). Sequences are available under the GenBank accession numbers GU184252 to GU184335.

Values of *alkB* gene copy numbers (*alkB* copies µg^{-1} DNA) from MPN-qPCR and rt-qPCR were tested for correlation. As observed in Fig. 1, values showed a scattered distribution and were poorly correlated ($r = 0.27$; $p = 0.396$). In all cases, results from rt-qPCR were between one and three orders of magnitude higher compared to data obtained from MPN-qPCR.

To assess differences in the diversity of the amplicons resulting from the two PCR approaches, two clone library containing 42 clones from MPN-qPCR products and 42 clones from rt-qPCR products were obtained. Results showed substantial differences in the diversity found in the two libraries; surprisingly no shared sequences were found in both libraries and only 12% of the MPN- and qPCR clones showed an amino acid sequence similarity above 90%. Cluster analysis led to two major groups (clusters I and II). Cluster I further branched into various subgroups (Fig. 2). Cluster II was exclusively composed of sequences obtained from MPN-qPCR, closely related to *Microscilla marina* ATCC 23134. Within subcluster Ia sequences from both qPCR methods were found (75% of MPN-qPCR sequences vs. 25% of rt-qPCR sequences). In contrast subcluster Ib was dominated by sequences obtained from rt-qPCR (83% rt-qPCR vs. 17% MPN-qPCR), most sequences in this subcluster were phylogenetically related to *Nocardiodes* sp. CF8.

Our results clearly indicate differences in the diversity data for *alkB* obtained by both qPCR methods. This observation may also occur with other functional genes. Our results also indicate that differences observed are not only related to redundancy but also to the abundance data. These differences may be related to i) the lower efficiency of polymerase after 35 PCR cycles, which forms the basis for MPN-qPCR quantification compared to polymerase efficiency in the exponential phase (cycles 10–15) which is the basis for rt-qPCR quantification, ii) the DNA detection chemistry (ethidium bromide for MPN-qPCR vs. SybrGreen for rt-qPCR); iii) the calibration method (no calibration for MPN-qPCR vs. standard curve calculation for rt-qPCR), iv) the statistical basis (probability for MPN-qPCR vs. regression for rt-qPCR), v) different levels of sensitivity of different polymerases to potential inhibitors and vi) subjectivity for the detection baseline.

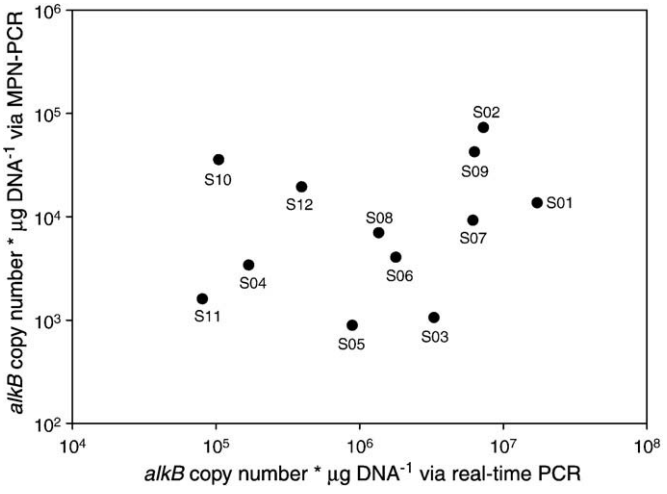

Fig. 1. Comparison of *alkB* abundance using MPN- and rt-qPCR.

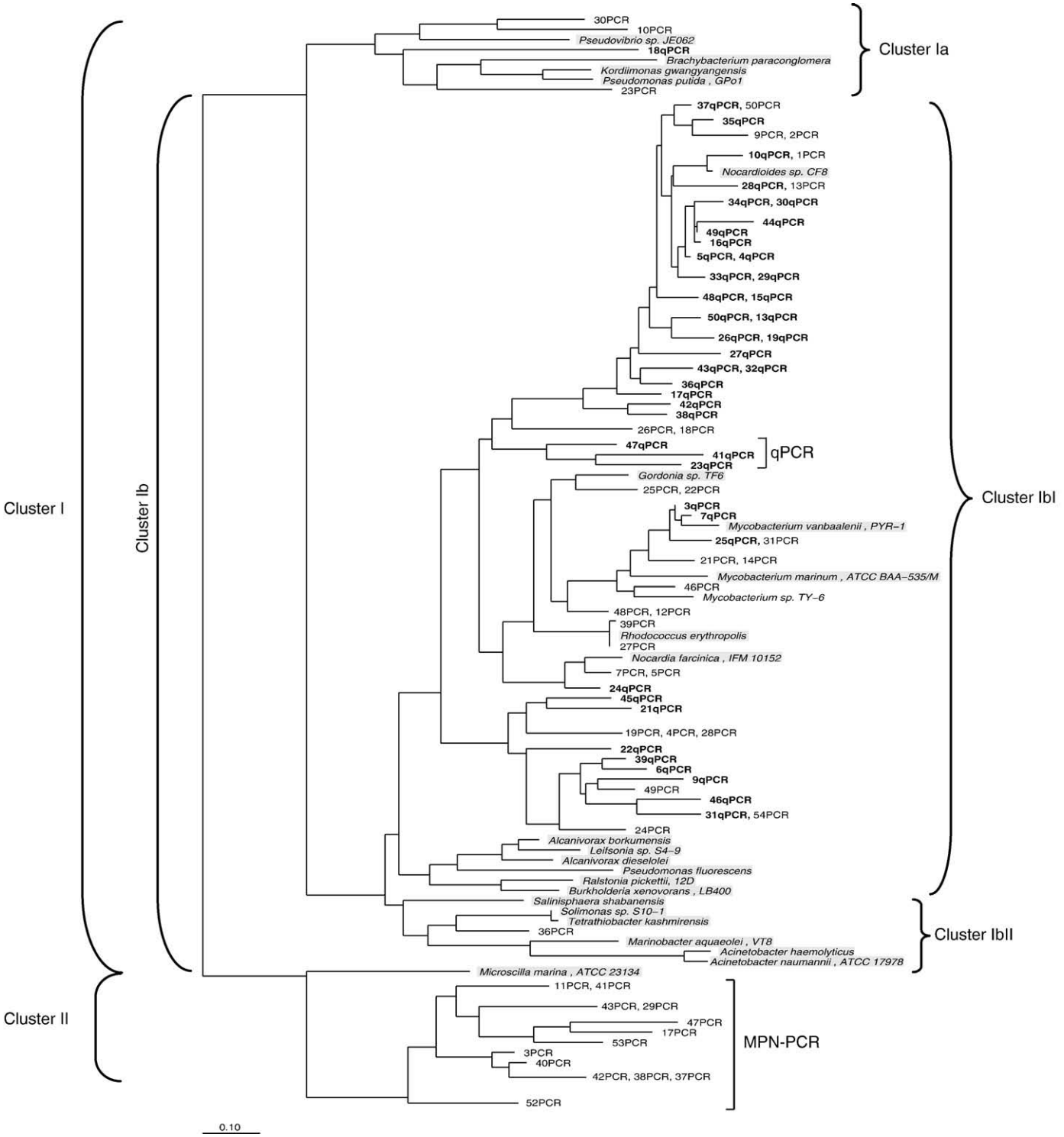

Fig. 2. Phylogenetic, aminoacid based PHYLIP-tree of clone sequences obtained from soil 1 using MPN-qPCR (PCR) and real-time-qPCR (qPCR) approaches. NCBI reference sequences are marked in gray.

Acknowledgements

This work has been supported by a grant from the Deutsche Forschungsgemeinschaft (DFG) in the frame of the priority program 1315 (Biogeochemical Interfaces in Soil).

References

Baek, K.-H., Byung-Dae, Y., Hee-Mock, O., Hee-Sik, K., 2006. Biodegradation of aliphatic and aromatic hydrocarbons by *Nocardia* sp. H17-1. Geomicrobiology Journal 23, 253–259.

Baldwin, B.R., Nakatsu, C.H., Nies, L., 2003. Detection and enumeration of aromatic oxygenases by multiplex and real-time PCR. Applied and Environmental Microbiology 69, 3350–3358.

Beilen van, J.B., Funhoff, E.G., Loon, A.v., Just, A., Kaysser, L., Bouza, M., Holtackers, R., Röthlisberger, M., Li, Z., Witholt, B., 2006. Cytochrome P450 alkane hydroxylases of the CYP153 family are common in alkane-degrading eubacteria lacking integral membrane alkane hydroxylases. Applied and Environmental Microbiology 72, 59–65.

Birnboim, H.C., Doly, J., 1979. A rapid alkaline extraction procedure for screening recombinant plasmid DNA. Nucleic Acid Research 7, 1513–1523.

Cochran, W., 1950. Estimation of bacterial densities by means of the "most probable number". Biometrics 6, 105–116.

Gasteiger, E., Gattiker, A., Hoogland, C., Ivanyi, I., Appel, R.D., Bairoch, A., 2003. ExPASy: the proteomics server for in-depth protein knoledge and analysis. Nucleic Acid Research 31, 3784–3788.

Griffiths, R.I., Whiteley, A.S., O'Donnell, A.G., Bailey, M.J., 2000. Rapid method for coextraction of DNA and RNA from natural environments for analysis of ribosomal DNA- and rRNA-based microbial community composition. Applied and Environmental Microbiology 66, 5488–5491.

Hamamura, N., Fukui, M., Ward, D.M., Inskeep, W.P., 2008. Assessing soil microbial populations responding to crude-oil amendment at different temperatures using phylogenetic, functional gene (*alkB*) and physiological analyses. Environmental Science & Technology 42, 7580–7586.

Hara, A., Baik, S., Syutsubo, K., Misawa, N., Smits, T.H.M., Beilen, J.B.v., 2004. Cloning and functional analysis of *alkB* genes in *Alcanivorax borkumensis* SK2. Environmental Microbiology 6 (3).

Kloos, K., Munch, J.C., Schloter, M., 2006. A new method for the detection of alkane-monooxygenase homologous genes (*alkB*) in soils based on PCR-hybridization. Journal of Microbiological Methods 66, 486–496.

Kuhn, E., Bellicanta, G.S., Pellizari, V., 2009. New *alk* genes detected in Antarctic marine sediments. Environmental Microbiology 11, 669–673.

Ludwig, W., Strunk, O., Westram, R., Richter, L., Meier, H., Yadhukumar, Buchner, A., Lai, T., Steppi, S., Jobb, G., Förster, W., Brettske, I., Gerber, S., Ginhart, A.W., Gross, O., Grumann, S., Hermann, S., Jost, R., König, A., Liss, T., Lüßmann, R., May, M., Nonhoff, B., Reichel, B., Strehlow, R., Stamatakis, A., Stuckmann, N., Vilbig, A., Lenke, M., Ludwig, T., Bode, A., Schleifer, K.-H., 2004. ARB: a software environment for sequence data. Nucleic Acid Research 32, 1363–1371.

Marchant, R., Sharkey, F.H., Banat, I.M., Rahman, T.J., Perfumo, A., 2006. The degradation of n-hexadecane in soil by thermophilic geobacilli. FEMS Microbiology Ecology 56, 44–54.

Margesin, R., Labbe, D., Schinner, F., Greer, C.W., Whyte, L.G., 2003. Characterization of hydrocarbon-degrading microbial populations in contaminated and pristine alpine soils. Applied and Environmental Microbiology 69, 3085–3092.

Mehboob, F., Junca, H., Schraa, G., Stams, A.J.M., 2009. Growth of *Pseudomonas chloritidis* mutants AW-1^T on n-alkanes with chlorate as electron acceptor. Applied Microbiology and Biotechnology 83, 739–747.

Pérez-de-Mora, A., Madejón, E., Cabrera, F., Buegger, F., Fu, R., Pritsch, K., Schloter, M., 2008. Long-term impact of acid resin waste deposits on soil quality of forest areas I. Contaminants and abiotic properties. Science of the Total Environment 406, 88–98.

Powell, S.M., Ferguson, S.H., Bowman, J.P., Snape, I., 2006. Using real-time PCR to assess changes in the hydrocarbon-degrading microbial community in Antarctic soil during bioremediation. Microbial Ecology 52, 523–532.

Rasband, W.S., 1997–2009. ImageJ 1.41o. National Institutes of Health, USA.

Smits, T.H.M., Balada, S.B., Witholt, B., Beilen, J.B.v., 2002. Functional analysis of alkane hydroxylases from gram-negative and gram-positive bacteria. Journal of Bacteriology 184, 1733–1742.

Throne-Holst, M., Wentzel, A., Ellingsen, T.E., Kotlar, H.-K., Zotchev, S.B., 2007. Identification of novel genes involved in long-chain n-alkane degradation by *Acinetobacter* sp. strain DSM 17874. Applied and Environmental Microbiology 73, 3327–3332.

Vomberg, A., Klinner, U., 2000. Distribution of *alkB* genes within n-alkane-degrading bacteria. Journal of Applied Microbiology 89, 339–348.

Whyte, L.G., Greer, C.W., Inniss, W.E., 1996. Assessment of the biodegradation potential of psychrotrophic microorganisms. Canadian Journal of Microbiology 42, 99–106.

Whyte, L.G., Schultz, A., Van Beilen, J.B., Luz, A.P., Pellizari, V., Labbé, D., Greer, C.W., 2002. Prevalence of alkane monooxygenase genes in Arctic and Antartic hydrcarbon-contaminated and pristine soils. FEMS Microbiology Ecology 41, 141–150.

Publication III

The ISME Journal (2012), 1–12

www.nature.com/ismej

ORIGINAL ARTICLE

Plant litter and soil type drive abundance, activity and community structure of *alkB* harbouring microbes in different soil compartments

Stephan Schulz[1,2,5], Julia Giebler[3,5], Antonis Chatzinotas[3], Lukas Y Wick[3], Ingo Fetzer[3], Gerhard Welzl[4], Hauke Harms[3] and Michael Schloter[2]

[1]*Chair of Soil Ecology, Technische Universität München, Neuherberg, Germany;* [2]*Research Unit for Environmental Genomics, HelmholtzZentrum München, German Research Center for Environmental Health, Neuherberg, Germany;* [3]*Department of Environmental Microbiology, Helmholtz Centre for Environmental Research – UFZ, Leipzig, Germany and* [4]*Institute of Developmental Genetics, HelmholtzZentrum München, German Research Center for Environmental Health, Neuherberg, Germany*

Alkanes are major constituents of plant-derived waxy materials. In this study, we investigated the abundance, community structure and activity of bacteria harbouring the alkane monooxygenase gene *alkB*, which catalyses a major step in the pathway of aerobic alkane degradation in the litter layer, the litter–soil interface and in bulk soil at three time points during the degradation of maize and pea plant litter (2, 8 and 30 weeks) to improve our understanding about drivers for microbial performance in different soil compartments. Soil cores of different soil textures (sandy and silty) were taken from an agricultural field and incubated at constant laboratory conditions. The abundance of *alkB* genes and transcripts (by qPCR) as well as the community structure (by terminal restriction fragment polymorphism fingerprinting) were measured in combination with the concentrations and composition of alkanes. The results obtained indicate a clear response pattern of all investigated biotic and abiotic parameters depending on the applied litter material, the type of soil used, the time point of sampling and the soil compartment studied. As expected the distribution of alkanes of different chain length formed a steep gradient from the litter layer to the bulk soil. Mainly in the two upper soil compartments community structure and abundance patterns of *alkB* were driven by the applied litter type and its degradation. Surprisingly, the differences between the compartments in one soil were more pronounced than the differences between similar compartments in the two soils studied. This indicates the necessity for analysing processes in different soil compartments to improve our mechanistic understanding of the dynamics of distinct functional groups of microbes.

The ISME Journal advance online publication, 8 March 2012; doi:10.1038/ismej.2012.17
Subject Category: microbial ecology and functional diversity of natural habitats
Keywords: alkane monooxygenase; microbial community function; plant litter; soil compartments; waxes

Introduction

Soil harbours a multitude of different microhabitats for (micro)-organisms that form the basis for the vast diversity and functional heterogeneity often found in soils (Curtis and Sloan, 2005). Such habitats are characterised by multidimensional interfaces at the μm to mm scale, and are the result of the interplay of soil microbiota with their physical and chemical environment (Totsche *et al.*, 2010). As these structural elements are highly dynamic in response to the surrounding environmental conditions, they can be considered as hotspots for microbial activity and the basis of all ecosystem services provided by soils (Yaalon, 2000). In particular, the degradation of polymeric substances and other complex molecules might be depending on the structure of microhabitats either due to present varying microbial communities, different sorption properties and/or oxygen and nutrient availability. Such heterogeneity remains undetected, if vast amounts of bulk soils are sampled with a soil auger, homogenised and divided into subsamples for analysis.

Alkanes are major compounds of plant leaves (Eglinton *et al.*, 1962). The corresponding cuticulary waxes are produced as protective systems against phytopathogens or to minimise water loss by uncontrolled evaporation (Avato *et al.*, 1990;

Correspondence: M Schloter, Research Unit for Environmental Genomics, HelmholtzZentrum München, German Research Center for Environmental Health, Ingolstädter Landstraße 1, Neuherberg 85764, Germany.
E-mail: schloter@helmholtz-muenchen.de
[5]These authors contributed equally to this work.
Received 23 October 2011; revised 10 February 2012; accepted 10 February 2012

Gniwotta *et al.*, 2005). Compound concentration and composition of these waxes vary between plants, thus allowing differentiation of several plant families or plants with different metabolic properties like C3 and C4 plants (Rieley *et al.*, 1993; Collister *et al.*, 1994; Maffei, 1996). Earlier studies revealed the release of plant wax-derived alkanes during litter degradation and their transport into the surrounding soil (Lichtfouse *et al.*, 1994; Cayet and Lichtfouse, 2001; Dignac and Rumpel, 2006). Mainly alkanes with a chain length shorter than C_{20} can be transported into deeper soil layers and enter different soil compartments, where their bioavailability can be drastically reduced by physicochemical mechanisms such as (i) adsorption to soil organic matter and clay minerals (Manilal and Alexander, 1991; Richnow *et al.*, 1995), (ii) adsorption to non-aqueous-phase liquids and (iii) diffusion into smaller pores inaccessible for microbes (Bosma *et al.*, 1996). Soil microbes may also influence the bioavailability of alkanes. For example, bacteria can actively promote bioavailability by reducing their distance to these substrates by chemotaxis (Lanfranconi *et al.*, 2003), changing their cell wall properties (de Carvalho *et al.*, 2009) or producing biosurfactants such as rhamnolipids or the bioemulsifying protein. These processes facilitate bacterial attachment to substrate reservoirs (Wick *et al.*, 2000) and transfer of hydrocarbons into aqueous phases (Holden *et al.*, 2002). Beside alkane bioavailability other biotic and abiotic parameters like the presence of dissolved organic carbon (Smith *et al.*, 2009), the access to nutrients or the amount of oxygen present influence alkane biodegradation in different soil compartments.

The capability of alkane catabolism via aerobic and anaerobic degradation pathways is found among a broad range of fungi and bacteria. Although the chemically inert alkanes are activated by the addition of fumarate (Heider *et al.*, 1999; Widdel and Rabus, 2001; Wilkes *et al.*, 2003) during anoxia, aerobic activation is accomplished by the terminal (Sepic *et al.*, 1995; Koma *et al.*, 2001; Van Hamme *et al.*, 2003) or subterminal (Whyte *et al.*, 1998; Kotani *et al.*, 2006, 2007) introduction of oxygen. For alkanes with a chain length $<C_{30}$, which can be considered as typical for plant waxes, terminal oxygen introduction is mainly catalysed by the membrane bound, rubredoxin-dependent di-iron alkane monooxygenase (AlkB), which is found among *Actinobacteria*, α-, β- and γ-*Proteobacteria* (van Beilen *et al.*, 2003; van Beilen and Funhoff, 2007).

In this study, we report on the dynamics of the abundance, activity and community structure of microbes harbouring the alkane monooxygenase gene *alkB* during the degradation of litter-derived alkanes in different soil compartments (litter layer; litter–soil interface; bulk soil). We postulate that in soil compartments close to the litter material, the type of litter material highly influences abundance, activity and community structure of *alkB* harbouring bacteria. With increasing distance from the litter layer, the influence of the soil type should increase. For this, intact soil cores of two arable soils, differing significantly in their composition and texture, were incubated with litter of maize and pea. These two plants were chosen as they represent different assimilation pathways (C3 and C4 plants, respectively) and contain different alkane concentrations as well as different compositions (Avato *et al.*, 1990; Gniwotta *et al.*, 2005). The different compartments were analysed after 2, 8 and 30 weeks of incubation. The *alkB* gene copy numbers and amounts of *alkB* transcripts were quantified using SybrGreen-based real-time PCR, whereas the community structure of *alkB*-harbouring microbes and the corresponding transcripts was determined using terminal restriction fragment polymorphism (T-RFLP) analysis. Furthermore, the amount and composition of litter-derived alkanes were determined in the three different compartments.

Materials and methods

Soil sampling and microcosm experiment

A total of 96 soil cores (diameter 5 cm; height 5 cm) were taken with a soil auger from two different top soils (0–5 cm; 48 cores each) at an agricultural research farm located 45 km north of Munich (www.helmholtz-muenchen.de/scheyern) in autumn 2008 after the harvest of winter wheat. The soil texture of the silty (60.6% silt, 18% sand, 21.4% clay) and the sandy soil (31.4% silt, 55.2% sand, 13.4% clay) was determined in 2003 after Sinowski and Auerswald (1999). Both soils had a pH of 6.0 after extraction with 0.01 M $CaCl_2$. The soil cores were equilibrated for two weeks at 14 °C and 55% of the maximum water holding capacity to reset soil microbial activity. Three cores of each soil type were sampled after equilibration and served as time point zero treatments (T0). Nine soil cores of each soil type were incubated with 1 g dry weight (dw) fresh litter material from maize (*Zea mays* L), respectively, pea (*Pisum sativum* L) with a piece size of 25 mm^2, which was applied carefully on the top of the soil core. Additionally, for each litter and soil type nine cores were incubated using litter material in litterbags (1 g litter material per bag; 50 μm mesh size of the bags), which were carefully covered by soil to determine litter degradation rates. Nine cores of each soil type without litter addition served as controls. All cores were incubated in the dark up to 30 weeks at a constant temperature of 14 °C and soil moisture of 55% of maximum water holding capacity.

Sampling of three soil cores per treatment (sand-pea; sand-maize; sand-control; silt-pea; silt-maize; silt-control) was performed 2 (T1), 8 (T2) and 30 (T3) weeks after litter addition. For each sampling three compartments (litter layer, litter–soil interface and

bulk soil 1–1.5 cm below the interface) were sampled from each core and treated as true replicates from the treatments. To obtain the litter–soil interface, the remaining litter material was carefully removed with a pair of forceps and then carefully sampled using a clean spatula up to a depth of 2–3 mm below the litter layer. Samples were either shock frozen in liquid nitrogen and stored at −80 °C for molecular analysis or, respectively, dried with anhydrous Na_2SO_4 (ca 10–15 g) for the analysis of alkane amount and composition. For the determination of litter degradation rates, litter bags were removed from the soils of the corresponding treatments at T1, T2 and T3, and the air-dried litter material quantified gravimetrically.

Alkane analysis

Abundance and composition of alkanes were determined in triplicate from either 1.5 g soil or 0.5 g of pooled litter. Samples were extracted twice with 20 ml (60 min extraction time) and 10 ml (30 min) hexane (HPLC-grade; Merck, Darmstadt, Germany) using a horizontal shaker at room temperature, and then concentrated to 1 ml using a Turbo Vap II vacuum system (Zymark, Idenstein, Germany). In order to correct potential alkane losses during extraction, 50 ng of deuterated hexadecane per ml of hexane (Dr Ehrenstorfer GmbH, Augsburg, Germany) was used as extraction standard. Litter extracts were split into two fractions of 0.5 ml, where each of the fractions was further purified by using silica gel columns containing 0.5 g of cleaned and activated silica 60 (35–50 mesh, Merck) and 3–5 ml of hexane (HPLC-grade; Merck). Joined extracts of the columns were concentrated (Turbo Vap II vacuum system) to 0.5 ml. Gas chromatographic mass spectrometry (GC-MS) measurements of concentrated extracts were performed with an HP 6890 gas chromatograph (Hewlett Packard, Palo Alto, CA, USA), which was equipped with an HP-5 MS column and an HP 5973 mass spectrometer for detection (both Agilent Technologies, Santa Clara, CA, USA). Final temperature was set to 320 °C, at a final time of 7 min and an initial helium flow of 0.8 ml min^{-1}. For the MSD Transfer Line Heater an initial temperature of 280 °C was used.

Extraction of nucleic acids and cDNA synthesis

DNA and RNA were co-extracted as recently described (Töwe *et al*., 2011) and subsequently separated using the AllPrep DNA/RNA Mini Kit (Qiagen, Hilden, Germany) following the manufacturer's instructions. Quality and quantity of isolated nucleic acids were determined spectrophotometrically at 260 and 230 nm (Nanodrop ND-1000, Peqlab, Erlangen, Germany). First strand cDNA was synthesised with SuperScript II Reverse Transcriptase (Invitrogen, Darmstadt, Germany) using 1 pmol of random hexamer primer.

Table 1 Primers used for the quantitative PCR and T-RFLP analysis

Primer	*Sequence*[a,b]	*Reference*
alkB-1f	5′-AAYACNGCNCAYGARCTNGGNCA YAA-3′	Kloos *et al*. (2006)
alkB-1r	5′-GCRTGRTGRTCNGARTGNCGYTG-3′	Kloos *et al*. (2006)

[a]Underlined positions were substituted by an inosine nucleotide to improve amplification efficiency.
[b]*N* bases A, T, C or G; *Y* bases C or T; *R* bases G or A.

Quantification of alkB *genes and transcripts*

SybrGreen-based quantitative real-time PCR (qPCR) was performed with the ABI Prism 3300 (Applied Biosystems, Foster City, CA, USA) system for the DNA and cDNA. PCR reaction mixtures with 25 µl reaction volume contained 2 mM magnesium chloride, 0.1 µM of *alkB* specific primers (Table 1; Kloos *et al*., 2006), 0.06% BSA, 1 × Power Sybr Green Master Mix (Applied Biosystems) and 5–15 ng DNA or 10–40 ng cDNA, respectively. The qPCR was carried out as previously described (Pérez-de-Mora *et al*., 2010) using a cloned fragment of *alkB* (550 bp) from *Pseudomonas putida* as standard.

Standard curves were linear ($r^2 > 0.99$) over five orders of magnitude and amplification efficiency was around 86%. No fluorescence signals were detected in the non-template controls. Signal acquisition at 78 °C impeded biased fluorescence signal detection due to primer dimers.

Community structure of alkB harbouring bacteria and their transcripts

DNA and cDNA were used for T-RFLP analysis to track changes in the diversity of *alkB* harbouring bacteria on DNA as well as mRNA level. Briefly, PCR reaction mixtures with 25 µl volume were composed of *alkB* specific primers (Table 1), with alkB_1f labelled with 6-carboxyfluorescein (6-FAM), 15–20 ng DNA or 120 ng cDNA, 1 × *Taq* PCR Master Mix Kit (Qiagen) and 0.12% BSA. The annealing temperatures were set to 58.7 °C for 30 cycles for DNA and 58 °C for 35 cycles in the case of cDNA. PCR reactions were accomplished with no further changes in the PCR protocol described in the previous section. Afterwards, amplification products were purified with Wizard SV Gel and PCR Clean-UP System (Promega, Mannheim, Germany) according to the manufacturer's instructions and subsequently quantified spectrophotometrically at 260 nm (Nanodrop ND-1000, Peqlab). An amount of 100 ng purified DNA-derived PCR product or 10–50 ng of cDNA-derived PCR product, respectively (pooled from three independent PCR reactions), was digested at 37 °C over night using two units of *HpyCH4V* (New England BioLabs, Beverly, MA, USA). After precipitation of the restriction fragments with ethanol, T-RFLP was run in an ABI PRISM 3100 genetic analyzer system (capillary injection time of 15 s) using GeneScan 500 ROX as

size standard (both Applied Biosystems). Data were analysed with GeneMapper V3.7 software (Applied Biosystems).

Statistical analysis
Multifactorial ANOVA calculations were run with log-transformed data. For statistical analyses of the abundance of the *alkB* genes and transcripts as well as the community structure of *alkB* harbouring bacteria, the statistical software R version 2.10.0 (R Development Core Team, 2009) was used. Normal data distribution was checked by using histograms and the Kolmogorov–Smirnov test at a level of significance of $P \leqslant 0.05$. See details on the statistical analysis of T-RFLP data in the Supplementary Material S1.

qPCR data were calculated on the basis of the amount of soil or litter material. The alternative to relate functional gene abundance to 16S rRNA gene abundance has been not feasible, as a shift from *r*- to *k*-strategists may occur during the incubation time that excludes the use of constant conversion factors, because *r*- and *k*-strategists are known to contain different rRNA operon copy numbers (Klappenbach *et al.*, 2000).

Results

Litter degradation rates
Litter degradation rates based on the litter bag experiments performed followed a logarithmic function as described previously (Wang *et al.*, 2004; Ha *et al.*, 2007). The decay of pea litter was significantly faster than the degradation of maize litter ($P < 0.001$) independent of the soil type. Whereas after 2 weeks of incubation only half of the initial maize litter amount remained, nearly 80% of the initial pea litter was degraded. The soil type did not significantly influence the litter decay (Supplementary Materials S2 and S5).

Alkane analysis in the different compartments
Even- and odd-numbered, straight-chain alkanes of chain-lengths between C_{10}–C_{40} as well as pristane and phytane were quantified in all compartments (litter layer; litter–soil interface and bulk soil) at all sampling time points (Table 2 and Figure 1). Alkane amounts in plant litter exceeded the alkane loads of the underlying soil compartments by two to four orders of magnitude. Fresh plant material comprised alkane contents of about $180\,\mu g\,g^{-1}$ for maize litter and $6500\,\mu g\,g^{-1}$ for pea litter (Table 2). Alkane degradation rates were comparable in all litter samples with 43–87% of the total alkane concentration being lost within the first 8 weeks of incubation. Independent of the soil type ($P > 0.1$), maize and pea litter differed significantly ($P < 0.05$) in their relative chain-length distribution over time with considerably higher fractions of very long chained alkanes (C_{31}–C_{40}) in pea litter. Nonacosane (C_{29}) and hentriacontane (C_{31}), which are known to prevail in maize and pea (Avato *et al.*, 1990; Gniwotta *et al.*, 2005), constituted between 76–97% of the total alkane content in pea litter and 40–62% of the total alkanes in maize (Figure 1).

Similar concentration dynamics were monitored for the different soil compartments in both soil types with no significant influence ($P > 0.1$) of the litter type over time (Table 2). Starting with comparable alkane loads in silty and sandy soil ($206\,ng\,g^{-1}$ soil, respectively, $167\,ng\,g^{-1}$), the total alkane concentrations decreased to 20–47% of the initial concentration after 2 weeks (T1) in all soil samples. The differences

Table 2 Total alkane concentration at the three analyzed compartments during the incubation of sandy and silty soil microcosms with maize and pea litter

Compartment	*Time*	*Maize*		*Pea*	
		Sandy soil	*Silty soil*	*Sandy soil*	*Silty soil*
Litter ($\mu g\,g^{-1}$)	FM	183.4 (22.0)	183.4 (22.0)	6544.8 (2013.4)	6544.8 (2013.4)
	T1	29.9 (ND)	169.3 (ND)	7524.3 (ND)	6021.0 (ND)
	T2	26.3 (ND)	36.4 (ND)	881.3 (ND)	3705.9 (ND)
	T3	25.4 (ND)	56.6 (ND)	2111.4 (ND)	1428.5 (ND)
Interface (0-1 mm) ($ng\,g^{-1}$)	T1	52.0 (13.0)	46.0 (2.0)	52.0 (16.0)	50.0 (6.0)
	T2	39.0 (15.0)	36.0 (1.0)	66.0 (31.0)	47.0 (4.0)
	T3	49.0 (12.0)	105.0 (29.0)	81.0 (17.0)	96.0 (27.0)
Bulk soil ($ng\,g^{-1}$)	T0	167.0 (52.0)	206.0 (ND)	167.0 (52.0)	206.0 (ND)
	T1	67.0 (26.0)	52.0 (6.0)	78.0 (7.0)	40.0 (5.0)
	T2	128.0 (6.0)	39.0 (9.0)	71.0 (3.0)	48.0 (14.0)
	T3	120.0 (40.0)	74.0 (2.0)	79.0 (22.0)	108.0 (24.0)

Sampling time points for bulk soil were at the beginning (T0) and after 2 (T1), 8 (T2) and 30 (T3) weeks of incubation. Besides the fresh litter material (FM), litter has been also analyzed at T1–T3. Samples from the soil–litter interface have been analyzed from time points T1–T3. Note that concentrations are given in $\mu g\,g^{-1}$ (litter samples) or $ng\,g^{-1}$ (soil samples), respectively. Standard deviations are given in brackets ($n = 3$). As the amount of remaining litter material was too low for single measurements at T1, T2 and T3 litter material was pooled from the three replicates; thus no standard deviation is given (ND).

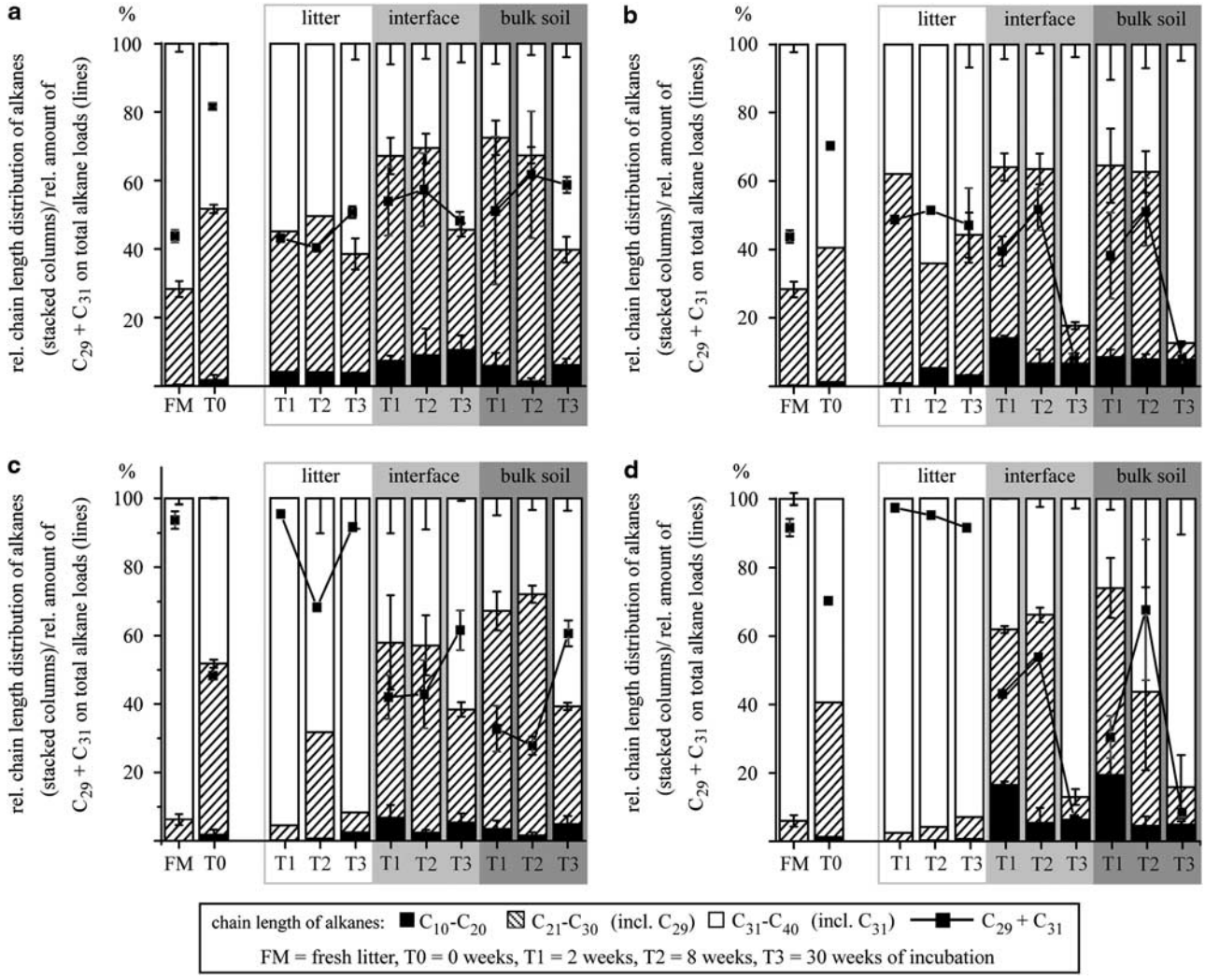

Figure 1 Relative distribution of medium- (C_{10}–C_{20}), long- (C_{22}–C_{30}) and very long-chain (C_{32}–C_{40}) alkanes and for the dynamics of nonacosane and hentriacontane (C_{29} and C_{31}) as control for the most abundant plant wax alkanes during the incubation of sandy (**a**, **c**) and silty (**b**, **d**) soil microcosms covered with litter of maize (**a**, **b**) or pea (**c**, **d**). The litter layer, litter–soil interface (0–1 mm) and the bulk soil are indicated. Error bars represent standard deviations ($n = 3$).

in the residual amounts at T1 were significantly dependent on the soil type ($P < 0.05$) but independent of the soil compartment ($P > 0.1$). Until the end of the experiment, further significant changes in total alkane amounts were observed only for bulk sandy soil incubated with maize at T2 (8 weeks) as well as both litter–soil interface and bulk soil compartments from the silty soil treatments at T3 (30 weeks) where up to three times higher alkane loads ($P < 0.05$) were monitored compared with the preceding time point.

Changes in the relative chain-length distribution of alkanes in soil were significantly influenced by the soil type and additionally by the incubation time ($P < 0.05$). Although sandy and silty soils shared a similar distribution of alkanes with different chain-lengths at T0 (2%; 50%; 48%, respectively, 1%; 40%; 59% for C_{10}–C_{20}; C_{21}–C_{30}; C_{31}–C_{40}) with nonacosane and hentriacontane constituting 82 and 70% of the total alkane content, pronounced differences were observed at T3. Whereas moderate changes of chain-length distribution patterns were observed during the incubation in sandy soils only, long-chained alkanes (C_{31}–C_{40}) represented the dominating alkane fraction (85%) in silty soils at T3. At this time a highly significant impact of the soil type was monitored ($P < 0.001$) while the litter type had no influence. Interestingly, only the relative amount of nonacosane and hentriacontane was influenced by the litter type at this time ($P < 0.05$), which is coincident to earlier results (Avato *et al.*, 1990; Gniwotta *et al.*, 2005).

Quantification of alkB *genes and transcripts in the different compartments*

All results of the quantification of *alkB* genes and transcripts are summarised in Figure 2. The initial *alkB* gene copy number differed in both litter types significantly ($P < 0.05$). While in maize litter

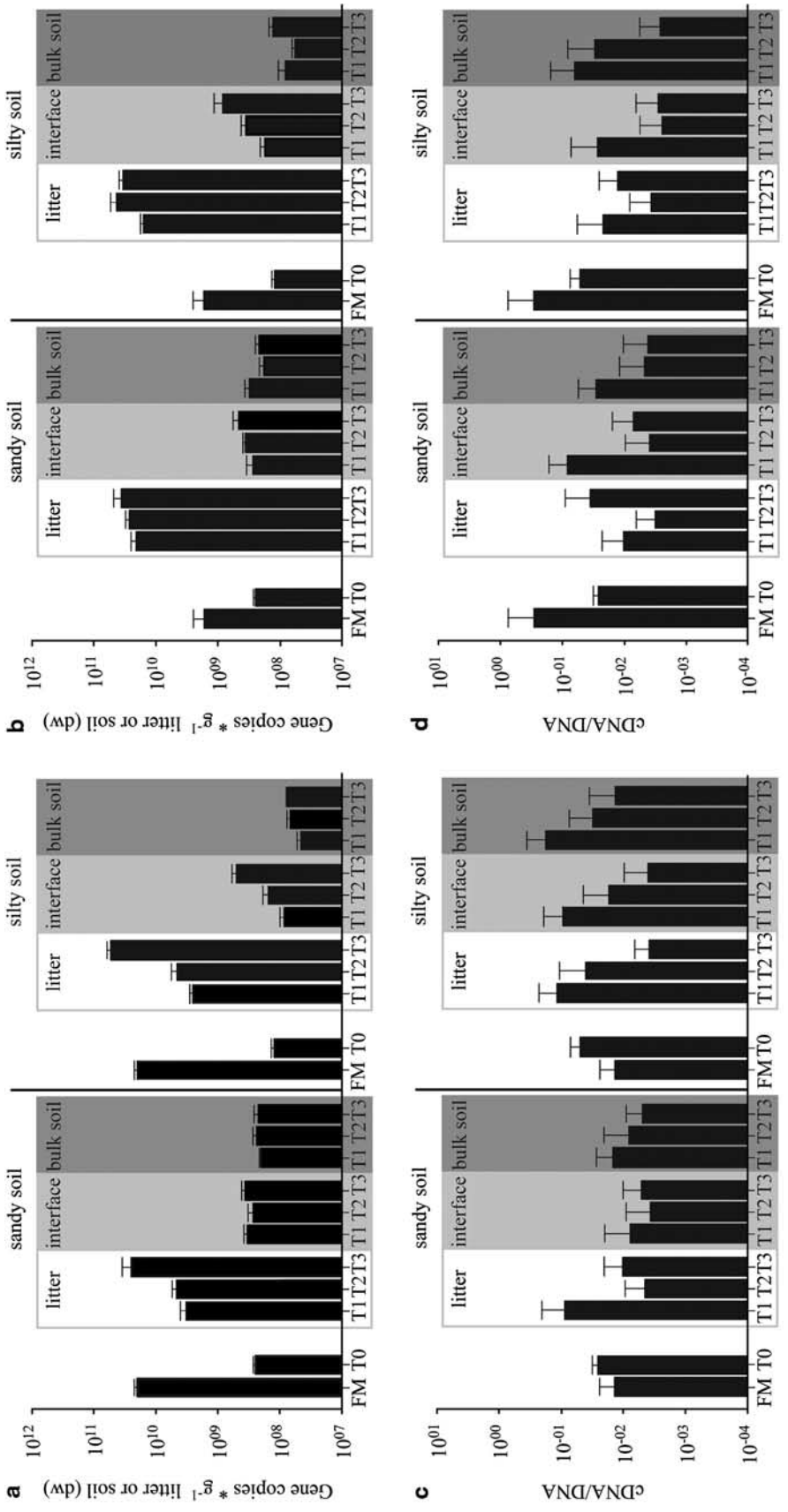

Figure 2 Changes in the abundance patterns (**a**, **b**) and the specific induction of the *alkB* gene (**c**, **d**) in the litter layer, the litter–soil interface and bulk soil during the incubation with maize (**a**, **c**) and pea (**b**, **d**) litter. The specific induction is referred to the ratio of *alkB* mRNA and DNA. Error bars represent standard deviations ($n = 3$).

3×10^{10} copies g^{-1} litter (dw) were monitored in the fresh litter material, gene copy numbers in pea litter were one order of magnitude lower. In the litter layer significant interactions between incubation time and litter type ($P = 0.001$) reflect the influence of both factors on *alkB* abundance. Although *alkB* gene copy numbers dropped at T1 and increased again towards T3 in all maize litter samples, in pea litter a significant increase in *alkB* copy numbers was mainly visible at the first 2 weeks of incubation towards T1. After 30 weeks of incubation *alkB* gene copy numbers were comparable in both litter types and reached almost 1×10^{11} copies g^{-1} litter (dw). The soil type had no significant influence on *alkB* gene copy dynamics in litter. *AlkB* gene copy numbers at the litter–soil interfaces and in the bulk soil compartments were significantly lower ($P < 0.001$) than in the respective litter layer and ranged between 2×10^{8} and 9×10^{8} copies g^{-1} soil (dw). In silty soil samples a clear reduction of *alkB* copy numbers from the litter–soil interface towards the bulk soil was visible. Over the time, gene copy numbers at the litter–soil interface increased, whereas no significant changes could be detected in bulk soil independent of the type of litter. In contrast, in the sandy soil samples no differences were monitored between both soil compartments and *alkB* gene copy numbers remained stable in the litter–soil interface over time.

Overall copy numbers of *alkB* transcripts followed the same trend like described above (data not shown). To describe specific transcription rates of *alkB* in the different compartments the ratio between mRNA and DNA copy numbers were calculated. Specific induction of *alkB* transcripts could be clearly observed independent from the soil type ($P = 0.95$) at the maize litter compartment within the first 2 weeks of incubation followed by a remarkable decrease. In contrast, highest specific induction rates for *alkB*-related transcripts were found in the fresh pea litter and decreased mainly in the first 2 weeks of incubation towards T1. In the silty soil samples treated with maize litter a clear influence of the litter addition was visible on the specific induction rates of *alkB* in the litter-soil compartment as well as in the bulk soil compartment after 2 weeks of incubation. In all other treatments, the addition of the litter material did not increase specific transcription rates in the two soil compartments towards T1. At T2 and T3, specific induction rates of *alkB* genes were reduced in all treatments compared with T0 independent of the plant litter type, the soil compartment analysed or the soil type ($P = 0.873$).

Gene and transcript copy numbers of *alkB* did not change significantly over time in control microcosms without litter addition (data not shown).

Community structure of alkB harbouring bacteria and their transcripts in the different compartments

Two weeks after the litter addition, an increase of total T-RF numbers (that is, richness of *alkB* genes) was observed in the litter-soil and bulk soil compartment irrespective of the soil type (Supplementary Material S7). Nonmetric multidimensional scaling plots calculated on the basis of Bray–Curtis similarity indices (including presence and relative abundance of T-RF) displayed a strong differentiation between communities on the DNA level in response to the sampled compartment, the litter type and the incubation time (Figure 3; Supplementary Material S4). Overall, *alkB*-harbouring communities in the litter–soil interface as well as in the bulk soil were more related to each other than to communities colonising the litter material. For example, T-RF 63, 117 and 475 were detected in most DNA samples from soil, but were far less frequent in litter samples. Conversely, the T-RF 260, 324 and 401 were far more specific for litter samples and occurred in only few soil samples (Supplementary Material S8) if at all. Interestingly, although less frequent in the litter samples based on DNA analysis, T-RF 63 and 117 were dominant members of the T-RF profiles of the mRNA samples, indicating high transcription rates of the corresponding genes at least at the time point of sampling. The analysis of samples derived from replicate treatments did not reveal significant differences in T-RFLP pattern (data not shown); therefore data in Figure 3 and others is based on analysis of pooled samples from replicated treatments for clarity reasons.

Nonmetric multidimensional scaling plots of amplified mRNA displayed no differentiation among communities in the different compartments, as observed on DNA level, irrespective of the litter material (Figures 3c and d). However, the composition of transcripts of *alkB* based on T-RF analysis was significantly impacted by the soil type in soil cores incubated with maize litter, whereas incubation time and the relative amount of C_{10}–C_{20} influenced the *alkB* genes and *alkB* transcripts significantly in cores incubated with pea litter (Supplementary Material S4).

Based on ongoing cultivation studies using samples from the same experiment, several of the T-RF could be tentatively assigned to T-RF obtained from *alkB* sequences originating from soil and litter isolates (Supplementary Material S3). For example, T-RF 324 and 459 were specific for *Actinomycetales*-related isolates harbouring *alkB* sequences homologous to the *alkB* sequence types of *Rhodococcus* sp. Q15 *alkB*2 (AF388182) and *Gordonia* sp. TF6 (AB112870), respectively. These T-RF were more common in DNA from litter samples and were, if at all, only detectable in soil samples incubated with litter, but never in controls.

A total analysis with nonmetric multidimensional scaling of T-RFLP patterns of all treatments and layers (including controls) on genomic and transcriptomic scale revealed differentiation between the *alkB*-harbouring and *alkB*-expressing communities (Supplementary Material S9). The *alkB*-harbouring communities especially from the litter–soil

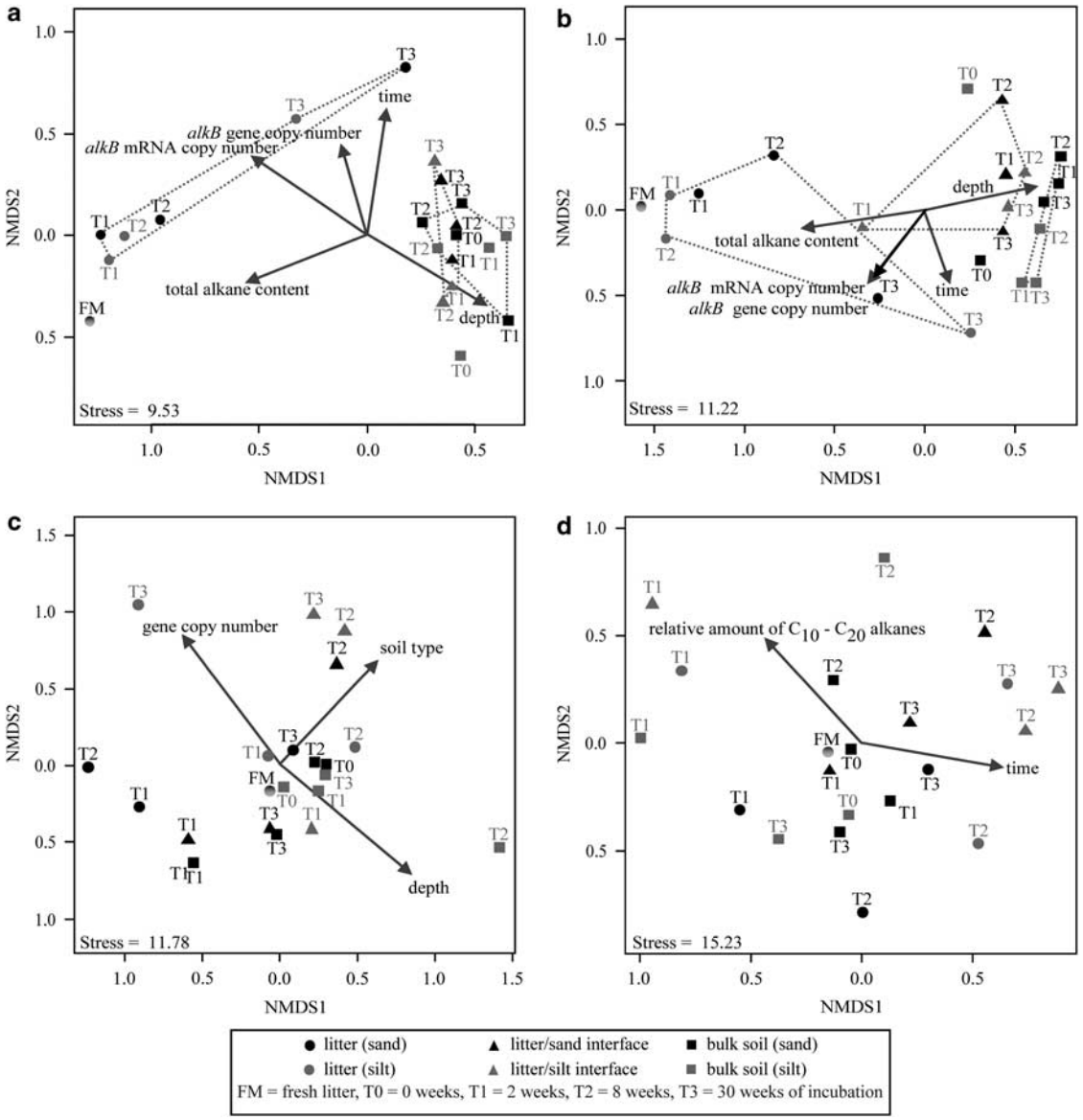

Figure 3 T-RFLP based NMDS plots of *alkB* gene harbouring communities based on DNA-derived T-RFLP analysis (**a**, **b**) and mRNA-derived T-RFLP-analysis (**c**, **d**) in sandy and silty soil microcosms covered with maize (**a**, **c**) and pea litter (**b**, **d**). Community similarity was calculated using Bray–Curtis similarity measurement, which includes presence and relative abundance of T-RF. Note that only bulk soil was sampled at T0, as no differences between litter–soil interface and bulk soil were expected at the beginning of the incubation. Arrows are correlation vectors of diversity differences and environmental conditions with significance factors $P<0.1$ (for exact significance level see Supplementary Material S4). Monte–Carlo permutation model based analysis with 1000 permutation and final ANOVA was applied to test for significance.

interface and bulk soil (irrespective of the soil type) shared more similarity to each other (domination sector III) than to the respective *alkB*-expressing communities (mainly sectors II) (molecule type, $P<0.001$). This indicates a high similarity to litter communities expressing *alkB* (sector II). The litter type had significant influence on the differentiation between *alkB*-harbouring and -expressing communities of all samples including controls ($P<0.001$) as also observed for the soil type ($P<0.05$) and the vicinity to the litter (depth, $P<0.001$). Control samples especially of bulk soil incubated without litter had similar patterns for *alkB* genes and transcripts (mainly sector I) and differed from soil samples incubated with litter (dominating sector III). Overall, the community structure of *alkB* harbouring bacteria genes and their transcripts in the non-litter controls did not change (Supplementary Materials S6 and S9).

Discussion

In this study, we related gene copy numbers, structure and activity of a functional community in different soil compartments to the presence of the

corresponding substrate. We could demonstrate that the investigated bacterial populations are highly dynamic in the different soil compartments, which have been investigated and at least partly controlled by substrate availability.

Surprisingly litter application resulted only in a growth of *alkB*-harbouring bacteria in the litter layer of soils where pea litter has been added. This increase in biomass could not be related to the degradation of alkanes only, as the amounts in litter are too low. Therefore, the use of other plant-derived compounds by the alkane degraders and co-metabolic degradation must be postulated. This hypothesis is also verified by the fact that in pea litter, which is easily degradable compared with maize litter and nutrient release is much faster, a steady increase of *alkB*-harbouring bacteria could be observed. In the litter–soil interface in silty soils also an increase in *alkB*-harbouring bacteria could be detected at T3 independent from the litter type. This observation might be related to the fact that leaching of alkanes is much slower in silty soils compared with sandy soils as indicated by the higher alkane concentrations in silty soil samples at T3; this prolonged substrate availability in silty soil samples obviously stimulated the growth of *alkB*-harbouring bacteria.

Generally, prolonged incubation time of the soil cores with the litter material resulted in distinct changes in *alkB* expression and diversity of *alkB*-harbouring bacteria. These shifts as well as the increased abundance were most pronounced in the litter layer likely indicating that significant parts of the available alkanes were readily degraded. This fact is supported by data from earlier studies, where extensive community structure changes of *alkB*-harbouring bacteria in nutrient-enriched soils as compared with control plots over time has been described in several field studies (Röling *et al*. 2004; Hamamura *et al*. 2006; Vázquez *et al*., 2009).

Substrate loads and relative chain-length distribution of alkanes in the compartments were significantly responsible for the distinct T-RFLP *alkB* fingerprints from litter and soil on the DNA level. These strong differences reflect changes in the presence as well as in the relative abundance of T-RF in litter and soil. This might indicate that alkane degraders in the litter layer were specific to or possibly introduced with the plant material rather than being part of the soil microbial community.

However, on the expression level the similarity in the number of transcripts between litter and soil samples indicates that external environmental conditions rather than the high abundance of certain degraders are responsible for shaping the community structure of active alkane degraders harbouring the *alkB* gene. Furthermore, specific *alkB* gene paralogues could be expressed similarly in litter and soil in response to the comparable growth conditions. The paralogues functions are yet unclear, but it was hypothesised that they are preferentially expressed depending on the chain-length of the available alkanes or on the growth state of bacteria (Marin *et al*., 2001; van Beilen *et al*., 2003; Amouric *et al*., 2010).

Alkanes released upon decay of litter material are possibly solubilised by surface-active agents (Holden *et al*., 2002), facilitating their transport into the surrounding soil, for example, with flowing water (Lichtfouse *et al*., 1994). Interestingly, total alkane loads in the litter–soil interface decreased significantly rather than increased, after litter amendment. Together with the stable numbers of *alkB* genes and transcripts in some soil compartments, this could support degradation activity of alkane degraders relying on enzyme systems others than AlkB (for example, Cyp153). In contrast, elevated *alkB* gene and transcript numbers in bulk soil compartments were detected after litter amendment, thus hinting at a concomitantly stimulated alkane degradation activity and a fast consumption of the substrate by *alkB*-harbouring bacteria.

Soil type dependent differences in the bioavailability of alkanes might occur due to the different porosities and mineral compositions of sandy and silty soils. In fact, the macroporosity of sandy soils, as opposed to the microporosity and high clay content of silty soils, may favour the transport of alkanes (Galin *et al*., 1990; Arthurs *et al*., 1995) and therefore influence the structure and activity of *alkB*-harbouring bacteria differently. At T3, the strong soil type dependent differences in the relative chain-length distribution and a concomitantly higher total alkane amount in silty soil were accompanied by elevated *alkB* gene numbers in the interface compartments of this soil type. Soil texture induced alkane sequestration, hence could have been responsible for a reduced *ad hoc* bioavailability and concomitantly retarded substrate consumption in silty soil.

The present study, interestingly, could not verify any influence of the soil type on the community structure of bacteria harbouring the *alkB* gene, as they were remarkably similar between sandy and silty soils, whereas simultaneously expressing similar *alkB* gene abundance and expression. In contrast, the differences in the community structure of *alkB*-harbouring bacteria were much higher in the soil compartments within one soil type than in the same soil compartments between the two soil types. This points to a distinct influence of the plant litter on the community structure of potential degraders that is more pronounced in communities located closer to the litter layer. Factors such as the availability of nutrients or electron acceptors introduced by the plant litter may accordingly be important (Wiesenberg *et al*., 2004; Dignac and Rumpel, 2006) forming steep gradients and thus preferentially influencing the community structure. Furthermore, plant litter-derived degraders could be transferred to the litter–soil interface along fungal

hyphae (Kohlmeier *et al*., 2005), without reaching the deeper soil layers.

However, on the expression level, the depth differentiation between the two soil compartments was less pronounced as also observed for the *alkB* transcripts in litter and soil. This and the dependency of the community structure of bacteria expressing the *alkB* gene in pea litter incubated samples on the relative amount of medium-chain alkanes (C_{10}–C_{20}) further supports the hypothesis of preferentially expressed *alkB* gene paralogues. The changes in the *alkB* expression patterns of maize litter incubated samples significantly correlated with the soil type, which had not been observed on the DNA-level and could thus be explained by the soil type-dependent relative chain-length distribution of the alkanes. At T3, the higher fraction of very long-chain alkanes in silty soil (C_{31}–C_{40}) at both compartments possibly induces *alkB* gene paralogues others than expressed with long-chain alkanes (C_{21}–C_{30}), which were more abundant although not dominant in sandy soil. Furthermore, the significant differences in the relative amounts of nonacosane and hentriacontane between the soil types might have a role.

Conclusion and outlook

The observed dynamics of abundance, community structure and activity of functional communities are often overlooked when soil samples are taken with a soil auger and further processed by mixing and sieving. However, to understand the functionality of soils in relation to the performance of microbial communities, the spatial resolution of analyses close to biogeochemical interfaces as they have been defined by Totsche *et al*. (2010) have to be improved. These authors stated that 'linking the heterogeneous architecture of soil interfaces with the diverse structure of microbial communities in predictive ways in order to understand soil functions and the role for ecosystem services has yet to be seen as one of the grand decadal challenges in science'. The structural and compositional heterogeneity of these interfaces is one likely reason for the vast diversification of microbes (Curtis and Sloan, 2005; Gans *et al*., 2005). Biogeochemical interfaces may stimulate the metabolic activity and are supposedly sites for horizontal gene transfer (Top and Springael, 2003; van der Meer and Sentchilo, 2003). This role of interfaces has also been demonstrated impressively using model biofilms (Molin and Toker-Nielsen, 2003). Therefore, future studies must address even smaller scales than those addressed by the present study to get more mechanistic insight into the functioning of biogeochemical interfaces and their dynamics. There is a particular need to employ minimally destructive sampling techniques and *in situ* analysis to obtain an unbiased view of the ecology of communities at high resolution.

Obviously in our study litter type-specific abundance of *alkB* and its expression patterns thereby seem to reflect not solely the different bioavailability of alkanes but might be also the result of the succession of *alkB*-harbouring bacteria by alkane degrading fungi (for example, *Fusarium* sp, *Aspergillus* sp, *Penicillium* sp). These fungi are known as important drivers of litter degrading communities and likely competitors with the bacteria for the same substrate. These alkane-degrading microbes do not use the alkane monooxygenase pathway for alkane degradation and therefore cannot be tackled by using *alkB*-specific primers. Therefore, to describe total functional communities involved in the degradation of plant-derived alkanes abundance, the community structure and the activity pattern of those microbes need to be described in future experiments, for example, by using metagenomic analysis and expression cloning approaches.

Finally T-RFLP analysis is a very useful technique for a high thruput analysis of changes in the community structure without clear phylogenetic assignments, which was the aim of this study. However, to link a certain *alkB* type to the given environmental conditions in a compartment, there is a need to better understand ecophysiology and phylogenetic position of the corresponding organisms. Furthermore, in many cases an analysis of the T-RFLP pattern is done using normalisation; as small peaks are not considered for analysis, this technique may not be able to describe changes in the rare biosphere of *alkB*-harbouring bacteria. As the number of *alkB* operons and its heterogeneity of so far uncultivated organisms is not known a direct link of number of T-RFs and diversity must be carefully considered. In this respect, sequence-based analysis of metagenomic libraries may help in the future to improve our understanding on *alkB*-harbouring microbes.

Acknowledgements

This work is part of the priority programme 1315 'Biogeochemical Interfaces in Soil' and was funded by the German Research Foundation (DFG). Financial support is greatly acknowledged. For support on GC-MS measurement, we are very grateful to Birgit Würz. We wish to thank the three reviewers of the original manuscript for their very helpful and constructive comments, which formed the basis for this revised version.

References

Amouric A, Quéméneur M, Grossi V, Liebgott PP, Auria R, Casalot L. (2010). Identification of different alkane hydroxylase systems in *Rhodococcus ruber* strain SP2B, an hexane-degrading actinomycete. *J Appl Microbiol* **108**: 1903–1916.

Arthurs P, Stiver WH, Zytner RG. (1995). Passive volatilization of gasoline from soil. *J Soil Contam* **4**: 123–135.

Avato P, Bianchi G, Pogna N. (1990). Chemosystematics of surface lipids from maize and some related species. *Phytochemistry* **29**: 1571–1576.

Bosma TNP, Middeldorp PJM, Schraa G, Zehnder AJB. (1996). Mass transfer limitation of biotransformation: quantifying bioavailability. *Environ Sci Technol* **31**: 248–252.

Cayet C, Lichtfouse E. (2001). $\delta^{13}C$ of plant-derived n-alkanes in soil particle-size fractions. *Org Geochem* **32**: 253–258.

Collister JW, Rieley G, Stern B, Eglinton G, Fry B. (1994). Compound-specific $\delta^{13}C$ analyses of leaf lipids from plants with differing carbon dioxide metabolisms. *Org Geochem* **21**: 619–627.

Curtis TP, Sloan WT. (2005). Exploring microbial diversity—a vast below. *Science* **309**: 1331–1333.

de Carvalho CCCR, Wick LY, Heipieper HJ. (2009). Cell wall adaptations of planktonic and biofilm *Rhodococcus erythropolis* cells to growth on C5 to C16 *n*-alkane hydrocarbons. *Appl Microbiol Biotechnol* **82**: 311–320.

Dignac M-F, Rumpel C. (2006). Relative distributions of phenol dimers and hydroxy acids in a cultivated soil and above ground maize tissue. *Org Geochem* **37**: 1634–1638.

Eglinton G, Gonzalez AG, Hamilton RJ, Raphael RA. (1962). Hydrocarbon constituents of the wax coatings of plant leaves: a taxonomic survey. *Phytochemistry* **1**: 89–102.

Galin T, Gerstl Z, Yaron B. (1990). Soil pollution by petroleum products, III. Kerosene stability in soil columns as affected by volatilization. *J Contam Hydrol* **5**: 375–385.

Gans J, Wolinky M, Dunbar J. (2005). Microbiology: computational improvements reveal great bacterial diversity and high toxicity in soil. *Science* **309**: 1387–1390.

Gniwotta F, Vogg G, Gartmann V, Carver TLW, Riederer M, Jetter R. (2005). What do microbes encounter at the plant surface? Chemical composition of pea leaf cuticular waxes. *Plant Physiol* **139**: 519–530.

Ha KV, Marschner P, Bünemann EK, Smernik RJ. (2007). Chemical changes and phosphorus release during decomposition of pea residues in soil. *Soil Biol Biochem* **39**: 2696–2699.

Hamamura N, Olson SH, Ward DM, Inskeep WP. (2006). Microbial population dynamics associated with crude-oil biodegradation in diverse soils. *Appl Environ Microbiol* **72**: 6316–6324.

Heider J, Spormann AM, Beller HR, Widdel F. (1999). Anaerobic bacterial metabolism of hydrocarbons. *FEMS Microbiol Rev* **22**: 459–473.

Holden PA, LaMontagne MG, Bruce AK, Miller WG, Lindow SE. (2002). Assessing the role of *Pseudomonas aeruginosa* surface-active gene expression in hexadecane biodegradation in sand. *Appl Environ Microbiol* **68**: 2509–2518.

Klappenbach JA, Dunbar J, Schmidt TM. (2000). rRNA operon copy number reflects ecological strategies of bacteria. *Appl Environ Microbiol* **66**: 1328–1333.

Kloos K, Munch JC, Schloter M. (2006). A new method for the detection of alkane-monooxygenase homologous genes (*alkB*) in soils based on PCR-hybridization. *J Microbiol Methods* **66**: 486–496.

Kohlmeier S, Smits THM, Ford RM, Keel C, Harms H, Wick LY. (2005). Taking the fungal highway: mobilization of pollutant-degrading bacteria by fungi. *Environ Sci Technol* **39**: 4640–4646.

Koma D, Hasumi F, Yamamoto E, Ohta T, Chung S-Y, Kubo M. (2001). Biodegradation of long-chain *n*-paraffins from waste oil of car engine by *Acinetobacter sp*. *Soc Biotechnol Jpn* **91**: 94–96.

Kotani T, Kawashima Y, Yurimoto H, Kato N, Sakai Y. (2006). Gene structure and regulation of alkane monooxygenases in propane-utilizing *Mycobacterium sp*. TY-6 and *Pseudonocardia sp*. TY-7. *Soc Biotechnol Jpn* **102**: 184–192.

Kotani T, Yurimoto H, Kato N, Sakai Y. (2007). Novel acetone metabolism in a propane-utilizing bacterium, *Gordonia sp*. Strain TY-5. *J Bacteriol* **189**: 886–893.

Lanfranconi MP, Alvarez HM, Studdert CA. (2003). A strain isolated from gas oil-contaminated soil displays chemotaxis towards gas oil and hexadecane. *Environ Microbiol* **5**: 1002–1008.

Lichtfouse É, Elbisser B, Balesdent J, Mariotti A, Bardoux G. (1994). Isotope and molecular evidence for direct input of maize leaf wax *n*-alkanes into crop soils. *Org Geochem* **22**: 349–351.

Maffei M. (1996). Chemotaxonomic significance of leaf wax *n*-alkanes in the Umbelliferae, Cruciferae and Leguminosae (Subf. Papilionoideae). *Biochem Syst Ecol* **24**: 531–545.

Manilal VB, Alexander M. (1991). Factors affecting the microbial degradation of phenanthrene in soil. *Appl Microbiol Biotechnol* **35**: 401–405.

Marin MM, Smits THM, Beilen van JB, Rojo F. (2001). The alkane hydroxylase gene of Burkholderia cepacia RR10 is under catabolite repression control. *J Bacteriol* **183**: 4202–4209.

Molin S, Toker-Nielsen T. (2003). Gene transfer occurs with enhanced efficiency in biofilms and induces enhanced stabilisation of the biofilm structure. *Curr Opin Biotechnol* **14**: 255–261.

Pérez-de-Mora A, Schulz S, Schloter M. (2010). MPN- and real time-based PCR methods for the quantification of alkane-monooxygenase homologous genes (*alkB*) in environmental samples. In: Cunningham S (ed). *Methods in Molecular Biology*. Human Press: New York, pp 59–68.

R Development Core Team. (2009). *R: A Language and Environment for Statistical Computing,*. R Foundation for Statistical Computing: Vienna, Austria, ISBN 3-900051-07-0. http://www.R-project.org.

Richnow HH, Seifert R, Kästner M, Mahro B, Horsfield B, Tiedgen U *et al.* (1995). Rapid screening of PAH-residues in bioremediated soils. *Chemosphere* **31**: 3991–3999.

Rieley G, Collister JW, Stern B, Eglinton G. (1993). Gas chromatography/isotope ration mass spectrometry of leaf wax *n*-alkanes from plants of differing carbon dioxide metabolisms. *Rapid Commun Mass Sp* **7**: 488–491.

Röling WFM, Milner MG, Jones DM, Fratepietro F, Swannell RP, Daniel F *et al.* (2004). Bacterial community dynamics and hydrocarbon degradation during a field-scale evaluation of bioremediation on a mudflat beach contaminated with burried oil. *Appl Environ Microbiol* **70**: 2603–2613.

Sepic E, Leskovsek H, Trier C. (1995). Aerobic bacterial degradation of selected polyaromatic compounds and *n*-alkanes found in petroleum. *J Chromatogr A* **697**: 515–523.

Sinowski W, Auerswald K. (1999). Using relief parameters in a discriminant analysis to stratify geological areas with different spatial variability of soil properties. *Geoderma* **89**: 113–128.

Smith KEC, Thullner M, Wick LY, Harms H. (2009). Sorption to humic acids enhances PAH biodegradation. *Environ Sci Technol* **43**: 7205–7211.

Top EM, Springael D. (2003). The role of mobile genetic elements in bacterial adaptation to xenobiotic organic compounds. *Curr Opin Biotechnol* **14**: 262–269.

Totsche KU, Rennert T, Gerzabek MH, Kögel-Knabner I, Smalla K, Spiteller M *et al.* (2010). Biogeochemical interfaces in soil: the interdisciplinary challenge for soil science. *J Plant Nutr Soil Sci* **173**: 88–99.

Töwe S, Wallisch S, Bannert A, Fischer D, Hai B, Haesler F *et al.* (2011). Improved protocol for the simultaneous extraction and column-based separation of DNA and RNA from different soil. *J Microbiol Methods* **84**: 406–412.

van Beilen JB, Funhoff EG. (2007). Alkane hydroxylases involved in microbial alkane degradation. *Appl Microbiol Biotec* **74**: 13–21.

van Beilen JB, Li Z, Duetz WA, Smits THM, Witholt B. (2003). Diversity of alkane hydroxylase systems in the environment. *Oil Gas Sci Technol* **58**: 427–440.

van der Meer JR, Sentchilo V. (2003). Genomic islands and the evolution of catabolic pathways in bacteria. *Curr Opin Biotechnol* **14**: 248–254.

Van Hamme JD, Singh A, Ward OP. (2003). Recent advances in petroleum microbiology. *Microbiol Mol Biol Rev* **67**: 503–549.

Vázquez S, Nogales B, Ruberto L, Hernández E, Christie-Oleza J, Lo Balbo A *et al.* (2009). Bacterial community dynamics during bioremediation of diesel oil-contaminated Antarctic soil. *Microb Ecol* **57**: 598–610.

Wang WJ, Baldock JA, Dalal RC, Moody PW. (2004). Decomposition of plant materials in relation to nitrogen availability and biochemistry determined by NMR and wet-chemical analysis. *Soil Biol Biochem* **36**: 2045–2058.

Whyte LG, Hawari J, Zhou E, Bourbonnière L, Inniss WE, Greer CW. (1998). Biodegradation of variable-chain-length alkanes at low temperatures by a psychrotrophic *Rhodococcus sp*. *Appl Environ Microbiol* **64**: 2578–2584.

Wick LY, Colangelo T, Harms H. (2000). Kinetics of mass transfer-limited bacterial growth on solid PAHs. *Environ Sci Technol* **35**: 354–361.

Widdel F, Rabus R. (2001). Anaerobic biodegradation of saturated and aromatic hydrocarbons. *Curr Opin Biotechnol* **12**: 259–276.

Wiesenberg GLB, Schwarzbauer J, Schmidt MWI, Schwark L. (2004). Source and turnover of organic matter in agricultural soils derived from *n*-alkane/*n*-carboxylic acid compositions and C-isotope signatures. *Org Geochem* **35**: 1371–1393.

Wilkes H, Kühner S, Bolm C, Fischer T, Classen A, Widdel F *et al.* (2003). Formation of *n*-alkane- and cycloalkane-derived organic acids during anaerobic growth of a denitrifying bacterium with crude oil. *Org Geochem* **34**: 1313–1323.

Yaalon DH. (2000). Down to earth. *Nature* **407**: 301.

Supplementary Information accompanies the paper on The ISME Journal website (http://www.nature.com/ismej)

Supplemental Material

S1 *Statistical analysis of the T-RFLP data*

In order to avoid the incorporation of primer induced signals in the T-RFLP analysis, fragments smaller than 50 bp were excluded. An upper fragment length threshold of 560 bp was applied to consider also sequences with no restriction site as criterion for the community structure (complete amplicon length was 550 bp). Noise removal from the final signal measurements, peak binning to account for inter-run differences in T-RF size and normalization of signal intensity was conducted according to Abdo *et al.* (2006) using a cut-off value of four times the standard deviation to remove background noise. Multivariate statistical analysis of the resulting normalized sample-peak tables were run with the R package “vegan” (Oksanen *et al*., 2006). Non-metric multidimensional scaling (NMDS) analyses performed with the Bray-Curtis similarity index (including presence and relative abundance of T-RF) iteratively tried to plot the rank order of similarity of communities in a way that community point distances are exactly expressed on a two-dimensional sheet (greater distances represent greater dissimilarities). The major compositional environmental variations were fitted using a linear regression and the ”envfit” algorithm provided with the ”vegan” package. Significances of single environmental and experimental parameters on the NMDS results were tested using the Monte-Carlo permutation test with 1000 permutations and final ANOVA. These parameters included incubation time, depth, soil type, litter type, *alkB* gene and mRNA copy number as well as the total alkane amount, the relative amount of alkane fractions with different chain-length and the nucleic acid molecule type (for the overall analysis the *alkB* harbouring and expressing communities were combined).

S2 Significance levels of factors influencing the litter decay in microcosms covered with maize or pea litter respectively.

	maize	pea
soil type	n.s.	n.s.
time	* * *	* *
time * soil type	n.s.	n.s.

* P <0.05, ** P<0.01, *** P <0.001, n.s. = not significant

S3 Relative abundances of terminal restriction fragments (T-RF) in DNA or cDNA samples from litter, soil and control compartments detected also in soil and litter isolates. For the calculation, all samples in one sampling group (litter; soil; control) were summed with no differentiation of litter-, soil type, compartment and incubation time.

***alkB* sequence homology to published sequences**	**T-RF[a]**	**% detection in DNA[b]**			**% detection in cDNA[b]**		
		litter	**soil**	**control**	**litter**	**soil**	**control**
	63 (69)	21	100	**100**	93	**88**	**92**
e.g. H. phototrophica (ZP_02166109)	117[#] (120)	21	**100**	**100**	79	**85**	75
	124 (127)	21	100	67	43	54	33
	234 (240)	57	**80**	**58**	86	77	75
	260 (263)	**86**	15	25	**79**	**62**	17
	282 (285)	50	100	67	57	88	33
Rhodococcus sp. Q15 *alkB2* (AF388182)	324* (328)	57	0	0	14	4	0
	362 (366)	86	**100**	92	86	85	100
	401	21	0	0	0	0	42
Gordonia sp. TF6 (AB112870)	459* (464)	21	12	0	43	35	8
	475	0	42	83	0	0	50

*) Taxon Specific; #) Specific for one particular alkB-paralog occurring in phylogenetically different isolates. All other T-RF occurred in different isolates.

a) Theoretical T-RF from *in silico* restrictions of cloned *alkB* sequences derived from microcosm isolates are given in brackets.

b) Dominant T-RF (5x mean relative fluorescence unit of all T-RF in more than 50% of the respective sample group) are given in bold.

S4 Significance levels of environmental factors correlating with diversity changes in *alkB* harbouring (DNA) or expressing (cDNA) communities (based on NMDS of T-RFLP data) in the sandy and the silty soil microcosms incubated with maize or pea straw, respectively. In addition, litter communities are also included (maize; pea). Significance levels for the overall analysis including T-RFLP analysis of all treatments and layers on *alkB* gene and expression level are given in the last column (all). P values are based on Monte-Carlo permutation with 1000 permutations and final ANOVA.

	DNA		**cDNA**		
	maize	**pea**	**maize**	**pea**	**all**
time	***	*	-	.	-
depth	***	***	*	-	***
soil type	-	-	.	-	*
litter type	n.d.	n.d.	n.d.	n.d.	***
***alkB* gene copy number**	*	**	.	-	***
***alkB* mRNA copy number**	***	**	-	-	***
total alkane	***	***	-	-	n.d.
relative amount of C_{10}-C_{20} alkanes	*	*	-	.	n.d.
relative amount of C_{21}-C_{30} alkanes	-	**	-	-	n.d.
relative amount of C_{31}-C_{40} alkanes	-	**	-	-	n.d.
relative amount of C_{29} and C_{31}	-	**	-	-	n.d.
molecule type	n.d.	n.d.	n.d.	n.d.	***

·P < 0.1, * P <0.05, ** P <0.01, *** P <0.001, n.d. = not determined

S5 Relative amount of remaining litter of maize and pea plants after incubation of sandy and silty soil microcosms, referred to an initial amount of 1g (dw) of fresh litter material. Error bars denote standard deviation (n = 3).

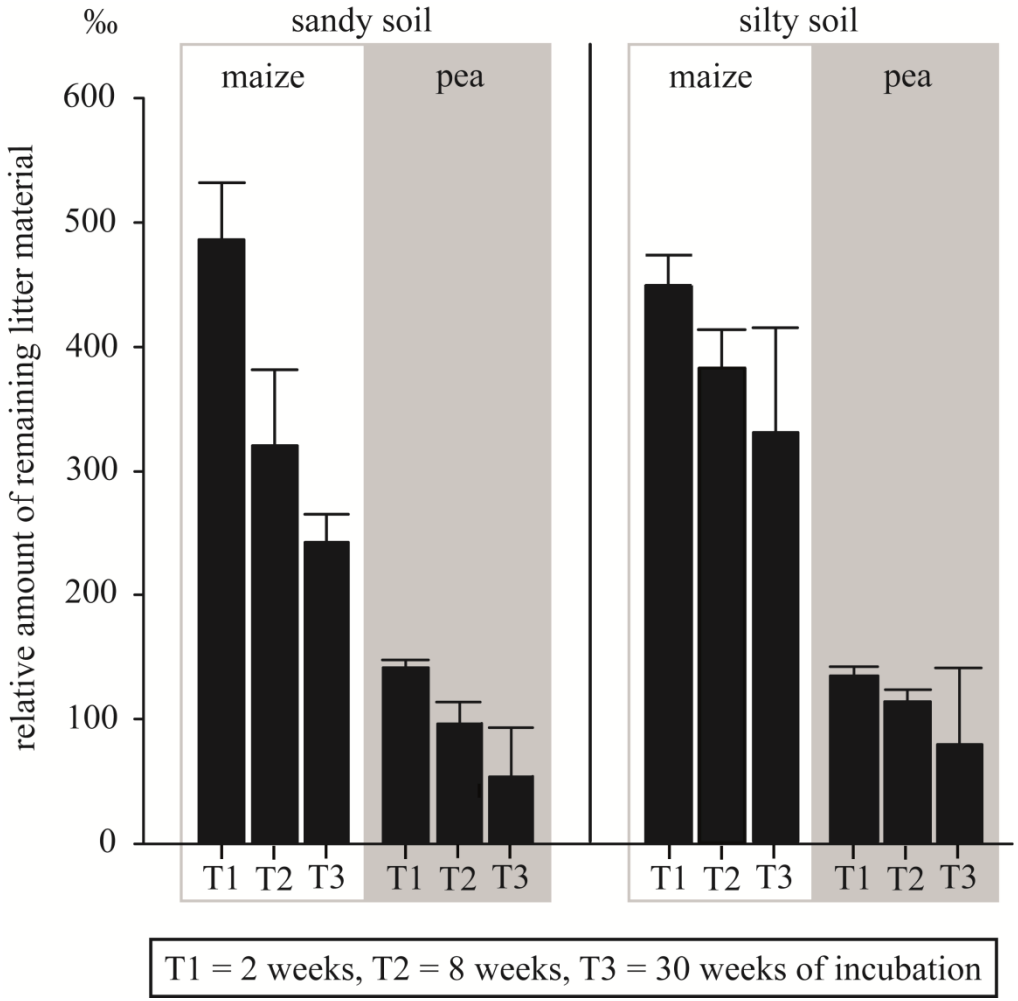

S6 Diversity cluster analyses of *alkB* genes (A, B) and transcripts (C, D) in silty and sandy soil microcosms covered either with maize (A, C) or pea (B, D) litter as well as in the non-litter controls.

FM = fresh litter T0 = 0 weeks, T1 = 2 weeks, T2 = 8 weeks, T3 = 30 weeks of incubation

S7 Number of T-RF (i.e. richness) detected in two soil compartments (litter-soil interface, bulk soil) after the incubation with maize and pea litter with differentiation of T-RF exclusively detected in sand, silt and shared T-RF between both soil types. For reasons of simplification no differentiation between the two soil compartments was included.

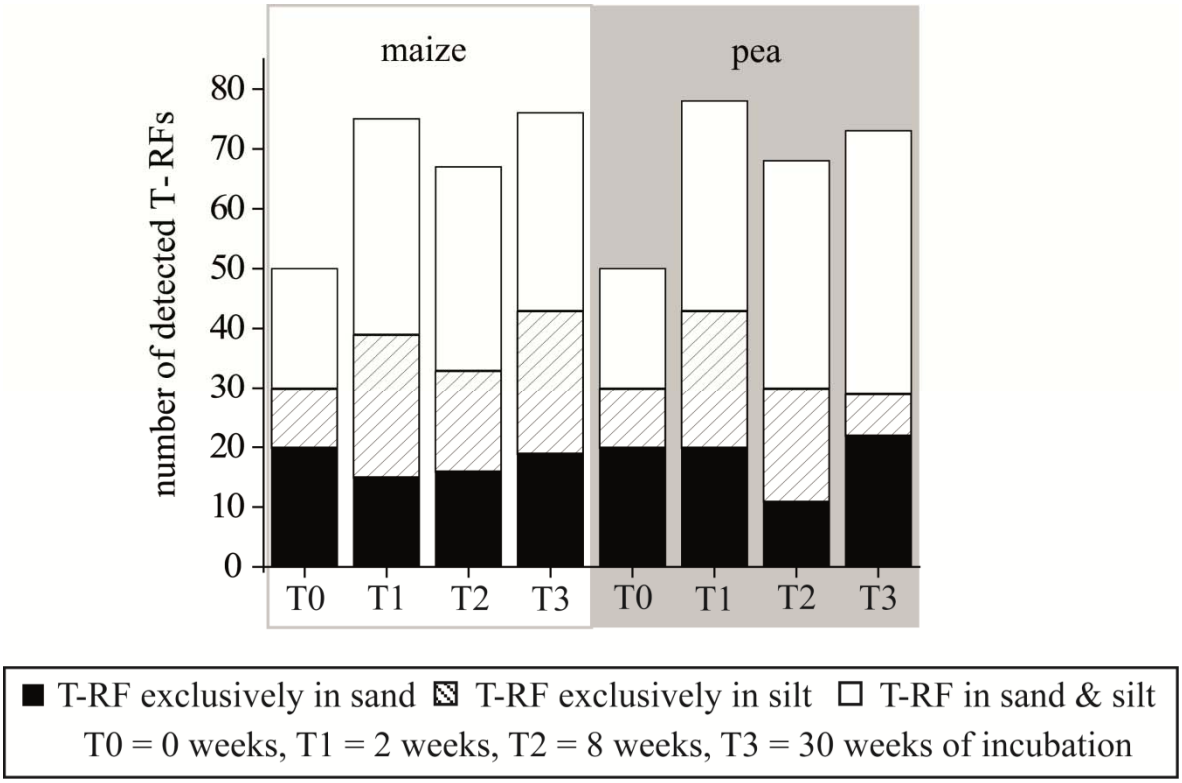

S8 T-RF in soil microcosms incubated with maize and pea litter with differentiation of T-RF exclusively detected in litter, soil and shared T-RF between litter and soil samples. For reasons of simplification no differentiation between the two soil compartments was included.

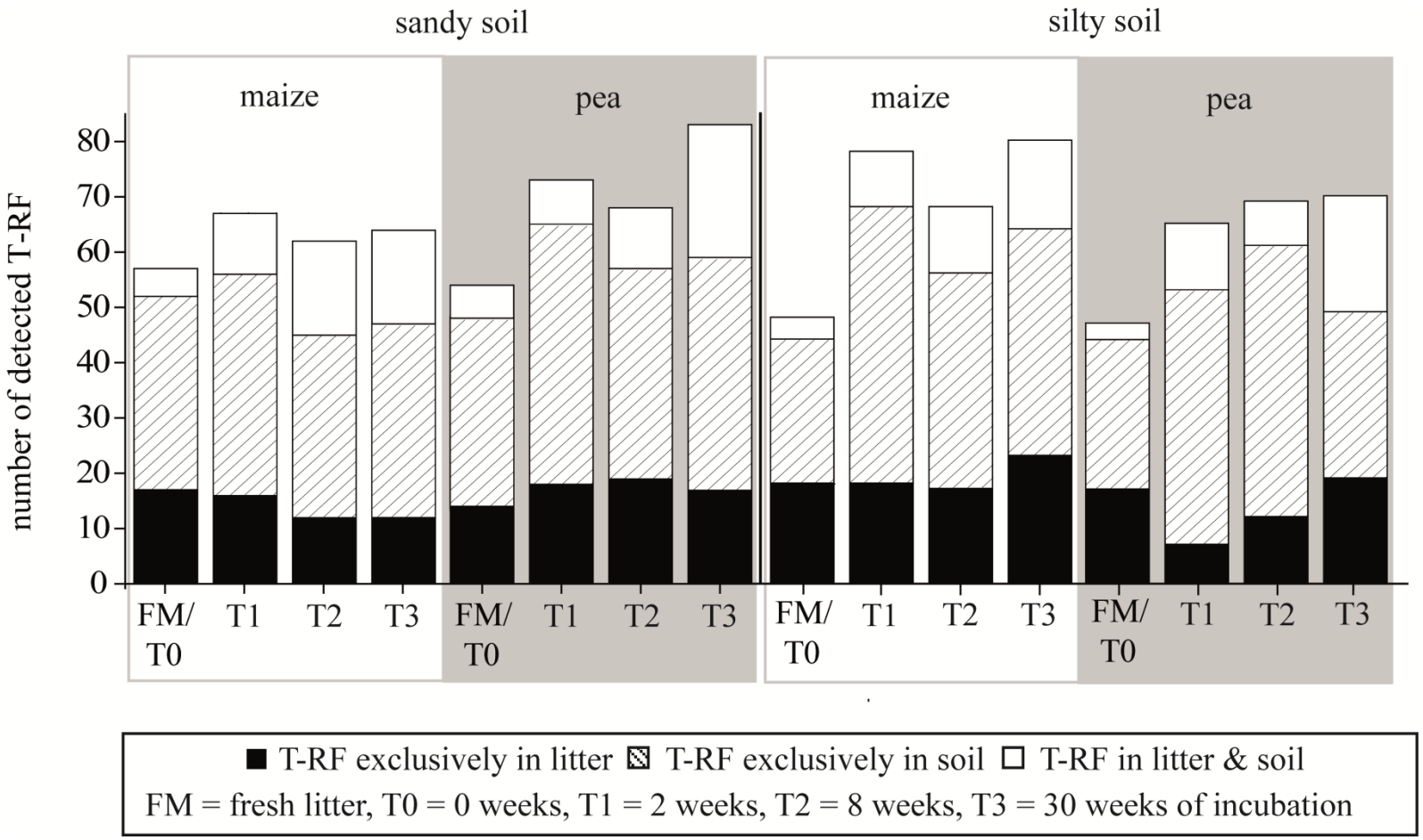

S9 T-RFLP based NMDS blot of all *alkB* gene harbouring and expressing communities of the microcosm experiments. Community similarity was calculated using Bray-Curtis similarity measurement. Arrows are correlation vectors of diversity differences and environmental conditions with significance factors P < 0.1 (for exact significance level see S4). Monte-Carlo permutation model based analysis with 1000 permutation and final ANOVA was applied to test for significance.

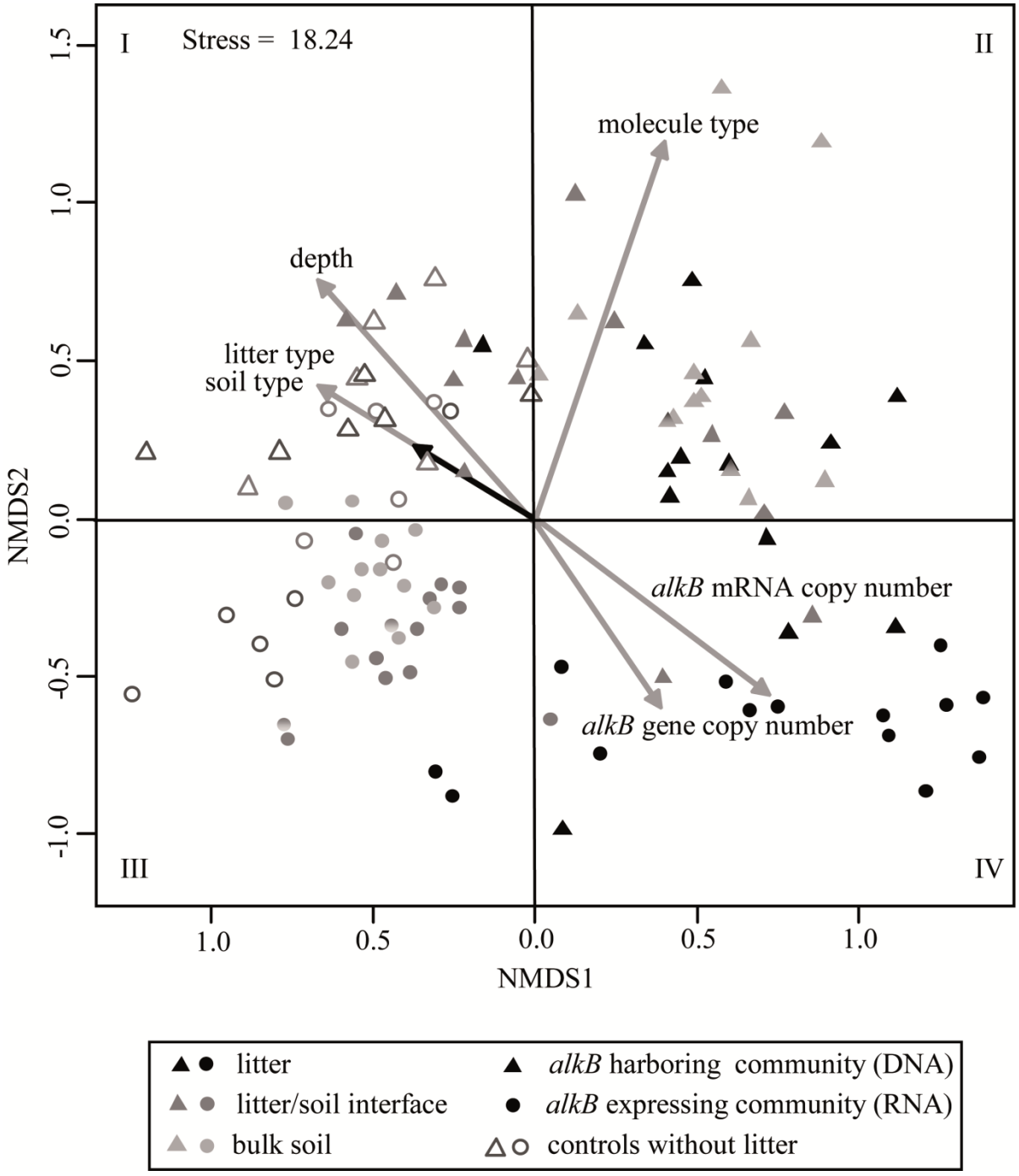

Publication IV

Biol Fertil Soils
DOI 10.1007/s00374-012-0685-2

ORIGINAL PAPER

The influence of the herbicide 2-methyl-4-chlorophenoxyacetic acid (MCPA) on the mineralization of litter-derived alkanes and the abundance of the alkane monooxygenase gene (*alkB*) in the detritusphere of *Pisum sativum* (L.)

Stephan Schulz · Tatiana Yuyunkina · Holger Pagel · Lukas Y. Wick · Christian Poll · Thilo Streck · Ellen Kandeler · Michael Schloter

Received: 16 December 2011 / Revised: 20 March 2012 / Accepted: 28 March 2012

Abstract In the present study, the temporal and spatial variation of the abundance of the alkane monooxygenase gene *alkB* and 16S rRNA genes in different soil compartments was analysed in the presence or absence of 2-methyl-4-chlorophenoxyacetic acid (MCPA) after the addition of pea litter to soil in a microcosm study. Samples were analysed shortly after litter addition (T0) and 1 week (T1), 3 weeks (T3) and 6 weeks (T6) after the addition of litter. In addition also, the quantity and quality of litter-derived alkanes was analysed and measured. The results revealed a fast and complete degradation of MCPA in all compartments throughout the experiment. Nevertheless, significant changes in the distribution patterns of short- and middle-chained alkanes suggest an interaction of MCPA and alkane degradation. *alkB* gene copy numbers were highly influenced by the time point of analysis and by the investigated soil compartment. Overall, an increase in *alkB* gene copy numbers from T0 to T3 was visible in the upper soil compartments whereas a decrease compared to T0 was measured in the deeper soil compartments. MCPA addition resulted in an increase of alkB abundance at T6. Gene copy numbers of 16S rRNA were not influenced by sampling time and soil compartment. In contrast to the control treatments, a slight increase in 16S rRNA gene copy numbers was visible at T1 and T3 compared to T0 in all soil compartments.

Keywords Alkane monooxygenase · MCPA · Alkane degradation · Plant litter

Ellen Kandeler and Michael Schloter contributed equally to this study.

S. Schulz · T. Yuyunkina
Chair of Soil Ecology, Technische Universität München,
Ingolstädter Landstr. 1,
85764 Neuherberg, Germany

T. Yuyunkina · C. Poll · E. Kandeler
Institute of Soil Science and Land Evaluation,
Soil Biology Section, University of Hohenheim,
Emil-Wolff-Str. 27,
70599 Stuttgart, Germany

L. Y. Wick
Department of Environmental Microbiology,
Helmholtz Centre for Environmental Research–UFZ,
Permoserstr. 15,
04318 Leipzig, Germany

H. Pagel · T. Streck
Institute of Soil Science and Land Evaluation,
Biogeophysics Section, University of Hohenheim,
Emil-Wolff-Str. 27,
70599 Stuttgart, Germany

M. Schloter (✉)
Research Unit for Environemtal Genomics,
Helmholtz Zentrum München,
German Research Center for Environmental Health (GmbH),
Ingolstädter Landstr. 1,
85764 Neuherberg, Germany
e-mail: schloter@helmholtz-muenchen.de

Introduction

Phenoxyacetic acids (PAA) like 4-chloro-2-methylphenoxyacetic acid (MCPA) are one of the most commonly used groups of herbicides for weed control. They are applied as post-emergence agents (Tomlin 2003) and taken up by broad-leaved plants, where they act as phytohormones and result in a nutrition deficiency and subsequent plant death. MCPA, which is either rinsed from the leaves by irrigation

Published online: 18 April 2012

or directly reaches the soil during its dispersion, can be rapidly degraded by soil microorganisms (Crespín et al. 2001). Therefore, over the last decades, the environmental fate of this herbicide and its impact on MCPA-degrading microorganisms has been studied intensively. For example, Greer and Shelton (1992) identified the soil organic matter content as one of the key factors influencing the degradation of 2,4-dichlorophenoxyacetic acid (2,4-D), an analogue to MCPA. Furthermore, it was shown that the degradation activity of MCPA degraders was enhanced after repeated herbicide application (Kearney and Kellogg 1985; Cederlund et al. 2007). Intensive studies of the *tfdA* gene, encoding the enzyme which catalyses the initial step in bacterial degradation of phenoxyacetic acid herbicides, have been performed on genomic and transcriptomic levels and demonstrated a rapid increase of gene copy numbers and transcripts after MCPA application (Baelum et al. 2008; Nicolaisen et al. 2008; Poll et al. 2010).

Although obviously MCPA is rapidly degraded in soil after application, there is still a concern if the herbicide has an impact on soil microbes and their activities. Whereas some studies could not reveal a negative impact of MCPA on soil microbial community structure even at doses 10 times higher than the approved levels (Anderson 1978; Duah-Yentumi and Johnson 1986; Vieublé Gonod et al. 2006; Zabaloy et al. 2008; Tejada et al. 2010), knowledge about its effects on functional groups of microbes and their activity is rare. In this respect, there is a need to consider also microbes involved in litter degradation, since due to the application of MCPA, a large amount of dead plant biomass accumulates, which needs to decompose, to recycle nutrients and to avoid colonisation of the plant litter material by phytopathogenic microbes like *Fusarium*.

Alkanes are a major constituent of cuticulary waxes of plant leaves, which form a barrier against water loss and phytopathogens. During the decay of plant litter, these alkanes reach the detritusphere (Lichtfouse et al. 1994; Cayet and Lichtfouse 2001; Dignac and Rumpel 2006), which represents a "hot spot" of microbial activity with high importance for the mineralization of litter-derived compounds (Gaillard et al. 2003; Poll et al. 2006). Therefore, in the present study, we investigated the influence of MCPA on alkane-degrading bacteria. Since MCPA is supposed to be a potential inhibitor of soil enzymatic activities (Tejada et al. 2010), it might also have a hampering effect on alkane-degrading bacteria reflected by a feedback reduction of abundance and activity.

The alkane monooxygenase gene *alkB* encodes the homonymous enzyme, which catalyses the initial step in aerobe bacterial degradation of linear aliphatic hydrocarbons with a chain length between C_5 and C_{16} (van Beilen et al. 2003) and is thus a good indicator for degraders of plant litter-derived alkanes. We hypothesise that MCPA (1) inhibits activity of *alkB*-harbouring bacteria and (2) changes the distribution pattern of alkanes of different length in the investigated soil compartments. To prove these hypotheses, we conducted a microcosm experiment using soils spiked with MCPA or water, respectively, and investigated the temporal changes of gene copy numbers of *alkB* as well as the mineralization of alkane species with different chain lengths in the detritusphere of plant litter.

Materials and methods

Microcosm experiment

For the microcosm experiment, topsoil (0–30 cm) of an arable Luvisol soil (18 % sand, 60.6 % silt, 21.4 % clay, pH_{CaCl2} 5.3) was collected from a research farm in Scheyern (www.helmholtz-muenchen.de/scheyern), 40 km north of Munich (Germany). To avoid the influence of living plant biomass, sampling was performed in December 2009. After sampling, the soil was sieved (<2 mm) and filled into 32 soil cores (5.6-cm diameter × 3-cm height, with a bulk soil density of 1.2 $g cm^{-3}$) which were pre-incubated for 2 weeks in the dark at 20°C and 35 % of the maximum water holding capacity to reset microbial activity. In order to study the effect of MCPA on *alkB*-harbouring bacteria, 12 soil cores were spiked with MCPA (50 mg kg^{-1} dry soil); the remaining soil cores received water and served as controls. All soil cores were covered with 0.5 g of small pieces (5 mm^2) of dried pea litter (*Pisum sativum* L.), which represents a plant litter type with high amounts of alkanes in the leaves (Schulz et al. 2010), and were incubated as described by Poll et al. (2010). During the incubation, the soil moisture was set to a corresponding water suction of −63 hPa. The microcosms were incubated for 6 weeks at 20°C in the dark and weekly irrigated with a 0.01 M $CaCl_2$ solution. Four microcosms of each treatment (MCPA or control) were sampled after 1 week (T1), 3 weeks (T3) and 6 weeks (T6) of incubation. In addition, soil aliquots were taken in four replicates 10 min directly after MCPA or water amendment at the start of the experiment (T0). For sampling, the remaining litter material was carefully removed; the soil cores were frozen at −21°C and subsequently sliced into thin layers ("compartments") using a cryostat microtome (HM 500 M, MICROM International GmbH, Germany). Soil samples from the detritusphere were taken in the following distances to the litter: 0–3, 3–6 and 6–9 mm. They were stored at −21°C until further use.

MCPA extraction and quantification

MCPA was extracted from the soil samples by a sequential extraction procedure where an amount of 1.5 g of fresh soil was mixed with 7.5 ml 0.01 M $CaCl_2$ (Merck, Darmstadt, Germany) and shaken vigorously for 20 min at 250 rpm.

After subsequent centrifugation (2500×*g*, 15 min), an aliquot of the resulting supernatant was additionally mixed with methanol (HPLC grade, Geyer Chemsolute, Renningen, Germany) in a ratio of 1:1 and incubated at 50°C for another 30 min. Prior MCPA concentration measurement, both extracts ($CaCl_2$ and methanol) were filtered using 0.45-μm syringe filters (Chromafil PP/RC-45/25, Macherey-Nagel, Düren, Germany) to avoid potential precipitation fragments. Afterwards, quantification was performed according to Moret et al. (2005). Briefly, separation of extracted MCPA was accomplished by using a HPLC-analytical column, equipped with a 3.5-μm Kromasil 100C18 silica phase (150×3 mm, MZ Analysentechnik GmbH, Germany) and a mixture of acetonitrile/water (30:70, *v*/*v*) and 10 mM tetrabutyl ammonium hydroxide serving as mobile phase (pH 7.2). The flow rate was set to 0.5 ml min^{-1}. Detection of the herbicide was done at 228 nm using an UV detector (Beckman Coulter, System Gold 166).

Alkane extraction and determination of quantity and quality

The quantitative and qualitative analysis of *n*-alkanes at the different soil compartments was done by mixing 4 g of fresh soil with anhydrous Na_2SO_4 and a subsequent two-stage extraction procedure using a total of 120 ml hexane (HPLC grade, Merck, Darmstadt, Germany). Gas chromatographic mass spectrometry (GC-MS) measurements of concentrated extracts were performed with an HP 6890 gas chromatograph (Hewlett Packard, Palo Alto, CA, USA), which was equipped with an HB-5 ms column and an HP 5973 mass spectrometer for signal detection (both Agilent Technologies, Santa Clara, CA, USA). Final temperature was set to 320°C, at a final time of 7 min and an initial helium flow of 0.8 ml min^{-1}. For the MSD transfer line heater, an initial temperature of 280°C was used.

Nucleic acid extraction and quantification of the alkane monooxygenase gene (*alkB*) and the gene coding for the 16S rRNA

The isolation of nucleic acids from soil samples was performed according to Töwe et al. (2011) without adding β-mercaptoethanol to the extraction buffer. Quality and quantity of the isolated DNA was determined spectrophotometrically at 260 and 230 nm (Nanodrop® ND-1000, Peqlab, Germany). Sybr® Green-based quantitative real-time PCR (qPCR) was accomplished by using the ABI Prism 3300 system (Applied Biosystems, Foster City, CA, USA). For qPCR of *alkB* genes, modified primers carrying inosine nucleotides at every fourfold-degenerated base have been used for the improvement of amplification efficiency (Kloss et al. 2006; Schulz et al. 2010), whereas primers for the quantification of 16S rRNA genes were used without modification (Bach et al. 2002).

The preparation of reaction mixtures and subsequent amplification reactions was performed as previously described (Bach et al. 2002; Pérez-de-Mora et al. 2010) using 2 to 25 ng of template DNA in each PCR setup. Cloned fragments of *alkB* (550 bp) from *Pseudomonas putida* and 16S rRNA (260 bp) from *Clavibacter michiganensis michiganensis* were used as standards. Amplification efficiencies ranged between 83 and 85 % (*alkB*) and 84 to 95 % (16S rRNA) with standard curve linearities (r^2>0.99) over six orders of magnitude for both standards.

Statistical analyses

Significance levels of the obtained data were calculated using a multifactoral ANOVA algorithm which is included in the SPSS software version 11.5 (SPSS Inc., USA). Data of gene abundances of *alkB* and 16S rRNA genes were log-transformed to fulfil the assumptions of normal data distribution and homogeneity of variances. The level of significance was set to $P \leq 0.05$.

Results

MCPA concentrations were in all soil compartments and at all time points significantly higher in the $CaCl_2$ extracts compared to the methanol extracts ($P<0.05$), indicating that the major part of the MCPA added to soil was still bioavailable and not covalently bound to the soil matrix. Only about 1/5 of the applied MCPA could be measured in the methanol extracts. This sorption process to soil was very fast and already visible some minutes after application (T0). The determination of the MCPA degradation rates revealed a fast decomposition already after 1 week (T1) of application in both fractions ($CaCl_2$ and methanol) in all soil compartments (Fig. 1). The degradation of the applied MCPA was higher ($P=0.02$) in the upper soil compartment (0–3 mm) compared to the deeper soil layers (3–6 and 6–9 mm) at T1. However, a leaching of MCPA from the upper to the lower soil compartments over time cannot be excluded. With ongoing incubation (T3), the remaining concentration of MCPA was further reduced (7 to 10 μg g^{-1} soil dry weight (dw)) in the $CaCl_2$ fraction as well as in the methanol extracts (1 to 2 μg g^{-1} soil dw) and resulted in concentrations below the detection limit of 5 ng g^{-1} soil (dw) at the end of the experiment after 6 weeks (T6) (Fig. 1) in all layers in both fractions. Overall, degradation rates did not change over time in all soil compartments.

Short-chain alkanes with a chain length less than C_{20} significantly increased over time up to 7 ng g^{-1} (Fig. 2a and d, Table 1). However, the increase in the MCPA-treated samples was overall more pronounced, indicating a reduced degradation of these alkanes in the presence of MCPA. The

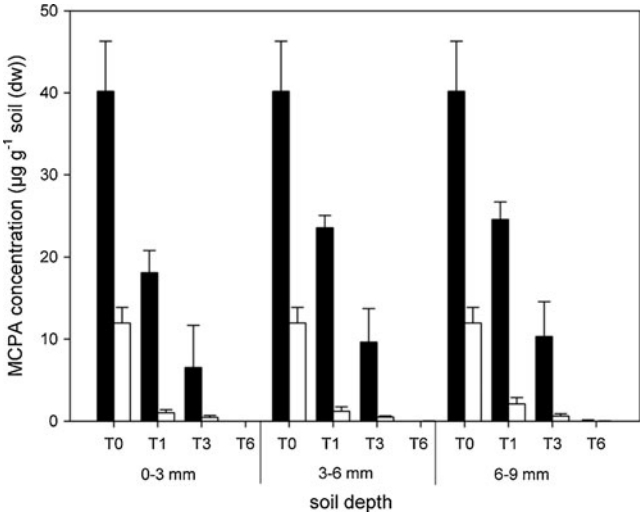

Fig. 1 Concentrations of MCPA in different soil compartments (0–3, 3–6 and 6–9 mm under the litter layer) during a microcosm experiment of 6 weeks. The herbicide concentration was measured in replicates (n=4) at the beginning (T0) and after 1 week (T1), 3 weeks (T3) and 6 weeks (T6) of incubation using a sequential extraction with $CaCl_2$ (*black bars*) and methanol (*open bars*). The *error bars* represent standard deviation

amount of short-chained alkanes (C_{10}–C_{19}) increased after 3 weeks (3–6 mm) and 6 weeks (0–3 mm) of incubation, respectively, in the control soils, whereas in MCPA-treated microcosms, the amounts already strongly increased in the first week and decreased in the following period only at 0–3 mm. For the deeper soil compartments (3–6 and 6–9 mm), trends were comparable to the controls, but the increase of alkanes was attenuated which indicates a slower reduction of alkane degradation. However, a significant difference of the alkane concentrations in the different soil compartments under investigation was not visible, which might be related to the fast leaching of this fraction.

Alkanes with a chain length between C_{20} and C_{29}, which were released during plant litter decay, were also influenced by the time and the availability of MCPA (Fig. 2b and e, Table 1). However, concentrations were much higher compared to the short-chain alkanes. In average, the amount ranged between 30 and 50 ng g^{-1} dry soil but did not exceed 55 ng g^{-1}. In the control microcosms, the amount of middle-chained alkanes (C_{20}–C_{29}) increased in the first week of incubation whereas concentrations remained constant or

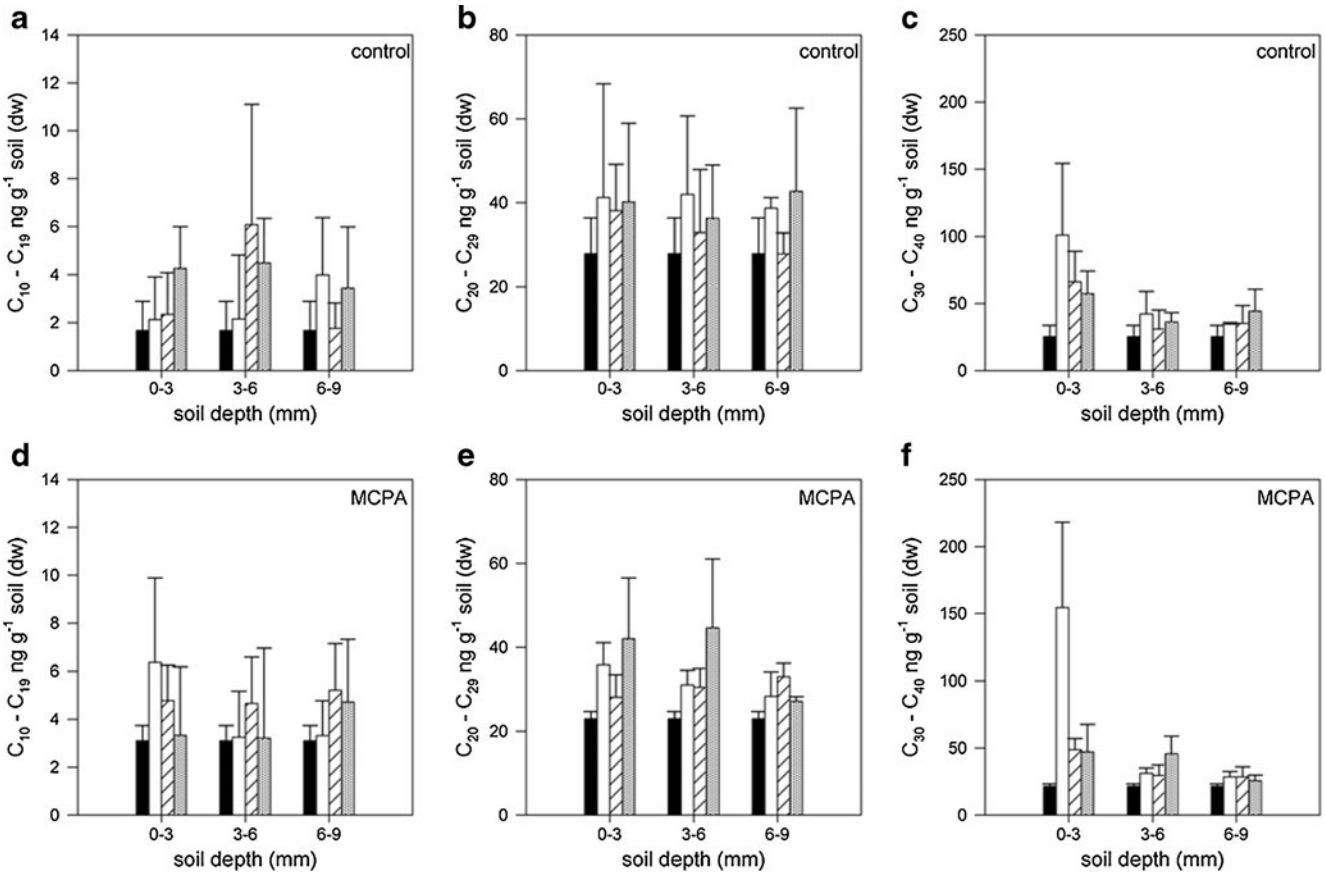

Fig. 2 The response of total short- (**a**, **d**), middle- (**b**, **e**) and long-chained (**c**, **f**) alkanes, without discrimination of even- and odd-numbered chains, to MCPA amendment in different soil compartments of the microcosms during an incubation time of 6 weeks. Amounts of alkanes in control (**a**–**c**) and MCPA (**d**–**f**) spiked microcosms at the beginning (*black bars*) and after 1 week (*open bars*), 3 weeks (*shaded bars*) and 6 weeks (*dotted bars*) of incubation are given. The different soil microsites are indicated. The *error bars* represent standard deviations (n=4)

Table 1 Correlation of gene copy numbers and concentration of total alkane species by multifactorial ANOVA with time, treatment and soil compartment. *P<0.05

Factor	ANOVA P values				
	alkB	*16S rRNA*	C_{10}–C_{19}	C_{20}–C_{29}	C_{30}–C_{40}
Time	0.263	0.558	0.036*	0.002*	0.000*
Soil compartment	0.008*	0.116	0.950	0.338	0.000*
Treatment	0.928	0.162	0.024*	0.040*	0.680
Time × compartment	0.691	0.605	0.461	0.949	0.000*
Time × treatment	0.694	0.200	0.390	0.777	0.264
Compartment × treatment	0.746	0.299	0.223	0.665	0.353
Time × compartment × treatment	0.773	0.837	0.185	0.244	0.042*

decreased at T3 and T6, indicating a degradation of these released hydrocarbons in all soil compartments. Contrary, in microcosms that have been spiked with MCPA, the amount of alkanes changed only slightly in the first 3 weeks of incubation in the first 6-mm soil depth and steeply increased at T6 to an amount of 45 ng g^{-1} soil (dw), indicating a decreasing degradation at the end of the experiment in microcosms spiked with MCPA.

Interestingly, the amount of long-chained alkanes (C_{30}–C_{40}) at T1 increased to a maximum of 110 and 150 ng g^{-1} soil in the first compartment (0–3 mm) of the control and MCPA-spiked microcosms, respectively (Fig. 2c and f, Table 1) at T1, indicating a fast litter decomposition and the release of hentriacontane (C_{31}) which is known to be predominant in cuticulary waxes of pea leaves (Gniwotta et al. 2005). With ongoing incubation, these high amounts dropped to a level of around 50 ng g^{-1} soil (dw) and changed only slightly towards T6.

The quantification of the alkane monooxygenase gene *alkB* demonstrated that copy numbers did not exceed 1×10^5 copies g^{-1} soil (dw) during the whole incubation. At the topsoil compartment representing the litter/soil interface (0–3 mm), the *alkB* gene copy number increased over time in control treatments (T0–T3), whereas in soil depths below that compartment, a clear decrease of *alkB* genes was measured over time (Fig. 3a and b, Table 1). A significant influence of the MCPA application on the abundance of *alkB* was not detectable at the early time points of sampling (T0, T1 and T3); however, the MCPA addition resulted in slightly higher gene *alkB* gene copy numbers compared to the controls at T6 in the two upper soil compartments

The 16S rRNA gene copy numbers in the control soils were very constant and did not change significantly with time or soil compartment (Table 1). The overall abundance of 16 S rRNA genes did not exceed 1×10^9 copies g^{-1} soil (dw) and ranged between 1×10^8 and 1×10^9 copies g^{-1} soil (dw). Also, in the microcosms treated with MCPA, 16S rRNA gene copy numbers did not change with soil depth. In contrast to the control treatments, a slight increase in 16S rRNA gene copy numbers was visible at T1 and T3 compared to T0 in all soil compartments in the MCPA-treated samples.

Discussion

PAA herbicides like MCPA are highly soluble and can be easily transported into deeper soil layers after field application. Despite the intensive use of these herbicides in agriculture, the concentrations in soils are low due to the fast microbial degradation and adsorption to soil particles. Although the amount of MCPA commonly used for weed control is in the range of 20 μg g^{-1} soil (dw), the resulting concentration in soils after field amendment is expected to undercut a limit of 4–5 μg g^{-1} (Anon 1987). Therefore, PAAs are considered by many authors as ecologically irrelevant.

The major fraction of MCPA in our study was rapidly degraded, and only a minor part was adsorbed to soil particles. The reduction of 50–60 % within the first week after application is in line with other studies. For example, Thorstensen and Lode (2001) as well as Boivin et al. (2005) demonstrated a clear reduction of about 50 % of the bioavailable MCPA in clayey and loamy soils within 14 days after application. In addition, the high microbial activity of MCPA degraders, which was repeatedly observed after MCPA application, could be further improved by the addition of external nutrient sources called biostimulants (Poll et al. 2010; Tejada et al. 2010).

Since previous studies could not show a negative impact of MCPA on the soil microflora even when applied in excess (Duah-Yentumi and Johnson 1986; Tejada et al 2010), an elevated concentration of 50 μg g^{-1} soil (dw) of MCPA was used in this study to create harsh conditions and check for influences on the *alkB*-harbouring bacterial community in soils. Even for such extremely high doses, our results revealed a complete disappearance of MCPA after 6 weeks of incubation, which was also shown recently (Hiller et al. 2009; Poll et al. 2010), as a consequence of microbial activity, adsorption to soil particles and organic matters as well as leaching processes.

Our results clearly indicate significantly higher MPCA degradation in the compartment, which represents the litter/soil interface supporting also the beneficial effect of litter-derived, easy degradable biostimulants and possibly

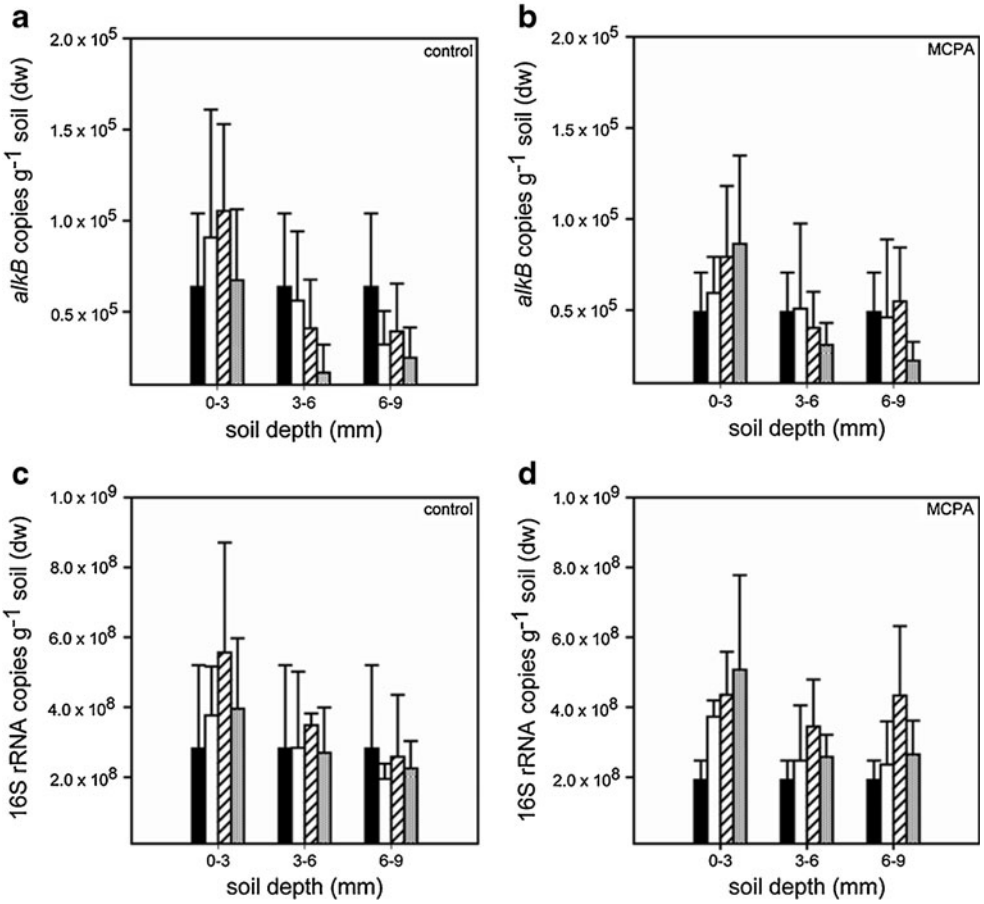

Fig. 3 Quantification of *alkB* (**a**, **b**) and 16S rRNA (**c**, **d**) genes in a microcosm experiment after litter addition to soil at the beginning (*black bars*) and after 1 week (*open bars*), 3 weeks (*shaded bars*) and 6 weeks (*dotted bars*) of incubation with water (**a**, **c**) and MCPA (**b**, **d**). The different soil compartments are indicated. The *error bars* represent standard deviations (n=4)

cometabolic degradation of MCPA. These higher microbial activities related to the degradation of biopolymers on a very small vertical scale or resolution have been also described by Baldrian et al. (2010), who investigated spatial heterogeneity pattern of selected soil enzymatic activities in forest soils.

The results of the present study confirm that the majority of bacteria is not affected by the addition of MCPA to soil. On the contrary, even a slight increase in 16S rRNA gene copy numbers could be measured in those treatments with MCPA addition at T1 and T3. This might indicate that probably fungi are more affected by the MCPA addition than bacteria. In this respect, a study by Herrmann et al. (2004) is of interest which could show pronounced effects of auxin on selected fungi. Taking into account that MCPA is an auxin analogue, effects on soil fungi could be postulated. Due to the reduced competition for resources, bacteria might benefit from the MCPA addition. The importance of soil fungi in the detritusphere might also explain that 16S rRNA gene copy numbers did not differ between the three soil compartments, which is in contrast to other studies where a clear gradient formation of 16S rRNA genes with highest numbers in the litter layer has been described (Poll et al. 2010). The litter compartment is a hot spot of general microbial activity (Beare et al. 1995), where water-soluble and easily degradable compounds (e.g. glucose, amino acids) are highly available and reach the soil during the first phase of plant litter decay. In our study, pea litter with a narrow C/N ratio was used, and it might be speculated that the high amount of N in pea litter highly influenced bacterial abundance not only in the litter compartment but by leaching also in deeper soil compartments resulting in an improved N supply in all soil compartments. This indicates the importance of the litter amount and quality for the development of bacterial communities in soil. However, a direct link between bacterial cell numbers and 16S rRNA genes is not possible due to the well-described variability in numbers of 16S rRNA gene operons between different bacterial taxa (Acinas et al. 2004).

In contrast to 16S rRNA gene copy numbers in the upper soil compartment (0–3 mm), a temporal increase of *alkB* abundance could be monitored independently from the addition of MCPA in the same soil compartment. The decrease of *alkB* gene copy numbers in the soil layers 3–6 and 6–9 mm during the incubation might indicate transport limitations of alkanes into deeper soil layers. It is known that mobility of alkanes correlates strongly with the chain length (Leythaeuser and Schae 1982) as sorption to soil particles increases and dissolving in liquids decrease with increasing carbon numbers and vice versa.

Our results clearly support this fact as the amounts of higher alkanes (>C_{30}) were comparable to T0 during the incubation in the deeper soil layers (3–6 and 6–9 mm), whereas a strong increase in the uppermost compartment within the first week was observed. Furthermore, the limitation of other factors like the availability of electron receptors or the succession by other bacteria and fungi could result in decreasing *alkB* gene copy numbers.

However, the present study could demonstrate MCPA-dependent changes in the distribution patterns of short- and middle-chained alkanes. On the one hand, this might point to changes in the communities of alkane degraders towards other alkane degradative systems like the monooxygenases of the cytochrome P450 superfamily (e.g. Cyp153, Cyp52) (van Beilen et al. 2003). Furthermore, evidences for the temporal changes in the soil microbial community induced by MPCA application were also shown on genomic scale by Vieublé Gonod et al. (2006). On the other hand, MCPA could also influence the activity of alkane-degrading enzymes as earlier shown for autochthonous laccases and glutamic dehydrogenases (Polemio et al. 1981; Ruggiero and Radogna 1985), resulting in a delayed response to litter-derived alkanes.

Therefore, to gain more detailed insight, further studies should focus on abundances and diversity analyses of other genes involved in degradation of alkanes mainly of fungal origin like *cyp153* and *cyp52* genes; in addition, geophysical analyses of the migration of short-, middle- and long-chained alkanes in the respective soil would be very useful to link microbial performance and availability of substrates more closely. Although sieved soil has been used in this microcosm study, clear effects related to the different compartments studied were visible, mainly related to MCPA and alkane distribution; however, it must be taken into account that the use of undisturbed soil columns may change some of the response pattern, mainly the abundance of 16S rRNA genes. To perform such experiments, larger microcosms might be needed to ensure reproducibility.

Acknowledgments We thank Birgit Würz for the alkane extraction and the GC-MS measurements. Financial grant was provided by the German Research Foundation (DFG) via the priority programme SPP1315: "Biogeochemical Interfaces in Soil".

References

Acinas SG, Marcelino LA, Klepac-Ceraj V, Polz MF (2004) Divergence and redundancy of 16S rRNA sequences in genomes with multiple rrn operons. J Bacteriol 186:2629–2635

Anderson JR (1978) Pesticide effects on non-target soil microorganisms. In: Hill IR, Wright SJL (Eds) Pesticide microbiology. Academic, London, pp 611–628

Anon TT (1987) Recommended laboratory tests for assessing the side effects of pesticides on soil microflora. Proceedings of the 3rd international workshop, Cambridge, September 1985. In: Somerville L, Greaves MP (Eds) Pesticide effects on the soil microflora. Taylor and Francis, London, pp 205–229

Bach HJ, Tomanova J, Schloter M, Munch JC (2002) Enumeration of total bacteria and bacteria with genes for proteolytic activity in pure cultures and in environmental samples by quantitative PCR mediated amplification. J Microbiol Meth 49:235–245

Baelum J, Nicolaisen MH, Holben WE, Strobel BW, Sörensen J (2008) Direct analysis of *tfdA* gene expression by indigenous bacteria in phenoxy acid amended agricultural soil. ISME J 2:677–687

Baldrian P, Voriskova J, Dobiasova P, Merhautova V, Lisa L, Valaskova V (2010) Production of extracellular enzymes and degradation of biopolymers by saprotrophic microfungi from the upper layers of forest soil. Plant Soil 338:111–125

Beare M, Coleman D, Crossley D, Hendrix P, Odum E (1995) A hierarchical approach to evaluating the significance of soil biodiversity to biogeochemical cycling. Plant Soil 170:5–22

Boivin A, Amellal S, Schiavon M, van Genuchten MT (2005) 2,4-Dichlorophenoxyacetic acid (2,4-D) sorption and degradation dynamics in three agricultural soils. Env Poll 138:92–99

Cayet C, Lichtfouse E (2001) $\delta^{13}C$ of plant-derived *n*-alkanes in soil particle-size fractions. Org Geochem 32:253–258

Cederlund H, Börjesson E, Önneby K, Stenström J (2007) Metabolic and cometabolic degradation of herbicides in the fine material of railway ballast. Soil Biol Biochem 39:473–484

Crespín MA, Gallego M, Valcárcel M (2001) Study of the degradation of the herbicide 2,4-D and MCPA at different depths in contaminated agricultural soil. Env Sci Technol 35:4265–4270

Dignac MF, Rumpel C (2006) Relative distributions of phenol dimers and hydroxy acids in a cultivated soil and above ground maize tissue. Org Geochem 37:1634–1638

Duah-Yentumi S, Johnson DB (1986) Changes in soil microflora in response to repeated applications of some pesticides. Soil Biol Biochem 18:629–635

Gaillard V, Chenu C, Recous S (2003) Carbon mineralisation in soil adjacent to plant residues of contrasting biochemical quality. Soil Biol Biochem 35:93–99

Gniwotta F, Vogg G, Gartmann V, Carver TLW, Riederer M, Jetter R (2005) What do microbes encounter at the plant surface? Chemical composition of pea leaf cuticular waxes. Plant Physiol 139:519–530

Greer LE, Shelton DR (1992) Effect of inoculant strain and organic matter content on kinetics of 2,4-dichlorophenoxyacetic acid degradation in soil. Appl Env Microbiol 58:1459–1465

Herrmann S, Oelmüller R, Buscot F (2004) Manipulation of the onset of ectomycorrhiza formation by indole-3-acetic acid, activated charcoal or relative humidity in the association between oak microcuttings and *Piloderma croceum*: influence on plant development and photosynthesis. J Plant Physiol 161:509–517

Hiller E, Bartaľ M, Milička J, Čerňanský S (2009) Environmental fate of the herbicide MCPA in two soils as affected by the presence of wheat ash. Water, Air Soil Poll 197:395–402

Kearney PC, Kellogg ST (1985) Microbial adaption to pesticides. Pure Appl Chem 57:389–403

Kloss K, Munch JC, Schloter M (2006) A new method for the detection of alkane-monooxygenase homologous genes (*alkB*) in soils based on PCR-hybridization. J Microbiol Meth 66:486–496

Leythaeuser D, Schae R (1982) Role of diffusion in primary migration of hydrocarbons. Am Assoc Pet Geol Bull. doi:10.1306/03B59B2A-16D1-8645000102C1865D 66

Lichtfouse É, Elbisser B, Balesdent J, Mariotti A, Bardoux G (1994) Isotope and molecular evidence for direct input of maize leaf wax *n*-alkanes into crop soils. Org Geochem 22:349–351

Moret S, Sánchez JM, Salvadó V, Hidalgo M (2005) The evaluation of different sorbents for the preconcentration of phenoxyacetic acid herbicides and their metabolites from soils. J Chromatogr A 1099:55–63

Nicolaisen MH, Bælum J, Jacobsen CS, Sørensen J (2008) Transcription dynamics of the functional tfdA gene during MCPA herbicide degradation by *Cupriavidus necator* AEO106 (pRO101) in agricultural soil. Environ Microbiol 10:571–579

Pérez-de-Mora A, Schulz S, Schloter M (2010) MPN- and real time-based PCR methods for the quantification of alkane-monooxygenase homologous genes (*alkB*) in environmental samples. In: Cunningham S (ed) Methods in molecular biology. Humana, New York, pp 59–68

Polemio M, Genchi G, Palmieri F, Testini C (1981) Glutamic-dehydrogenase activity inhibition by phenoxyacilic acids. Plant Soil 63:369–375

Poll C, Ingwersen J, Stemmer M, Gerzabek MH, Kandeler E (2006) Mechanisms of solute transport affect small-scale abundance and function of soil microorganisms in the detritusphere. Eur J Soil Sci 57:583–595

Poll C, Pagel H, Devers-Lamrani M, Martin-Laurent F, Ingwersen J, Streck T, Kandeler E (2010) Regulation of bacterial and fungal MCPA degradation at the soil–litter interface. Soil Biol Biochem 42:1879–1887

Ruggiero P, Radogna VM (1985) Inhibition of soil humus-laccase complexes by some phenoxyacetic acid and *s*-triazine herbicides. Soil Biol Biochem 17:309–312

Schulz S, Perez de Mora A, Engel M, Munch JC, Schloter M (2010) A comparative study of most probable number (MPN)-PCR vs. real-time-PCR for measurement of abundance and assessment of diversity of *alkB* homologous genes in soil. J Microbiol Meth 80:295–298

Tejada M, García-Martínez AM, Gómez I, Parrado J (2010) Application of MCPA herbicide on soils amended with biostimulants: short-time effects on soil biological properties. Chemosphere 80:1088–1094

Thorstensen CW, Lode O (2001) Laboratory degradation studies of bentazone, dichloroprop, MCPA and propiconazole in Norwegian soils. J Env Qual 30:947–953

Tomlin CDS (2003) The pesticide manual. The British Crop Protection Council, Alton, pp 347–348

Töwe S, Wallisch S, Bannert A, Fischer D, Hai B, Haesler F, Kleineidam K, Schloter M (2011) Improved protocol for the simultaneous extraction and column-based separation of DNA and RNA from different soils. J Microbiol Meth 84:406–412

van Beilen JB, Li Z, Duetz WA, Smits THM, Witholt B (2003) Diversity of alkane hydroxylase systems in the environment. Oil Gas Sci Technol 58:427–440

Vieublé Gonod L, Martin-Laurent F, Chenu C (2006) 2,4-D impact on bacterial communities, and the activity and genetic potential of 2,4-D degrading communities in soil. FEMS Microbiol Ecol 58:529–537

Zabaloy MC, Garland JL, Gómez MA (2008) An integrated approach to evaluate the impacts of the herbicides glyphosate, 2,4-D and metsulfuron-methyl on soil microbial communities in the Pampas region, Argentina. Appl Soil Ecol 40:1–12